Department of Energy
Washington, DC 20585

JUN 2 2 2017

Mr. John Greenewald
The Black Vault
[redacted]

Via email: john@greenewald.com

Re: HQ-2017-00045-C

Dear Mr. Greenewald:

This is the final response to the request for information that you submitted to the National Aeronautics and Space Administration (NASA) under the Freedom of Information Act (FOIA), 5 U.S.C. § 552. You asked for the following:

Title: (U) Proposal Nuclear Radiation Effects on Materials at Cryogenic Temperatures

In response to your request, the NASA located one (1) document that required the Department of Energy (DOE) review. The document was sent to DOE's Office of Nuclear Energy (NE) for review and direct response.

Upon review, DOE has determined that the document should be released to you in its entirety.

You may contact DOE's FOIA Public Liaison, Alexander Morris, FOIA Officer, Office of Public Information, at 202-586-5955 or by mail at MA-46/Forrestal Building 1000 Independence Avenue, S.W. Washington, D.C. 20585 for any further assistance and to discuss any aspect of your request. Additionally, you may contact the Office of Government Information Services (OGIS) at the National Archives and Records Administration to inquire about the FOIA mediation services they offer. The contact information for OGIS is as follows: Office of Government Information Services, National Archives and Records Administration, 8601 Adelphi Road-OGIS, College Park, Maryland 20740-6001, e-mail at ogis@nara.gov; telephone at 202-741-5770; toll free at 1-877-684-6448; or facsimile at 202-741-5769.

If you have any questions about the processing of your request, or this letter, you may contact Ms. Melissa Darr or me at:

MA-46/ Forrestal Building
1000 Independence Avenue, SW
Washington, DC 20585
(202) 287-6745

I appreciate the opportunity to assist you with this matter.

Sincerely,

Alexander C. Morris
FOIA Officer
Office of Public information

Enclosure
cc: Josephine Sibley
NASA FOIA Officer

INDEX

Request #: HQ-2017-00045-C

Final response for NE to the request from Mr. John Greenewald for:

Title: (U) Proposal Nuclear Radiation Effects on Materials at Cryogenic Temperatures

In response to your request, the NASA located one (1) document that required the Department of Energy (DOE) review. The document was sent to DOE's Office of Nuclear Energy (NE) for review and direct response.

NE has reviewed one (1) document responsive to your request.

- The document is *being released in its entirety.*

[redacted]

H. Grice

COPY 4

CLASSIFICATION CHANGED

To Unclassified —

By authority of Ltr. 1-15-60

NASA Hdqs. 1-15-60

PROPOSAL

NUCLEAR RADIATION EFFECTS on MATERIALS at CRYOGENIC TEMPERATURES

"DTIC USERS ONLY"

for the NATIONAL AERONAUTICS & SPACE ADMINISTRATION

NUCLEAR

CONFIDENTIAL

CLASSIFICATION CHANGED

To Unclassified

By authority of letter

Date 1-15-60

Class No. 66615

Proposal

Nuclear Radiation Effects on Materials at Cryogenic Temperatures

for the National Aeronautics and Space Administration

NP-33

July 1959

This document contains information affecting the national defense of the United States, within the meaning of the Espionage Laws, Title 18, U. S. C., Sections 793 and 794, the transmission or revelation of which in any manner to an unauthorized person is prohibited by law.

Copy / of 80

LOCKHEED NUCLEAR PRODUCTS

LOCKHEED AIRCRAFT CORPORATION

GEORGIA DIVISION MARIETTA, GEORGIA

12

"DTIC USERS ONLY"

UNCLASSIFIED

CONFIDENTIAL

FOREWORD

This proposal is submitted in response to the June 19, 1959, Request for Quotation No. HS-225 from the National Aeronautics and Space Administration, Washington, D. C. It presents a program for the study of nuclear radiation effects on the engineering properties of materials at cryogenic temperatures.

The proposed tasks will be performed by Lockheed Nuclear Products, as prime contractor, at the Georgia Nuclear Laboratories (GNL).

Lockheed has retained Arthur D. Little, Incorporated, of Cambridge, Massachusetts, to perform the refrigerator design and cryostat heat removal calculations and to consult with Lockheed on the cryostat design.

CONTENTS

ILLUSTRATIONS

SUMMARY

In nuclear missile components, the combination of cryogenic temperatures resulting from the use of liquid hydrogen as the propellant fluid and nuclear radiation is expected to produce effects on the engineering properties of materials that are new both to materials engineers and to missile design engineers. Before reliable systems can be designed, these effects on the properties of materials must be known.

To meet this requirement, Lockheed Nuclear Products outlines in this proposal to NASA a program for a study of the combined effects of nuclear radiation and cryogenic temperatures on the engineering properties of pertinent materials that may be used in the construction of nuclear missiles.

This proposal includes an analysis of the state-of-the-art relative to the effects of cryogenic temperatures, nuclear radiation, and low-temperature annealing on the engineering properties of materials. The rationale for choosing the temperatures, integrated radiation doses, radiation under stressed and unstressed conditions, materials, and specific tests to be used in the test program is presented. These specific tests will include evaluation of engineering design characteristics and the determination of fundamental properties of the materials of interest; these will be compared to give extrapolation of limited data. Conceptual designs and the basis for the selection are given for the cryostats, special test equipment and instrumentation, and the refrigeration equipment. Presented also is a preliminary study of a method for reducing gamma heating and radioactivation in the reactor cryostat and virtually eliminating

any perturbation of the reactor during insertion or removal of cryostats from the reactor beam hole. Also included is a preliminary analysis of the factors that could possibly affect the safety of reactor operation. And a test program based on the concepts and equipment discussed is presented. It includes materials to be tested, types and number of tests to be made, the number of specimens to be tested for each determination and the statistical basis for establishing this number, and the methods for preparation and selection of individual test specimens. · The capabilities of Lockheed Nuclear Products as the prime contractor and Arthur D. Little, Incorporated, as the major subcontractor include pertinent experience of the two companies, resumes of the personnel available for the project, the project organization, and facilities available to the project. Furthermore, a schedule for the entire program is presented.

1. STATEMENT OF WORK

The method by which Lockheed Nuclear Products proposes to determine the effects of nuclear radiation at cryogenic temperatures on the physical and mechanical properties of materials is outlined in this section.

1.1 PHASE I - PLANNING AND DESIGN

1.1.1 Test Procedures and Test Program

A comprehensive test program, including test procedures, for obtaining engineering design data on structural materials that will be submitted to NASA for approval will be formulated.

1.1.2 Cryostats

The cryostats incorporating special test equipment for implementing the NASA approved test program will be designed. The design will include both heat calculations and mechanical designs.

1.1.3 Refrigerator

The refrigerator equipment needed for obtaining and maintaining the required temperatures in the cryostats during testing operations will be designed. This design will include both heat calculations and mechanical design.

1.1.4 Instrumentation

All instrumentation required for operating the cryogenic and test equipment, for reactor safety, and for measuring and recording test parameters will be designed. Commercially available instrumentation will be utilized where applicable.

1.1.5 Remote Handling Equipment

The equipment for remote handling of the cryostats at Plumbrook will be designed.

1.1.6 Gamma Heating Analysis

The gamma heating problem will be analyzed both theoretically and experimentally. The GNL Critical Experiment Facility will be utilized for experimental studies. Required shields will be designed.

1.1.7 Reactor Safety Analysis

A complete reactor safety analysis conforming to the requirements of the Plumbrook Reactor Safety Committee will be prepared for the operation within the beam hole of all test equipment.

1.1.8 Project Management and Project Support

A project manager will be provided for the overall direction of the program. Included are clerical personnel and scientific personnel necessary for the support of the program. This task will apply also to Phases II and III.

1.1.9 Reports

Reports to be submitted for this phase of the program will include the following:

a. Monthly letter reports

b. Topical reports as appropriate

c. A summary report for Phase I

1.2 PHASE II - FABRICATION AND INSTALLATION

1.2.1 Cryostats

The cryostats, including special test equipment designed in Phase I, will be fabricated, and the operating characteristics will be determined at GNL. After proper operating characteristics have been established, they will be installed at Plumbrook and GNL as required.

1.2.2 Refrigeration Equipment -- Plumbrook

The refrigeration equipment designed in Phase I for providing the required temperatures in the cryostats at Plumbrook will be fabricated and installed at the Plumbrook Reactor Facility. After installation, the operating characteristics will be determined and any required modifications completed.

1.2.3 Refrigeration Equipment -- GNL

Refrigeration equipment will be installed at GNL for calibration and test operations.

1.2.4 Instrumentation

The instrumentation specified in Section 1.1.4 will be fabricated, installed at Plumbrook, and its operating characteristics calibrated. Normal laboratory instrumentation will be available at GNL for use in this program.

1.2.5 Shields

The shields required for reducing the incident gamma and thermal neutron flux on the cryostats will be fabricated and installed in the beam hole at Plumbrook. The effectiveness of this shield in preventing reactor perturbations during cryostat changes will be determined by direct measurement.

1.2.6 Remote Handling Equipment

The equipment for remote handling of the cryostats at Plumbrook will be fabricated and installed.

1.2.7 Flux Mapping

Maps of fast neutron flux and spectrum in the interior of the cryostats installed in the shielded beam hole of the Plumbrook reactor will be made by using foil techniques.

1.2.8 Test Samples

The test sample program will be conducted as follows:

a. Materials from which test specimens are to be made will be procured.

b. The required test samples will be fabricated.

c. A pretest examination of each specimen will be made to determine specimen characteristics.

1.2.9 Reports

Reports to be submitted for this phase of the program will include the following:

a. Monthly letter reports

b. Topical reports as appropriate

c. A summary report for Phase II

1.3 PHASE III - TESTING

1.3.1 Tests at GNL

Tests conducted at GNL will include the following:

a. Tests to establish correlation between standard and miniature specimens and between standard and special physical test equipment

b. Screening tests to be conducted without irradiation

c. Tests required for establishing engineering design data under nonirradiated conditions at room and cryogenic temperatures

1.3.2 Tests at Plumbrook

All irradiation testing will be conducted at the Plumbrook facility.

1.3.3 Reports

Reports to be submitted for this phase of the program will include the following:

a. Monthly letter reports

b. Topical reports as appropriate

c. A final report, which will include an engineering design manual, incorporating the results of the test program

2. PRELIMINARY ANALYSIS

This section reflects Lockheed's analysis of the present state of accomplishments in the field of determining effects of radiation on materials at cryogenic temperatures.

There is a substantial amount of information on the effects on crystalline materials of irradiation alone and cryogenic temperatures alone. To minimize complex effects in these investigations, most of the work has been performed on pure metals, with the emphasis on single-crystal studies. Some investigations, however, have been made on the effects of these factors on the mechanical properties of metals.

Following are discussions of the various effects of concern in establishing test parameters.

2.1 CRYOGENIC TEMPERATURE EFFECTS

The effects of cryogenic temperatures on the tensile, fatigue, and creep properties of various materials are discussed in this section.

2.1.1 Tensile Properties

As early as 1930, Boas and Schmid reported that as the temperature was reduced to 36°R, the critical shear stress of cadmium single crystals increased considerably.[1] A few years later -- in 1933 -- de Haas and Hadfield reported their experiments on polycrystalline metals and alloys, which included pure iron (99.85%), carbon steels, alloy steels, nonferrous alloys, and high-purity copper and nickel.[2]

In all cases, the tensile strength increased as the metal was heated from room temperature to 140°R and there was no further increase in tensile strength for iron and most of the steels; brittle fracture occurred in this temperature range. Steels with a high nickel content did not exhibit brittle fracture. The tensile strength of the nonferrous alloys, copper, and nickel continued to increase with the decrease in temperature to 36°R, the minimum temperature at which tests were conducted. Eldin and Collins[3] reported results of experiments on 1020 steel that confirmed the work reported by de Haas and Hadfield. They found that brittle fracture did occur below 140°R, but that there was a slight increase in the stress required to produce fracture as the temperature was reduced to 22°R. McCammon and Rosenberg have also measured the tensile strength of a number of high-purity polycrystalline metals as a function of temperature from 7.6 to 540°R.[4] Figure 1 presents some of the results.

Figure 1 Variation of Tensile Strength of Copper, Gold, Silver, and Aluminum with Temperature

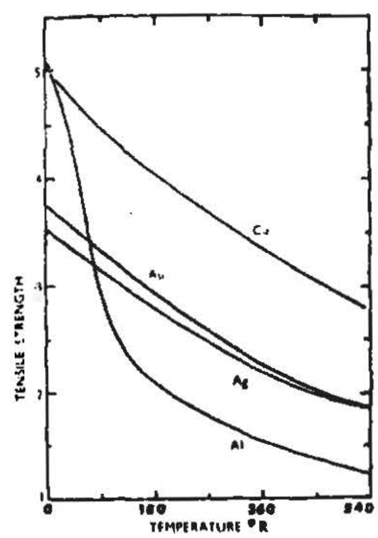

These data show an increase of 400% in the tensile strength of aluminum and about 200% increase for the other metals between 540°R and 7.6°R; the increase continues all the way. These metals all have a face-centered cubic structure, while iron and its alloys exhibiting brittle fracture at low temperatures are body-centered cubic. Bechtold and Wessel found that in molybdenum, tantalum, niobium, and steel the yield strength increases below room temperature and that the rate of increase is greatest just above the ductile-brittle transition temperature.[5]

Two explanations have been proposed for the yield-point phenomena in those metals that exhibit brittle fracture. One is that small amounts of alloying or impurity elements, such as carbon or nitrogen in iron, are attracted to and become concentrated around a dislocation, pinning the dislocation and inhibiting its movement. Consequently, for slip to occur a higher stress is required. Wessel has suggested that after the dislocations have broken away from the impurity agglomerate, they pile up against grain boundaries or other barriers, producing the pre-yield-point plastic strain, and that the yield point does not occur until new dislocation sources are activated by the large stresses in these pile-ups, which are able to break through the barriers. Because of the decrease in the thermal activity at lower temperatures, the stress at a pile-up must be increased before any breakthrough can occur, thus increasing the pre-yield-point plastic strain. At sufficiently low temperatures, the strains produced will be of a magnitude to produce highly localized stresses in the dislocation pile-ups, which cause cleavage in unfavorably oriented sites and thus develop microcracks. In favorably oriented regions, plastic flow will still occur, but the microcracks will reduce the stress required for yield. Decreasing the temperature increases the formation of microcracks to the point where brittle fracture results with very little plastic flow. Wessel also postulated that the ductile-brittle transition temperature might be lowered by reducing the grain size in the metal, since this would minimize the possibility of large dislocation pile-ups. His theory has been substantiated by the work of Basinski and Sleeswyk on very fine-grained (20,000 grains/mm^2), high-purity iron.[6] And later, Smith and Rutherford obtained similar results.[7]

A second explanation of the yield-point phenomena has been formulated by Cottrell.[*] He suggests that the pre-yield strain is due to premature yielding in small localized regions of the specimen. Because of this premature yielding, dislocations are released to pile up against the grain boundaries. The stress in the adjacent grain, resulting from this pile-up added to the external stress, is sufficient to release the nearest dislocation; so the process continues as a chain reaction. Brittle fracture may result from the rapid spreading of a microcrack at the head of a dislocation pile-up. Cottrell points out, however, that this cannot be the only mechanism that can cause failure, because brittle fracture does occur in single crystals in which such dislocation pile-ups are very unlikely. He therefore suggests that crack formation may result from the combination of two dislocations in the absence of a pile-up. This could result when two dislocations with Burgers vectors $\frac{a}{2}[\bar{1}\bar{1}1]$ and $\frac{a}{2}[111]$ gliding in the $(10\bar{1})$ and $(1\bar{0}\bar{1})$ planes, respectively, of a body-centered cubic lattice (a is the lattice constant), combine with a lowering of elastic energy at the intersection of the planes to form another dislocation with Burgers vectors $\frac{a}{\sqrt{2}}[001]$, which lies in the cleavage plane of the crystal. This dislocation, acting as a wedge in the plane, will tend to force the atoms apart to start a crack. When the stresses are great enough, the crack will spread and cause brittle failure.

As shown in some of the work previously cited, metals with face-centered cubic lattice structure do not exhibit ductile-brittle transition, but do increase markedly in strength at low temperatures. This increase in strength, according to Rosenberg, results from the hardening of the metal at low temperatures rather than an increase in interatomic attraction forces.[*] Current theories attribute this hardening to the introduction of obstacles that limit the motion of dislocations. To explain the phenomenon, Rosenberg utilizes the tensile stress-strain curves shown in Figure 2.

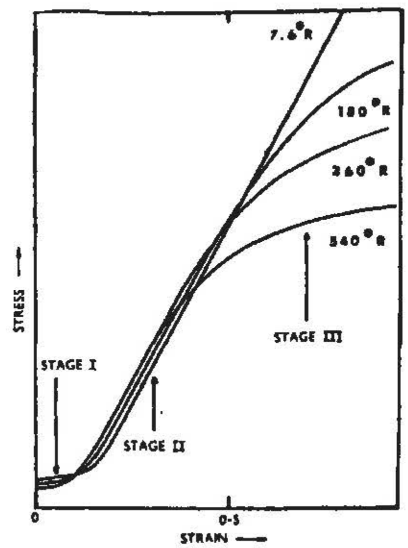

Figure 2 Stress-strain Curves for a Face-centered Cubic Single Crystal at Various Temperatures

Each curve can be divided into three main sections, marked Stages I, II, and III. Stage I is the so-called easy-glide region, in which very little hardening takes place. It occurs in crystals so oriented that only one glide system operates under the applied stress. Stage II is the region of rapid work-hardening, where the stress/strain curve is linear. Stage III begins where this linear section of the curve bends over to what is usually a parabolic form. Whereas Stages I and II are not very temperature dependent, the stress at which Stage III begins increases as the test temperature decreases. During Stage I, slip occurs on only one set of planes. Since there are few obstacles to the movement of dislocations, they move a considerable distance with the application of small external stresses. As the end of Stage I is approached, slip and dislocations are generated on other sets of glide planes. Some of these dislocations will cross the primary glide plane and combine with dislocations on that plane to form what Rosenberg terms sessile dislocations.[9] These sessile dislocations are common to two intersecting slip planes; consequently, they act as obstacles to the movement of the dislocations in the primary glide plane. These tend to pile up behind the sessile, with the result that as the deformation proceeds more obstacles are formed and the number of pile-ups increases, causing the stress required to continue the deformation to increase rapidly. These phenomena will produce a linear stress/strain curve that is independent of temperature, as shown in Stage II, Figure 2. Polycrystalline materials in which single slip cannot occur because of constraints on the crystallites produce stress/strain curves in which Stage I is absent.

The decrease in rate of hardening shown in Stage III is believed to result from the fact that, at higher stresses, the dislocations at the head of the pile-ups avoid the sessiles by cross-slip onto adjacent planes that are free of obstacles. Since a given amount of energy is required to activate the cross-slip, at higher temperatures the thermal energy of the crystal lattice will reduce the external stress demand. This explains the temperature dependency for Stage III shown in Figure 2.

In summary, it must first be stated that the tensile strength of a metal is dependent on ductility and work-hardening characteristics. Except for the body-centered cubic crystal structures, which exhibit a ductile-brittle transition point, the ductility remains fairly constant as the temperature is reduced. These materials follow the general trend until this transition is reached. Since most metals fracture when they are in Stage III, greater stresses must be applied at the lower temperatures to produce fracture. This accounts for the observed increase in tensile strength at the lower temperatures. A contributing factor to this temperature dependence is the fact that for dislocations to move in a slip plane they must cut through the many dislocations that intersect that plane. Thermal activity within the crystal contributes to this movement; consequently, with lower temperatures, the accompanying thermal energy is lessened and a greater external stress is required to produce rupture. This phenomenon should be more pronounced in polycrystalline materials than in single crystals, because of the greater number of obstacles.

One other phenomenon has been observed in stress/strain curves resulting from low-temperature tensile tests. These curves contain serrations, although tests on the same materials at higher temperatures produce smooth curves. Blewitt, Coltman, and Redmond attribute this phenomenon in copper single crystals to twinning, the presence of which they confirmed by X-ray diffraction experiments.[10] They do show, however, that it is only for certain orientations that twinning occurs. This indicates that the serrations are not necessarily due to twinning. Other investigators have suggested that the serrations are caused by local heating within the specimen, but experiments performed to confirm this hypothesis are not entirely conclusive. Rosenberg suggests that another plausible explanation for discontinuous slip at low temperatures may be local yielding in which a few dislocation pile-ups break through their barriers;[9] at higher temperatures, this would be accomplished with the aid of the thermal activity within the crystal.

2.1.2 Fatigue Properties

The first experiments on the fatigue properties of metals at low temperatures were reported by Fontana and co-workers on aluminum alloys, magnesium alloys, stainless steels, titanium, and titanium alloys.[11, 12, 13] The results show that at 138°R the fatigue life at a given alternating stress was about ten times the life at room temperature. Tests at 349°R gave intermediate curves, and tensile tests on the same materials at these temperatures correlated very favorably with the fatigue tests. The effect of temperature on notched specimens was much less than on unnotched ones.

McCammon and Rosenberg,[14] in work on pure copper, silver, gold, aluminum, cadmium, and magnesium, confirmed the results of Fontana's group. Their work extended to 7.6°R, and they found that increases in fatigue and tensile strengths increased in the same ratio from room temperature to liquid helium temperature. Between room temperature and 7.6°R the fatigue life of aluminum under a given alternating stress increased by a factor of approximately 10^7. Experiments were also conducted on zinc and iron (body-centered cubic crystal structures). Their low-temperature brittle fracture characteristic was reflected in their fatigue behavior. Below the brittle-ductile transition temperature, there was a very narrow stress range where fatigue failure occurred. Below this stress range, the metal never failed; above, it broke immediately.

Rosenberg explains the correspondence between fatigue and tensile data by assuming that a small fatigue crack has been formed and that for failure to occur this crack must spread.[9] The theory of the spread of such a crack assumes that the fracture stress must be attained at the tip of the crack so that the metal will yield and increase the length of the crack. If, as the temperature is decreased, the fracture stress increases (it behaves similarly to tensile strength), then for the crack to spread at a given rate, the applied stress must be increased in the same proportion as was the fracture stress.

The fact that fatigue failure occurs in a normal manner even at 7.6°R throws some light on which processes are not possible for the original formation of the fatigue crack. Many theories postulate some diffusion mechanism for the formation of the microcrack; for example, the agglomeration of vacancies produced during the slip. Others suggest that a corrosion process is required. It is highly unlikely that processes of this nature can occur at liquid helium temperatures. The most plausible mode of crack formation appears to be purely geometrical interaction of dislocations or slip planes. In explaining the small extrusions and intrusions observed on copper when it was fatigued at temperatures from room temperature down to 7.6°R, Cottrell and Hull show that if there are two intersecting slip planes, one of which is activated before the other, it is possible to obtain small extrusions and intrusions on the surface of the specimen purely by geometrical interaction.[15] This could represent the beginning of fatigue cracks. It must be emphasized, however, that although diffusion or corrosion mechanisms seem very unlikely in low-temperature fatigue, they may be present at higher temperatures; but they are not essential to the formation of the fatigue crack.

Evidence is beginning to accumulate that indicates the cold work introduced into a metal when it is fatigued is different from that produced in a metal during unidirectional extension. It appears that fatigue work hardening results from the formation of point defects. Experiments by Broom and Ham have shown that according to stress/strain curves taken at 162°R and at 527°R after a specimen has been cold-worked at room temperature either by fatigue or by tension, the flow stress of the specimen is much more temperature-dependent for the fatigued specimens than for the extended specimens.[16] They suggest that this may be because the fatigue hardening resulted from interactions of dislocations with point defects, and these would tend to be more mobile at room temperature. Such point defects might be expected to result from fatigue hardening, since large dislocation movements are unlikely under these conditions. Certain processes that are activated by fatigue can be quenched if the fatiguing is done at 162°R. If a metal is strained at a given stress and then fatigued at a lower stress level, considerable softening of the metal occurs. Presumably this process involves the production and movement of point defects, which tend to unlock the dislocations and cause a softening of the metal. This process is practically eliminated and very little softening is observed when the fatiguing is conducted at 162°R. In some work reported by Broom and co-workers on aluminum alloys, this was demonstrated by the fact that at room temperature the fully hardened and the initially overaged specimens gave similar fatigue curves, indicating that the fully hardened material had become overaged during fatiguing.[17] In tests at 162°R, the overaging during fatigue was inhibited, with the result that the fatigue characteristics of the fully hardened metal were much better than those of the overaged samples.

2.1.3 Creep Properties

Investigations of the creep characteristics of metals show that the phenomena are extremely temperature-dependent. For a given load, the amount of creep increases with temperature. One explanation of this relationship is that thermal activation supplied by higher temperatures is required to overcome barriers that block the movement of dislocations, thus permitting further slip (creep) to occur.

At temperatures in the 162°R range, it has been found that the extension E = AT log Vt, where A and V are constants, t is the time of load application, and T is the absolute temperature of the specimen. Thus, the extension is proportional to the absolute temperature. The theory explaining these phenomena is called the "exhaustion theory." It assumes that within the metal there are minute areas of varying degrees of softness. These soft spots require additional stress or thermal activation to produce yield. They exist in a range requiring different activation energies; consequently, those with lower energy requirements will yield quickly, leaving the ones with higher energies still awaiting activation. The theory also assumes that once a soft spot has yielded and slip has occurred, it cannot be activated again. Hence, with time the supply of soft spots becomes exhausted, with a corresponding decrease in creep rate. This situation lends itself to the derivation of a logrithmic creep law, and a theoretical expression for the value of A in terms of the slope of the static stress/strain curve of the specimen. In this manner, theory and experiment may be compared. Wyatt performed such experiments at temperatures in the 140°R range and found that the creep is proportional to temperature.[18] In 1930, Meissner, Polanyi, and Schmid measured the creep of cadmium crystals at liquid helium temperatures.[19] Their results showed creep extensions of the order of a few tenths of a percent at 2.2°R. It was, however, of the same order of magnitude as they found at 7.6°R. These results did not agree with the theory which, if applicable at these temperatures, would have indicated considerable difference in creep at the two temperatures. Glen repeated the experiments and confirmed the earlier results.[20] He showed that the value of A calculated from his stress/strain curves is not in agreement with the value of A calculated from stress/strain curves on the same material at higher temperatures (138 and 162°R). At the lower temperatures, the creep is 10 times that expected from theory. This indicates that this theory is not valid in the near absolute zero temperature region. Glen suggests that at these low temperatures the soft spots may be activated by the quantum-mechanical tunnel effect. If there is a potential barrier retarding the slip of a soft spot, even without thermal activation, there is a finite probability that the barrier may be overcome. This probability can be calculated with quantum mechanics. The calculations of Mott indicate that, in the liquid helium temperature range, most if not all of the activation is caused by the tunnel effect.[21]

2.2 RADIATION EFFECTS

Many authors have discussed the mechanisms by which neutron irradiation affects the properties of metals. Dienes has summarized these phenomena in the following manner: the interaction of high-energy radiation with matter introduce several types of disturbances (crystalline defects and radiation-induced processes) which affect the properties of the solid.[22] These disturbances are vacancies, interstitial atoms, thermal spikes, impurity atoms, ionization effects, displacement spikes, replacement collisions, crowdions, and dislocations.

In discussing radiation effects in metals and alloys, Billington states that one of the most important factors governing the behavior of metals under irradiation is the temperature of irradiation.[23] Other important variables are melting point, crystal structure, prior thermal and mechanical history, radiation environment, neutron flux, and the property being studied.

The temperature of irradiation is important since it exerts considerable influence on the mobility of induced defects that in turn affect the production of secondary effects. The irradiation effects observed are related both to the melting point of the material and to the temperature of irradiation. As a rough approximation, at temperatures somewhat above half of the absolute melting point, many solid state reactions will proceed at an appreciable rate. The annealing as well as the production of defects is closely allied with this relationship.

The crystal structure provides an indication of some physical property changes that may be expected to result from irradiation. For instance, body-centered cubic materials, such as iron and carbon steel, that exhibit low-impact strength at room temperature and a sensitivity to notch embrittlement, show an increased weakness in regard to these properties under neutron irradiation. Conversely, face-centered cubic metals, such as aluminum alloys and stainless steels, do not exhibit brittle fracture under irradiation, although they do suffer some loss in ductility. Uranium and graphite are good examples of anisotrophy in crystal structure. The relationship between crystal structure and these properties is insufficiently understood to permit broad generalizations in regard to radiation behavior, but it is recognized as being a factor of some importance.

Billington states that the importance of neutron flux as an important variable has been demonstrated in a few instances, but lack of suitable reactor conditions has prevented comprehensive studies in all areas of interest.[23] The question of whether the total dose of radiation or the rate of irradiation is the more important factor in radiation damage to metals has not been resolved.

Billington also states that some mechanical properties of metals are more affected by radiation than others; furthermore, a knowledge of the unirradiated state is often not a good criterion for estimating the relative behavior of various properties under irradiation.

All metals and alloys examined have shown substantial increases in mechanical properties under appropriate conditions of irradiation. The chemical composition and the prior thermal and mechanical history of the metal or alloy greatly affect radiation damage observed. The chemical composition may exert a strong influence, particularly on post-irradiation annealing kinetics, at low temperatures. It may also influence radiation-induced changes in such properties as internal friction and apparent elastic constants.[24] The effects of irradiation on high-purity aluminum have been found to be much less than on impure aluminum. If a metal is only slightly alloyed, more pronounced effects are produced, even for a room-temperature irradiation.[25,26] The introduction of a very small number of impurity atoms may contribute to the production of a concentration of crowdion effects to which certain annealing phenomena are attributed. Consequently, for radiation effects studies on metals and alloys to provide true pictures of the phenomena they investigate, the chemical analysis of the materials studied must be exact and include the minor impurities as well as the major alloying elements.

The initial condition of a metal has been shown to exert considerable influence on the effect of irradiation.[27, 28, 29] Annealed metals exhibit significantly greater changes than those in an initially hardened state when irradiated. Although the exception rather than the rule, there have been instances in which mechanical property values have decreased as a result of irradiation. Makin and Minter observed this phenomenon on the yield strength of specimens of heavily cold-worked zirconium.[30] Ultimate tensile strength is increased by irradiation, but to a lesser extent than tensile yield strength.[31] A comparison of typical increases, after irradiation, in tensile ultimate and tensile yield strengths of several metals and alloys is given in the following tabulation.[23]

	Tensile Strength Psi		YS/US	
MATERIAL	YIELD	ULTIMATE	PRE-	POST-
2S H14 Aluminum	+ 5,000	+ 7,000	0.90	0.85
2SO Aluminum	+ 10,000	+ 9,000	0.51	0.65
High Purity Iron	+ 13,000	1,000	0.50	0.84
Normalized Carbon Steel	+ 43,000	+ 22,000	0.67	0.96
Hardened & Tempered Alloy Steel	+ 43,000	+ 34,000	0.93	0.99
Austenitic Stainless Steel	+ 60,000	+ 17,000	0.38	0.84
Titanium, Commercial 75A	+ 42,000	+ 23,000	0.75	0.99
High Purity Zirconium	+ 18,000	+ 3,000	0.33	0.73

The yield strength effects in steels appear to be more sensitive to the temperature of irradiation than changes in ultimate strength. A result of large integrated doses of fast neutrons is a loss of ductility. Carbon steels and beryllium exhibit considerable sensitivity in this respect. In low-carbon steels, which are body-centered cubic in crystal structure, the major loss of ductility occurs in the uniform elongation prior to necking in tension tests. Loss of impact strength in carbon steels becomes significant after room-temperature exposures as low as 5×10^{18} n/cm^2. Accompanying this phenomenon is an increase in the ductile-brittle transition temperature.

Faris reports that Berggren and Kernohan, at ORNL, observed that an exposure of 2.5×10^{19} n/cm^2 at 581°R caused the transition temperature of a pressure vessel steel to rise from 437°R to 581°R.[26] Sutton and Leeser have reported similar results.[32] And Wilson and Billington reported that samples of high-purity irons and steels with high sulphur and phosphorus content are more susceptible to radiation embrittlement than pure iron and high-quality steels.[33] Since the effects of irradiation on tensile properties, impact strength, and ductile-brittle transition temperature are sensitive to irradiation temperature, irradiations and radiation effects measurements should be conducted at the temperatures of interest.

Most creep experiments on polycrystalline metals have shown no strong effects of irradiation. Jones, Munro, and Hancock found only nominal change in creep rate in aluminum after irradiation with fast neutrons.[34] Jeppson, et al, in creep experiments on cyclotron irradiated aluminum and copper, found similar effects.[35] Wilson and Billington reported a slight increase in the creep rate of stainless steel under irradiation. Faris summarized various radiation creep investigations by reporting no significant effect of neutron irradiation for aluminum at 1121°R, constantan at 1031°R, or nickel at 1751°R; and a slight increase in creep in austenitic stainless steel at temperatures above 1859°R, with a decrease at lower temperatures.[24]

The absorption of neutrons by nuclei often results in the formation of a chemically new species of atoms. The concentration of impurity atoms that are so formed is increased so slowly that their effect on commercial alloys will largely be overshadowed by the impurities that are initially present. The effects become metallurgically important when the transmuted atoms are highly insoluble.[36] Embrittlement may occur and, in addition, some atoms tend to separate out in a gaseous form, since rare-gas atoms are a fairly common product of nuclear reactions.

2.3 ANNEALING

The preceding discussion has shown that the mechanical properties of metals and alloys are greatly influenced by the type, concentration, and distribution of defects in the solid state. The effects on the property results from the presence or absence of the defects, and it is not dependent on the mechanism by which they are produced.[23] Since the advent of nuclear radiation as a tool for investigation of the solid state, many studies have utilized it to produce defects so that annealing characteristics could be determined. Consequently, most reported studies of solid-state defect annealing concern defects produced by irradiation. Similar defects produced by thermal and mechanical mechanisms, such as heat treatment or cold work, would respond to annealing in the same manner.

Dienes and Vineyard state that the defects produced by irradiation are capable of moving about if the temperature is sufficiently high. In this way, the effect of irradiation is altered and may be completely annealed out. In most common metals, defects are mobile at temperatures as low as $54^{\circ}R$, and Cottrell reports that in high-purity copper, after irradiation below $18^{\circ}R$, with 1.35 Mev electrons, most of the electrical resistivity change anneals out by about $63^{\circ}R$.[36] Thus it may be seen that annealing, even during irradiation, is the rule rather than the exception. Consequently, studies of the effects of irradiation on metals at cryogenic temperatures must be made at the temperatures of interest. It is not enough that the irradiation be performed at these temperatures; the test measurements must also be made without permitting the specimen to be warmed.

At an international roundtable meeting held in 1958, various models for the recovery of the physical property changes resulting from lattice defects in metals induced by irradiation were discussed.[37] The defects considered were interstitial atoms, di-interstitial, interstitial agglomerate, vacancy, di-vacancy, vacancy agglomerate, crowdion, spike or zone, dislocation, close pair, and impurity trap. A schematic representation of the recovery of a physical property following low-temperature damaging treatment is presented in Figure 3.

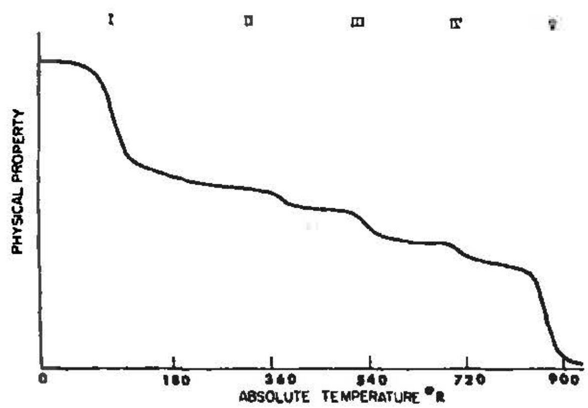

Figure 3 Physical Property Recovery vs. Temperature

Initially, only interstitial atoms, vacant lattice sites, and dislocations were considered adequate to explain the observed phenomena. As more recovery stages were identified and their detailed character examined, the inclusion of more complex effects were required in the explanation. Preliminary evidence indicates that in copper, Stage I recovery following neutron irradiation begins as low as 14°R. The mechanism for recovery in the lower temperature substages of Stage I is thought to be close-pair recombination. Complete agreement has not been reached on the recovery processes for the higher temperature portions of this stage. The simplest interpretation is that the interstitials undergo free migration. Some data indicate that many interstitials are trapped by impurity atoms or dislocations, thereby leaving an equal number of vacancies that have not been annihilated.

Based primarily on internal friction measurements after plastic deformation, the recovery processes in Stage II have tentatively been attributed to the migration of small vacancy or interstitial agglomerates.

Considerable disagreement exists among the investigators concerning the interpretation of the recovery phenomena of Stage III. It is possible that either Stage III or the higher substages of Stage I are to be associated with static crowdion migration, the other being associated with interstitial migration. Although there are some objections to this interpretation, it does fulfill an important requirement imposed by data on lattice parameter and density measurements following deuteron irradiation. Another possibility is that Stage III is associated with vacancy migration.

Active recovery mechanisms for Stage IV are also a subject of controversy. Some investigators think that the vacancy migration mentioned as a possibility for Stage III is the mechanism prevalent in Stage IV. Others think that Stage IV annealing must be explained in terms of a more complex defect. They do not, however, define the defect.

There appears to be universal agreement that annealing in Stage V is accomplished through recrystallation with the reduction of the dislocation concentration.

Dienes and Vinyard summarize by stating that the annealing behavior of irradiated substances is complicated and not yet well understood in even favorable cases. A number of hypotheses have been put forward, but no single interpretation has proved to be entirely satisfactory.

Results of annealing experiments on metals cold-worked below 36°R have disclosed an absence of the annealing that has been observed in the 54-81°R range in radiation damaged specimens, although other processes are present, including one with an activation energy of 0.7 ev. When these results are interpreted according to Huntington's theoretical values of 1.4 ev for the formation of a vacancy and approximately 4.5 ev for an interstitial, they indicate that cold work produces vacancies and not interstitials, whereas irradiation produces both. These data also indicate that the annealing observed in the 54-81°R range results from some type of migration of interstitials with vacancy migration.

Blewitt and his coworkers at ORNL deduced that the effects of structural and chemical defects on the low-temperature annealing processes are quite significant.[38,39] They report that in high-purity copper, annealing peaks exist in the ranges 50-90°R, 414-486°R, and 1026-1206°R, with a steady decrease in radiation-induced resistivity in the temperature range 90-414°R. Similar results were observed for high-purity aluminum and nickel. The temperature-annealing kinetics of copper alloyed with minor amounts of smaller and larger atoms were studied to test the validity of the crowdion interstitialcy process, the effect of dislocation density, and the density of radiation-induced defects on the annealing spectrum. In the crowdion interstitialcy process, displaced atoms are constrained to migrate in a line, with movement being blocked with either a large or small atom.

McReynolds found that two-thirds of the radiation-induced resistivity in copper was annealed out in the range 347-527°R, with an activation energy of approximately 0.6 ev and no decrease in critical shear stress.[40] At 1067°R, both effects were annealed with 2.0 ev activation energy. In aluminum, both effects were completely annealed at 383°R with 0.55 ev energy.

Broom summarizes the results of annealing experiments with the following comments:

> "There are conflicting ideas as to the recovery mechanisms . . . The outstanding thing about all experiments is the amount of damage which can be annealed below room temperature . . . Release of stored energy in the temperature range of resistivity recovery gives values so small that interstitial mechanisms appear unlikely."[41]

3. TEST PROGRAM

This section is devoted to a discussion of Lockheed's proposed test program. The first step, the general approach employed, presents the philosophy established to provide the desired design data. Next, the methods of performing the tests are presented. Following this, the test machines and cryostats are described. And finally, the two-part test program is outlined. The entire program is amplified in Tables I through XII in Appendix A, beginning on page

3.1 APPROACH

The survey of the present state of the art in the field of the effects of nuclear radiation and cryogenic temperatures on the mechanical properties of engineering materials, presented in Section 2, substantiates the need for a comprehensive testing program to provide nuclear missile engineers with reliable design data on the construction materials that must operate in these combined environments. Since the data in Section 2 show that metals exhibiting body-centered cubic crystal structure are subject to severe embrittlement at cryogenic temperatures below the ductile-brittle transition temperature and that nuclear irradiation usually raises this transition temperature, metals of this type may justifiably be eliminated from the test program to avoid unnecessary testing.

The program outlined herein is designed to produce, at minimum cost, reliable engineering design data for a limited number of materials for applications in combined cryogenic and radiation atmospheres specified in NASA RFQ HS-225. Programs for the evaluation of additional materials and for the evaluation of components can be more efficiently planned through consideration of the results obtained in this initial program.

The proposed program consists of two parts. In Part I, screening tests will be conducted to reduce the number of materials that will be subjected to comprehensive tests in Part II.

In the selection of the materials to be evaluated and the specific physical and mechanical properties needed to provide engineering design data, the suggestions presented by NASA, in RFQ HS-225, and the results of the preliminary analysis were utilized.

A number of decisions that are incorporated into this proposal are based on the recommendations of the missile design engineers of Lockheed Missile and Space Division. Among these are the following:

- Adding a buckling test on a limited number of specimens
- Making an additional measurement during a tensile test to permit the determination of Poisson's ratio, which is needed for the calculation of discontinuity stresses[42]
- Testing of 5052, rather than 7075, aluminum alloy because of the relative sensitivity of the two materials to notch effects[43]

The screening tests will probably eliminate the 400-series stainless steel alloys for pump applications, as these alloys undergo a very large loss in ductility at temperatures approaching 36°R. They will, however, be acceptable at temperatures beginning at about 100°R.

The turbine materials have been omitted from this program because the turbine is in contact with gases at cryogenic temperatures for only a few seconds, and during this time it is not subjected to significant doses of radiation. To furnish significant data for use in nuclear missile design, tests of these materials should consist of thermal shock from the temperature of liquid hydrogen to the temperature of the operating gas from the reactor recycle followed by irradiation and the determination of pertinent mechanical properties at the temperature of the hot gas. This is outside the scope of this proposal, as specified in NASA RFQ HS-225.

Tests of the shield materials have not been included because these materials will not be subjected to cryogenic temperatures with the possible exception that, in some designs, the hydrogen inlet to the reactor may penetrate the shield. Mechanical property data for the use of these materials as radiation shields under other than cryogenic conditions have been accumulated during the many materials programs conducted or sponsored by the AEC and the military agencies for the ANP and related projects. Among the materials listed in RFQ HS-225 for shield applications, only one, lithium hydride, requires canning to prevent excessive decomposition. Some of the materials that could be used for canning will be evaluated in this program for applications in other components.

Since the scope of this study is limited to an evaluation of the characteristics of basic structural materials, problems related to fabrication methods such as welding (which would change the hardness characteristics of the metals, thus affecting their mechanical properties) should be considered in a follow-on program devoted to fabrication and manufacturing problems.

The temperature of liquid hydrogen, 36°R, has been selected as the minimum temperature at which tests will be conducted. This temperature was selected primarily because it corresponds to the minimum temperature for applications in a nuclear missile and because testing at lower temperatures would add significantly to the cost of the program. Tests at either higher or lower temperatures would not produce data valid for the properties of materials at 36°R, because a significant amount of annealing occurs even at these low temperatures. These phenomena are discussed in Section 2.3 and on page 20 of Section 2.2.

In this proposed program, mechanical property determinations on irradiated specimens will be made at the irradiation temperature with no interim heating of the specimen since annealing of lattice defects is temperature sensitive, as discussed in Section 2.3. To prevent annealing due to temperature changes between irradiation and testing, which would produce erroneous data, mechanical property measurements will be conducted in the cryostat in which the specimen is irradiated. These tests will be made without removing the cryostat from its position in the beam hole, except for fatigue and creep measurements. To conserve reactor time and to permit accurate correlation of these property values with integrated irradiation dose, the cryostat will be removed from the reactor after irradiation and positioned in the pool for the tests. Another cryostat can then be positioned in the beam hole and, as shown in Section 4, the refrigeration system will cool two cryostats at once, one in the pool and one in the beam hole being irradiated. This will be accomplished without changing the temperature of the specimen.

The proposed cryogenic system to be installed at the Plumbrook facility provides for simultaneously maintaining a specimen temperature of $36^{o}R$ in one cryostat under irradiation and in one other cryostat outside the reactor. This will permit the testing arrangement described above. Tests can be conducted in as many as four cryostats at one time when no irradiation is in progress.

Several factors contributed to minimizing the refrigeration capacity requirements. One of these is the use of miniaturized test specimens and equipment. Special test machines for determining the properties of interest in a cryostat under irradiation will be designed, constructed, and calibrated. Conceptual designs of some of this test equipment are included in Section 4 of this proposal. Test specimens will be miniaturized, as required, to conform to the limitations imposed by the gamma heating. This gamma heating limits the mass of material (which includes both test specimen and test apparatus) that can be cooled to cryogenic temperatures.

Another factor that reduces the cooling requirements and also simplifies handling problems is the use of special gamma and thermal-neutron shields within the beam hole. By reducing the incident gamma rays generated within the reactor and eliminating the greater part of the thermal neutrons that would generate gamma rays within the cryostat and its contents, the gamma heat to be removed will be reduced by a factor of ten from that which would be generated without the shield. Another desirable result of using this shield is that the operation of the reactor will not be perturbed when cryostats are inserted or removed, as discussed in Section 4.3.

Those parts of this program that do not involve irradiation will be accomplished at the Georgia Nuclear Laboratories. The necessary refrigeration equipment will be available at the Georgia Nuclear Laboratories to perform the cold tests. This will permit calibration of test equipment, development of test methods, and the accumulation of basic cryogenic data before the Plumbrook facility is available for irradiation testing.

The various tests specified in this program were selected to provide the nuclear missile design engineer with the engineering data required for nuclear missile design. The state-of-the-art survey discussed in Section 2 indicates that drastic changes in the values of these properties occur at cryogenic temperatures. In Section 2.2, radiation is shown to exert its influence also. In some instances, the effect of the two environments is additive; in others (creep, for example) the opposite trend is sometimes in evidence. The interaction of the two factors and the exact values for such properties as tensile strength, tensile yield strength, elongation, Poisson's ratio, fatigue, creep, notch strength, tensile impact, buckling, and wear will be determined for a limited number of materials.

In addition to the engineering tests, certain fundamental measurements -- resistivity and stored energy -- are listed. These later tests will determine the temperatures above $36^{o}R$ at which mechanical properties will be determined, as discussed in Section 3.2.2. They will serve as a means for extrapolating limited engineering data.

3.2 TEST DESCRIPTIONS

The test program is designed primarily to provide engineering design data on commercial-quality improved alloys under the simultaneous conditions of nuclear radiation, cryogenic temperature, and stress. Hardenable either by heat treatment or cold work, high strength-to-weight ratio alloys will be carefully evaluated to provide critical design data on combined effects as required by the NASA. In addition, wear and endurance data on typical seal and bearing materials will be obtained.

Work will be performed at the Nuclear Laboratory Division facility and at the NASA Plumbrook facility by personnel of the Lockheed Nuclear Products, with assistance from the Engineering Research and Development Division and the Mathematical Analysis Department of the Lockheed Georgia Division and the Lockheed Missile and Space Division.

Since certain limitations are imposed by the test environments -- cryogenic temperatures and irradiation -- modifications of conventional methods to permit testing in the specialized equipment described in Section 3.3 will be necessary.

3.2.1 Engineering Properties Tests

The engineering properties of nonirradiated specimens at room temperature and at the cryogenic temperatures are listed in Tables I, II, and III in Appendix A. The values for these properties will also be determined on irradiated specimens under the same conditions.

The following sequence of operations is the typical procedure for testing irradiated specimens.

a. Load sample into cryostat and check instrumentation.

b. Seal cryostat and evacuate air to 0.5 mm or less.

c. Purge cryostat with room-temperature helium at 1 atmosphere.

d. Evacuate cryostat, flush with helium at least three times, charge with warm helium, and close valves.

e. Connect cryostat to helium refrigeration manifold.

f. Evacuate between valves and start refrigeration to cool test chamber.

g. Position cryostat in reactor beam hole.

h. Adjust refrigeration to provide temperature; wait for equilibrium.

i. Expose the sample until it has received the specified irradiation . . .

- For tests other than fatigue and creep, perform the test.

- For fatigue and creep tests, remove the cryostat from the reactor, position it in pool, perform the test.

j. Disconnect cryostat from refrigeration source, place in shielded cask, transport it to hot cell.

k. Replace with a second cryostat, previously connected to common manifold and conditioned for test.

3.2.1.1 Tensile

The tensile test cryostat will be specially designed by Lockheed Nuclear Products and Arthur D. Little, Inc., to be operable within a horizontal beam hole of the Plumbrook Reactor Facility.

The operating characteristics of the tensile test cryostat will simulate those of a standard tensile test machine.[44,45] They will be limited only by the accuracy of the sensing elements such as load cells, microformers, and strain gages operating within the environment of cryogenic temperature and radiation. Tranducers least likely to be affected by radiation rate or total dose will be selected. (A more complete summary of tranducers and instrumentation is presented in Section 3. 3. 4.)

Thermocouples will be attached to the reduced section of the specimen to maintain a constant record of temperature level and gradient throughout the testing period. Tests will be conducted at various temperatures and doses as indicated in Table IV. Specimen temperature at any one point will be controlled within $\pm$ 2°R.

All sensing, indicating, and recording devices will be calibrated periodically throughout the program. Typical flat and round test specimens for the tensile stress-strain and notch sensitivity properties are shown in Figures 4 and 5.

All tensile data will be presented in detail. The test parameters to be measured are as follows:

Tensile yield strength
Ultimate tensile strength
Percentage of elongation
Reduction in area
Poisson's ratio
Young's modulus

Ultimate tensile strength will be calculated from the maximum load during a tension test and the original cross-sectional area of the specimen.

$$\text{UTS (psi)} = \frac{\text{load, max, (pounds)}}{\text{original cross sectional area (sq in.)}}$$

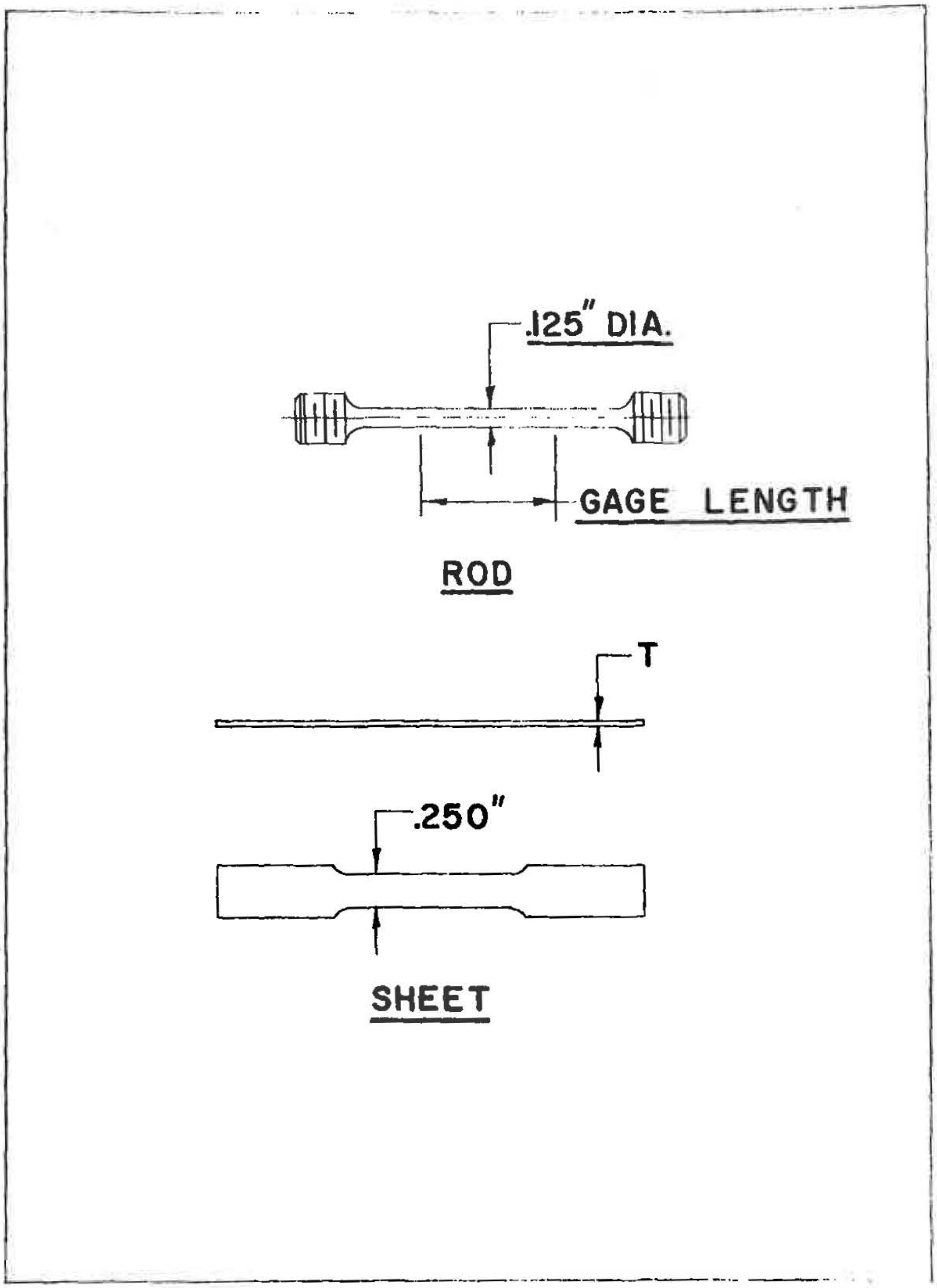

FIGURE 4 TENSILE TEST SPECIMENS

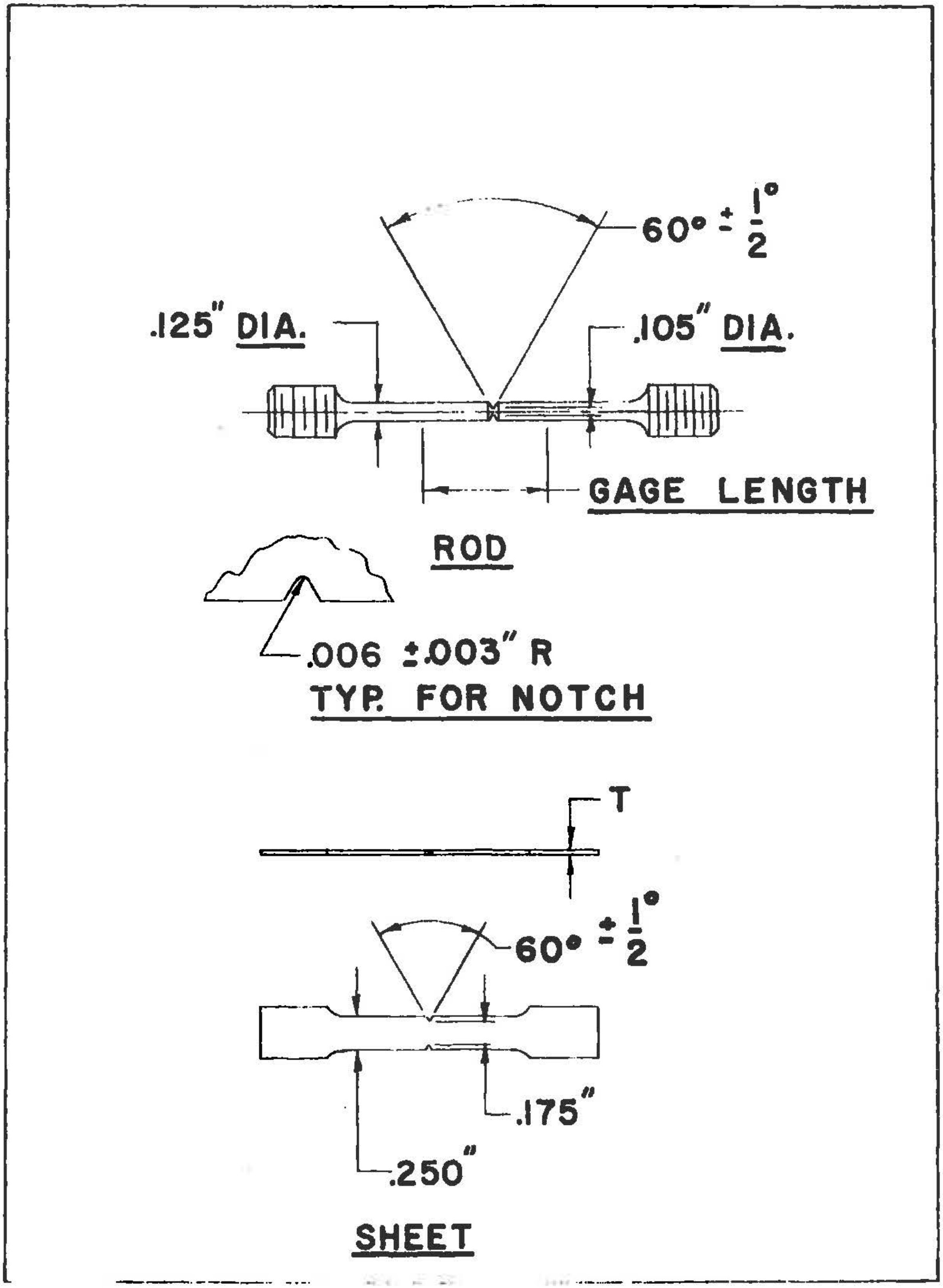

FIGURE 5 TENSILE TEST SPECIMENS – NOTCH SENSITIVITY

Yield strength will be expressed in terms of the stress corresponding to permanent strain.

$$\text{YS (psi)} = \frac{\text{load (0.2\% strain offset, pounds)}}{\text{original cross sectional area (sq in.)}}$$

Poisson's ratio will be calculated from the absolute value of the ratio of transverse strain to the corresponding axial strain under uniform stress, below the proportional limit.

Percentage of elongation will be taken as the percentage increase in gage length of the tensile test specimen.

$$\text{Percentage of elongation} = \frac{\text{final gage length - original gage length}}{\text{original gage length}} \times 100$$

Reduction of area will be measured as a function of stress.

3.2.1.2 *Tensile Notch Strength*

The notch strength of flat and round specimens will be determined by using the tensile test cryostat.

Each test specimen will be notched with a $60^{\circ} \pm 1/2^{\circ}$ groove as shown in Figure 5. Table V lists the materials for test.)

A constant speed of jaw separation will be used for this portion of the test and will be identical to the speed used for unnotched tensile specimens.

The speed of testing has been found in some materials at low temperatures to affect the notch strength. It will be consistent with the purpose of the first phase to test for each material one or two samples at higher speeds than those normally used for tensile testing, but still within the range of a conventional tensile machine. However, a thorough study of the effects of testing speed on the strength of alloys at cryogenic temperatures and radiation is recommended for a later period.

3.2.1.3 Tensile Impact

In this test, the tensile load required for failure will be applied to the specimen in approximately 10 milliseconds, which is much beyond the maximum rate of loading allowable in most tensile test machines. The purpose of this special test is to determine the effects of rates of loading approaching impact.

Specimens may be either notched or unnotched. Notch geometry and specimen size are identical to those used in tests described in the previous paragraphs.

3.2.1.4 Tensile Shear

Empirical relations have been established between the shear strength and the ultimate tensile strength for many ductile alloys. Design engineers often use as the shear strength the value of 50 to 60% of the ultimate tensile strength for ductile materials. Theories of failure based on standard shear data are well correlated with experimental values obtained in the laboratory and are considered useful for the prediction of structural failure.

A relatively simple test that will simulate shear in a specially designed specimen will be conducted to determine the following:

- The application of the empirical relation of shear strength and ultimated tensile strength at cryogenic temperatures and under nuclear radiation.

- The presence of abrupt discontinuities in the ultimate tensile shear strength relationship.

The shear test specimen design is shown in Figure 6 . The cross sectional area of the test specimen is a rectangle 0.250 $\pm$ 0.010 inch times the thickness of the sheet material. Shear stress in psi will be calculated as the pounds of force required to fail the test specimen divided by the cross sectional area as described above.

3.2.1.5 Buckling

Associated with the increased use of pressure-vessel type structure in space vehicles is a greater dependence on buckling criteria.

The design of shell or wall structures with high buckling strength-to-weight ratio calls for the use of hat, Z, and other cross sections.

Work by the NACA has helped to provide good correlation of experimental and theoretical data for sections of this type over a wide range of temperatures.[46,47,48,49] However, the spectrum of tests at cryogenic temperatures under nuclear radiation has not been investigated. Various shapes were correlated on the same structural index curve.[50]

The purpose of this portion of the test program is to evaluate a typical cross section of interest to the space vehicle design engineer and to provide needed data on the buckling strength of shaped elements at cryogenic temperatures and under radiation.

A typical buckling test specimen is shown in Figure 7 , and the number and types of specimens required are listed in Table VI. Tests will be performed in the tensile test cryostat by the application of a compressive load. The load in pounds required to cause buckling will be recorded; temperature and total dose will also be recorded for each specimen.

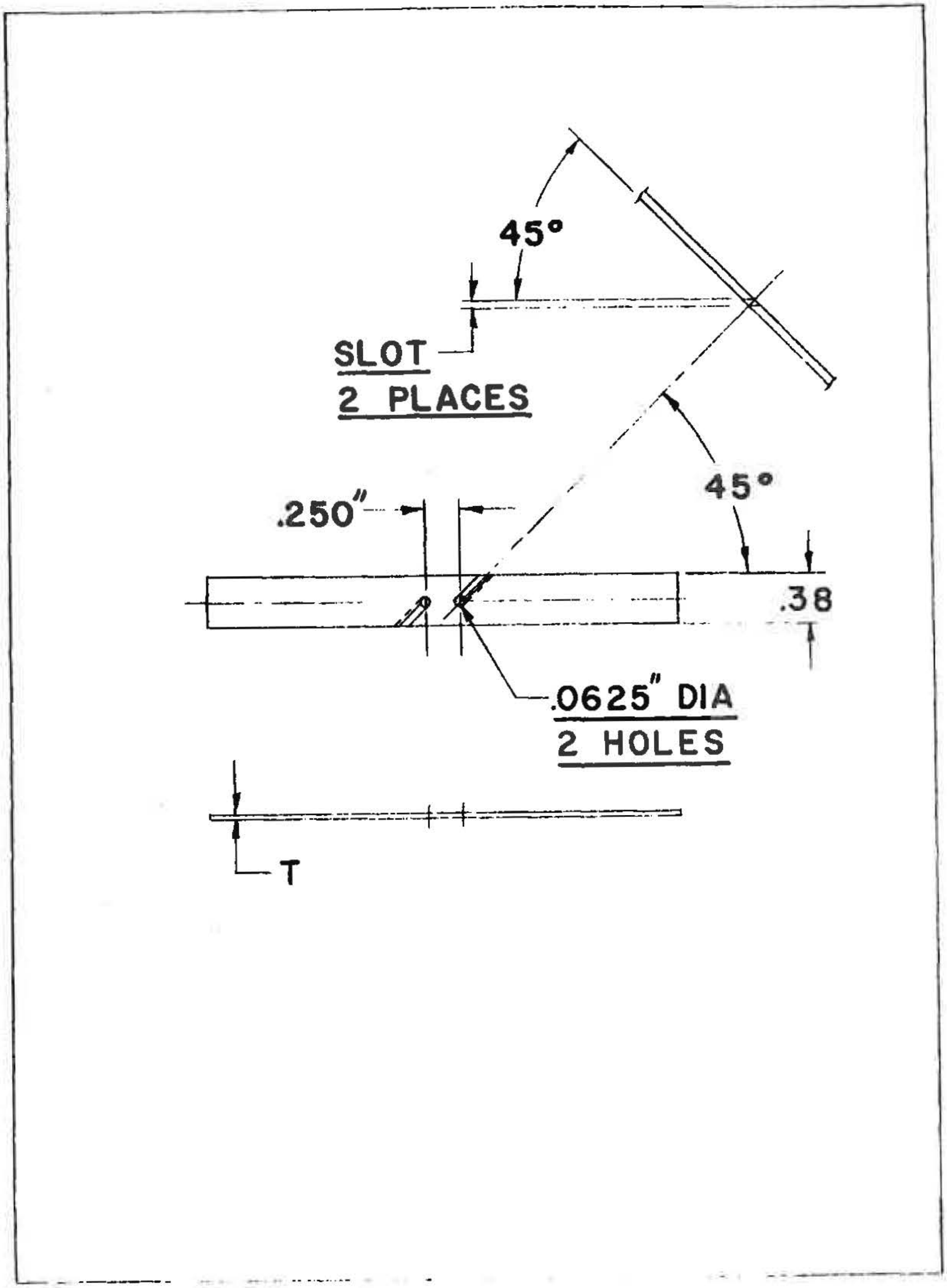

FIGURE 6 SHEAR TEST SPECIMEN

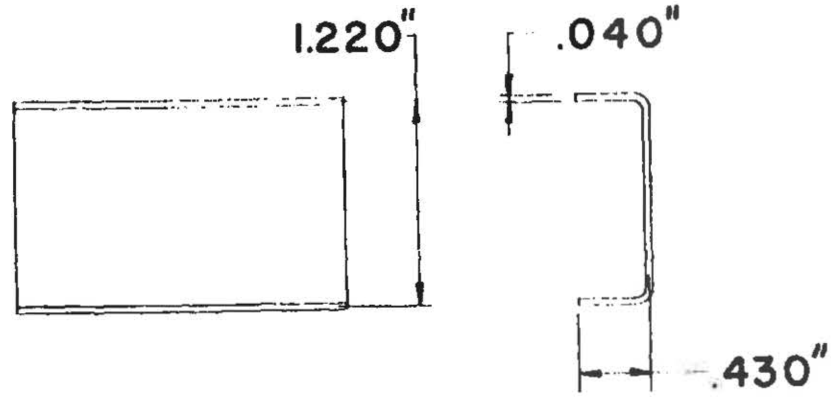

FIGURE 7 BUCKLING TEST SPECIMEN

3.2.1.6 Creep

This test measures the influence of irradiation on the generation of dispersed microscopic "soft spots" in the test samples, as discussed in Section 2.1.3. This condition may give rise to a process comparable to creep when structures at constant stress are exposed to nuclear radiation. The assessment of this phenomenon for short-time creep will be made in the tensile test cryostat. Isostress plots will be made with strain and time as the ordinate and abscissa, respectively, for irradiated and unirradiated test specimens.

A typical creep test is shown in Figure 8. Table VII lists the test conditions and the number of test specimens required.

3.2.1.7 Fatigue

In the design of advanced space vehicles and missiles, an adequate supply of airframe materials that are resistant to long-term repeated loads and short-term shock loads at low temperature and under irradiation is of utmost importance.

The purpose of the bending fatigue test is to simulate the long-term repeated loads imposed on parts of the space vehicle in these environments. The technique of applying a resonant frequency to the test specimen in tension will also be evaluated and a test method selected.

An alternating amplitude of approximately 0.05 inch (peak to peak) will be applied to the sample vibrating from 100 to 500 cycles per second.

A stress level will be selected for each alloy so that the number of cycles required for failure will be approximately 10^6 cycles, which represents about one hour of cycling at 500 cycles. Selection of 10^6 as the number of cycles and a single-stress level for each alloy will reduce considerably the number of specimens required, but will still provide basic fatigue design data for the engineer.

A fatigue test specimen to be used is shown in Figure 9. A final inspection of all surfaces of the specimens will be made at 25X prior to testing and will be in addition to the quality control procedure described in Section 3.6 for test specimens.

For all fatigue tests, the sample will be irradiated at cryogenic temperatures to the specified total dose in the fatigue test cryostat. Without changing the temperature, the cryostat will be removed from the reactor and positioned on a test rack in the pool where the fatigue testing will be conducted. In this manner, the total dose received by the specimen can be accurately measured.

All specimens will be tested as described in Section 3.3.2, by applying magnetic excitation at resonance.

Table VIII lists the parameters of the fatigue test and the number of specimens required for each parameter.

Fatigue data for all of the alloys will be tabulated in terms of the number of stress cycles endured, test temperature, and amount of dosage for each of the alloys tested.

3.2.1.8 Wear

Wear tests for both bearings and seals are described in this section.

For a careful evaluation of bearing design, axial and radial load, rotating rate, temperature, and atmosphere must all be considered.

Within the bearing assembly, the races, balls, retainers, and lubricant play an important part and selection is based on the bearing task.

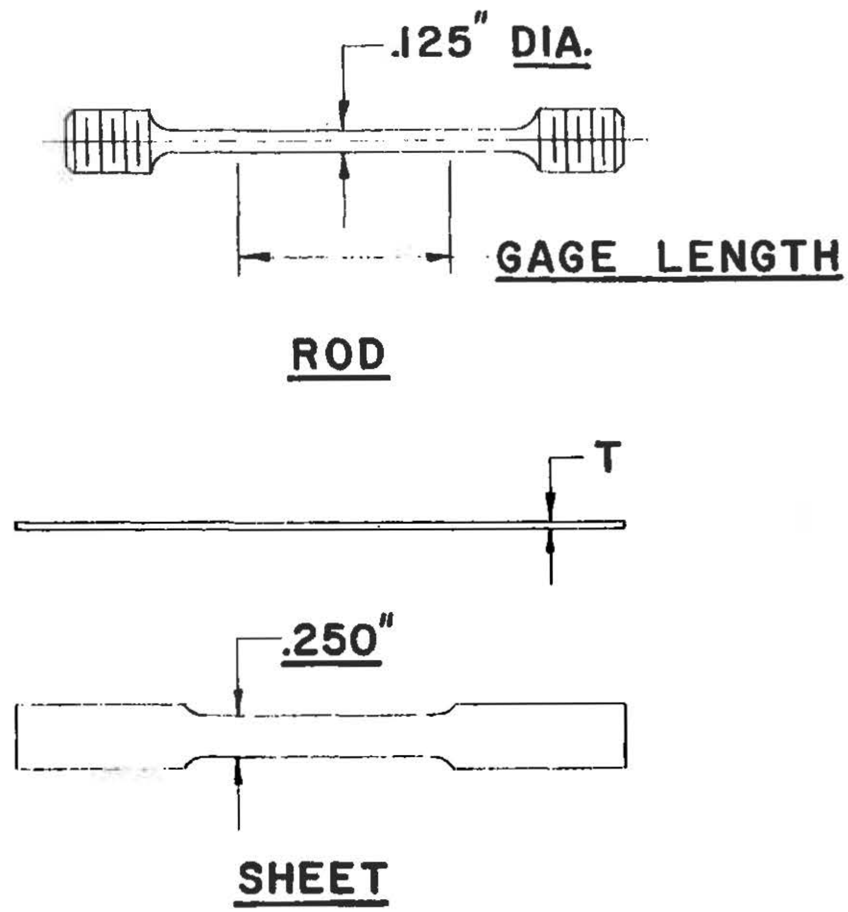

FIGURE 8 CREEP TEST SPECIMENS

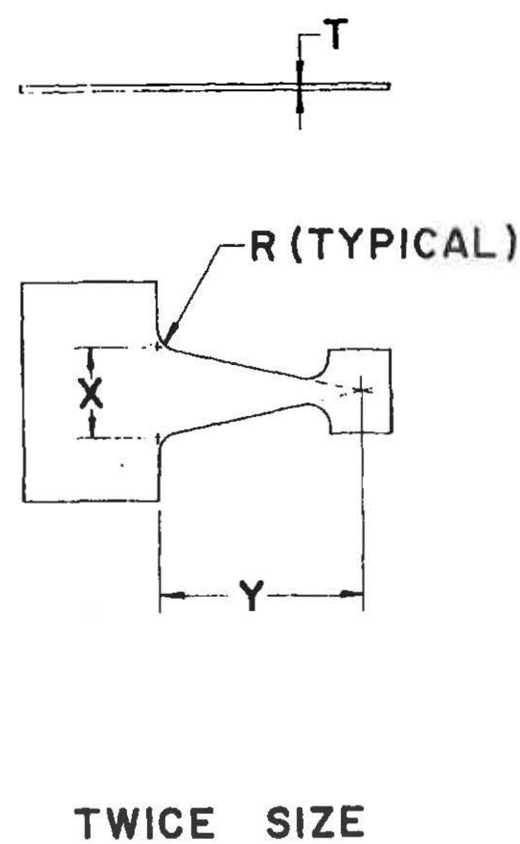

FIGURE 9 FATIGUE TEST SPECIMEN

Considerable work on bearing wear has been done by the NACA and the Armed Forces.[51] The alpha, Falex, and MacMillan testers have been used in this application.[52,53]

Figure 10 shows the test specimen configuration for bearing wear and bearing hardness, and Table IX lists the material combinations planned.

A modified MacMillan wear tester, incorporated in the Wear Test Cryostat, will be used to wear combinations of ball and race material and lubricants.

The end of the rotating shaft, fitted with a ring of the test material, will be loaded in contact with a block of identical or different test material held stationary. A thermocouple will be inserted in the stationary block to indicate temperature.

As the material wears, the torque in the shaft increases. At a preset value of torque, the motor is stopped and the run is completed. This type of test provides a qualitative method of comparing bearing materials and lubricants, based on wear, run time, and load.

It is to be emphasized here that for these tests helium gas rather than hydrogen will be in contact with the bearing material. For a full-scale program the effect of a near vacuum, hydrogen, or other atmospheres on bearings should be considered. A critical evaluation of the method to provide the recommended atmosphere at cryogenic temperatures will be needed.

The ability of a rotary face seal, reciprocating seal, or static spring seal to perform its function on a space vehicle depends in part upon the materials from which the seal components -- such as the face, seal, and bellows -- are fabricated.

Of equal importance in job-rated quality is the seal configuration under the combined environment of stress, temperature, and radiation.

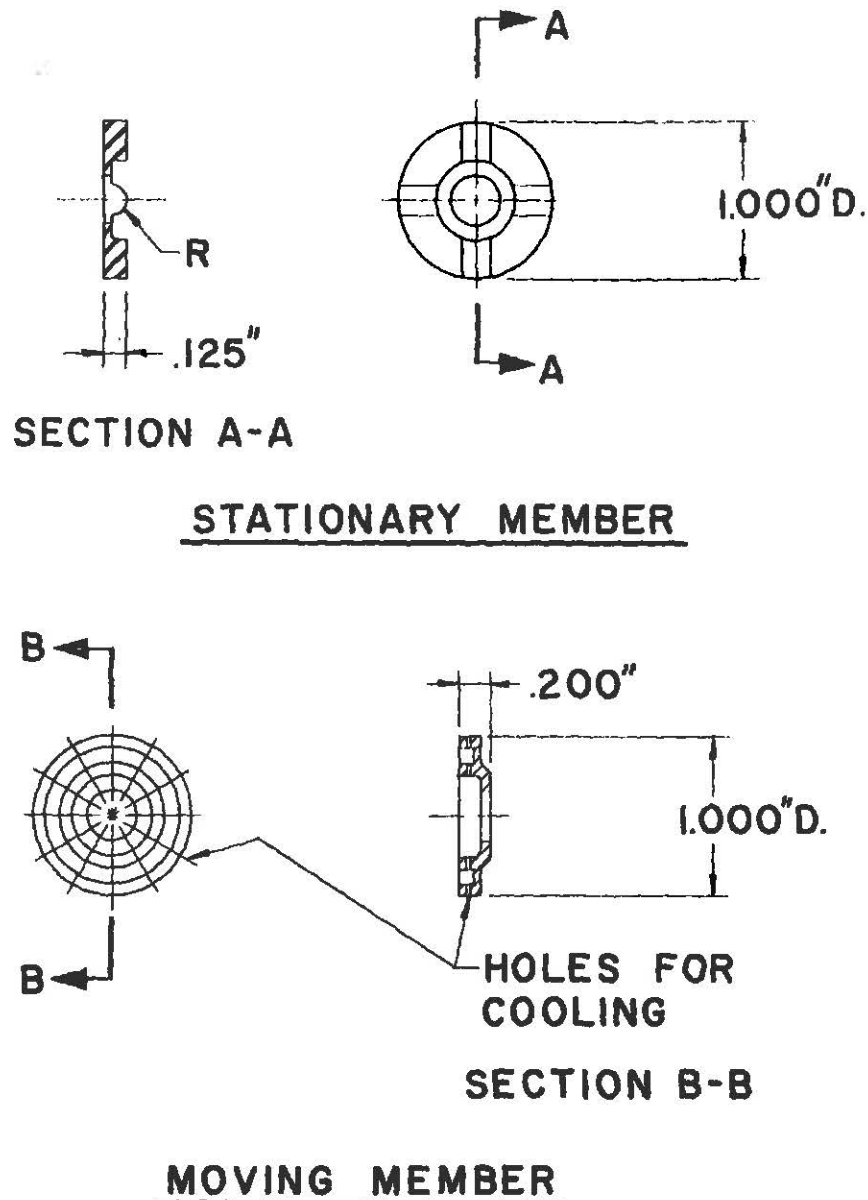

FIGURE 13 WEAR TEST SPECIMEN

The engineering tests described below are designed to impose upon the seal assembly the type of stresses it will receive in service.

Combinations of face seal and rotating shaft face material will include austenitic 304, 17-7 PH, and 440 martensitic stainless steels, ceramic, and amorphous and graphitic carbon impregnated with barium fluoride or cadmium iodide.

Molybdenum disulfide and other coatings will be evaluated for use between the face material and the rotating member. Figure 10 shows the seal test specimen configuration. Tables II and X list the test conditions and the combinations of seal, rotating surface, bellows, and coating materials.

In measuring wear, the wear test cryostat will be used; and a test block of the seal material equipped with a thermocouple will be loaded against the rotating edge of the face material. Some of the test runs will feature coated face and block material. Wear will be reported as a loss in weight of the seal material as a function of run time, seal load, temperature, and total dose.

Coating failure on either the rotating member or the stationary block will be determined by a sharp increase in temperature as sensed by the thermocouple and will be correlated to run time, load, temperature, and dose.

3.2.1.9 HARDNESS

After reaching temperature equilibrium and receiving the required integrated dose,the surface of the test specimen will be indented by a Rockwell type of indentor while in pile. The volume of the indentation or its surface area will be related to the hardness of the material.

Calibration curves will be established for the equipment through using materials of known hardness at varying temperatures.

Measurement of identation size will be made out-of pile. Dimensional changes in the identation due to a possible measureable difference between the temperature of testing and measuring will be incorporated into the calibration. Thus, it will not materially affect the data.

The indentor releasing mechanism will be designed to operate in two stages; the application of a minor load, followed by the application of a major load. The loading stage and related equipment will be designed as an integral part of the tensile test cryostat.

3.2.1.10 Bellows Ductility

Tests will be run in the tensile test cryostat. The compressive stress required to strain the bellows for finite increments of strain will be recorded as a measure of ductility. Various temperature and irradiation combinations are specified in Table XI. A load-strain plot will be made to show the relationship of strain, stress, temperature, and integrated dose to bellows material.

Correlations will be made between the basic mechanical strength properties and ductility of the bellows of the same material. A typical bellows test specimen is shown in Figure 11.

3.2.1.11 Bellows Endurance

The tensile test cryostat will also be used to apply an alternating load in tension and compression to typical bellows configurations. It will be placed in the beam hole until the sample has received the specified radiation, then it will be removed and placed in the pool for testing.

Cycling in the cryostat will continue until failure occurs, and the number of cycles to failure will be recorded. An alternating amplitude of stress will be applied to the bellows vibrating at about 10 cps. Failure of the sealed pressurized bellows will be detected by a change in pressure with the pressure sensing device located either inside the bellows or in the outer chamber.

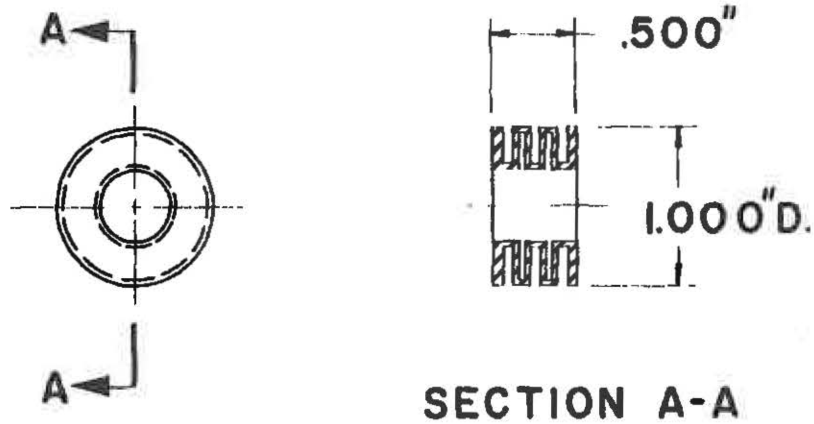

FIGURE 11 BELLOWS TEST SPECIMEN

Amplitude of movement, temperature, number of cycles to failure, and integrated dose will be recorded.

3.2.1.12 Bellows Torsion

The torsion transmitted to the bellows through the seal material will be measured by means of a torque sensitive device mounted as a part of the main shaft of the wear test cryostat. The Wear Test Cryostat will be designed by Lockheed Nuclear Products and Arthur D. Little, Inc., to run wear tests on bearing as well as seal material at cryogenic temperatures. A torque, alternating in direction, will be transmitted to the bellows test specimen until failure of the bellows occurs.

The torsion load and the number of cycles required to fail the bellows will be recorded, as well as the temperature and total dose.

3.2.2 Fundamental Correlation Tests

Stored energy and resistivity characteristics of alloys can be used to establish temperatures at which major annealing effects occur and to provide a basis for possible extrapolation of limited mechanical property data.

3.2.2.1 Stored Energy Measurements

Stored energy will be measured as suggested by Coltman, Blewitt, and Noggle of Oak Ridge National Laboratories.[54] The sample will be irradiated to a dose of about 10^{19} n/cm^2, at low temperature (about 36°R), so that energy is stored. The gamma radiation will be applied to raise the temperature of the sample and at the same time release the stored energy. A plot of temperature vs time will be obtained. The sample will then be restored to cryostat temperature and a second run made; this time the sample should contain no stored energy.

In the first run, where the temperature rise is caused by the release of stored energy, as well as by the heat imparted by gamma irradiation. The following equation may be used:

$$C_p \, dT = dQ \neq dE$$

where C_p = the specific heat of the material
dQ = the energy due to gamma irradiation
dE = the stored energy

When the external heat imput is at a constant rate, it may be expressed as follows:

$$C_p \, dT = r dt \neq dE$$

where r = the rate of external energy input $\frac{dQ}{dt}$, from which is obtained the expression

$$\frac{dt}{dT} = \frac{1}{r}\left(C_p - \frac{dE}{dT}\right)$$

For the second run, where no stored energy is present, the slope of the curve becomes

$$\left(\frac{dt}{dT}\right)_1 = \frac{C_p}{r}$$

Subtracting $\frac{dt}{dT}$ from $\left(\frac{dt}{dT}\right)_1$ and solving for dE gives

$$dE = r\left[\left(\frac{dt}{dT}\right)_1 - \frac{dt}{dT}\right] dT$$

The stored energy released in any temperature may then be determined by hand integration of the two temperature vs time recordings. This method will require a thermocouple to determine cryostat temperature and a second thermocouple to monitor sample temperature.

The testing method is shown in Figure 13, which appears in Section 3.3.1.

3.2.2.2 Resistivity

Changes in resistivity will also be determined by a method suggested by Coltman, Blewitt and Noggle.[54] In their method, the sample is kept at a low reference temperature (about 36°R), where the thermal component of resistivity is negligible and changes in the displacement component (which is quite small compared to the thermal component at higher temperatures) is readily observed. A known amount of energy is introduced into a heating coil in the proximity of the sample by discharging a capacitor charged to a selected voltage. By heating in this manner, the supplied power is independent of the heating element resistance and a given temperature rise may be obtained with good repeatability.

After the temperature rise, the sample is quenched to the reference temperature and the effect on resistivity by the annealing temperature excursion pulse is determined, as shown in Figure 14.

3.2.3 Hydrogen Permeability Properties

Various films and film combinations have been considered for sealing the inside of the liquid hydrogen tank in the space vehicle. Mylar has been recommended by the Lockheed Missile and Space Division as one film material to be tested.

Since NASA reactor safety regulations prohibit the use of hydrogen within the reactor containment vessel, the test material will be irradiated and subsequently tested for permeability outside of the reactor with hydrogen at about 36°R.

The test cell will consist of a dual chamber filled on one side with liquid hydrogen boiling at 1 atmosphere pressure. A sheet of test film will separate the two chambers and be exposed to cold hydrogen vapor on one side. The film will be reinforced to prevent rupture and exposed to a sealed, evacuated space. Measurement of the change in pressure of the evacuated chamber, when corrected for temperature and plotted against time, will give an accurate measure of the permeability of the film. Several thicknesses of film will be evaluated.

3.3 TEST EQUIPMENT

The three types of cryostats to be used in the test program -- tensile cryostat, fatigue cryostat, and wear cryostat -- are described in this section. Also included is a discussion of the equipment incorporated into each cryostat to determine the physical and mechanical properties of interest. This equipment makes it possible to irradiate and test the specimens while cryogenic temperatures are maintained.

3.3.1 Tensile Cryostat

The tensile tester consists of a chamber that houses the specimen and grips, surrounded for the most part by a vacuum jacket. Within the unit around the specimen, is a close-fitting duct, which conducts the coolant (gaseous helium) into the cryostat, to and past the specimen gage length and back, through a return line, to the refrigerator. The duct clearance on the specimen is designed to achieve a high flow velocity, thus producing a large Reynolds number and heat transfer coefficient, a necessary condition to effective extraction of gamma heating. Provision is made in this duct to house an extensometer of the differential transformer type; it will be mounted directly on the gage length of the specimen.

Because the cold helium duct is fitted closely to the specimen, the region inside the cryostat, but outside of the duct, will tend to be stagnant. Actually, the nonvacuum jacketed flange and the grips permit some heat influx by conduction. The helium gas will then develop thermal gradients circulating between the warm top and the cold internal duct, providing natural convective heat transfer into the cryostat. However, the over-all requirements are such that this loss of refrigeration is negligible.

It is important that facility in changing specimens be recognized in the design phase of the test rigs; and in tensile test units, this consideration is regarded as mandatory because of the necessity of remote handling. While a slight penalty on heat load has been taken to achieve this, the ease of assembly and disassembly reflected in the design of Figure 12 will more than compensate.

Specimen size has been dictated by two main considerations, refrigeration capacity of the cooling system and the load capacity of the supporting mechanical system.

The first item is a direct function of the amount of material that must be cooled. A large mass means large gamma heating, hence more refrigeration. As discussed in Section 4.1, the increase in size and mass tends to produce a correspondingly smaller rate of increase in surface area. Since the gamma [illegible] is concentrated at the surface, a relatively smaller [illegible] greater temperature difference between the test [illegible] coolant and a greater temperature difference [illegible] specimen cross section itself. For these reasons, it is essential to keep the test specimen size commensurate with low temperature gradients and near uniform sample temperatures.

The second point relates to the need of test rig compactness. The elements of the apparatus must have a considerable margin of safety over the strongest specimen tested. At high fracture stresses, the sudden release of stored energy in the mechanical system will produce a severe shock, which must be absorbed by the system itself. While provisions are made to minimize the shock load by controls in the hydraulic load system, it is still essential that a large safety factor be built in. To do this in the space allotted, small test specimens are required.

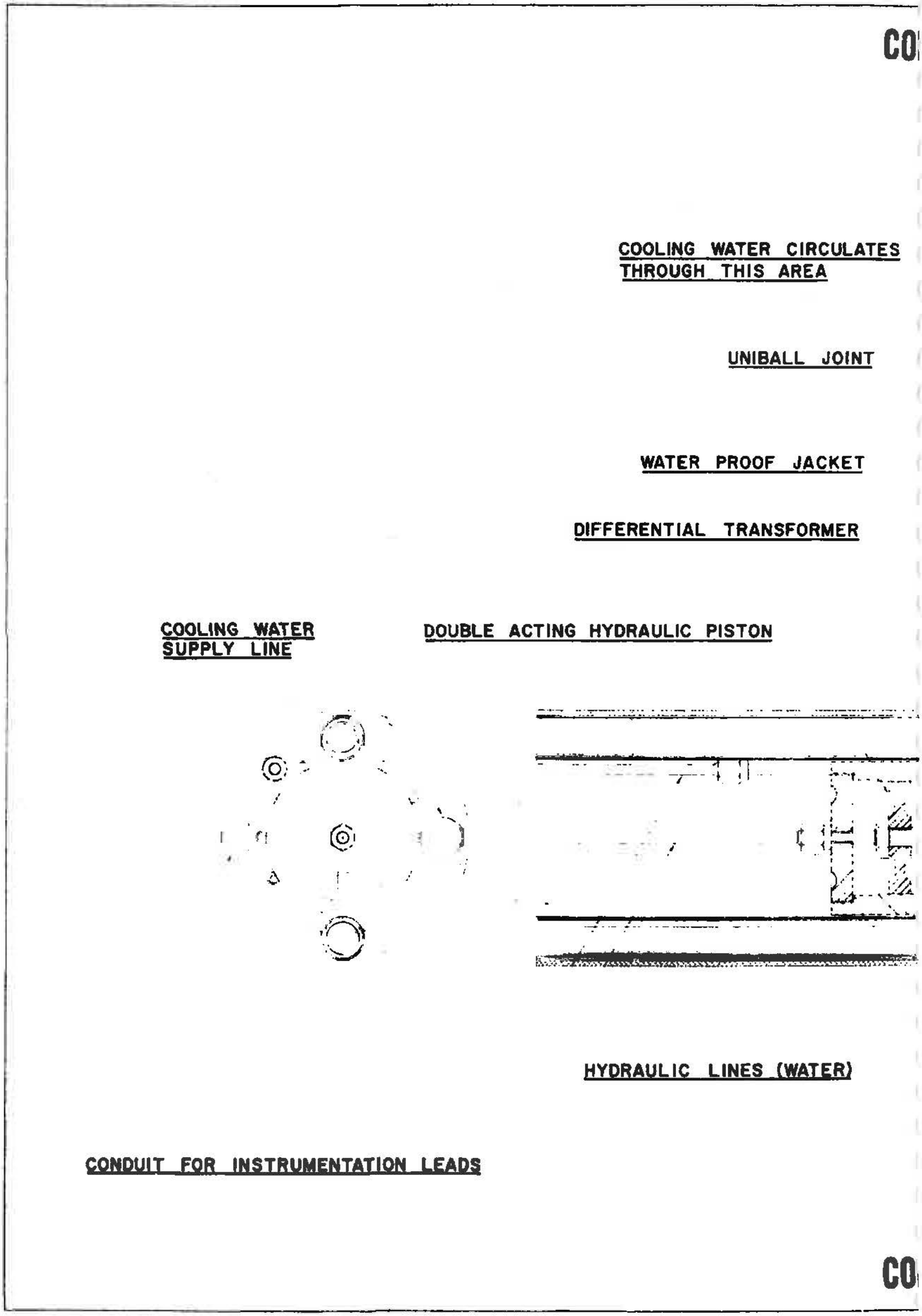
COOLING WATER CIRCULATES THROUGH THIS AREA
UNIBALL JOINT
WATER PROOF JACKET
DIFFERENTIAL TRANSFORMER
COOLING WATER SUPPLY LINE
DOUBLE ACTING HYDRAULIC PISTON
HYDRAULIC LINES (WATER)
CONDUIT FOR INSTRUMENTATION LEADS

CONFIDENTIAL

REVISIONS							
ZONE	SYM	DESCRIPTION	SERIAL NO	DFTMN	CHK	DATE	APP

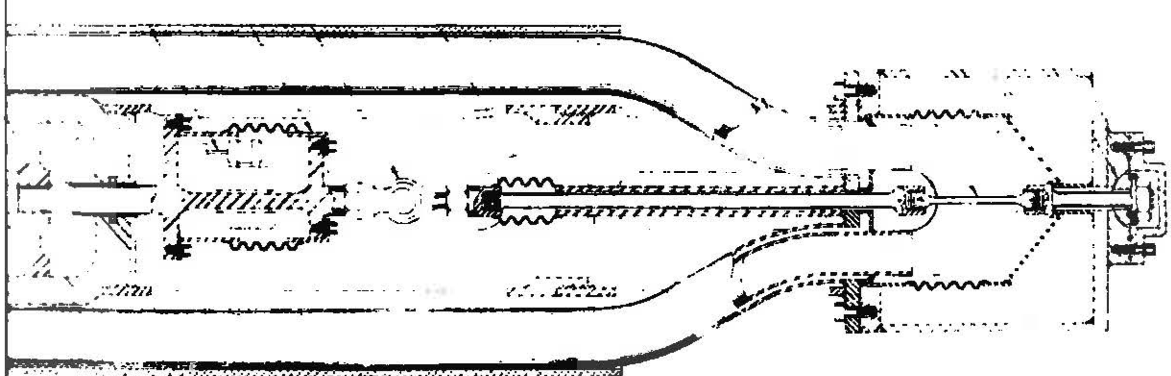

FIGURE 12

REQ'D	PART NO.	ZONE	DESCRIPTION	MATERIAL	SIZE	MATL. SPEC.	HEAT TREAT	FINISH

LIST OF MATERIAL

DATE	7-22-59
DESIGN	
CHK.	
MATL.	
STRESS	
SUPV.	
PROJ.	
APPD.	
APPD.	

APPLICATION | QTY REQ'D

LOCKHEED NUCLEAR PRODUCTS

LOCKHEED AIRCRAFT CORP. MARIETTA, GEORGIA

TENSILE TEST CRYOSTAT

TOLERANCES		SCALE	DWG. NO.
FRACTIONS ±	.XX ± .03		PD-II-0001
ANGLES ±	.XXX ± .010		

CONFIDENTIAL

The foregoing reasons have led to the testing of 1/8-inch diameter samples. A typical sample is shown in Figure 4.

The extensometer will be a differential transformer. For most purposes, a one-inch gage length to measure strains up to 0.100 inch, will be used. Where particularly ductile materials are tested, it may be necessary to reduce the gage length to cover the desired range of strains.

The outer housing will be made of 2002 aluminum. Grips and pull rods will have to be very high strength stainless alloys -- preferably one that can be heat-treated to high yield strength while still retaining ductility and notch strength at $36^{o}R$.

Figure 12 shows the load system for the cryostat. It will consist of a double-acting piston capable of putting tension and compression on a test sample. The piston will be hydraulically actuated. Leakage past the seal will enter the space between the cylinder and the cryostat. Since the latter is fully sealed against its environment, the space referred to can be open to cooling water, and the seal leakage will be no problem.

A hydraulic control system will govern the rate of loading and, if necessary, rate of unloading of specimens. It will be possible to apply loads at specified rates, rapid or slow.

Stored energy and resistivity measurements will be performed in this cryostat as indicated in Figures 13 and 14.

3.3.2 Fatigue Cryostat

The cryostat, as shown in Figure 15, is a cylindrical container mounted on the wall of a larger sealed cylinder, which contains the shaker. The small hole in the cryostat, through which the drive pin passes, is not sealed. The sealed housing contains warm helium and is pressurized to the same value as the cryostat, establishing a pressure balance that prevents serious leakage

CONFIDENTIAL

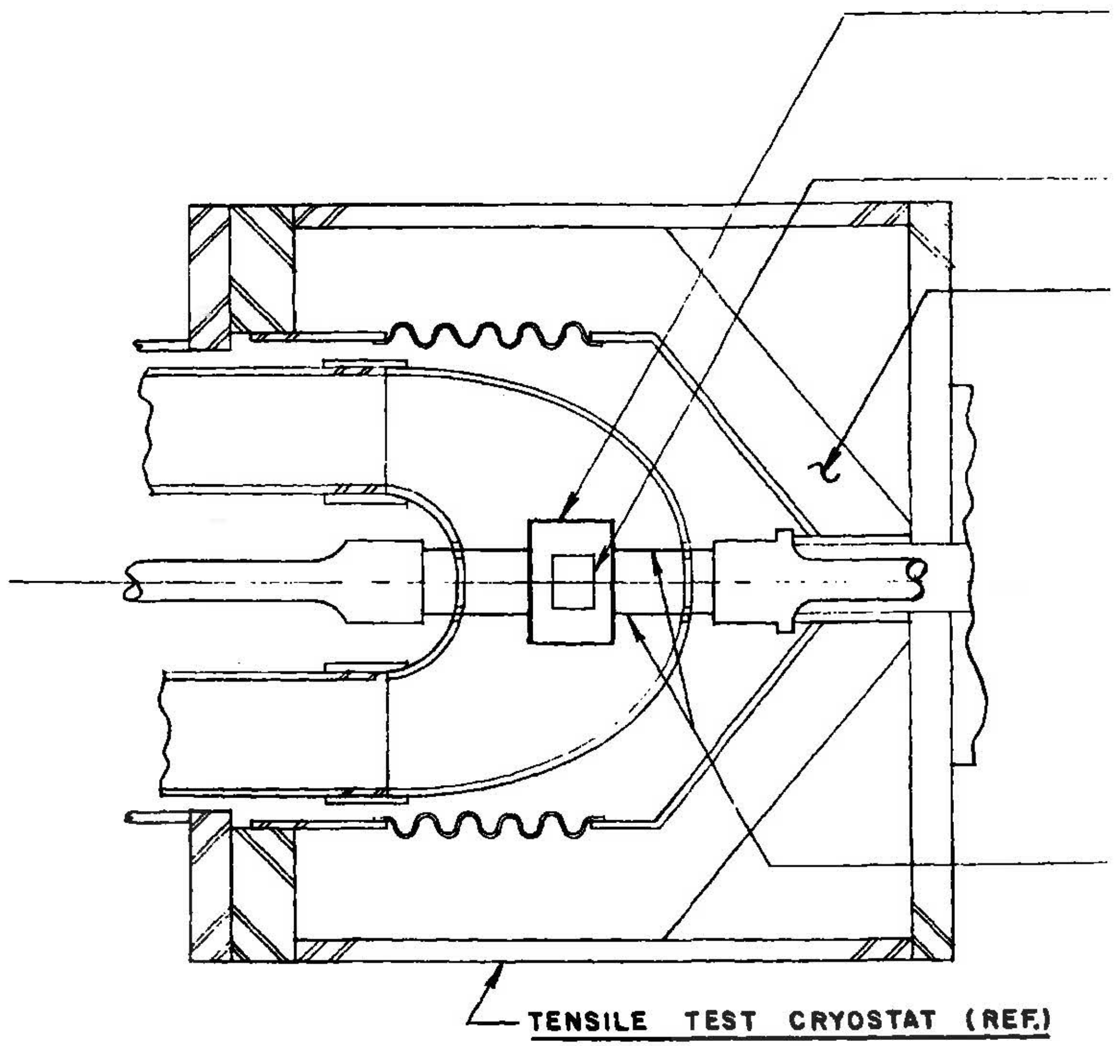

CONFIDENTIAL

ONFIDENTIAL

REVISIONS

ZONE	SYM	DESCRIPTION	SERIAL NO	DFTMN	CHK	DATE	APPD

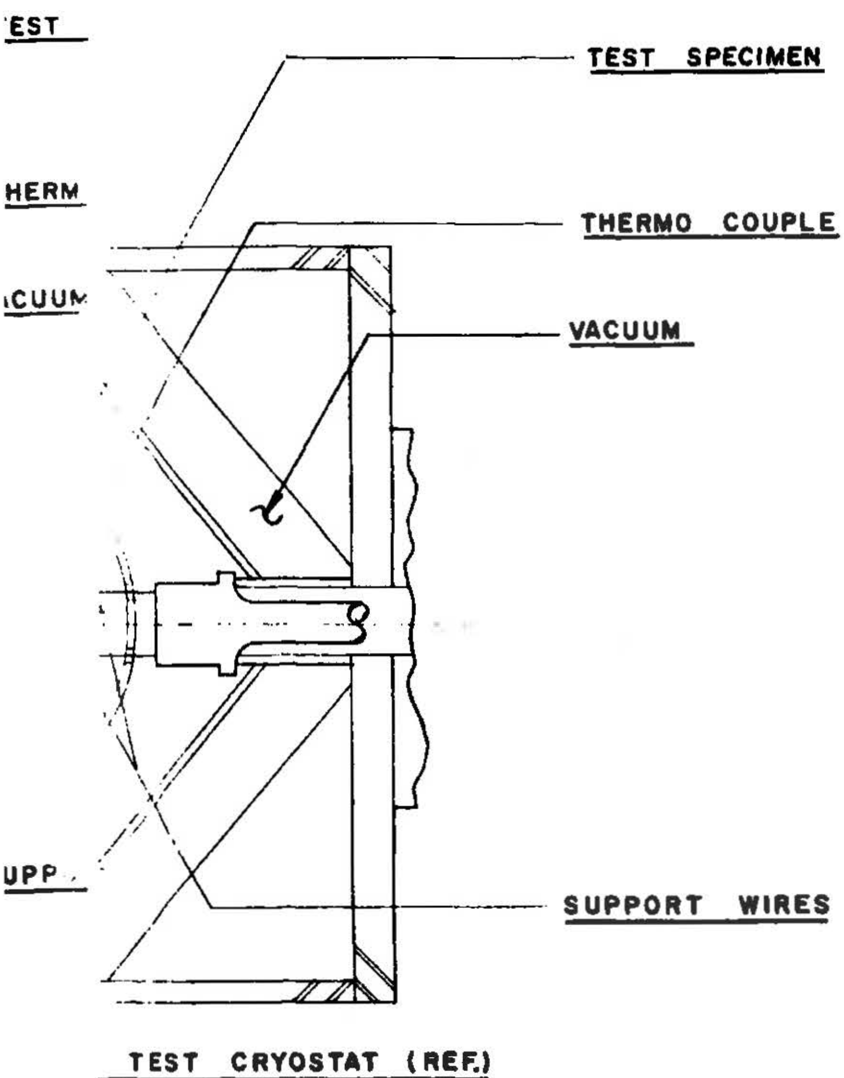

REQ'D	PART NO.	ZONE	DESCRIPTION	MATERIAL	SIZE	MATL. SPEC.	HEAT TREAT	FINISH
LIST OF MATERIAL								

DATE	7 22 59
DESIGN	
CHK	
MATL	
STRESS	
SUPV	
PROJ	
APPD	
APPD	

APPLICATION | QTY REQ'D

LOCKHEED NUCLEAR PRODUCTS

LOCKHEED AIRCRAFT CORP. MARIETTA, GEORGIA

EXPERIMENT - STORED ENERGY

TOLERANCES		SCALE	DWG. NO.
FRACTIONS ±	.XX ± .03		PD-II-0005
ANGLES ±	.XXX ± .010		

ONFIDENTIAL

FIGURE 13

CONFIDE

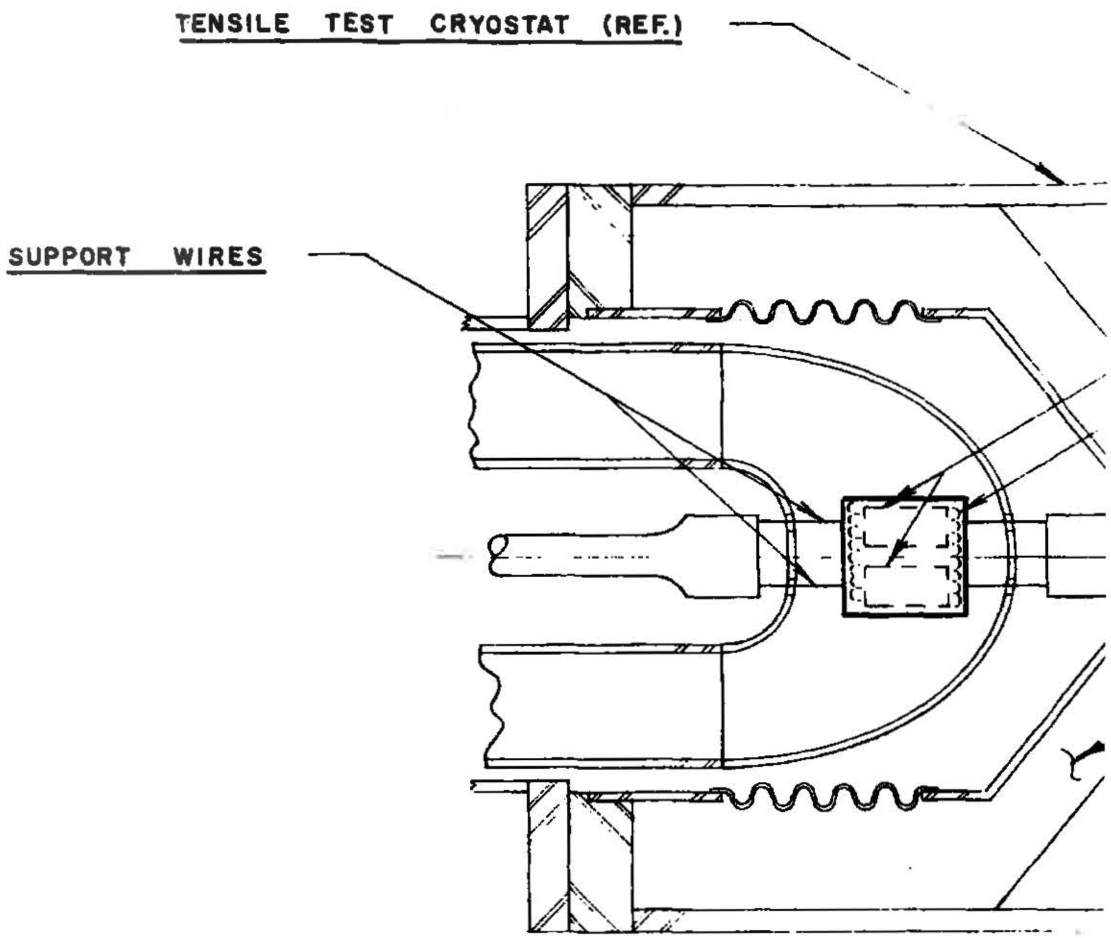

CONFID

CONFIDENTIAL

REVISIONS

ZONE	SYM	DESCRIPTION	SERIAL NO	DFTMN	CHK	DATE	APPD

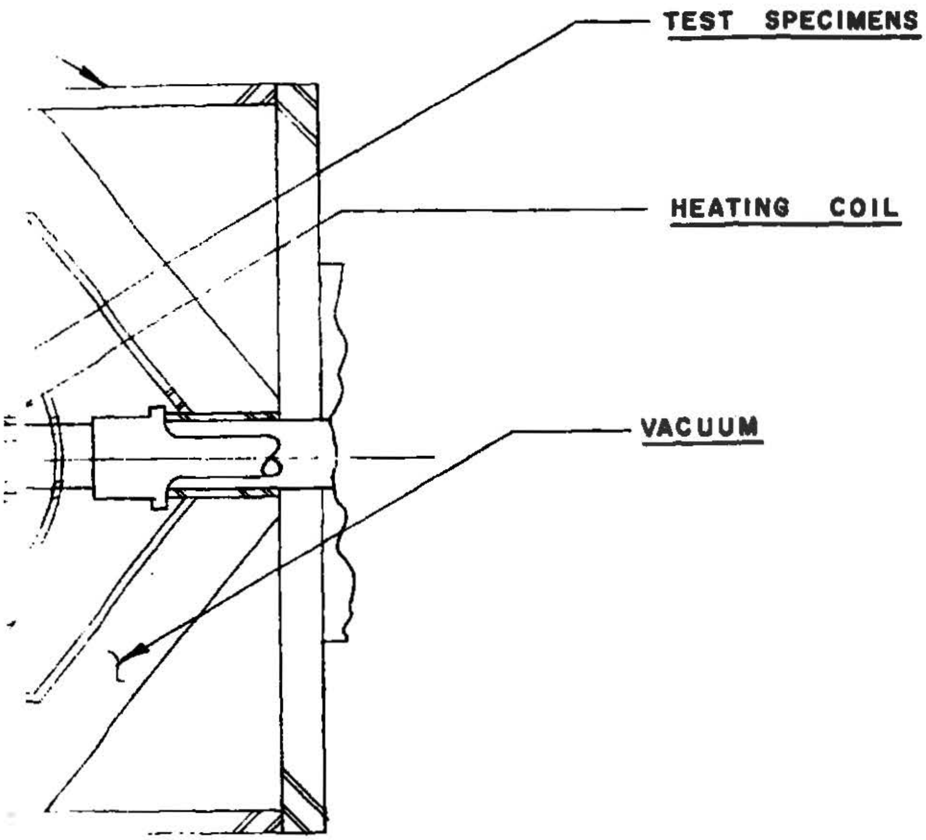

REQ'D	PART NO.	ZONE	DESCRIPTION	MATERIAL	SIZE	MATL. SPEC.	HEAT TREAT	FINISH

LIST OF MATERIAL

DATE 7-22-59

LOCKHEED NUCLEAR PRODUCTS
LOCKHEED AIRCRAFT CORP. MARIETTA, GEORGIA

EXPERIMENT- RESISTIVITY

TOLERANCES: FRACTIONS ± .XX ±.03; ANGLES ± .XXX ±.010

SCALE

DWG. NO. PD-11-0006

APPLICATION | QTY REQ'D

CONFIDENTIAL

FIGURE 14

CONFID

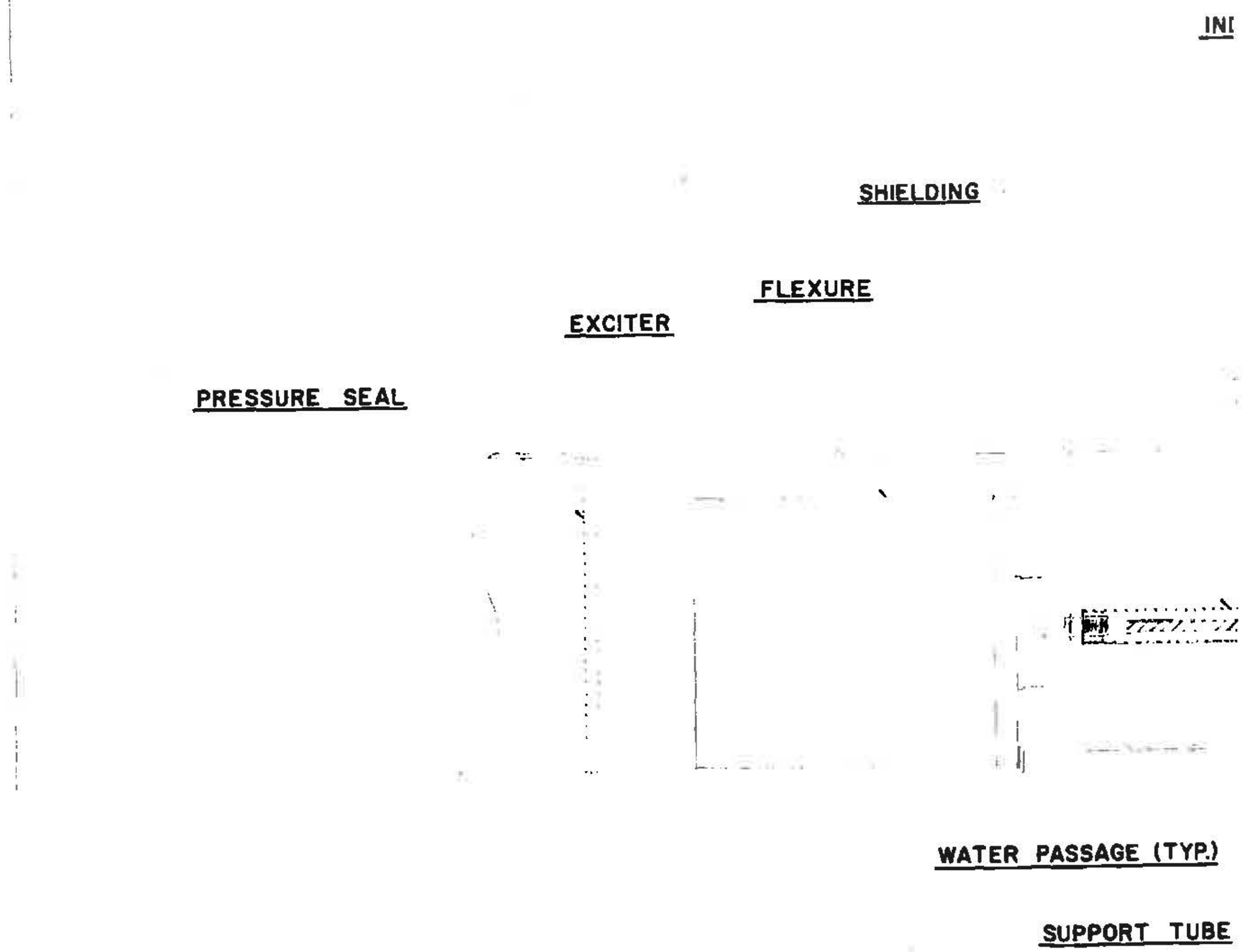

CONFI

CONFIDENTIAL

REVISIONS							
ZONE	SYM	DESCRIPTION	SERIAL NO	DFTMN	CHK	DATE	APP

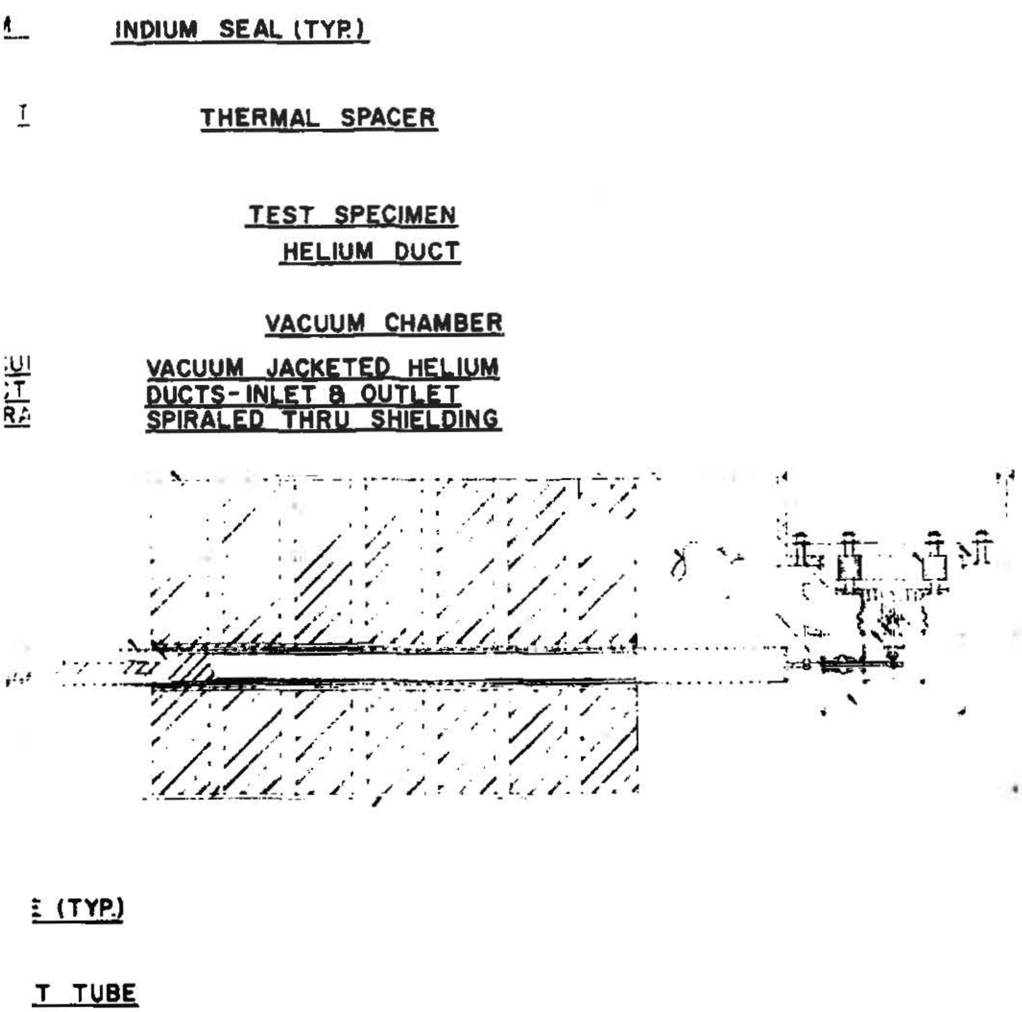

FIGURE 15

REQ'D	PART NO.	ZONE	DESCRIPTION	MATERIAL	SIZE	MATL SPEC	HEAT TREAT	FINISH
LIST OF MATERIAL								

		DATE	7-2-59	LOCKHEED NUCLEAR PRODUCTS LOCKHEED AIRCRAFT CORP. MARIETTA, GEORGIA		
		DESIGN				
		CHK.				
		MATL.		FATIGUE TEST CRYOSTAT		
		STRESS				
		SUPV.				
		PROJ.		TOLERANCES	SCALE	DWG. NO.
		APPD.		FRACTIONS ± / .XX ± .03		PD-11-0002
APPLICATION	QTY. REQ'D	APPD.		ANGLES ± / .XXX ± .010		

CONFIDENTIAL

of cold helium through the drive-pin hole. Surrounding the inner vessel of the cryostat is a vacuum jacket to inhibit conductive heat influx through the cryostat wall. The means of fastening the specimen holder block is designed to further reduce heat in-leakage at the supports by using multiple stainless steel washers in the vacuum space, a device that effectively increases the thermal conductive resistance.

The unit has been designed with easy assembly and disassembly as a primary requirement, in recognition of the large test load imposed by the program. Figure 15 shows how these operations will be accomplished.

The specimens will be tested in reversed bending at frequencies permitting the generation of about 1,000,000 cycles per hour. Because of the high rate of reversal, a resonant mechanical system will be employed, driven by an electromagnetic exciter. The specimens will be cantilevered as shown in Figure 15; the end of the specimen will be clamped through a pin connection to a push pull rod, which is in turn fastened to the moving mass of the exciter. The resonant mechanical system is comprised of the specimen, the rod, and the exciter mass; it will be tuned, if necessary, to give the desired frequency.

The exciter will be equipped with an automatic gain control so that a fixed amplitude can be maintained at the resonant frequency. This amplitude can be maintained even though mechanical damage caused by fatigue shifts the natural frequency of the specimen. In this case, the exciter can automatically (through the gain control) supply additional power to compensate the additional force required by detuning, up to the full capacity of the exciter. Provisions will be made to stop the test should failure cause a decrease or increase in the amplitude of vibration beyond allowable limits.

The entire fatigue machine will be housed in a sealed tube, which is long enough to minimize exposure of the exciter to irradiation, but at the same time short enough to prevent mechanical problems associated with a long, slender, push-pull rod.

To test at maximum frequency, the specimens must be small. The power available in an exciter small enough to fit into the beam port is limited to a maximum of about 10 pounds. At stresses below the fatigue limit, hysteresis effects can be expected to dissipate energy at a rate less than one inch-pound per cubic inch of material at the maximum stress.[55] Above the fatigue limits, this increases rapidly with increased stress, reaching in some materials an increase in damping by a factor of 1000 at stresses 25 per cent above the fatigue limit. Since tests will be at high stresses and small numbers of cycles to define the S-N curve, it is imperative that the specimens be small enough to permit testing with a 10-pound shaker.

With data and methods from WADC reports[55,56] an energy absorption of E/cycle = 0.00067 inch - pound per cycle at 100,000 psi reversed bending stress is estimated for the specimen exhibited in Figure 9. The force input per cycle will be approximately

$$\pi P_0 X_0 = 0.018 \text{ pound}$$

which gives a maximum applied force P_0 of about 0.020 pounds when the above stress is developed. It is clear that if the material in question has an endurance limit at 100,000 psi, increasing the reversed bending stress above this value will result in a much larger hysteresis. A factor of 500, for example, would tax the capacity of the shaker to its full limit.

Recognizing also that the specimen tends to become detuned as fatigue damage progresses and that at joints there may be friction losses that also contribute, the conclusion is that test specimens must be small.

In addition to power limitations, the size of the specimen will be limited by the refrigeration associated with the mass to be cooled. Aside from other heat sources, the generation of large amounts of heat by hysteresis must be considered. Considering the previous example, the deflection of the specimen at a maximum bending stress of 100,000 psi will be about 0.011 inches, the half amplitude of the vibrating specimen. Considering the mass of the pull rod, the shaker moving mass, and the specimen, a natural frequency of some 250 cps has been estimated. On this basis, about 0.0643 Btu/hr of heat would be generated and must be removed by the refrigeration, a figure that is virtually negligible. However, multiplied by a factor of 500, the heat would be appreciable, sufficient indeed to be taken into account in the refrigerator design. This is another deterrent to the use of large specimens.

Figure 9 shows a typical specimen. In the interests of achieving maximum rate of cycling, and to comply with power limits of the test shaker and the need of testing sheet of more than one material and thickness, the specimen size may have to be adjusted to achieve the maximum benefit from fatigue testing.

Materials will vary as described in Sections 3.7 and 3.8.

3.3.3 Wear Cryostat

The wear test cryostat will be used to determine the wear properties of several materials. To simplify the design and cut down specimen loading time, the test specimens will be disks, as shown in Figure 10. The grove and radial holes in the specimen are necessary to cool the specimen during test.

The fixture, as shown in Figure 16, has provisions for loading the wear surfaces and rotating one against the other. The mounting surfaces will be perfectly flat so that heat generated will be conducted to supporting structure for better cooling. Each of the pair will be pinned to its support. The load will be provided by a spring system, which will be set to a given load during specimen assembly in the fixture. The rotation will be provided by a synchronous motor, located about two feet from the test specimen. Shielding will be supplied as required.

The spring load on the specimen and the torque produced due to friction between the pair of test specimens will be measured continuously during test. This torque will also indicate excessive load on the fixture due to galling of the test specimens.

Each test specimen of the pair will be weighed before and after test to determine amount of wear. The coefficient of friction may also be calculated since the load and resulting torque will be measured.

3.3.4 Instrumentation

Measurements will be carried out by use of standard commercial instrumentation, where possible. It is expected that the principal transducers will be strain gages, thermocouples, and various types of differential transformers. Transducers will be selected on the basis of their resistance to the effects of radiation rate and dose. Calibrations involving more than one independent variable, while possible, would be extremely difficult to work with and would also involve several more channels of nuclear instrumentation.

Commercial recording systems containing all of the electronics necessary to obtain a chart record of the various parameters are available. The only external apparatus needed with these systems will be the transducers.

For each channel, the system will contain a recorder and recorder drive amplifier and a type of pre-amplifier selected to operate with the desired transducer type to be employed. The pre-amplifier will contain an oscillator unit for exciting the transducer.

These systems are available in one to eight channel packages and will be capable of performing the required measurements functions (where standard transducers are employed) without modifications. A typical system of this type is the Sanborn Type-150 recording system.

In the performance of complex measurement operations such as are involved in this program, it usually becomes necessary to develop a certain amount of specialized instrumentation ; however, as previously stated, commercial instrumentation will be utilized wherever possible.

3.4 FLUX MAPPING

To obtain precise neutron dose and spectral data in the cryostat test volume, measurements will be made by using neutron threshold detection foils. Each foil will consist of a nuclide whose activation cross-section for neutrons is known as a function of neutron energy, and each will be activated to an extent proportional to the neutron flux in a given energy interval and to the foil cross-section. Counting data will be reduced to neutron flux per unit energy interval. From these data, a complete flux and dose map of the cryostat will be obtained.

To monitor the dose during an irradiation, a wire sample will be in place in the cryostat and its activity determined after irradiation.

The gamma heating in the cryostat will be determined experimentally to check the calculated gamma heating values used for refrigerator design. Measurements similar to those listed above have been made at the Georgia Nuclear Laboratories in the Radiation Effects Reactor to determine neutron and gamma flux, dose, and spectra. So techniques have been developed, and the necessary instrumentation is available to perform such studies at Plumbrook.

CON

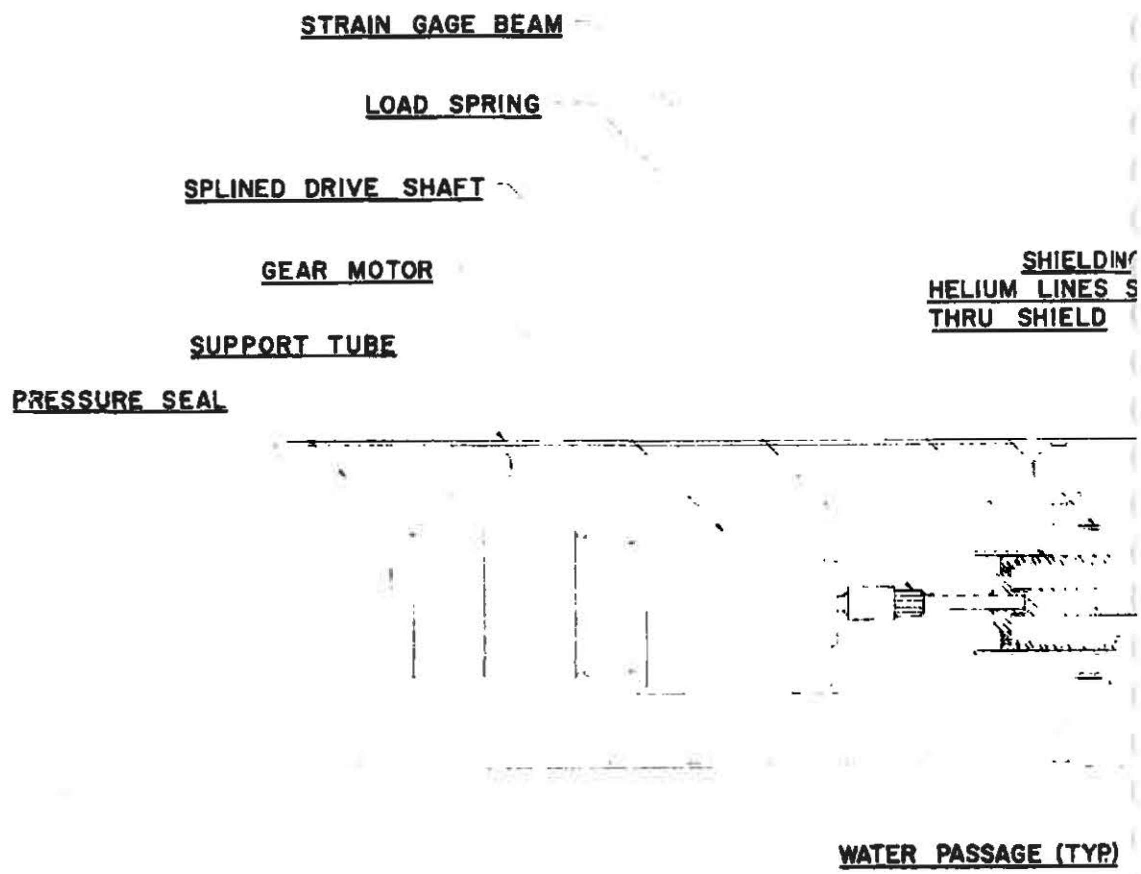
STRAIN GAGE BEAM
LOAD SPRING
SPLINED DRIVE SHAFT
GEAR MOTOR
SUPPORT TUBE
PRESSURE SEAL
SHIELDIN
HELIUM LINES S
THRU SHIELD
WATER PASSAGE (TYP.)

CON

CONFIDENTIAL

REVISIONS

ZONE	SYM	DESCRIPTION	SERIAL NO	DFTMN	CHK	DATE	APPD

FIGURE 16

REQ'D	PART NO.	ZONE	DESCRIPTION	MATERIAL	SIZE	MATL. SPEC.	HEAT TREAT	FINISH

LIST OF MATERIAL

LOCKHEED NUCLEAR PRODUCTS
LOCKHEED AIRCRAFT CORP. MARIETTA, GEORGIA

WEAR TEST CRYOSTAT

DATE / DESIGN / CHK / MATL / STRESS / SUPV. / PROJ. / APPD. / APPD

APPLICATION | QTY REQ'D

TOLERANCES: FRACTIONS ± | .XX ± .03 | ANGLES ± | .XXX ± .010

SCALE

DWG. NO. PD-11-0003

CONFIDENTIAL

3.5 REMOTE HANDLING AND SPECIMEN CHANGE

The cryostat will be removed from the beam port after irradiation and placed in a shielded, watertight cask, as shown in Figure 17. The cask will then be transported by means of the overhead crane to canal "F."

At this point, it will be placed in the canal and transported under water to the hot cell area.

The cryostat will then be lifted out of the water, removed from the watertight cask, and placed in the hot cell.

The test specimen will be removed from the cryostat by the use of the master slave manipulators. To minimize the time required for remote disassembly and reassembly of the cryostats, several special tools will be developed. Two of these may be the cryostat removal wrench assemblies shown in Figures 18 and 19. One assembly, which will be used on all three types of cryostats, uses a sun gear to operate planetary gears driving a series of wrenches that simultaneously remove all flange cap screws on the cryostat head. The other wrench assembly, needed only on tensile test cryostats, is used to disassemble and reassemble the back flange. Each assembly is actuated by a remotely operated impact wrench described in Appendix C. A new test specimen will be installed and the cryostat will be reassembled, again by using the several special tools.

After reassembly, the cryostat will be removed from the hot cell, placed in the cask, and transported via the canal to the reactor. Here it will be connected to the refrigeration system and returned to the proper beam port for irradiation.

This entire operation will take approximately one hour.

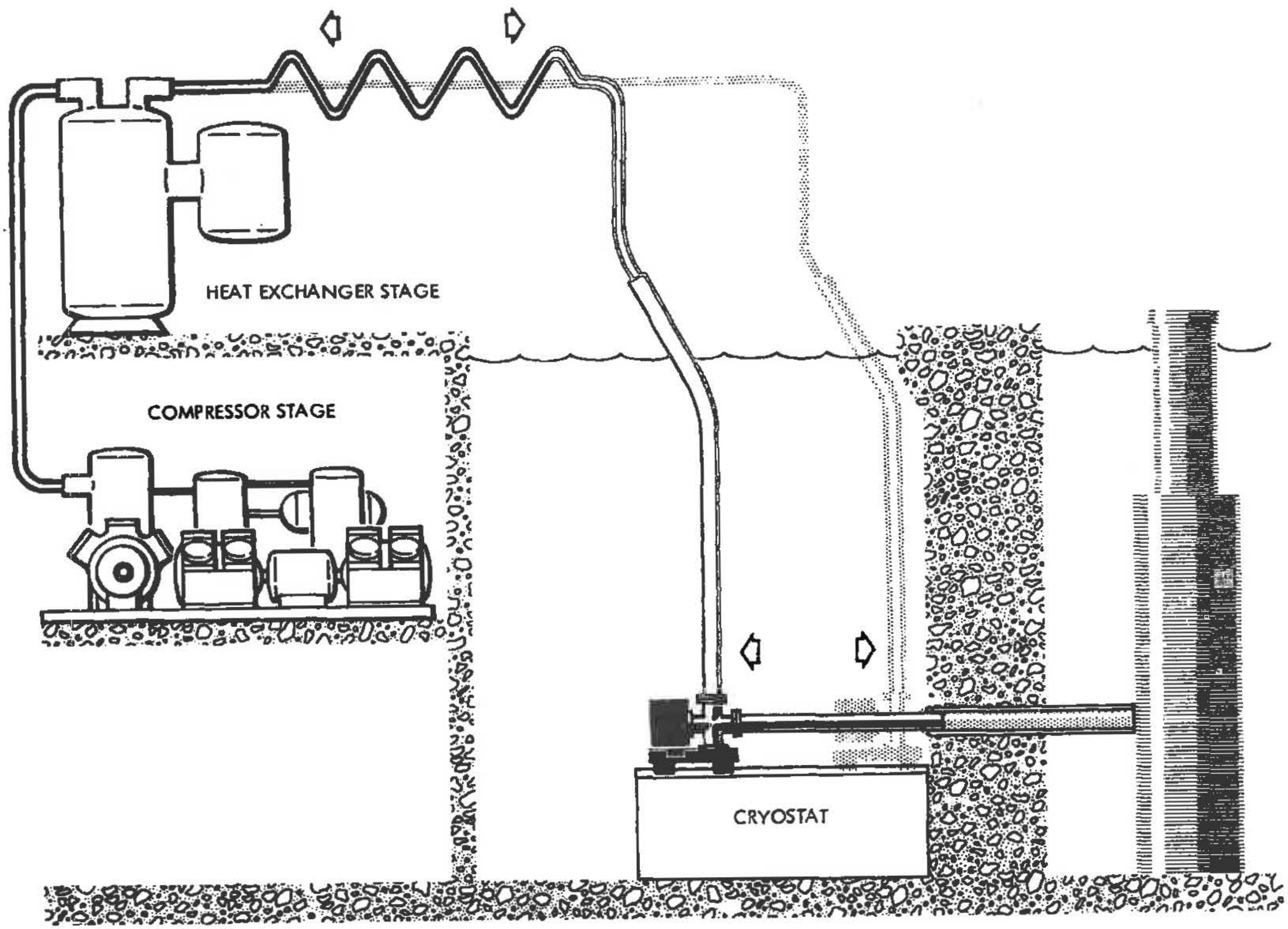

FIGURE 17 CRYOSTAT HORIZONTAL MOVEMENT SCHEMATIC

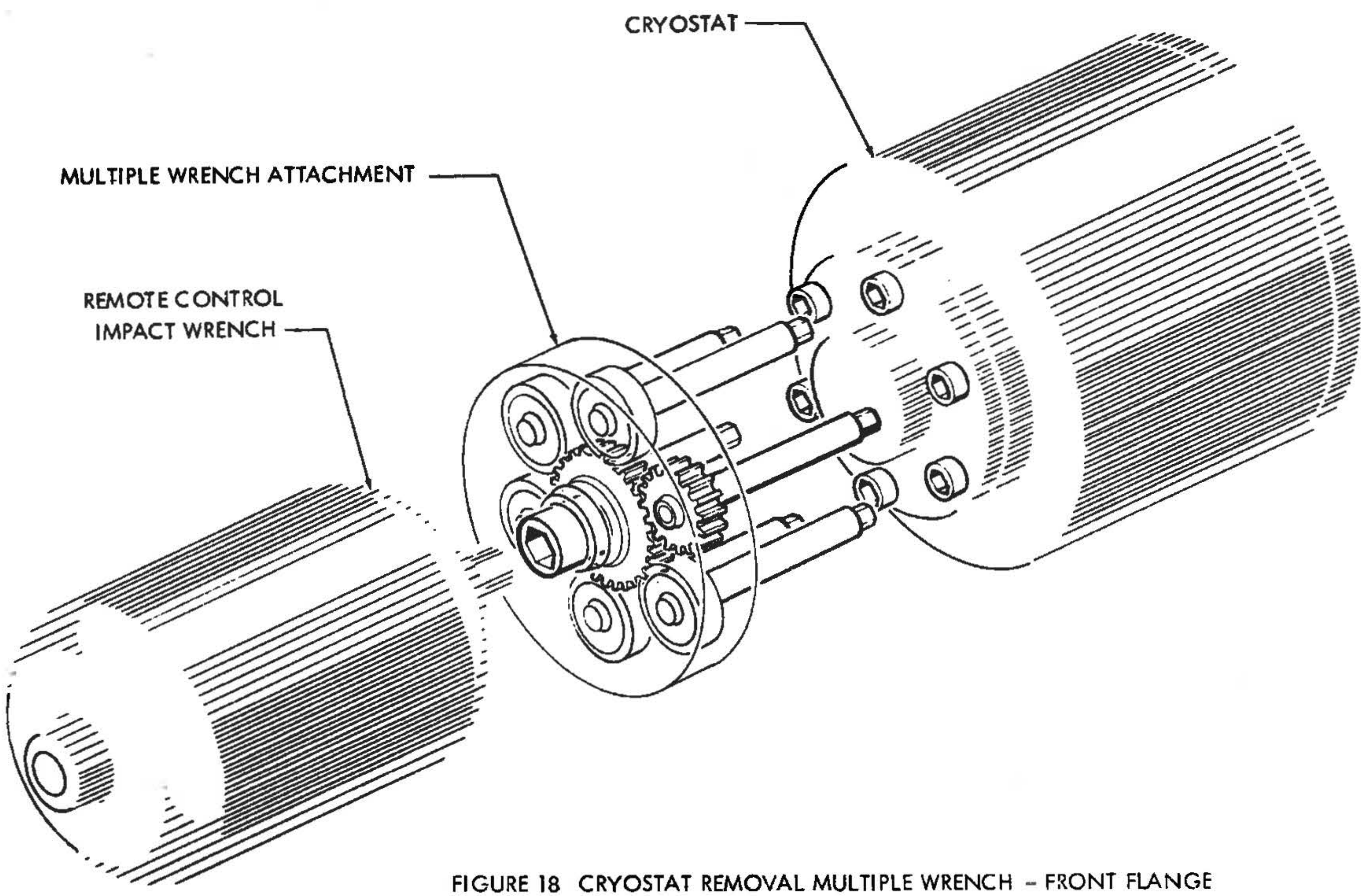

FIGURE 18 CRYOSTAT REMOVAL MULTIPLE WRENCH – FRONT FLANGE

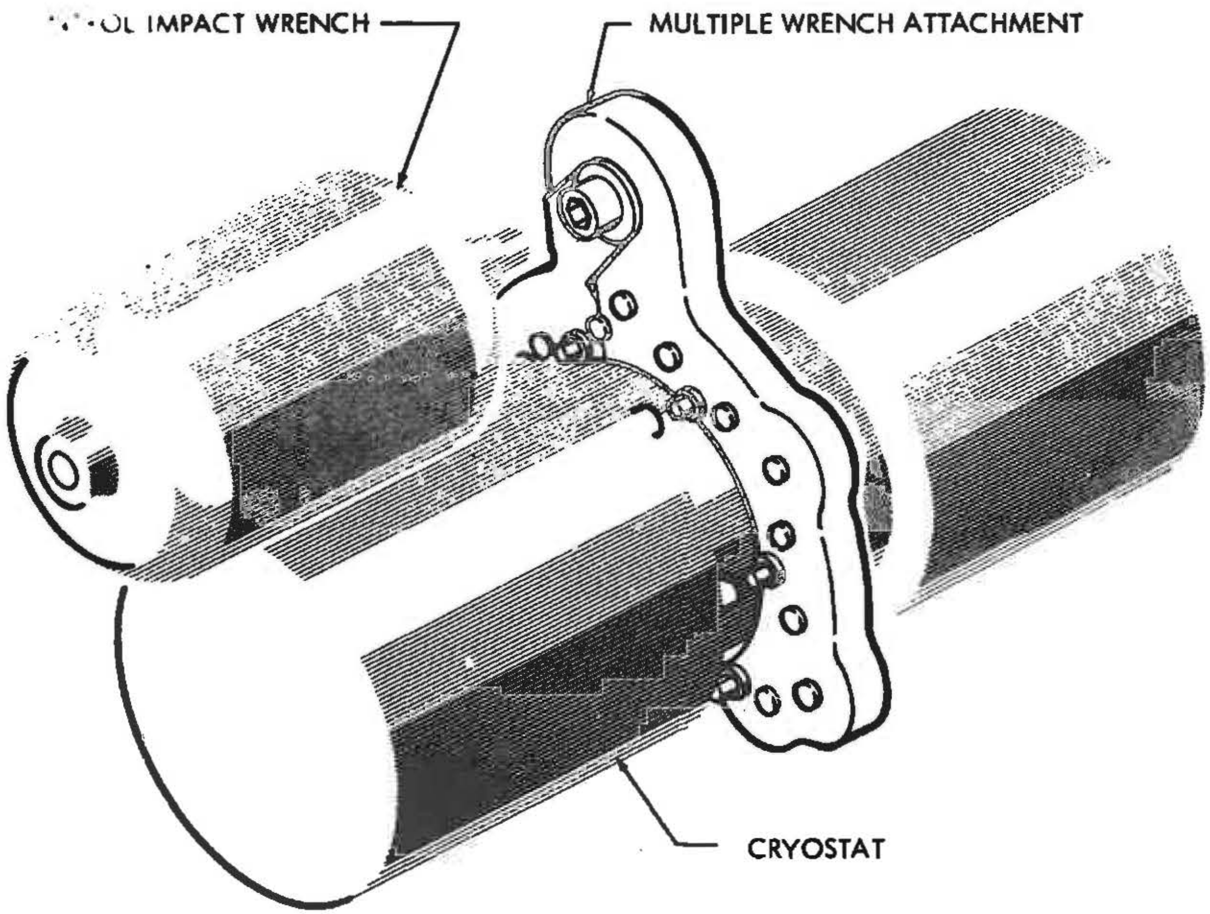

FIGURE 19 CRYOSTAT REMOVAL WRENCH ASSEMBLY – BACK FLANGE

3.6 SPECIMEN PREPARATION

Test material procurement, acceptance tests, specimen machining requirements, and specimen selection tests are explained in this section. A specimen preparation flow diagram is also included.

3.6.1 Selection of Test Materials

The specifications for procurement of both metal and plastic materials will be standard with two exceptions. One exception is that for metallic materials, the vendors will be required to furnish chemical analyses from two laboratories for each of the three separate batches of alloy requested (each analysis to be run in triplicate), plus a metallurgical analysis report on each. For a given alloy, batches will be selected to bracket the ASM normal chemical composition limits. The batches must be identified by number, and each piece of stock from such batches will be clearly identified by color coding, number stamping, or any acceptable means of ensuring the recipient of a positive means of identification.

The other exception involves plastic materials. The vendor must supply detailed information as to materials used, batch numbers, and any other pertinent information necessary to assure receipt of uniform dependable raw material.

Chemical and spectroscopic analyses will be performed on all metals to ascertain the exact composition of the alloys. Emission spectroscopy or X-ray fluorescent spectroscopy will be used as necessary to aid in determining trace quantities of elements in the alloys. These analyses will be limited to the raw metal stock as received.

Absorption spectrophotometry may be used to analyze plastic materials if normal tests indicate some deviation or doubt as to uniformity from batch to batch of these materials.

The flow diagram shown in Figure 20 indicates the controls on the materials and specimens prior to testing.

Standard metallurgical examination will be limited to randon samples selected from finished test specimens. Hardness, grain size, surface condition, and stage of heat treat or annealing will be of paramount interest for these examinations.

Where rolled metals are concerned, it will be necessary to prepare test specimens cut from the stock metal in a direction parallel to the rolling direction and similar sets of specimens cut from the stock in a direction normal to the rolling direction. This will determine whether grain flow direction has any effect on physical properties at cryogenic temperatures.

3.6.2 Specimen Preparation

A procedure will be established for machining each material for test as to speed, pressure, and depth of cut. This will ensure uniformity and reduce the possibility of residual stresses and strain hardening. Microscopic analysis will be made to verify the absence of edge cracks and notches due to machining.

All machining operations will be held to ±0.0002 inch as applicable on critical surfaces. In some cases, final polishing to a surface roughness of 10 microinches rms or less may be required. All specimens prepared for pre-, during-, or post-irradiation metallurgical examination will undoubtedly require mirror finish metallurgical polishing. These close tolerances are necessary to hold the number of variables encountered to an absolute minimum and to obviate the possibility of erroneous test data resulting from variation in roughness, waviness, necking down, or notching of test specimens.

Specimen layout diagrams will be drawn for each sheet of material with specimens dispersed through the sheets and serialized for identification.

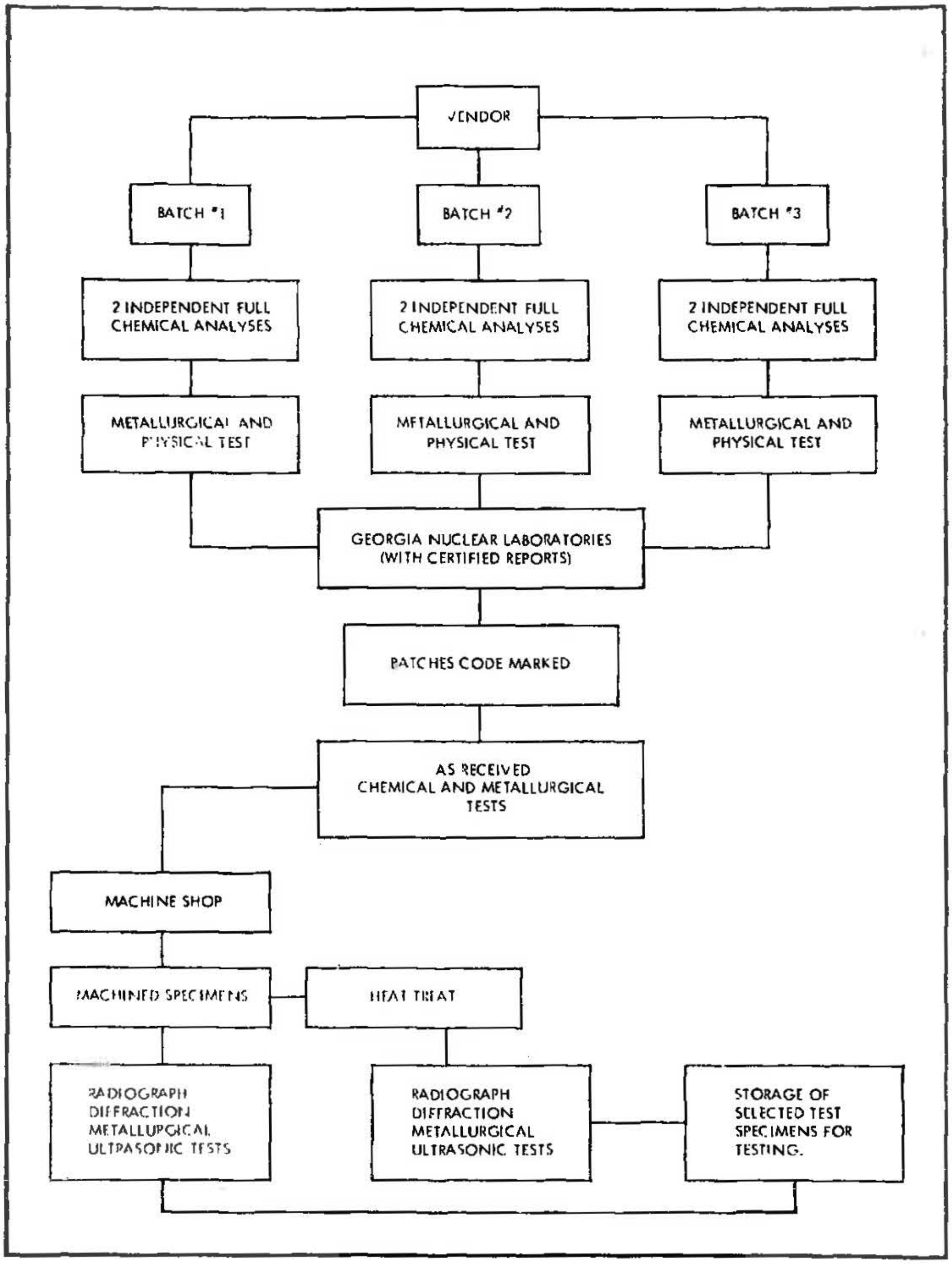

FIGURE 20 SPECIMEN PREPARATION FLOW DIAGRAM

Extreme care will be taken during heat treating of the test specimens to hold scale formation, decarburizing, hydrogen embrittlement, and other heat treating faults to an absolute minimum. Attempts will also be made to prevent specimen warping during heat-treatment, annealing, quenching, and cold working operations. The post heat-treat condition of the test specimens must be closely controlled and duplicated within reasonable limits.

Care will be exercised to ensure uniformity in cast or molded specimens. Detailed nondestructive and destructive tests will be used on plastic and ceramic materials to maintain uniformity.

Radiographic tests will be performed to determine whether subsurface defects exist and thus enable the examiner to discard unsound specimens.

Dye penetration surface inspection will be performed on all metals to detect any microscopic cracks from machining, grinding, or heat treatment. This test will be limited to finished specimens.

Debye-Scherrer X-ray diffraction pattern pictures will be taken of randomly selected representative specimens to determine crystal orientation, preferred orientation, internal stress, and annealing conditions in the pre-heat-treated and post-heat-treated or cold-worked specimens.

3.7 TEST PROGRAM - PART I

In this initial part of the test program, special test equipment and methods will be evaluated. In addition, screening tests will be conducted to select a limited number of materials for comprehensive testing. To provide a means for correlating data obtained from the miniaturized test specimens and equipment with that obtained from standard specimens and equipment and to obtain significant data for selecting materials for comprehensive testing at minimum cost, five specimens will be tested to establish the value for each test. The reason for choosing this number of specimens is discussed in Appendix B.

3.7.1 Test Equipment and Specimen Calibration

Data for evaluating any effect of specimen or test equipment miniaturization will be obtained by testing specimens machined from typical alloys of aluminum, of stainless steel, and of titanium. These tests will be conducted on standard size specimens in standard test machines and on miniature specimens in the special test equipment in the cryostat. In addition to tests at room temperature, tests will be conducted at liquid nitrogen temperature (139°R) to determine any changes in correlation that may result. The choice of 139°R, rather than 36°R, is primarily for economy. The cost of a liquid-nitrogen-cooled cryostat for standard test machines is negligible as compared to that of a helium cryostat. This apparent temperature discrepancy should not, however, affect the calibration results. Kropschot, at the National Bureau of Standards Cryogenic Laboratory, reported, in NBS Report 2708, data on tensile and impact properties of alloys of aluminum and stainless steel between 36°R and 139°R. These data show that the rate of change in property values is very low when compared to that between 139°R and room temperature. Consequently, tests at room temperature and at 139°R should reveal any lack of correlation between the two sizes of specimens and test equipment that is attributable to temperature differences.

If acceptable correlation is not obtained during these tests, miniature specimens will be tested at the two temperatures in standard test machines. Correlation in this test will indicate a need for modification of the special test equipment or its mode of operation. Lack of correlation will, of course, mean that specimen miniaturization has affected results, thus indicating a need for either specimen redesign or modification of some factors in the test procedure.

3.7.2 Screening Tests

Screening tests will be conducted under the following conditions:

At room temperature
At 36°R with no irradiation
At 36°R after irradiation to an integrated dose of 10^{17} n/cm^2 at 36°R

The choice of this irradiation level is based on information presented in Figure 1 of NASA RFQ HS-225. All screening test specimens (alloys) will be machined from commercial heat-treated materials. Evaluation of the effects of minor variations of chemical composition and heat treatment within standard specification limits will be made only during Part II of the test program.

The materials to be tested for each component application are presented in Table X. The tests to be conducted for each application and the number of specimens to be tested for each determination are given in Table II.

On the basis of the results obtained, one alloy each for the tank, for the pressure shell, and for the pump will be selected for comprehensive testing in Part II. For bearing applications, ball material and lubricant will be combined with metal, plastic, and ceramic race materials to select those combinations exhibiting the most desirable characteristics, as revealed by the results of these tests, for Part II testing. For seals, the metal, the carbon, and the ceramic material exhibiting the best wear properties and the sheet material with the best combination of properties will be tested in Part II.

Each material selected for testing in Part II of the proposed program will be chosen on the basis of the most favorable combination of mechanical properties and favorable strength-to-weight ratio, as determined by conferences with nuclear missile design engineers at NASA and Lockheed Missiles and Space Division.

3.8 TEST PROGRAM - PART II

This phase of the program will provide reliable engineering design data for those materials selected in Part I for each component application. The effect of many variables will be economically evaluated through the use of the statistical planning of the experiments presented in Appendix B. This planning dictated the number of samples chosen for analysis; the samples selected are shown in Table III.

The effects of variables to be evaluated have been chosen to provide the nuclear missile design engineer with data representative of the materials that will be used in production. Since construction materials will be produced at different times and under slightly varying conditions, these tests will define and provide justification for the degree of control required, for example, on such variables as chemical composition and heat treatment or cold work metal alloys for the specific applications.

3.8.1 Temperature and Irradiation Level Selection

Electrical resistivity and stored energy measurements will be made after a fixed irradiation dose to establish annealing curves for each alloy over the temperature range from 36°R to room temperature. These annealing curves will indicate the temperatures at which major annealing of radiation-induced lattice defects occurs. The temperatures at which mechanical property measurements are to be made will be chosen for each material to coincide with the temperatures at which major annealing of defects in the material of interest has been indicated by the resistivity and stored energy measurements. Although two temperatures in addition to

36°R are indicated in the schedule of tests in Table III, this number will be revised, if required, when the annealing curves have been established for the individual materials.

All specimens will be irradiated at 36°R to the integrated dose specified. Tests will then be conducted at the specified temperature. Initial irradiation doses for materials to be used in all components except the pressure shell and reflector will be $10^{17} n/cm^2$. For the pressure shell materials, the dose will be $5 \times 10^{17} n/cm^2$, and for the reflector it will be $10^{18} n/cm^2$. Since these dose levels are the maximum specified in NASA RFQ HS-235, if significant effects of radiation do not result, irradiations at other levels will not be warranted. If significant effects are observed, materials for components other than the pressure shell and reflector will be irradiated to an integrated dose of $5 \times 10^{15} n/cm^2$ to bracket the range specified for these components. Tests at intermediate irradiation level will be made only if the results obtained at the high and low ends of the dose range show sufficient sensitivity to irradiation dose level to warrant such tests. Should results of stressed and unstressed irradiations to the highest integrated doses specified for each material show negligible effect of the stressed condition on properties, the remainder of the irradiations on the stressed condition of that material for the property evaluated will be omitted.

The number of specimens to be used for the determination of each property and the conditions (subject to the alternatives described in the previous paragraphs of this section) for each determination are tabulated in Table III.

The effect of such variables as chemical composition and heat treatment, or cold work as discussed on pages 18 and 19, will be determined on 3 specimens for each identical combination for each of the nine combinations of these variables, making a total of 27 specimens for each value determination. The effect of these variables will be determined under the following conditions:

At room temperature
At $36^{o}R$ without irradiation
At $36^{o}R$ after irradiation to the maximum dose
for the particular application at $36^{o}R$

The standard deviation and limit of error of the mean will be determined. For a given test on a particular material at other specified conditions of temperature and irradiation, only 6 specimens will be tested. If the standard deviation and limit of error of the mean for these 6 values are in agreement with those of the 27 specimens tested under the original 3 conditions, no additional specimens will be tested. If not, more specimens will be tested, as required, to establish valid data. A diagram and discussion of this approach are presented in Appendix B.

4. DESIGN CRITERIA

This section shows the heat calculations necessary to determine refrigerator size, describes the refrigerator design, and shows the nuclear analyses of gamma heat, beam hole selection, reactor safety, and gamma activation.

4.1 HEAT EXTRACTION AND SPECIMEN SIZE

Gamma rays generate heat uniformly within the bulk volume of any material they penetrate. The heat thus generated must be dissipated at the surface of the material. For the case at hand, not only the specimen, but also that portion of the testing apparatus attached directly thereto must be cooled. To examine the surface heat flux generated in three specimens under identical conditions of gamma heating, a 1-inch length of a long bar is considered, which is of sufficient length to eliminate end effects. The gamma heating rate is 590 watts/lb (1.3 watts/gm) as calculated in Section 4.3.1, and the density is 0.3 $lb/in.^3$. For a 1/4-inch diameter rod, the surface heat flux is 5400 $Btu/hr\text{-}ft^2$; and for a 1/8-inch diameter rod, the flux is 2700 $Btu/hr\text{-}ft^2$. For a 0.040-inch by 0.306-inch flat bar, the surface flux is 1535 $Btu/hr\text{-}ft^2$. The cross sectional area, and hence the tensile strength of the flat bar, is the same as the 1/8-inch diameter round rod.

The rate of heat removal from the specimen by a gas is described by the equation:

$Q =$ $hA\Delta T$, where
$Q =$ heat removed, Btu/hr
$h =$ film coefficient Btu/hr-°F-ft^2
$\Delta T =$ difference in temperature between surface and gas, degrees Fahrenheit
$A =$ surface area ft^2

This may be rewritten as $\frac{Q}{A} = h\Delta T$ where $\frac{Q}{A}$ is the surface heat flux.

Determining the maximum value of $\underline{h}$ indicates the minimum value of ΔT for a given $\frac{Q}{A}$, which is a measure of the minimum temperature to which the specimen surface can be cooled with a given refrigerant gas temperature.

To estimate values of $\underline{h}$, it is assumed that the velocity of the gas is subsonic and that the dimensionless equation[57]

$$\frac{h_m D_o}{K_f} = B \left(\frac{D_o G}{\mu_f}\right)^n$$

represents the heat transfer to a gas from a single cylinder with transverse flow.

h_m = film coefficient Btu/ft^2 - °F - hr, mean value
D_o = diameter, feet of the cylinder
K_f = thermal conductivity of gas Btu/hr - ft - °F
G = mass flow - lbs/hr - ft^2
μ_f = absolute viscosity - lbs/hr-ft
C_p = specific heat Btu/lb - °F

Transverse flow has been assumed even though axial flow through a duct could yield higher values of $\underline{h}$. The positioning of the extensometer would interfere with axial ducting; therefore it seems inconvenient at the present.

Exceeding sonic velocity would result in a shock wave generation that yields lower integrated values of h and increases pressure drop.

The concept of using a boiling liquid to cool the specimen has been considered and rejected. While nucleate boiling coefficients would yield higher values of h, the only material that could exist as a liquid at the minimum test temperature is hydrogen, which has been forbidden from use.

For 36°R helium, the minimum specified specimen temperature,

$$K_f = 0.01156$$
$$\mu_f = 0.00824$$
$$C_p = 1.25$$
$$D_o = 0.125/12 = 0.0104$$
$$G = \text{mass flow per unit duct area}$$

A duct width of 0.189 inch and an effective height of 1.0 inch is assumed, giving duct area of 0.189 square inches. From refrigeration considerations, a 325-lb/hr helium flow is assumed.

Therefore $$G = \frac{325 \times 144}{0.189} = 246{,}000 \text{ lbs/ft}^2 - \text{hr}$$

$$h_m = \left(\frac{k_f}{D_o}\right)\left[B\left(\frac{D_o G}{\mu_f}\right)^n\right] = 710 \ *$$

Using this value of h in the equation quoted on the previous page and solving for ΔT results in the following:

$$\Delta T = \frac{Q}{h_m} = \frac{2700}{710} = 3.8\ F^\circ\ (R^\circ)\ 1/8\text{-inch diameter specimen.}$$

This film temperature difference added to a mean gas temperature of 29°R gives a surface temperature of 32.8°R.

In addition to the film temperature gradient, there will be, within the specimen, a gradient caused by the radial flow of heat. The center of the specimen will be warmer than the surface by the relationship

* The value for h_m is considered an approximation, since the prefix B and the n values are not precisely defined for this region.

shown below, which depends on the conductivity of the specimen material.

In an elemental ring of material of radius R and thickness dR and unit length, where Wi is the volume gamma heating in Btu/hr $-ft^3$, the steady state heat flowing through the elemental ring from the inside will be πR^2 Wi. The heat flow through the element is $K\, 2\pi R \frac{dT}{dR}$. Since these must be equal, $\pi R^2\, Wi = 2 K \pi R \frac{dT}{dR}$

$$\frac{dT}{dR} = \frac{Wi\, R}{2K}$$

$$T = \frac{Wi}{4K} R^2 \Big]_{R=0}^{R=R_o} = T_{\text{center line}} - T_{\text{surface}} = \frac{Wi\, R_o^{\,2}}{4K}$$

At 36°R, for a 1/8-inch diameter specimen the thermal conductivity, K, of a typically low conductivity material, such as Type 304 stainless steel, is equal to 1.16 Btu/hr - ft - °F. For this material:

$$T_{\text{center line}} - T_{\text{surface}} = \frac{1{,}045{,}000}{4 \times 1.16} \times \left(\frac{1}{16}\right)^2 \times \frac{1}{144} = 6.12\ F° \ (R°)$$

A 6.12R° increase in center line temperature added to the 32.8° R surface temperature gives a 38.9°R maximum specimen temperature.

However, for a high conductivity material, such as pure aluminum, at 36°R, K is equal to 1150 Btu/hr - ft -°F.

In addition, the gamma heating for aluminum is less by the ratio $\frac{0.9}{1.3} \times 1{,}045{,}000 = 724{,}000$ Btu/ft^3 – hr.

The surface-to-center line temperature rise for a 1/8-inch diameter aluminum specimen would therefore be

$$T_{\text{center line}} - T_{\text{surface}} = \frac{724{,}000}{4 \times 1150} \times \frac{(1)}{(16)}^2 \times \frac{1}{144} = 0.00427 F° \ (R°)$$

For a material of this type the internal temperature gradient is not significant.

The film ΔT will also be lower because of the lower gamma heating rate for aluminum.

$$\text{Film } \Delta T = 3.8R^\circ \times \frac{0.9}{1.3} = 2.6R^\circ$$

This ΔT added to a mean gas temperature of 29°R gives a surface temperature of 31.6°R.

The foregoing heat transfer considerations indicate that a 1/8-inch diameter specimen over the range of conductivities and gamma heating rates considered can be adequately cooled. Specimens 1/4 inch in diameter, with a surface heat flux of 5400 Btu/hr - ft^2, result in a film $\Delta T = \frac{5400}{710} = 7.6R^\circ$. The surface temperature is 29 + 7.6 = 36.6°R, which is above the specified specimen temperature. However, 1/8 inch was selected as the maximum diameter for round specimens because of the additional structure that would be necessary inside the cryostat to perform tensile tests and similar tests on larger samples. The heat load of a cryostat designed to perform tests on 1/4-inch specimens would be approximately double that value given below, or about 1128 watts, thus considerably increasing the refrigerator size. It is interesting to note that the film ΔT for the flat bar specimen is $\frac{1535}{710} = 2.2R^\circ$ and for any other configuration not exceeding the cross sectional area of the 1/8 inch round specimen the film ΔT will be less than 3.8R°.

The heating of the fatigue specimen due to internal damping has been calculated for the maximum anticipated frequency.

The maximum anticipated heating value is not significant when compared with the gamma heating so will not contribute measurably to the specimen temperature rise.

4.1.1 Cryostat Heat Load

In addition to the gamma heat generated in the specimen, gamma heat must be removed from all internal parts of the test chamber not cooled by water.

The total weight of these parts for a typical cryostat is estimated to be 0.75 pounds, or 340 grams.

$$340 \text{ grams} \times 1.3 \text{ watts/gram} = 433 \text{ watts gamma heating}$$

In addition to the internal gamma heating, there will be a heat leak into the low temperature chamber from the outside environment. Conduction will contribute largely to the heat leak and is estimated at 100 watts at 36°R.

Specimen gamma heat of 11 watts plus cryostat gamma heat of 433 watts plus the heat leak of 100 watts = 544 watts total cryostat heat load.

4.1.2 Helium Line Heat Load

It is estimated that the helium lines will be 35 feet long each and that there will be therefore a total of 70 feet of approximately 36°R helium line for each cryostat. Part of this system will be made up of flexible line and part will be rigid. If it is assumed that 20-foot rigid sections and 15 feet of flexible line will be used, there will be a total of 40 feet rigid and 30 feet of flexible. These lines will be 1-1/8 inches inside diameter, and representative heat leaks for high vacuum insulated lines of this type are as follows:

1-1/8 inch rigid	=	1.2	Btu/ft-hr
1-1/8 inch flexible	=	12	Btu/ft-hr
1-1/8 inch valve	=	20	Btu/valve-hr
1-1/8 inch joint	=	20	Btu/joint-hr

For one test cryostat cold piping system there will be the following heat leaks:

40 feet rigid	=	40 x 1.2	=	48
30 feet flexible	=	30 x 12	=	360
4 valves	=	4 x 20	=	80
4 joints	=	4 x 20	=	80
		Total	=	568 Btu/hr

$$\frac{568}{3.415} = \quad 167 \text{ watts line heat leak}$$

The total load associated with one in-reactor cryostat and lines is therefore 544 watts plus 167 watts = 711 watts.

The heat load associated with one out of reactor cryostat and connecting lines is 167 watts plus 100 watts = 267.

Thus, while operating 2 cryostats, one in reactor and one out, the total heat load is 978 watts.

4.2 REFRIGERATION

Refrigeration of the cryostats for testing will be accomplished at the Plumbrook site; but the facilities at GNL will permit effective non-irradiated tests for screening and reference purposes by the addition of a helium liquefier, which will be procured by Lockheed from Arthur D. Little, Inc. This unit is capable of producing 90 to 100 watts of refrigeration at 36°R. With this unit, it may be necessary to cool the outer jacket of the test cryostats with liquid nitrogen to reduce the heat leak; but there will be no need for long helium transfer lines with attendant heat loads, inasmuch as the tests will be conducted out of pile.

The liquefier to be used at GNL is one of 150 such units in use. It is provided with two 15-hp compressor sections; it requires 30 kw of 440-volt power and 10 gpm of cooling water.

The refrigeration system to be used at the Plumbrook site will have a capacity of 1000 watts at 36°R, which, as shown in Section 4.1, will be necessary. It will employ helium gas as the medium, which offers several attractive features: it is inert and it is unaffected by irradiation. This gas has considerable precedent in reactor cooling applications. For instance, units at ORNL and Brookhaven National Laboratory have used helium with complete success. At ORNL, such a refrigerator has been operated over 10,000 hours at 36°R without breakdown of the cryogenic equipment.

The plan is to employ three stages of compression instead of the customary two in order to prolong the life of the compressors through reducing the compression ratio per stage. The 1000-watt unit, a schematic-flow diagram of which is shown in Figure 21, employs two expansion engines of proved design and high reliability to remove heat from the gas. These engines are of the reciprocating, unlubricated, cryogenic expansion type, 300 of which have been manufactured by Arthur D. Little, Inc.

The refrigeration system to be used at Plumbrook consists of a closed-loop, dense-gas, helium-expansion cycle. It compresses 325 pounds of helium per hour in three stages, each stage followed by an aftercooler to remove the heat of compression. After the oil mist is removed, the helium flows through one side of a countercurrent regenerative heat exchanger, where it is cooled to approximately 41.5°R by giving up heat to the effluent helium stream. The helium at 300 psia and 41.5°R is expanded with approximately 75% adiabatic efficiency in two expansion engines to 50 psia and 27.6°R. The cold helium flows to the test cryostat and cools the specimen. It is in turn warmed to about 36°R. The helium returns through a dual charcoal filter bed, which removes any particulate matter that may have originated in the test chamber, then flows back through the counterflow heat exchanger, where it cools the incoming high pressure helium. After leaving the heat exchanger, it returns to the compressor section and repeats the cycle.

The refrigerator will be provided with a manifold, which will permit the connection of two test cryostats simultaneously. With 325 pounds per hour circulating, the allowable warmup of the helium at the load is

$$\frac{1000 \times 3.415 \text{ Btu/hr}}{325 \times 1.25 \quad \text{Btu/°R}} \qquad 8.4 \text{ R°}$$

The compressor section will require approximately 8 feet by 10 feet of floor space, and it will be 3 feet high. The cold box section will require approximately 5 feet by 7 feet of floor space and will be 8 feet high. The cold box will be located at the edge of the water shield, and the compressor section can be situated at any convenient location at the floor level. The compressor section will require 150 kw of 440-volt power, and 2 kw of 110-volt power will be required for controls, vacuum pumps, and other auxiliary equipment. The compressor section will require 25 gallons per minute of cooling water for aftercoolers. In addition,2 gallons per minute will be required at the cold box section.

All instruments and controls will be located at the cold box section with appropriate duplicate trouble annunciators located in the reactor control room. The refrigerator is provided with all temperature gages, pressure gages, tachometers, vacuum gages necessary for routine operation, and special systems to indicate and locate troubles that could affect the tést program.

Operation of the refrigerator is extremely simple. The compressor as well as the expansion engines are started by push button. The desired operating temperature is dialed into a thermostatic valve and the only manual adjustment will be engine speed adjustment. This adjustment is required only at the higher temperature levels.

Routine preventive maintenance of the refrigerator is required to assure trouble-free operation. This will involve daily checks on compressor oil levels and periodic blow down of filters and oil separators. The equipment should provide a minimum of 2000 hours operation before requiring any major overhaul.

The refrigerator has been planned and priced on the 1000-watt basis. A change in capacity of plus or minus 25% would result in a price change of perhaps plus or minus 15% since the cost of design, installation, testing, and operator instructions is not affected by size.

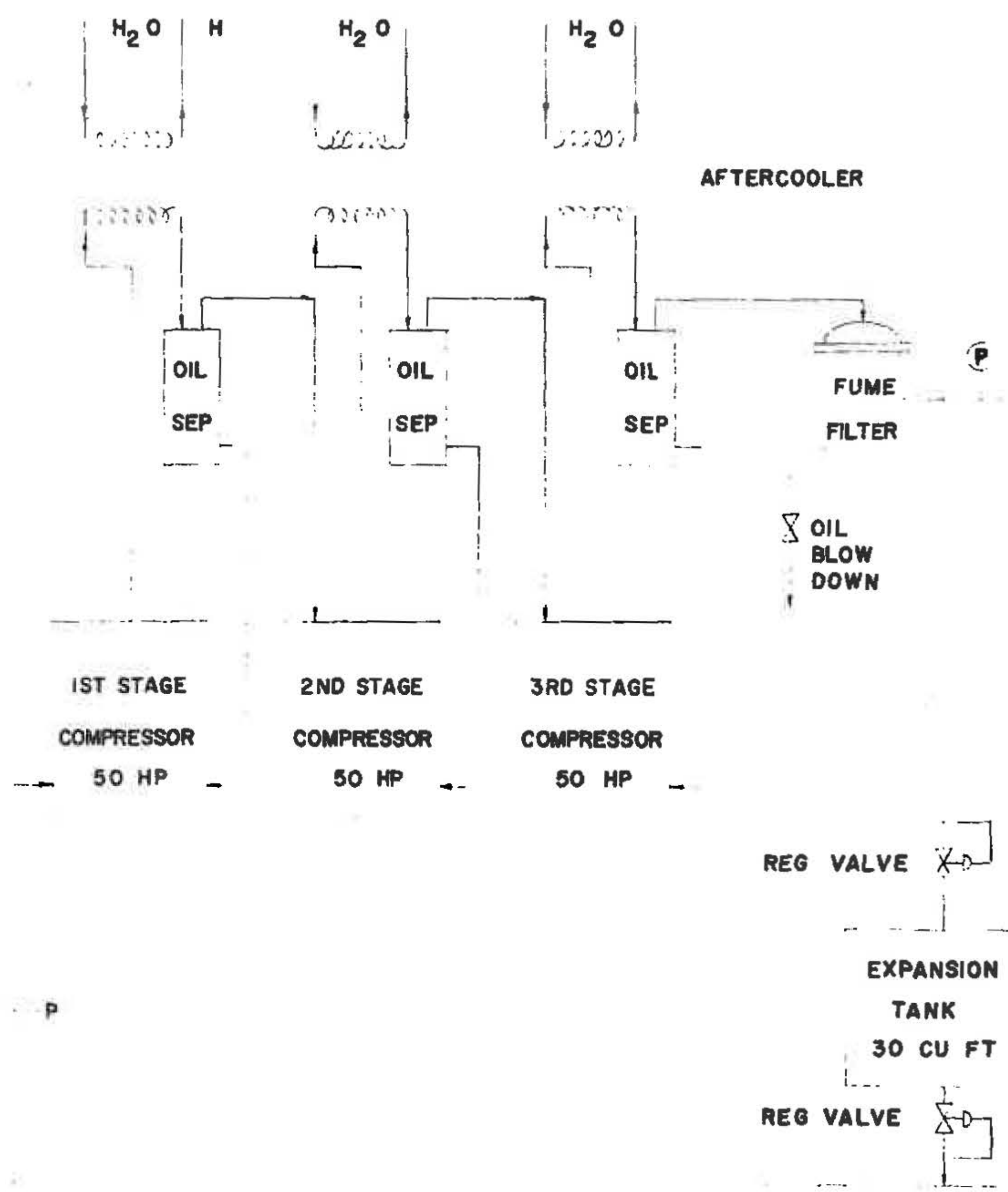

COMPRESSOR SECTION

FIDENT NFIDENTIAL

REVISIONS							
ZONE	SYM	DESCRIPTION	SERIAL NO	DFTMN	CHK	DATE	APPD

TE
CC
VA

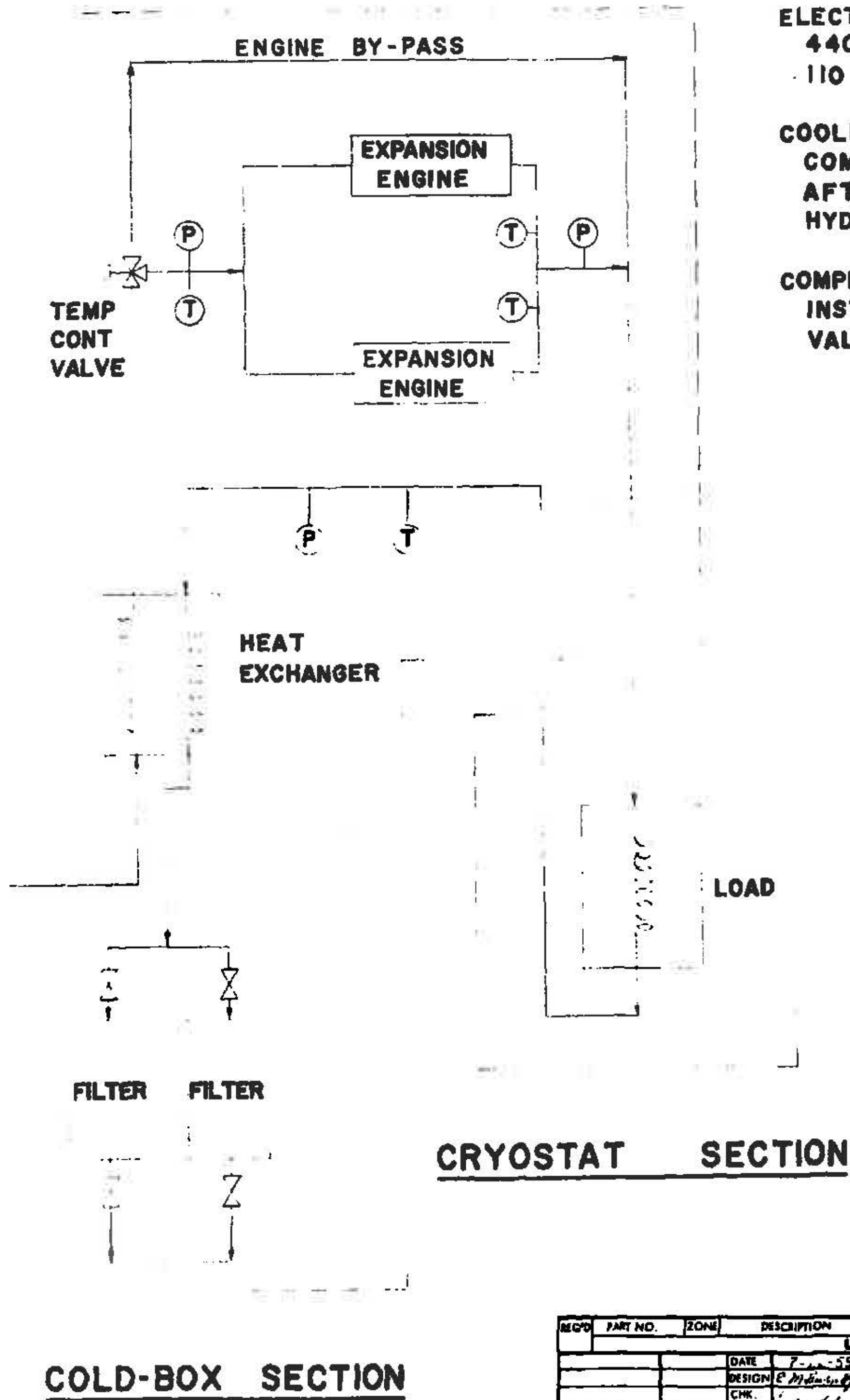

ELECTRIC POWER
440 V 3 0 60 CYCLE 150 KW
110 V 1 0 60 CYCLE 2 KW

COOLING WATER
COMPRESSORS
AFTERCOOLERS 256 GPM
HYDRAULIC CROSSHEAD 56 GPM

COMPRESSED AIR
INSTRUMENTS & CONTROL
VALVES 1 CFM - 80 PSI

C

REQ'D	PART NO.	ZONE	DESCRIPTION	MATERIAL	SIZE	MATL. SPEC.	HEAT TREAT	FINISH
LIST OF MATERIAL								

DATE	7-_-59
DESIGN	[illegible]
CHK.	
MATL.	
STRESS	
SUPV	[illegible]
PROJ.	
APPD.	[illegible]
APPD.	[illegible]

APPLICATION | QTY. REQ'D

LOCKHEED NUCLEAR PRODUCTS
LOCKHEED AIRCRAFT CORP. MARIETTA, GEORGIA

REFRIGERATION FLOW DIAGRAM

TOLERANCES		SCALE	DWG. NO.
FRACTIONS ±	.XX ± .03		PD 11 0004
ANGLES ±	.XXX ± .010		

INFIDE ONFIDENTIAL

FIGURE 21

4.3 NUCLEAR ANALYSIS

This section includes calculations of gamma heat, then discussions of beam hole selection, reactor safety, and gamma actuation of the cryostat.

4.3.1 Gamma Heat

In calculating the gamma heat to be expected in the Plumbrook Reactor, several conditions were established or assumed: the designated gamma heat value of 9 watts per gram in hole HB-2 was considered and determined to be valid;[58] the gamma spectrum was assumed to be similar to that of the BSR;[59] the gamma-heat generation rates on the BSR as calculated by Binford et al were assumed to be sufficiently close to those of concern for purposes of calculation after a power level correction factor had been applied.[60]

Upon establishing the validity of the gamma heating value and examining the refrigerator requirements necessary to remove this heat, it was decided to incorporate into the horizontal beam hole a Mallory-1000 gamma shield, as shown in Figure 22, and an enriched boron-10 thermal neutron shield, neither of which will be affected by radiation to a degree necessitating replacement. (The need for these shields is established in Section 4.3.1.2 and 4.3.1.3.) They decrease the gamma heating in the region of the cryostat to approximately 0.1 of the initial value with an additional 0.5 decrease due to geometry. This will provide a more efficient system, by reducing the requirements of the refrigeration unit for the cryostat and by allowing the use of more realistic size test specimens. The gamma heating values for the cryostat region are listed in the following tabulation.

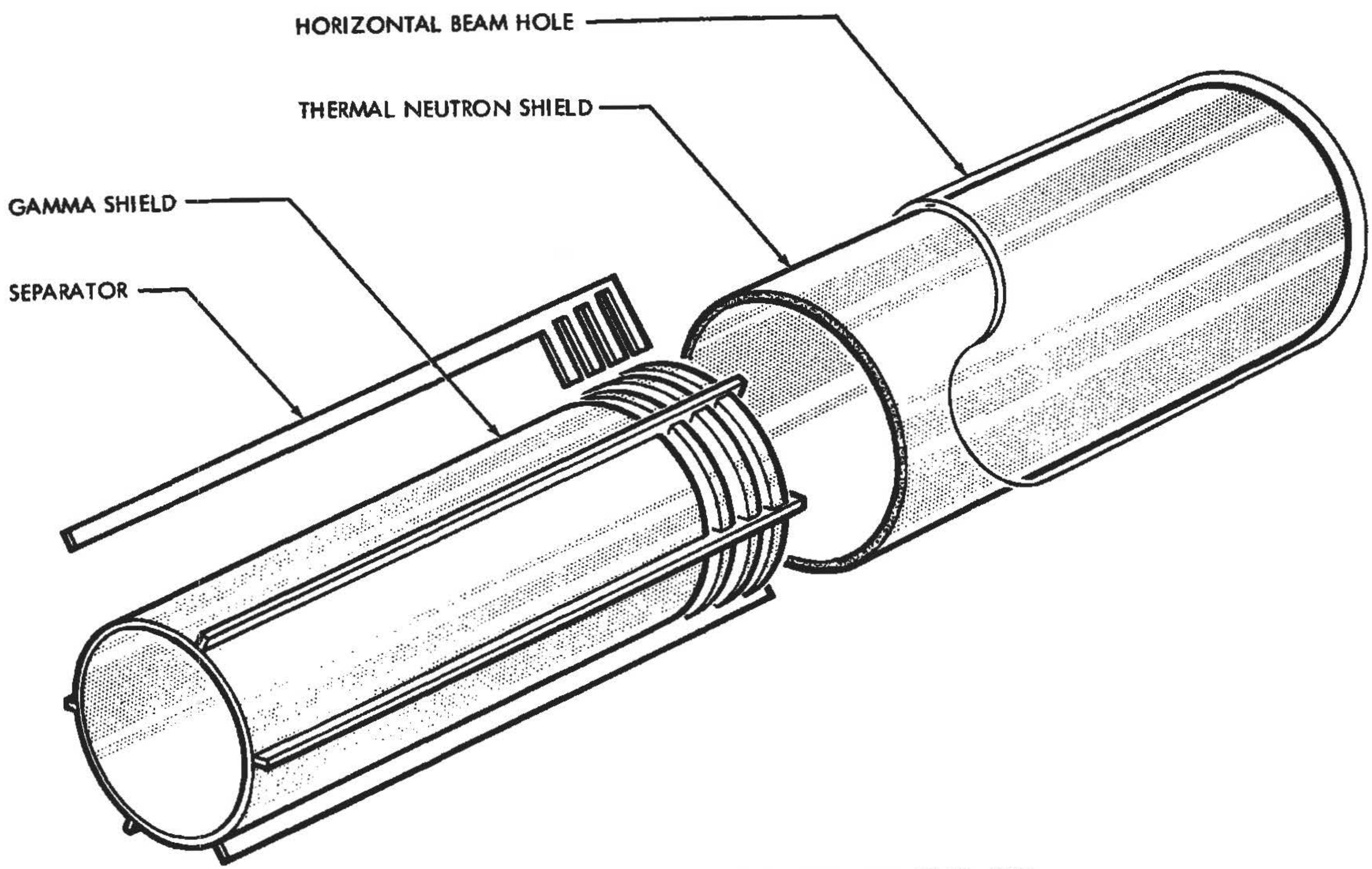

FIGURE 22 SHIELDING CONFIGURATION, EXPLODED VIEW

Distance from end of beam hole (in.)		Total heat generation (watts/gm) (shielded)
Aluminum	2	0.450
	4	0.281
	6	0.168
	8	0.106
Iron	2	0.650
	4	0.375
	6	0.225
	8	0.141

For the refrigerator conceptual design criteria, the maximum gamma heating values were used, i.e., 0.9 watts/gm for aluminum and water and 1.3 watts/gm for stainless steel and inconel X. These figures are a factor of 2 higher than the maximum values given in the preceding table. The higher values were used in order to allow for the effects of neutron inelastic scattering and for a small safety factor.

Figures 23 and 24 show the fast and thermal neutron flux distribution and the gamma dose rates along the axis of the HB-2 hole before and after the insertion of the gamma shield. Figures 23 and 25 show the fast and thermal neutron flux distribution and the gamma dose rates along the axis of the HB-2 hole before and after the insertion of the thermal shield. The reduction of the thermal neutron flux will decrease the target capture gamma rays, further reducing the gamma heating value. Figure 26 shows the flux distribution in the HB-2 hole due to the insertion of both the gamma and thermal shields. A slight attenuation of the fast neutron flux is exhibited in the irradiation volume because of the geometry of the shields and fast neutron removal; but the decrease is only a factor of 60 to 66%, still allowing a fast flux of 1×10^{14} n/cm^2-sec as a peak value.

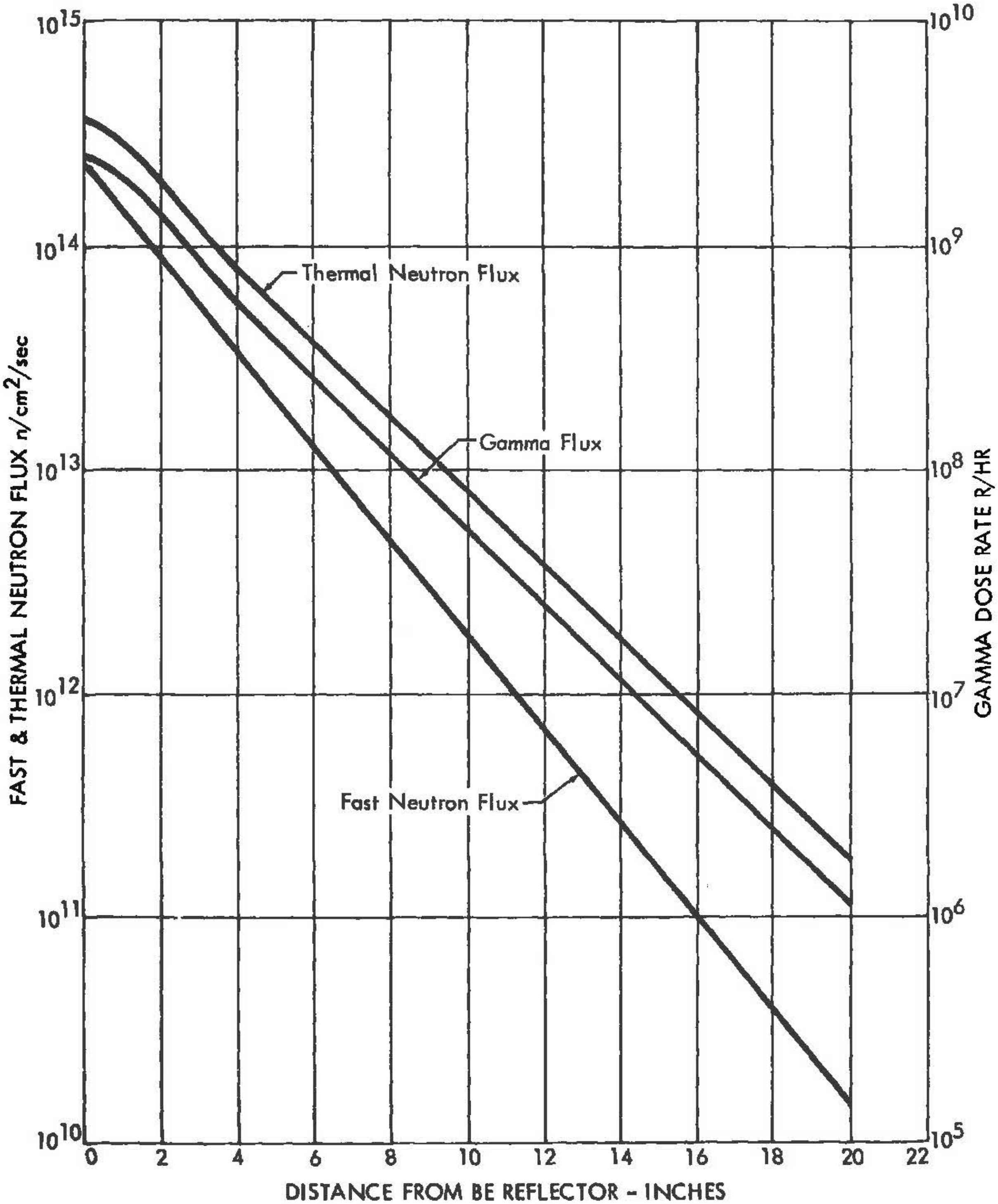

FIGURE 23 AXIAL FAST NEUTRON FLUX, THERMAL NEUTRON FLUX AND GAMMA FLUX IN HB-2 TUBE FROM BE REFLECTOR FACE

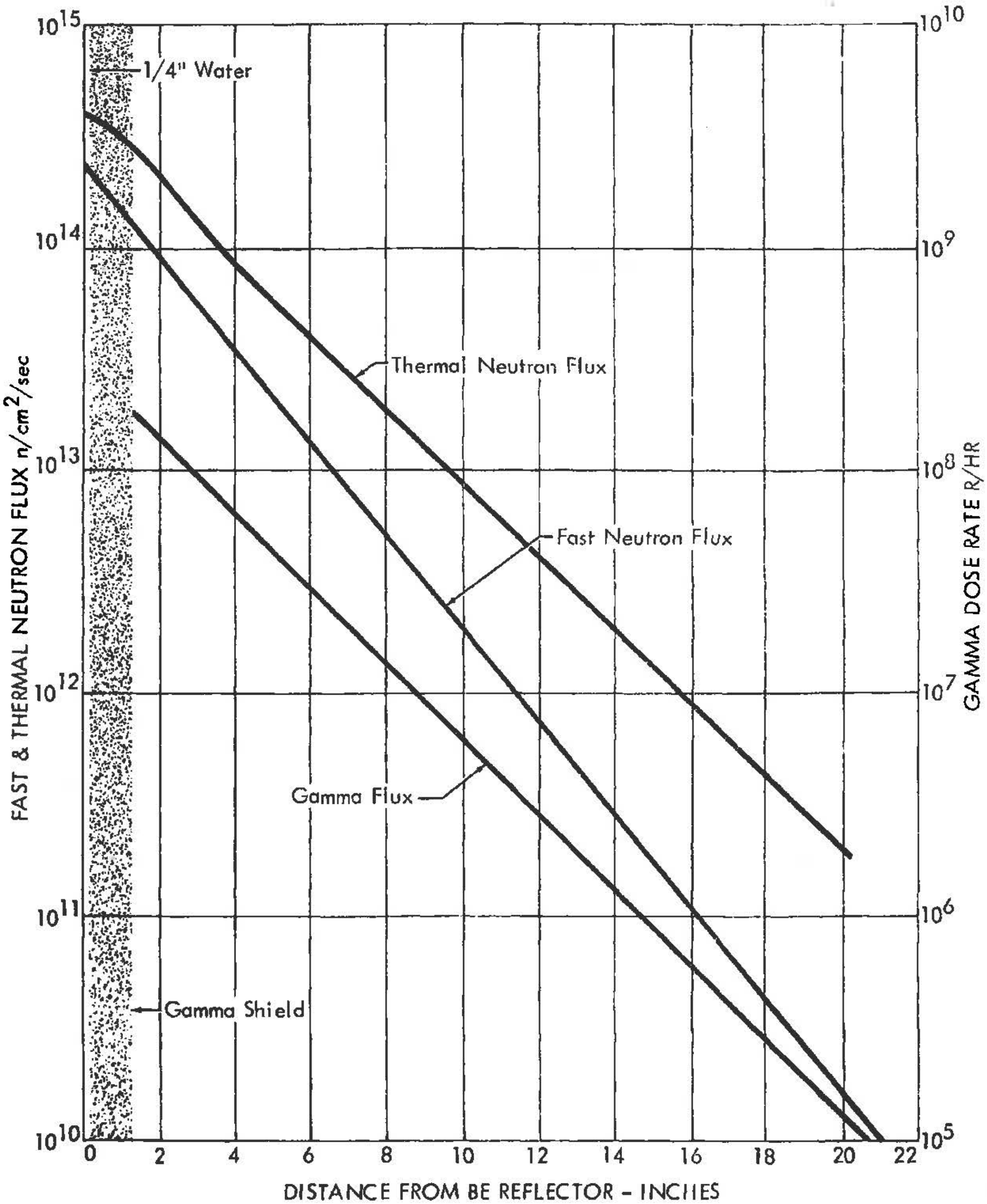

FIGURE 24 AXIAL FAST NEUTRON FLUX, THERMAL NEUTRON FLUX AND GAMMA FLUX IN HB-2 TUBE FROM BE REFLECTOR FACE WITH GAMMA SHIELD

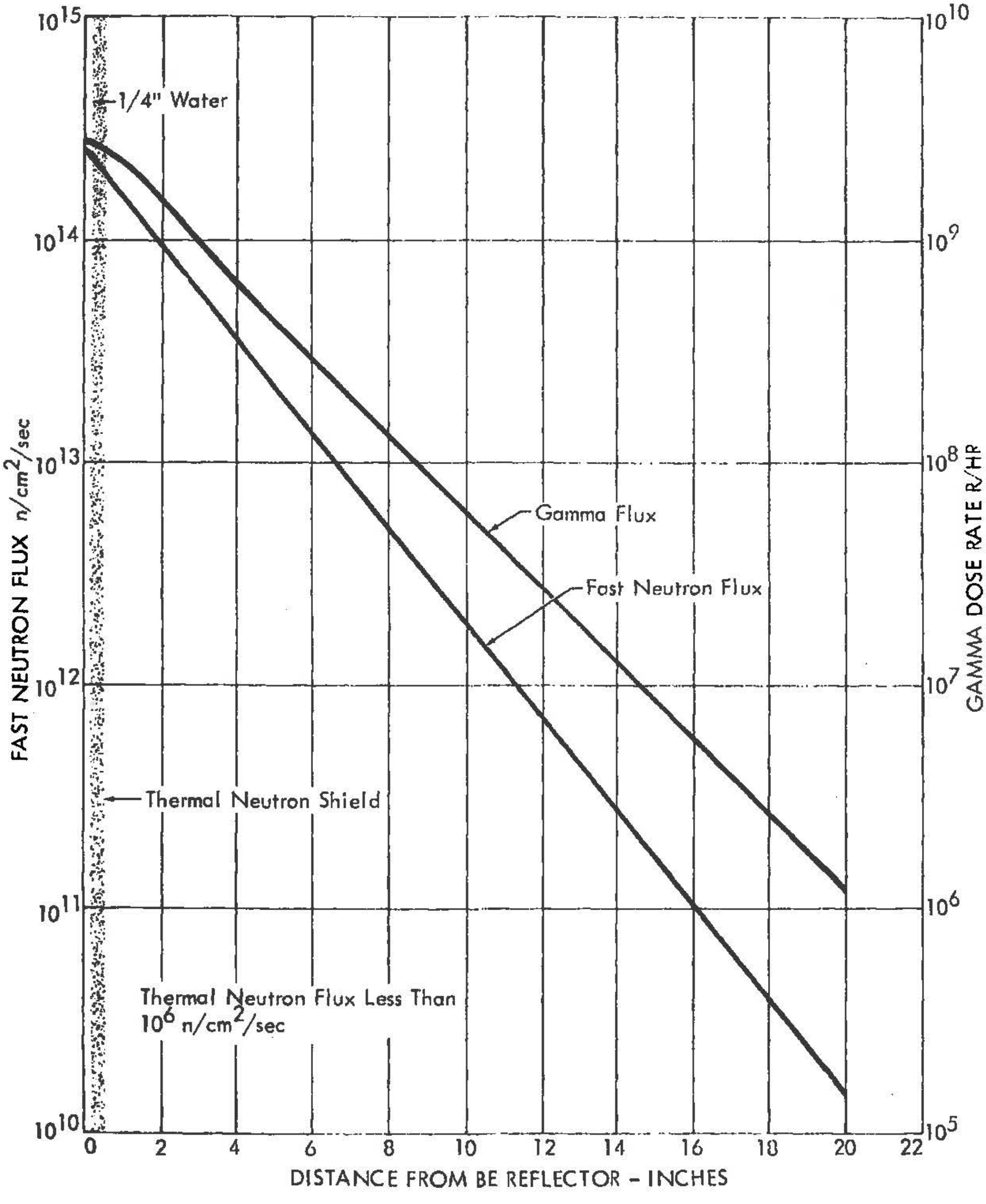

FIGURE 25 AXIAL FAST NEUTRON FLUX, GAMMA FLUX IN HB-2 TUBE FROM BE REFLECTOR FACE WITH THERMAL NEUTRON SHIELD

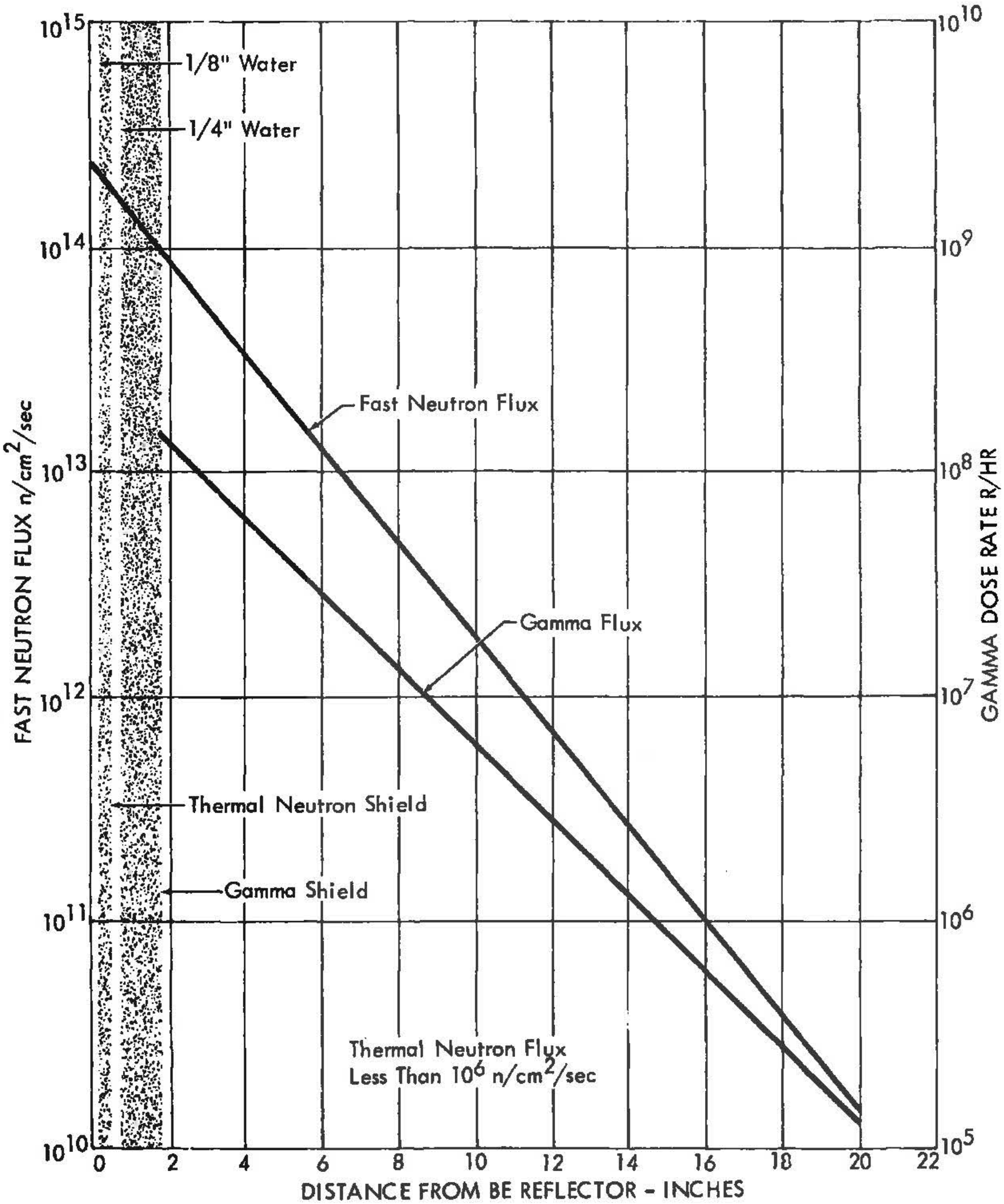

FIGURE 26 AXIAL FAST NEUTRON FLUX, GAMMA FLUX IN HB-2 TUBE FROM BE REFLECTOR FACE WITH THERMAL NEUTRON AND GAMMA SHIELDS

4.3.1.1 Heat Generation in the Gamma Shield

The amount of heat generated in the Mallory-1000 shield was calculated by considering target capture gamma rays. The calculations were made with the thermal neutron shield inserted in the beam hole. They were based on a shield composition of 90% tungsten, 6% nickel, and 4% copper.

a. Tungsten (n, γ) (0.115 Mev γ)

$$P \text{ (watts/gm)} = \phi_2 \quad \Sigma'(E_i)\,(\mu_i)\,(1.6 \times 10^{-13})$$

where ϕ_2 = thermal neutron flux

$\Sigma'(E_i)$ = cross section of (n, γ) reaction

μ_i = mass absorption cross section

P = 0.130×10^{-10} Btu/hr-gm

b. Nickel (n, γ) (1.33 Mev γ)

P (watts/gm) = 0.0026 watts/gm = 0.0089 Btu/hr-gm

c. Nickel (n, γ) (1.47 Mev γ)

P = 0.020×10^{-10} Btu/hr-gm

Therefore, the total gamma heating due to target gamma capture = 0.0466×10^{-10} watts/gm = 0.16×10^{-10} Btu/hr-gm.

To arrive at the core gamma contribution, the mean absorption coefficient was calculated to be greater in tungsten than in aluminum. This was determined by comparing the mass absorption coefficients of iron, aluminum, and tungsten in the following table for the four different energies. The calculations were weighted by the gamma spectrum of the BSR, and an allowance was made for an excess of 6 Mev gamma rays due to the (n, n') reaction and the beryllium reflector.[61] Since the gamma heating is a linear function of the mass absorption coefficient, the heating in the gamma shield will be increased by a factor of 1.4 times the value for aluminum. Therefore, the core gamma heat contribution is 12.6 watts per gram (9 watts/gm x 1.4).

Material	0.5 Mev	1 Mev	3 Mev	6 Mev
Iron	0.0840	0.0598	0.0359	0.0305
Aluminum	0.0844	0.0614	0.0353	0.0266
Tungsten	0.131	0.0655	0.0400	0.0426

The total gamma heating rate is then approximately 12.6 watts per gram, since the calculated gamma capture contribution is very small; the total gamma heating in the gamma shield = 208,000 Btu/hr.

4.3.1.2 Heat Generation in the Thermal Neutron Shield

To determine the total heat generated in the shields, the amount in the thermal neutron shield must be added to that in the gamma shield.

a. Boron (n, α) (2.35 Mev α)

$$_5B^{10} + {}_0n^1 \longrightarrow {}_5B^{11} \longrightarrow {}_3Li^7 + 2\,He^4 + Q$$

Where Q = the reaction energy of the α particle and recoil of the Li atom minus the gamma energy, therefore

$$P_1 = (\text{watts/gm}) = \phi_2 \quad \Sigma_\alpha \quad (Ei) \quad (1.6 \times 10^{-13}) \; \frac{1}{d}$$

Where ϕ_2 = the thermal neutron flux Σ_α = the alpha cross section
Ei = the energy of the α in Mev d = the density of the boron
P_1 = 0.014 watts/gm = 0.048 Btu/hr/gm

b. *Boron (n, γ) (0.5 Mev γ)*

In calculating the gamma rays in the boron, 93% of the capture gamma rays produce 0.5 Mev gamma.

$$P_2 = 0.11 \text{ Btu/hr-gm}$$

Since the 92% enriched B^{10} powder is sandwiched in 2002 aluminum cans, the heating contribution of the aluminum must also be considered.

c. Aluminum (n, γ) (6.78 Mev γ)

The amount of target gamma rays in the aluminum is

$$P_3 = 0.07 \text{ watts/gm} = 0.23 \text{ Btu/hr-gm}$$

d. Al^{28} (n, β) reaction

$$P_4 = 2.0 \text{ Btu/hr-gm}$$

Again using the mass absorption coefficient relationship and the 9 watts per gram gamma heating value, the core gamma contribution $P_5 = 4.56$ Btu/hr-gm.

The total heating in the thermal neutron shield is therefore:

$$P_t = P_1 (W_B) + P_2 (W_B) + P_3 (W_{Al}) + P_4 (W_{Al}) + P_5 (W_B + W_{Al})$$

where W_B = weight in grams of the B^{10} powder

W_{Al} = weight in grams of the aluminum can

$$P_t = 200{,}000 \text{ Btu/hr}$$

4.3.1.3 Thermal and Gamma Shield Cooling Analysis

To remove the 228,000 Btu/hr generated within the thermal and gamma shields, the required one inch of Mallory-1000 for the gamma shield was split into four plates with cooling channels between each plate as shown in Figure 27. Multiple plates are used in order to reduce the thermal gradient and thus the stress that would be present if only one or two plates were used. Also, the use of several plates increases the surface to volume ratio and thus reduces the heat flux in the shield. The space between the plates is divided into pie-shaped segments by means of separators as shown in typical section A-A, Figure 27. These separators ensure satisfactory distribution of coolant flow over the plates.

A thermal study has been made of this configuration;and the resulting flow rate, pressure drop, and temperature gradients seem quite reasonable.

The heat transfer coefficient, h, is obtained from the Colburn equation[57]

$$hD_e^{0.2} = 0.023\,K\left(\frac{G}{\mu}\right)^{0.8}\left(\frac{\mu C}{K}\right)^{0.33}$$

where

D_e = equivalent diameter = $\dfrac{4\ (\text{area of flow})}{\text{wetted perimeter}}$, ft

K = thermal conductivity, Btu/hr-ft-°F

G = mass flow rate = ρV, lb/ft^2-hr

μ = dynamic viscosity, lb/ft-hr

C = specific heat, Btu/lb-°F

The temperature rise across the liquid film is then found by

$$\Delta t\ \text{film} = \frac{q}{h}$$

q = heat flux Btu/ft^2-hr

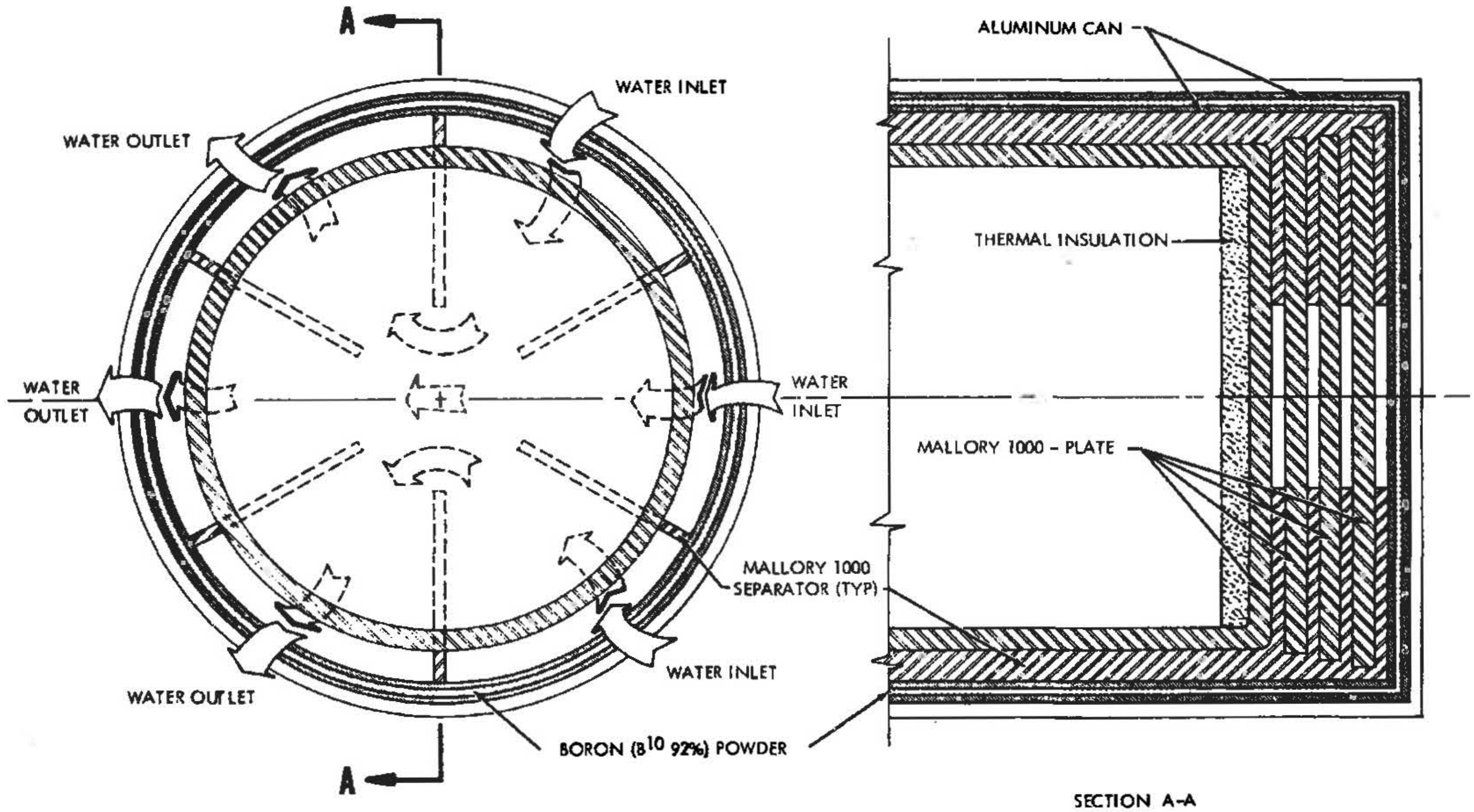

FIGURE 27 SHIELD TUBE COOLING

The temperature of the plate centerline is found by

$$t_{cl} = t_s + \frac{q''' l^2}{2k}$$

q''' = volumetric heat generation rate Btu/ft^3 -hr

l = plate half-thickness

t_s = surface temperature = t_{water} + Δt film

The pressure drop is comprised of frictional losses, turning losses, and contraction and expansion losses as follows:

$$\Delta P = \left(\frac{12fL}{D_e} + K_c + K_e + K_t \right) \frac{1}{12\rho} \left(\frac{G}{10^5} \right)^2$$

f = Moody friction factor
L = developed length, ft
K_c = contraction loss
K_e = expansion loss
K_t = turning loss
ρ = density, lb/ft^3

Therefore:

Flow rate, lb/hr	175,000
Coolant inlet temperature,°F	160
Coolant outlet temperature,°F	161.3
Maximum fluid velocity, ft/sec	45
Fluid pressure drop, psi	~ 3
Average heat flux, Btu/ft^2-hr	~ 140,000
Minimum temperature in shield, °F	~ 175
Maximum temperature in shield, °F	~ 220
Maximum surface temperature,°F	~ 195

Since fluid velocities can be expected to approach 45 ft/sec, the problem of erosion in the shield materials was considered. The erosion of the Mallory-1000 shield was found to be negligible, however; and the erosion of the aluminum can for the thermal shield will not be severe enough to warrant replacement.

In order to provide the necessary space requirements for the installation of the thermal and gamma shields, the stainless steel inserts and the aluminum sleeve will be removed from the horizontal beam hole. Adequate cooling for the shields can be provided by diverting some of the coolant from the primary reactor loop to the coolant channels in the beam hole. Both of these modifications are compatible with the Plumbrook Reactor Facility Hazards Summary, Volumes 1 and 2.

The use of water as the coolant raised the question of (n , γ) reactions in the water itself. However, the contribution to gamma heating of these reactions was found to be negligible, because of the incorporation of the thermal neutron shield and subsequent attenuation of the thermal neutron flux.

4.3.2 Beam Hole Selection

According to RFQ HS-225, it is very unlikely that the horizontal through holes will be available for this materials evaluation program; however, an analysis was made of the feasibility of using such holes. This analysis indicates that the additional flux afforded by these holes will not be sufficient to justify the effect of the added gamma heating, which would necessitate additional shielding and increase the refrigeration requirements.

The vertical through holes were rejected because of low fast neutron dose rates, even with modification of the fuel loading. Also, the locations of such holes would require impractical modification of the shrapnel shield. Of the horizontal beam holes, HB-2 is preferable to HB-1 or HB-3, because of the higher and more symmetrical fast neutron flux distribution it affords.

4.3.3 Reactor Safety

The maximum credible accident that could occur in a cryostat undergoing irradiation in a horizontal beam hole would be a chemical explosion -- nitrogen-ozone, ozone-organic, or a sudden decomposition of ozone. It has been noted further that any small amount of oxygen either in liquid or solid state in the cryostat constitutes a hazardous condition.[54]

In the event of an explosion caused by one of these reactions, several simultaneous events would take place: the helium gas refrigerant would exhibit a sharp increase in pressure and immediately thereafter drop below operating pressure; the cryostat would be damaged significantly with a remote possibility of rupture to the outer shell of the beam hole. It is inconceivable, however, that the explosion would cause any damage to the reactor or pressure vessel other than the rupture of the beam hole shell. With such a rupture, pressure would be lost in the reactor, lowering the boiling point of the primary coolant and incurring a hazardous situation. Therefore, provisions are made for an initial sharp increase in the helium gas pressure to initiate a reactor scram as described in Section 4.3.3.1. In addition, the inlet and outlet valves in the refrigeration lines to the cryostat would be closed automatically, thus eliminating the loss of helium refrigerant. A simultaneous loss of power to the material testing mechanism in the cryostat would occur.

The primary safeguard against any one or all of the stated reactions is a strict obedience to the operating procedures for the cryogenic system. The cryostat must be evacuated at room temperature and flushed at least three times with helium gas prior to cooling and irradiation. This procedure eliminates the probability of explosion.

Another accident that would be of consequence is the possibility of the rupture of an in-pile cryostat by a fragment from a test sample under stress. All calculations tend to discount the probability of such a rupture, however, because of the small mass and low kinetic energy of the fragment. For the maximum accident, it must be assumed that the fragment would cause a rupture in the walls of the cryostat, thus allowing a helium refrigerant leak. Even so, no severe thermal stresses would occur in any portion of the beam hole because of the low heat capacity and small volume of the helium gas. However, a sharp decrease in the helium refrigerant pressure would occur, thereby initiating an automatic closure of both the inlet and outlet refrigerant lines to the cryostat and a loss of power to the testing mechanism.

4.3.3.1 *Annunciator Panel and Test Console*

The control room will be provided with an annunciator-alarm panel to indicate any malfunctions in the cryogenic test setup. This panel, which will receive signals directly from the test console as illustrated in Figure 28, will consist of three annunciations: a rapid loss of helium refrigerant leak, which would indicate a rupture in the cryogenic loop or cryostat; a step function increase in helium pressure, which would indicate an explosion in the cryostat and initiate a reactor scram signal; and a general indication of troubles with the test mechanisms in the cryostats undergoing irradiation.

The test console will indicate all of these conditions in more detail so as to facilitate trouble-shooting and in addition monitor the helium refrigerant gas pressure and the temperature in the cryostats. (The alarm can be stopped by pushing an alarm reset button.)

4.3.3.2 Reactivity Changes

In computing a step change in reactivity, the horizontal beam holes (HB-1, 2, 3) were considered as a void and then as filled with water. An approximate calculational method was used instead of an extensive two-dimensional program calculation. The ratio $\frac{\Delta k}{k}$ was obtained through considering the horizontal through tube (HT-2) farthest from the core,[62] then

$$\left(\frac{\Delta k}{k}\right)_{HB-1,2,3} = \frac{\left(\int_v \Phi^2\, dv\right)_{HB-1,2,3}}{\left(\int_v \Phi^2\, dv\right)_{HT-2}} \left(\frac{\Delta k}{k}\right)_{HT-2}$$

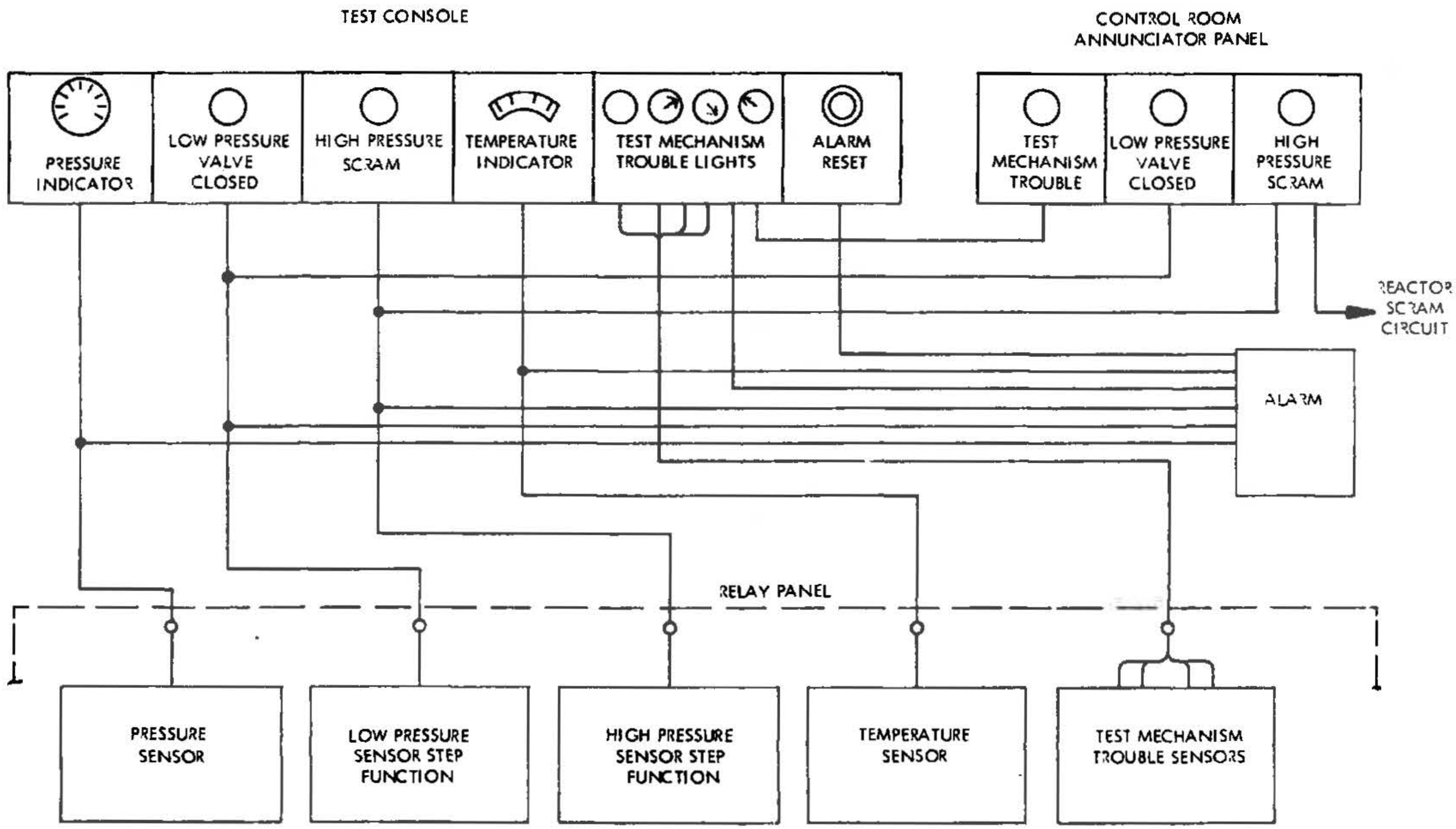

FIGURE 28 ALARM SYSTEM SCHEMATIC

where $\left(\frac{\Delta k}{k}\right)_{HT-2}$ = the change in reactivity in horizontal through tube

Φ_2 = the thermal neutron flux in the particular tube

$\left(\frac{\Delta k}{k}\right)_{HB-1,2,3}$ = the change in reactivity in the horizontal beam hole tubes

In this equation, the relative radial distances from the center of the core to both the HT-2 and HB holes are considered approximately the same, and the value chosen for the volume thickness of the HB holes is the same as that of the HT-2 hole. Therefore,the volume integrals are proportional to the subtended solid angles of HT-2 and HB holes, respectively.

$$\left(\frac{\Delta k}{k}\right)_{HB-1,2,3} = 0.002$$

In order to reduce the activation, a thermal neutron shield will be incorporated in the horizontal beam hole. Calculations indicate a negative $\frac{\Delta k}{k}$ of 0.002 for the replacement of the water in the beam hole with the thermal neutron shield.

Experimental data obtained with the BSR at ORNL indicate that a 6-inch diameter beam hole with a 3-inch beryllium oxide reflector is not worth more than 0.0025 in $\frac{\Delta k}{k}$,[42] which is consistent with the preceding calculations.

In the detailed analysis, the precise hazards associated with these aspects of loop operation will be determined by use of IBM 704 reactor codes -- WANDA, CANDLE, PDQ, and General Motors MAGNUM. In addition, a test will be performed at the Critical Experiment Facility of the GNL to determine the exact value of $\frac{\Delta k}{k}$ for the reactivity step changes prior to the irradiation tests.

It should be noted that all shielding material will be inserted prior to start-up of the reactor and left in a permanent position in the horizontal beam holes during the entire reactor operating time. The cryostat containing the test sample and test rig will then move in and out of the horizontal beam hole as required.

Due to the permanent perturbation of the thermal neutron flux by the thermal shield, the insertion or withdrawal of the cryostat will have a negligible effect on the reactivity of the reactor, less than $0.002 \frac{\Delta k}{k}$, and is well within the control of the regulating rod, which is worth approximately $0.006 \frac{\Delta k}{k}$.

4.3.4 Gamma Activation of the Cryostat

To determine conceptual design criteria and establish handling procedures for the irradiated cryostats, a study was made of the anticipated gamma dose rates from neutron activation. A permanent thermal neutron shield, described in Section 4.3.3.2, will be incorporated in the horizontal beam holes, as shown in Figure 29.

This shield will attenuate the thermal neutron flux to a sufficiently low level to eliminate the thermal neutron activation. The dose rates plotted in Figure 30 are principally due to threshold (n,p) and (n, α) reactions resulting from epithermal and fast neutron absorption.

The method of arriving at the dose rate curves plotted in Figure 30 was to peel curves plotted from experimentally determined data for the pertinent half-life contributors and reconstructing a composite curve with threshold reactions.[63,64,65,66] It was necessary to apply a correction factor to compensate for the difference in neutron fluxes and irradiation times between the experimental condition reflected in the reference curves and conditions associated with experiments to be conducted in hole HB-2 of the Plumbrook reactor. Half-lives shorter than 10 minutes have been ignored, since it is anticipated that a one-hour cooling period will be allowed in sample handling procedures.

The curves in Figure 30 depict the composite of relatively long half-lived elements. For example, the stainless steel 304 curve shows such components as Mn^{56} from the Co^{59} (n, α) Mn^{56} reaction with a 2.58-hour half-life; Fe^{59}, with a half-life of 45 days; and Co^{58}, with a 9-hour half-life. The curve levels off with the 45-day Fe^{59}, 26.5-day

Cr^{51}, 310-day Mn^{54}, and finally the 5.3-year Co^{60}.

The dose rates were computed at a distance of one foot from the material considered to be concentrated at a point source. This is somewhat conservative in that the actual measured activity will be less than the values shown in Figure 30.

In the final design, use will be made of codes for the IBM 704, which substitute a least-squares fit for the graphical peeling analysis used in this conceptual design.

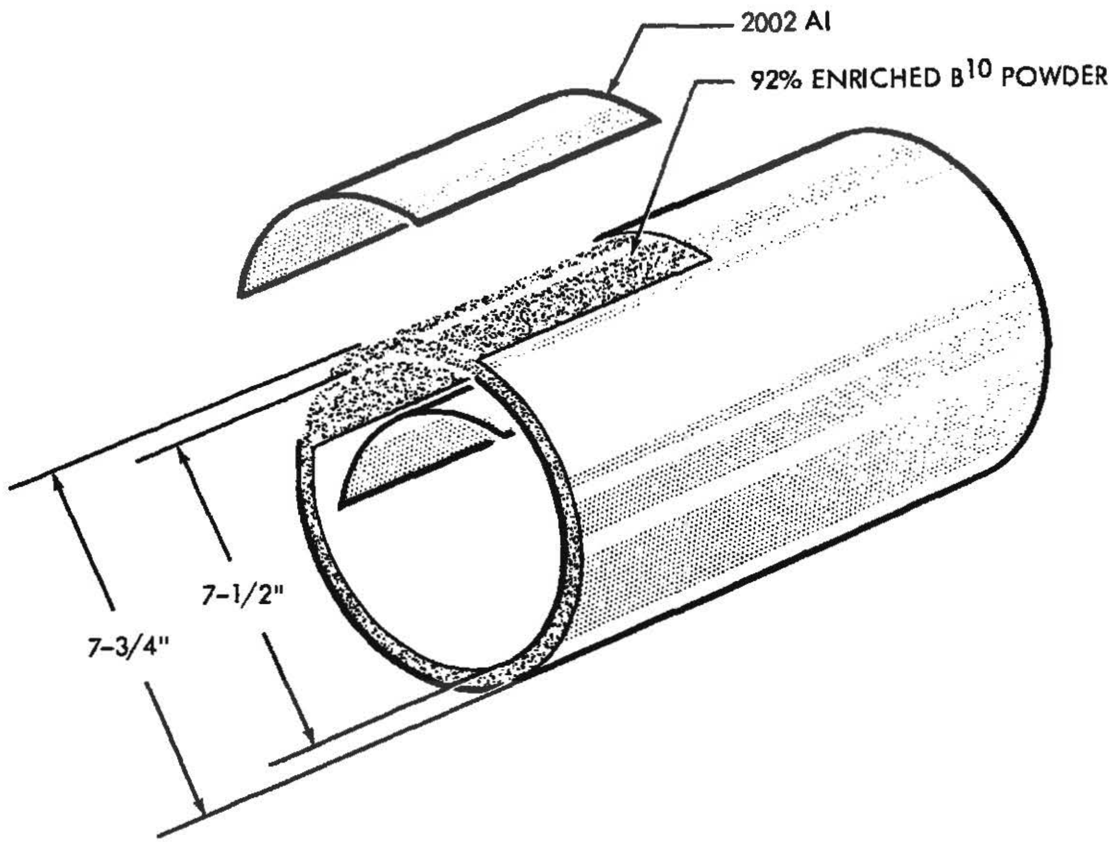

FIGURE 29 THERMAL NEUTRON SHIELD

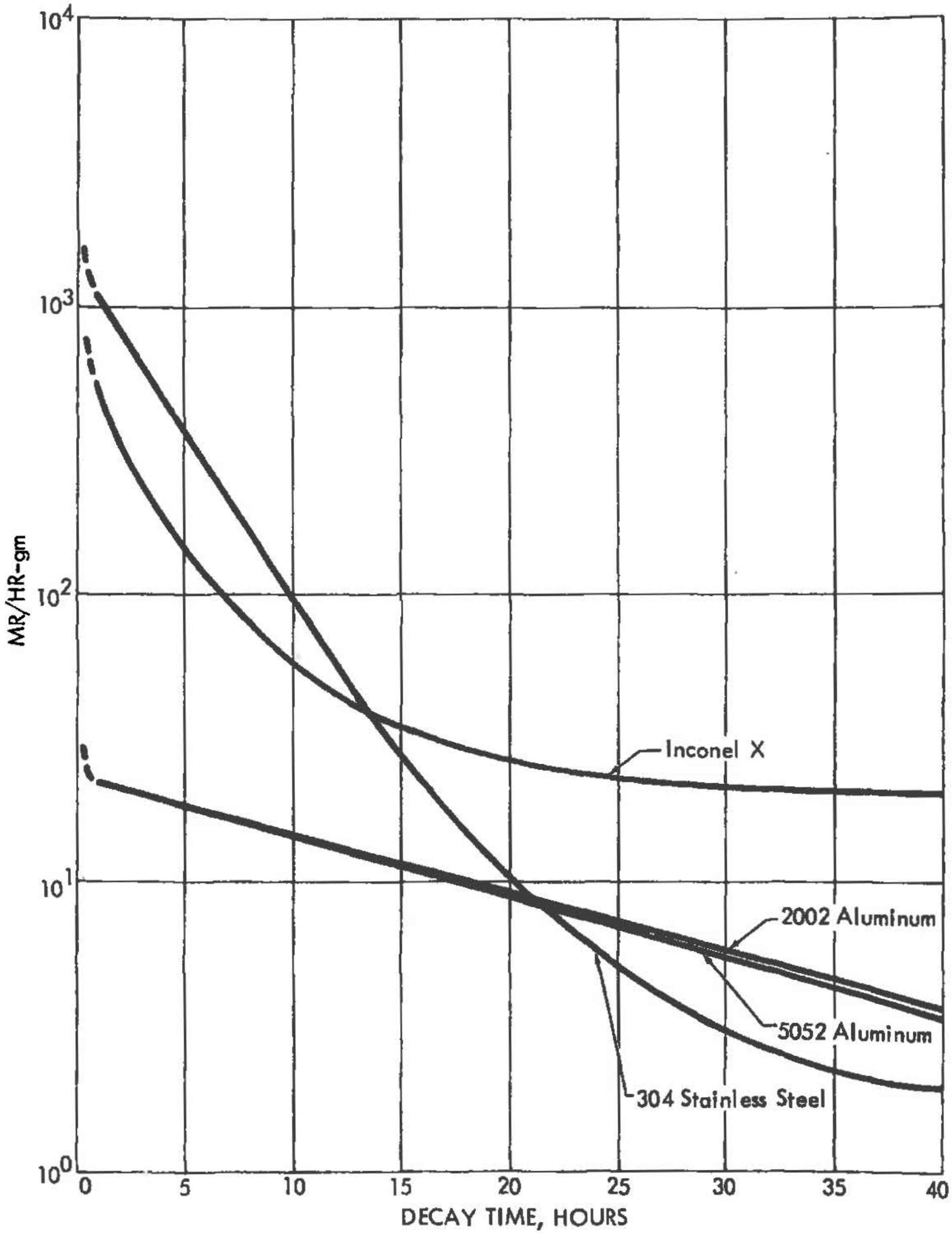

FIGURE 30 INDUCED GAMMA ACTIVITY IN CRYOSTAT (SHIELDED)

5. CAPABILITIES

This section describes the capabilities of Lockheed to accomplish the proposed program. Included is a discussion of Lockheed's facilities and experience along with the capabilities of Arthur D. Little, Inc. Also included are resumes of key personnel associated with the program.

Lockheed's capabilities in the nuclear field date from 1949, when the Company participated in the Nuclear Energy for the Propulsion of Aircraft project. Since then, Lockheed has worked on numerous research and development contracts for the Air Force.

Under Contract AF 33(600)-31845, Lockheed supervised the design and construction of the Georgia Nuclear Laboratories. This facility, designated Air Force Plant 67, occupies a remote, 10,000-acre tract of woodlands near Dawsonville, Georgia. Lockheed is responsible for managing and operating this facility under Contract AF 33(600)-38947 for AMC, Wright-Patterson Air Force Base.

This program includes operation of the 10-MW, light-water cooled and moderated Radiation Effects Reactor. This reactor is capable of simultaneously irradiating six railroad flat-car-loads of test articles, which may be operating systems, components, or other test articles. Support research and development facilities at AFP 67 include a Radiation Effects Laboratory, a Nuclear Measurements Laboratory, and a Critical Experiment Facility.

Lockheed Nuclear Products also has experience and capability for task planning, as well as conducting analytical and experimental test programs in the field of radiation effects, including test instrumentation and hot materials handling. As a consequence of the ANP program, dating back to 1952, Lockheed has analyzed numerous radiation effects problems dealing with nuclear aircraft. These problems in radiation effects are similar to those expected in a nuclear space vehicle.

In addition to the personnel and facilities of Lockheed Nuclear Products, other resources of the Lockheed Georgia Division will be available to this program as required. A number of current programs of the Georgia Division that are being conducted by branches other than LNP are applicable to this project. Representative of these are the programs discussed in the following paragraphs.

Lockheed Georgia Division is now spear-heading a program to develop forging techniques and procedures for heat-resistant magnesium alloys. This is an Air Force-sponsored project, contract AF 33(600)-36577; it involves the determination of the mechanical properties of HM21Xa (Dow alloy designation) for structural applications in the temperature range of 400°F to 700°F.

Another current program of Lockheed is sponsored by the Air Force, in contract AF 33(616)-6346, "Design Allowable Program on Four Titanium Alloys," under the guidance of the National Academy of Sciences. This is a large-scale materials testing program, designed to determine complete design allowables at room and elevated temperatures for four of the titanium alloys. Properties such as tensile, shear, creep, bearing, impact, compression, and fatigue are being determined at temperatures up to 900°F.

Also, Lockheed is currently working on contract AF 33(600)-36888 for AMC, Wright-Patterson Air Force Base on "Non-Metallic Tooling for High-Temperature Applications." This involves developing ceramics and non-metallics for use in development of high-temperature tooling. This ceramic tooling has been used in forming skins at 1900°F, brazing honeycomb, and making heat-treat fixtures.

The Georgia Division, by means of "Research Expenditure Proposal" funds, has been investigating RENE-41, UDI MET-500, UDI MET-700 high-temperature, high-strength alloys for possible aircraft application. In the past, work was done to varying degrees with 420, 422, PH 17-7, PH 15-7 MO, and Vasco-jet 1000 steel for possible aircraft use.

Lockheed Georgia Division completed contract AF 33(616)-3761 for WADC, Dayton, Ohio, in the latter part of 1958. This 18-month program, "Design, Development, and Testing of a 1000°F Pneumatic System," involved the design, development, and functional testing of a pneumatic servo and its associated components. Prior to the physical testing, wear tests were performed on more than 70 combinations of materials. Other work included surface treatment, hardness, and plating studies conducted with a MacMillan Wear Tester. Results of these tests were used to determine the choice of materials for the desired system components. This work demonstrated the applicability of various metals, finishes, and processes for hypersonic aircraft.

Lockheed will be able to provide a remote handling program that will include the development of special tools and techniques, a feasibility demonstration, and a final applications phase. LNP has also been actively engaged in the study of remote handling techniques and the development and construction of manipulator accessories and tools. The papers "Remote Disassembly of Aircraft Subsystems" and the "Remote Disassembly of ARC-34," Appendixes C and D, describe personnel and equipment capability.

As part of this proposal, a preliminary hazards analysis has been made. In this regard, Lockheed has recently provided the Air Research and Development Command of the USAF with a comprehensive Radiation Effects Reactor Hazards Report. The Air Force comments on this report are shown in the exhibit on the following page.

HEADQUARTERS
AIR RESEARCH AND DEVELOPMENT COMMAND
UNITED STATES AIR FORCE
Andrews Air Force Base
Washington 25, D. C.

ADDRESS REPLY TO
COMMANDER ARDC, ATTN
RDZNC

EXHIBIT

SUBJECT: Radiation Effects Reactor Approval

THROUGH: ARDC Liaison Office

TO: Lockheed Aircraft Corporation
Georgia Division
Attention: Mr. Sharp
Marietta, Georgia

1. The AEC Reactor Hazards Evaluation Staff and the Advisory Committee on Reactor Safeguards have judged that the RER may be operated as described in LAC-147 and in the ACRS meeting of 4 August 1958. Accordingly, operation of the RER up to 10 MW as so described is approved.

2. Some uncertainty continues to exist in the consideration of C^{14}, A^{41}, and dust activation problems in and around the REF. It is desired that experimental verification of data confirming concentrations of C^{14}, A^{41} and other radioisotopes in the air and ground be undertaken during early operation of the reactor. A report of the experimental results compared with the assumptions reported in LAC 147 and the 4 August meeting of the ACRS should be forwarded to RDZN for evaluation and transmitted to the AEC as soon as practicable.

3. This office wishes to commend the Lockheed personnel who supported and participated in the RER Hazards Report to the ACRS on 4 August 1958. The superlative effort obviously facilitated the rapid and wholehearted approval by the ACRS for RER operation as it was planned. The comprehensive nature of the report and the manner of presentation certainly attest to the outstanding capabilities of Lockheed personnel.

FOR THE COMMANDER:

Richard L. Johnson

RICHARD L. JOHNSON
Major, USAF
Chief, Subsystems and Support Division
Assistant Deputy Commander/Weapon
Systems for Nuclear Programs

Lockheed in conjunction with Arthur D. Little, Inc., has the capabilities to provide the organization, personnel, facilities, and equipment to perform the desired materials testing program at the specified cryogenic temperatures and in the specified nuclear environments.

5.1 ORGANIZATION

The Lockheed organizational structure and the organization of the NASA Cryogenics Project in relation to this overall structure is shown on the following pages. The project Review Board will meet at regular intervals to review the status of the program and to make recommendations for future program direction.

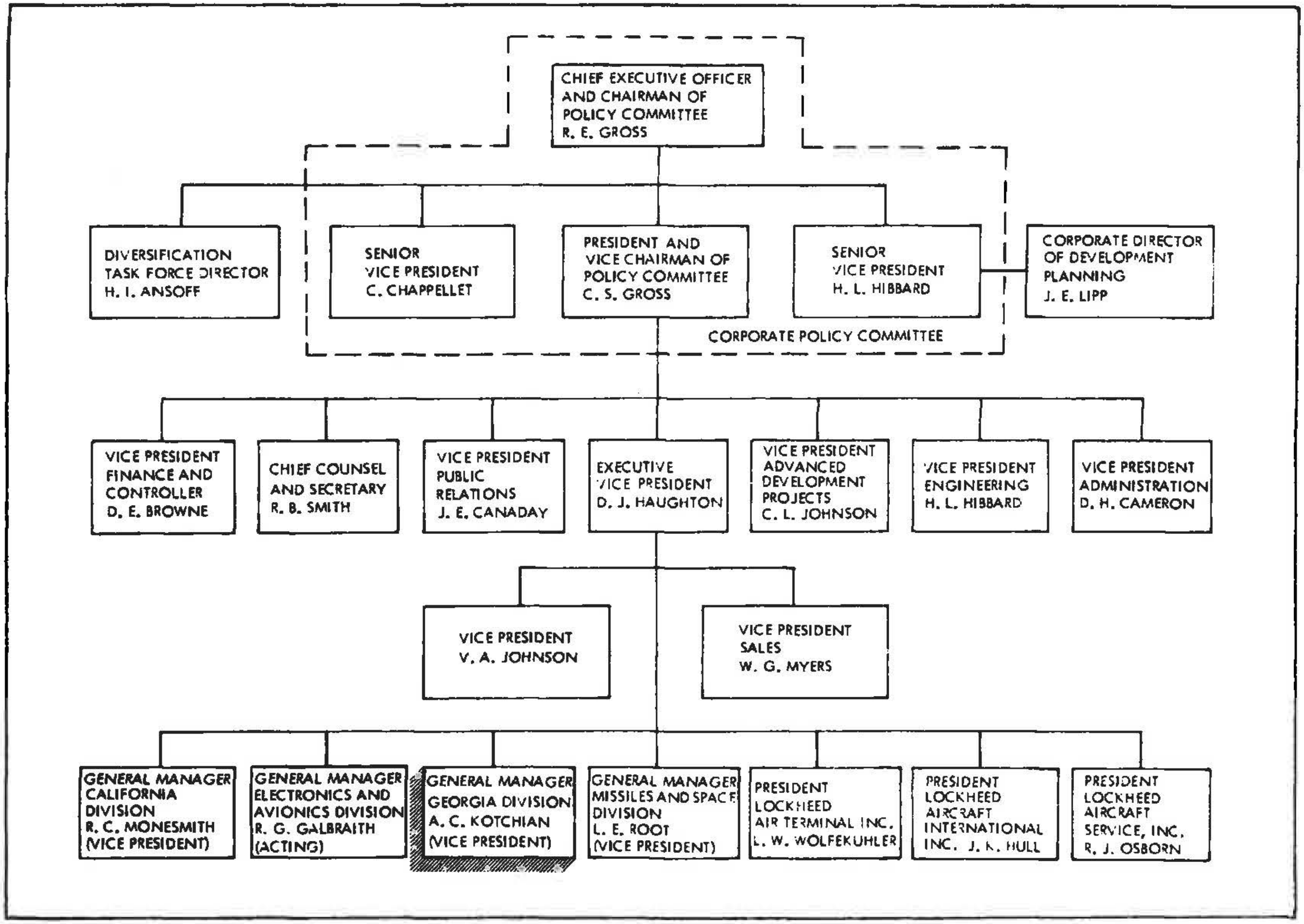

FIGURE 31 LOCKHEED AIRCRAFT CORPORATION CORPORATE ORGANIZATION

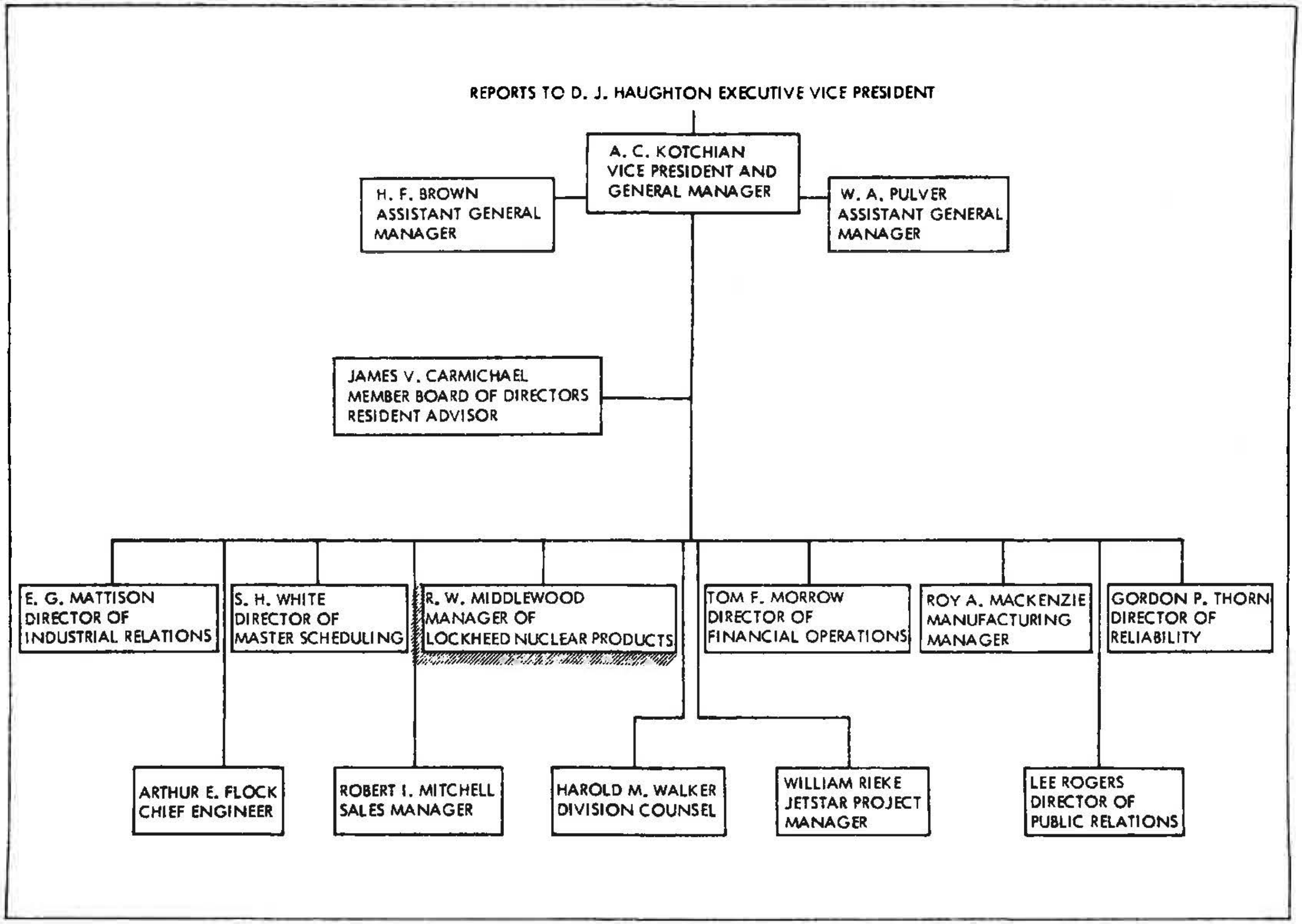

FIGURE 32 LOCKHEED AIRCRAFT CORPORATION, GEORGIA DIVISION, ORGANIZATION

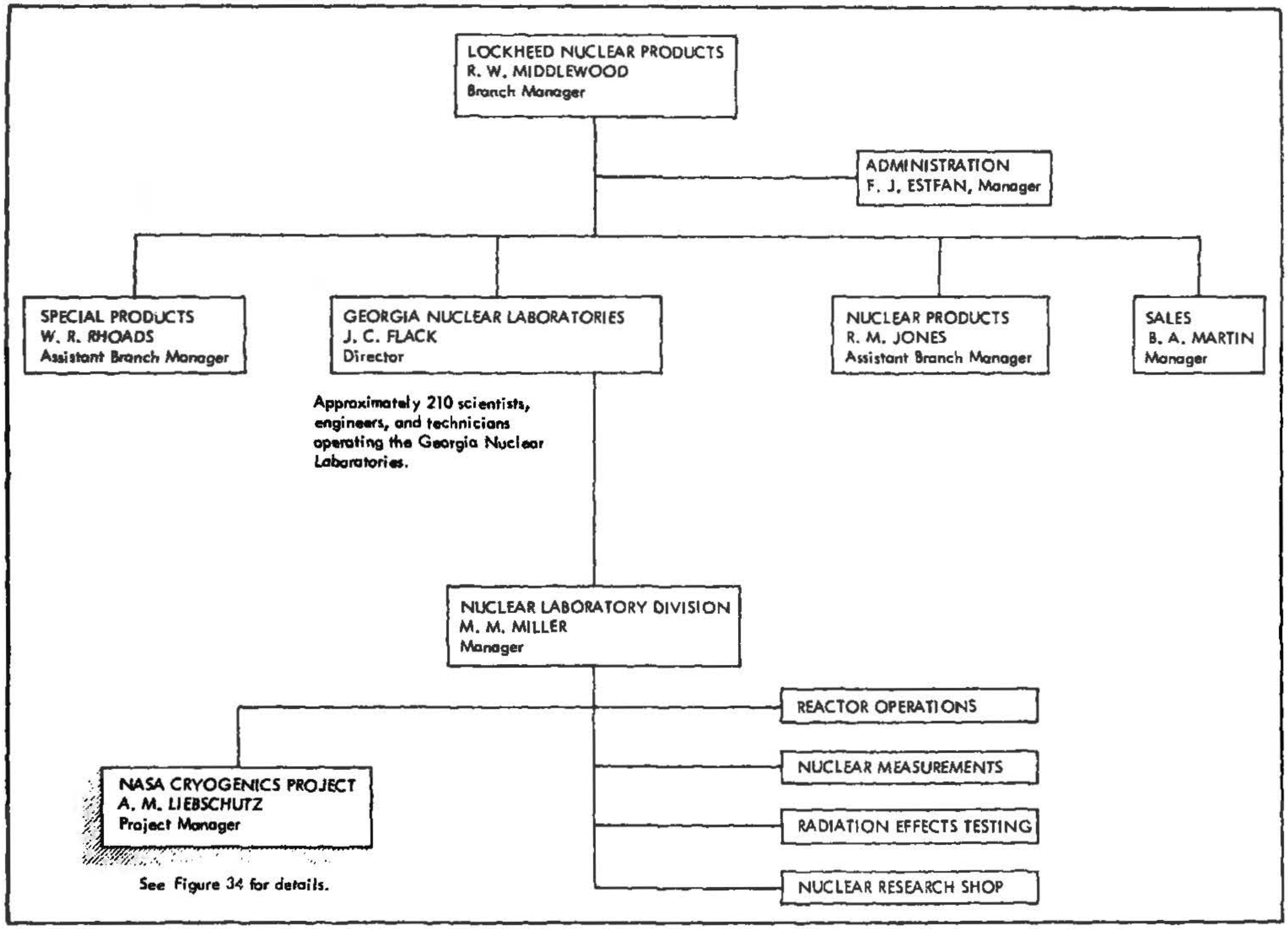

FIGURE 33 NASA CRYOGENICS PROJECT RELATIONSHIP TO LOCKHEED NUCLEAR PRODUCTS

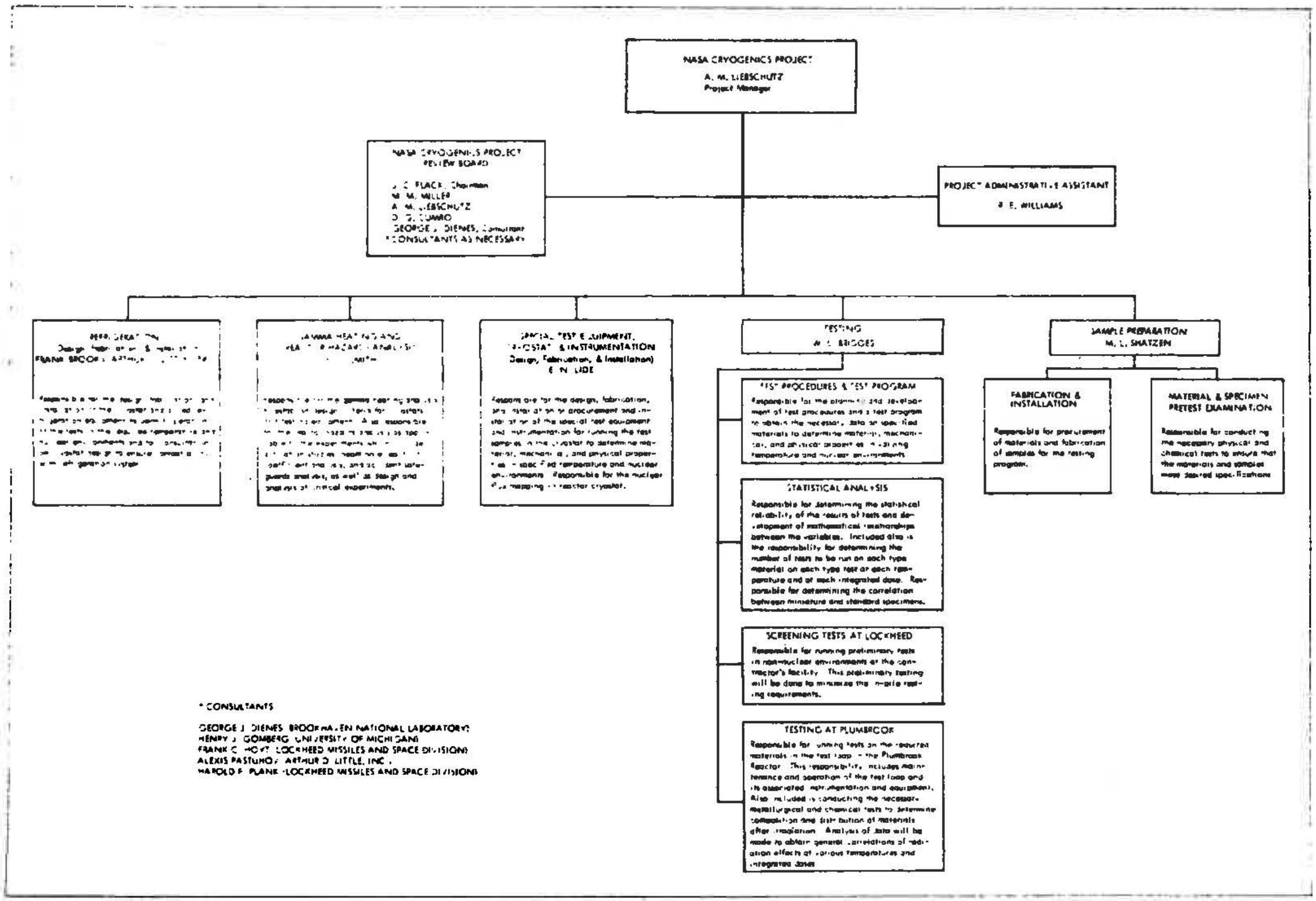

FIGURE 34 NASA CRYOGENICS PROJECT ORGANIZATION

5.2 PERSONNEL

The technical staff of Lockheed Nuclear Products is built around a core of scientists and engineers with capabilities encompassing a range of specialties that include reactor design, reactor operations, reactor safeguards analysis, radiological physics, solid state physics, thermodynamics, metallurgy, chemistry, physical testing, radiation effects analysis, radiochemistry, nuclear facility design, nuclear instrumentation design and fabrication, meteorology, servo-mechanisms, materials reliability, experimental nuclear physics, environmental engineering, theoretical physics, and remote handling operation and design. In addition, the capabilities of the staff will be supplemented by personnel of other Lockheed organizations, including the Lockheed Missiles and Space Division, and Arthur D. Little, Inc. The personnel of these organizations will provide capabilities in the fields of cryogenics, materials testing, mathematics, statistics, computers, and test equipment design.

The years of experience of Lockheed Nuclear Products engineers in specific categories of design engineering, nuclear engineering, research and development, analysis, and testing are graphically presented in Figure 35. The average experience per man is over 10 years, as shown in Figure 36.

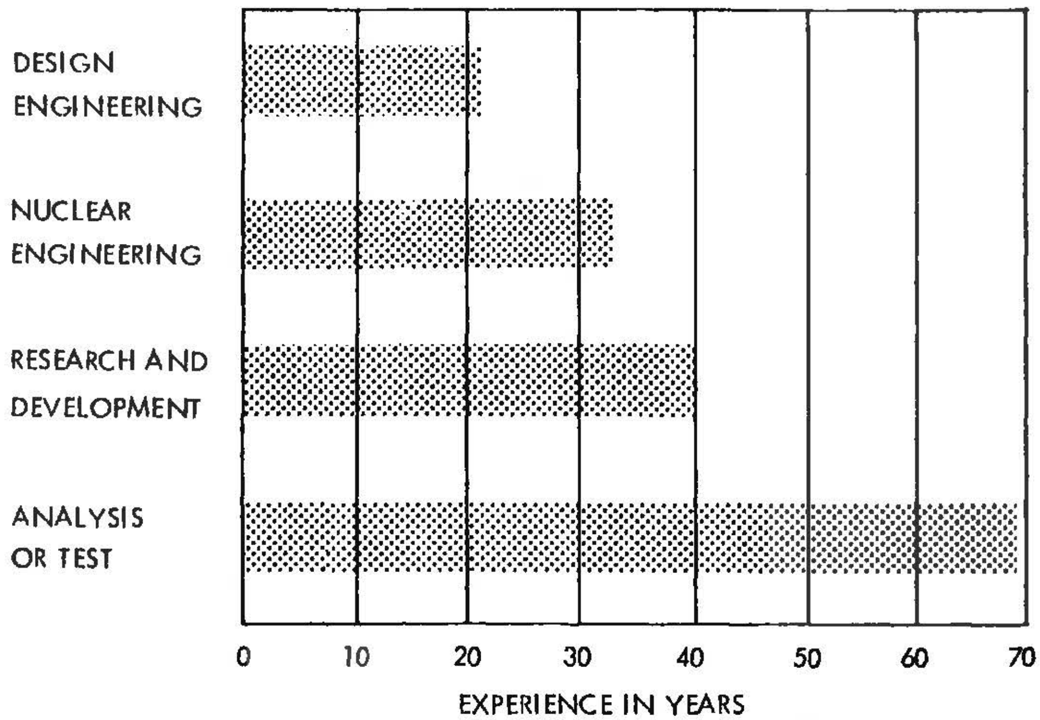

FIGURE 35 ENGINEERING AND SCIENTIFIC PERSONNEL EXPERIENCE

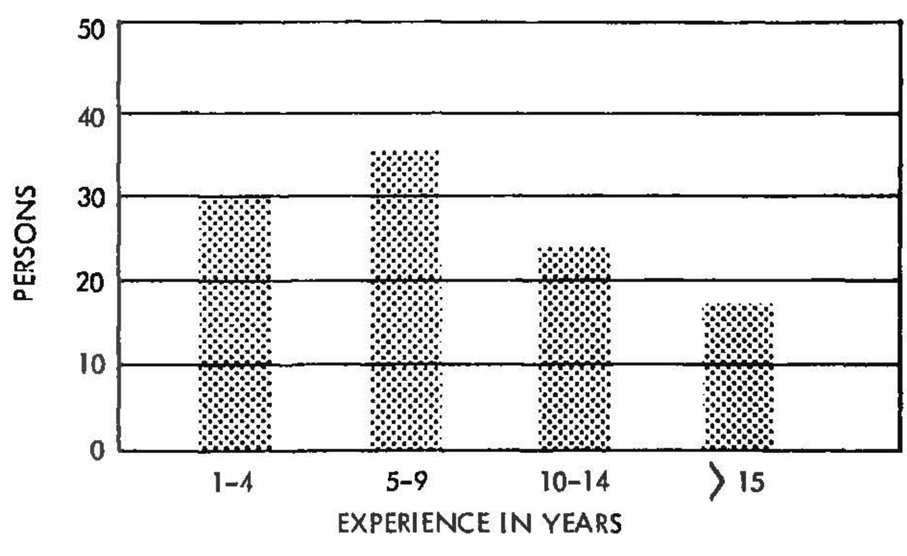

FIGURE 36 PERSONNEL EXPERIENCE IN NUCLEAR AND RELATED FIELDS

Resumes of key Lockheed people who will participate in the program follow. First is the resume of Dr. A. M. Liebschutz, who is the proposed Project Manager; then the resumes of other members of the Review Board, immediately followed by the resume of Mr. R. E. Williams, the proposed Project Administrative Assistant. Other resumes of personnel from whom key positions will be filled are included by function in the order indicated in the organization chart given in Figure 34.

A. M. LIEBSCHUTZ
Scientist, Nuclear Laboratory Division, Project Manager

With 12 years experience, Dr. Liebschutz directs the joint activities of scientific and technical personnel in the several departments. He is responsible for incorporating into reports the results of internal and external scientific studies in radiation effects, reactor technology, nuclear measurements, and related fields. He exercises technical approval authority over all reports and publications issued by the Nuclear Laboratory Division.

His experience includes research in corrosion, infrared sensing devices, radiation effects on materials, and theoretical and experimental studies of radiation effects in support of the Aircraft Nuclear Propulsion program. He participated in the conceptual design of the Georgia Nuclear Laboratories and supervised the conceptual design and detailed design liaison of the radiation effects laboratories. He was head of the experimental radiation effects group, which was responsible for electrical, electronic, hydraulic, pneumatic, physical, chemical, and metallurgical experimentation, materials and components, and activation analyses on hot cell operation.

His educational achievements include a BS in mathematics and physics, an MS in physics, and a PhD in experimental solid state physics. He was an instructor in physics and a Research Fellow and AEC Fellow at Purdue University for a number of years on several different projects. While at Purdue, he specialized in radiation effects studies and performed research in the fields of electron diffraction, electron microscopy, and X-ray diffraction.

He is a member of Sigma Pi Sigma and of the American Physical Society and is listed in the American Men of Science. He has published a number of papers, reports, and journal articles. He was the editor of the "Radiation Effects Handbook for Aircraft Designers."

J. C. FLACK
Director of Nuclear Laboratories

With 8 years experience, Dr. Flack is responsible for technical and administrative supervision of the Georgia Nuclear Laboratories. He is responsible for the continuing design and maintenance of this facility, as well as for the direction of personnel planning and conducting radiation effects programs.

He has conducted studies concerning the application of nuclear power to aircraft and has been responsible for radiation shield design, airframe activation studies, radiation damage analyses, and nuclear aspects of ground handling techniques for Lockheed's ANP efforts.

Before joining Lockheed, Dr. Flack was a Nuclear Group Engineer responsible for theoretical and experimental programs in shielding, radiation effects, and ground handling of ANP aircraft.

He possesses BS, MS, and PhD degrees, all in mathematics.

M. M. MILLER
Manager, Nuclear Laboratory Division

With 11 years of experience, Dr. Miller is Manager of the Nuclear Laboratory Division of Lockheed Nuclear Products. He was previously Department Manager supervising the operation of the nuclear laboratory. He also supervised the development of design criteria for the operation aspects of AFP 67 (Georgia Nuclear Laboratories).

Prior to his Lockheed experience, Dr. Miller served as a Staff Scientist, performing nuclear aircraft shielding design and conceptual nuclear facility design; as an Instructor in nuclear weapons; as a Staff Member of the Los Alamos Scientific Laboratory, where he conducted thermonuclear weapons research and critical experiments on uranium and plutonium assemblies; and as a Senior Nuclear Engineer in the experimental determination of gamma air scattering and conceptual design of nuclear aircraft facilities.

Dr. Miller's academic achievements include an AB and an MS in physics, and a PhD in experimental nuclear physics. He is a member of Sigma Xi and the American Physical Society and has contributed a number of papers to the Physical Review.

D. G. CUMRO
Manager, Structural Research Engineering Department

With 19 years experience, Mr. Cumro directs research tests and investigations of structural, dynamic, and fatigue problems. Mr. Cumro has held a number of positions in the fields of missiles and high-performance aircraft, including Structural Research Engineer, Materials and Process Engineer, Structural Engineer, Structural Test Engineer, and Test Consultant.

He studied mechanical engineering in the University of Nebraska and is a member of the Institute of Aeronautical Sciences.

R. E. WILLIAMS
Industrial Engineer

With 8 years experience, Mr. Williams is responsible for developing cost control programs; improving methods; recommending, writing, and implementing procedures; and compiling cost data for AFP 67 bids to perform work as requested by potential customers.

He has, in prior positions at Lockheed, been a Senior Methods and Time Standards Engineer, a Senior Tooling Standards Development and Methods Engineer, and a Methods and Time Standards Engineer.

In these positions, he was responsible for improving methods and for developing and maintaining cost control programs in the Fabrication and Tooling Divisions.

For 3 years prior to joining Lockheed, Mr. Williams had similar duties at Martin Aircraft Corporation in the Tool Engineering and Tool Manufacturing Organizations.

His academic achievements include a Bachelor's Degree in Industrial Engineering, as well as present work toward a Master's Degree in Industrial Engineering. He is a member of Alpha Pi Mu Industrial Engineering Society.

The following six resumes are for personnel comprising the capability in Refrigeration. These are all Arthur D. Little, Inc., personnel.

FRANK P. BROOKS

Mr. Brooks, a senior development engineer in the field of applied thermodynamics, was graduated from Tufts College with a BS degree in mechanical engineering. While with the Boston Edison Company, he specialized in stress analysis of high-pressure systems, applied electrolytic analysis of underground-transmission systems, and vault and tunnel design.

Since joining the staff of Arthur D. Little, Inc., in 1951, Mr. Brooks has been engaged principally in the field of cryogenic engineering. He has extensive experience in the design and production of low-boiling-point gas liquefaction equipment. He has, in addition, been responsible for project development in such areas as gas purification, paramagnetic demagnetization, infra-red detector cooling, low-temperature nuclear radiation damage research, and pressurization equipment for upper atmosphere research.

ROBERT P. EPPLE

Dr. Epple graduated from Juanita College with a BS degree in 1938 and obtained his advance degree in chemistry in 1947 at Massachusetts Institute of Technology. Before joining the staff of Arthur D. Little, Inc., in early 1956, Dr. Epple was Supervisor of the Analytical Laboratory of the Manhattan Project at Massachusetts Institute of Technology, Instructor and Assistant Professor of Chemistry at Brown University, and Head of the Inorganic Chemistry Department at Tracerlab. He is now in charge of the radioactivity laboratory at Arthur D. Little, Inc., where he is directing a number of studies of the usefulness of radiation for chemical processing and of radioisotopes for research and control of industrial problems. His primary fields of interest include the reaction rates of ionic systems, electrochemistry, radiochemistry of fission products and transuranic elements, radiochemistry of coolant contaminants, and radiation induced chemical and physical effects.

HOWARD G. McMAHON

Dr. McMahon received his BA degree (1935) and his MA degree (1937) in physical chemistry from the University of British Columbia. He was awarded a PhD in physical chemistry from Massachusetts Institute of Technology in 1941 at which time he was also associated with the Division of Industrial Cooperation of the Institute. He joined the staff of Arthur D. Little, Inc., in 1943 and was appointed Science Director in 1952. He was appointed Vice-president in charge of Advanced Research in 1956.

From 1943 to 1948, Dr. McMahon's experience was centered in the broad field of cryogenics; and he was largely responsible for the practical development of the ADL-Collins Helium Liquefier and other cryogenic equipment. Since that time he has directed advanced research projects in the fields of physical and chemical research, including phenomena of superconductivity, masers, glass fibre formation, dry friction, and the physics of high pressures. In addition, he has made a substantial contribution to the basic theory of thermal radiative properties of glass.

He is a member of Signa Xi, the American Association for the Advancement of Science, the American Chemical Society, and the American Physical Society. He was awarded the Longstreth Medal of the Franklin Institute for 1957 for his work in the development of the helium liquefier and the Frank Forrest Award of the American Ceramics Society for 1952 for his studies on thermal radiation from partially transparent reflecting bodies.

A number of U. S. and Canadian patents have been issued to Dr. McMahon, and he has been the author of a number of scientific publications.

ALEXIS PASTUHOV

Mr. Pastuhov, who is in charge of the applied-thermodynamics section at Arthur D. Little, Inc., is a mechanical engineering graduate of Massachusetts Institute of Technology. During four years with Du Pont as a development engineer, he worked on the design of high-pressure pumps and compressor systems and the design and development of rotary shaft seals.

Since joining the staff of Arthur D. Little, Inc., in 1951, he has been responsible for numerous low-temperature development projects, and has served as a special field consultant in the operation of many novel systems. Mr. Pastuhov has served one client as principal cryogenic engineer on a large-scale, liquefied natural gas program and has contributed significantly in this major undertaking to the evaluation of economic, as well as technical, aspects of the over-all process.

CHARLES A. SCHULTE

Mr. Schulte received his BS degree in engineering mechanics at the University of Michigan. The following three years he was associated with Farrell-Birmingham Company, Inc., Buffalo, New York. While there, he worked on stress and vibration analysis of gears, both theoretical and experimental; dynamics of mechanical systems, which included gearing design of test rigs; and design modifications of machine tools. His experience in analytical and experimental work on validating gas turbine designs and on effecting successful modifications in the designs, where needed, was obtained at the Elliott Company, Jeannette, Pennsylvania. A part of this experience included heat transfer analysis, used in designing for temperature distribution in turbine parts. Before joining Arthur D. Little, Inc., he was a design engineer and section supervisor in the Gas Turbine Department of the Ford Motor Company. His responsibility included primary supervision of mechanical analyses performed on the automobile engine, including heat exchanger and chassis mounts plus the basic engineering design and its details. With Little, he has worked on mechanical design of cryogenic processing equipment.

He is a member of the American Society of Mechanical Engineers and is also a Licensed Professional Engineer in Pennsylvania.

IVAN SIMON

Dr. Simon received his D. Sc. at Charles University in Prague, Czechoslovakia, in 1938. He was a physicist in the Research Department of Skoda, Ltd., from 1939 to 1947, an instructor in the Department of Physics at Charles University from 1945 to 1947, and a Research Associate in the Electronics Laboratory at Massachusetts Institute of Technology from 1948 to 1949.

Since joining Arthur D. Little, Inc., in 1949, Dr. Simon's primary work has been in experimental and applied physics, particularly solid state physics, X-ray diffraction, low-temperature physics, and the physics of high pressures. He has conducted theoretical and experimental research on the structure of quartz and glass by X-ray diffraction and infrared reflection and on the effects of very high pressures and neutron irradiation on crystalline and vitreous silicates. He has also had considerable experience in high vacuum technology, microwave electronics, and the design and construction of precision instrumentation required for new experimental techniques.

Dr. Simon is a member of the American Physical Society, American Association for Advancement of Science, and the New York Academy of Sciences.

He is the author of many technical papers.

The resumes on Mr. Bennett, Mr. Kemp, and Dr. Smith, following, indicate the capability in Gamma Heating and Reactor Hazards Analysis.

C. M. BENNETT
Senior Nuclear Engineer

With 10 years of experience, Mr. Bennett performs nuclear analysis and design on reactor core configurations in nuclear physics and engineering.

His experience at Lockheed includes reactor kinetics, nuclear and gamma heating, reactor hazard analysis, reactor optimization core design studies for radiation spectra, environmental nuclear studies in cryogenic engineering, and beta and gamma activity calculations.

During employment elsewhere, Mr. Bennett has held positions as Electronic Engineer, Reactor Engineer, and Senior Nuclear Engineer.

His academic achievements include an MS in physics, as well as a number of additional graduate courses in physics, engineering, and mathematics. He is a member of the American Physical Society, Sigma Pi Sigma, and American Nuclear Society.

S. N. KEMP
Senior Nuclear Engineer

With 3 years of experience, Mr. Kemp is responsible for a number of assignments on a project basis. These assignments require the close coordination of efforts on reactor hazard analysis, reactor engineering, core analysis and design, and the designing of special reactor experiments.

During employment elsewhere, Mr. Kemp operated and performed maintenance on several reactors; designed, performed, and analyzed reactor performance experiments; performed analytical reactor core and hazard analysis; and coordinated all studies, engineering, design, and fabrication in the complete modification of a shielding reactor.

His academic achievements include a BS in engineering physics, as well as a number of graduate level courses in nuclear reactor theory and nuclear reactor engineering. He is a member of Pi Mu Epsilon.

E. C. SMITH
Associate Scientist

With 9 years experience, Dr. Smith is technical assistant to the Manager of the Reactor Physics Department, and he is responsible for analytical studies on reactor systems. His experience at Lockheed includes the conduct of numerous theoretical studies in neutron activation, radiation effects, shield design, and reactor technology. He has also directed radiation effects testing and reactor systems design.

Dr. Smith participated in the development of basic design criteria for AFP 67. He was responsible for analyses of induced radioactivity, shielding design, and access limitations. He made evaluations of equipment and space requirements for laboratories and hot cells, assessed the data processing requirements, and served as a technical-liaison representative with the architect-engineer.

Before joining Lockheed, Dr. Smith was employed at Oak Ridge National Laboratory where he planned, executed, and analyzed measurements of neutron cross-sections, using a Van De Graff generator and a fast neutron chopper of his own design. He also performed studies involving neutron diffraction and spiral velocity selector.

Dr. Smith received his BA degree in mathematics and his PhD degree in physics, both from the University of Virginia.

The capability in Special Test Equipment, Cryostet, and Instrumentation is indicated in the following nine resumes. Some of the people described in these resumes will perform flux mapping.

R. M. CHAMBERS
Nuclear Engineer

With 4 years experience, Mr. Chambers, of the Reactor Physics Department, conducts analyses of thermodynamic and heat transfer characterists of systems in conceptual designs of reactor plants. He performed the heat transfer analysis for the core of a research reactor; he has also made a preliminary heat transfer study for a superheat reactor core; in addition, he has worked on systems design and analyses for a number of reactor conceptual designs.

Before joining Lockheed, he was a C A M E L Operations Test Engineer. In this capacity, he performed tests on system components of a liquid-metal cooled aircraft reactor and worked on an analysis of design and performance factors of the centrifugal pump.

Mr. Chambers has a BS degree in mechanical engineering.

G. W. CRAIG
Manager, Product Engineering Division

With 16 years experience, Mr. Craig is responsible for advanced and product design and development of all special products of a proprietary nature and for product design services for all nuclear reactors and associated nuclear devices. He also directs operations of the Electrical-Electronics Development Shop.

He has previously served as Department Manager responsible for the design of nuclear products and associated facilities. He was also responsible for establishing design criteria for the Georgia Nuclear Laboratory and for the design of special equipment required to maintain the Radiation Effects Reactor and Critical Experiment Facility.

Before joining Lockheed, Mr. Craig was responsible for the design of two research reactors and their supporting equipment. With another previous employer, he served as Chief Engineer and Chief of Quality Control.

A. D. DANIEL, JR.
Nuclear Engineer

With 8 years experience, Mr. Daniel designs reactor components and related mechanisms. He has held the previous positions of Draftsman, Project Assistant Engineer, Research Mechanic, and Associate Engineer.

Mr. Daniel studied at the University of Miami for three years. He later graduated from the Embry Riddle School of Aviation, specializing in small aircraft design.

R. L. GAMBLE
Nuclear Group Engineer

With 7 years of experience, Dr. Gamble prepares programs for the nuclear measurement laboratories, develops nuclear instrumentation, and supervises nuclear measurements functions. He has previously served as a Senior Nuclear Engineer, Leadman of a radiation effects group, and as a Research Fellow, engaged in research at Oak Ridge Institute of Nuclear Studies.

His work at Lockheed includes gamma and neutron flux mapping at the Radiation Effects Reactor, and gamma and neutron spectral measurements.

His academic achievements include a BA in physics, a BS in electrical engineering, an MS in physics, and a PhD in physics.

W. E. JORDAN, JR.
Snior Nuclear Engineer

With 17 years experience, Mr. Jordan designs remote handling equipment and other devices for hot cell operations. He has held previous positions of Aircraft Design Engineer and Senior Aircraft Design Engineer on flight controls and hydraulics systems.

Before joining Lockheed, he served as Mechanical Engineer engaged in design of models for wind tunnel testing, design of airfoil machines, and design of research equipment.

He has a BS in mechanical engineering.

L. LEWIS
Senior Nuclear Engineer

With 9 years experience, Mr. Lewis designs reactor components and associated systems.

His experience prior to joining Lockheed included positions of Engineering Ground Leader, with assignments in manufacturing in the steam and nuclear fields, and Sales Engineer and Consultant, involved with corrosion and prevention studies in nuclear and conventional power fields.

He has a BS in mechanical engineering and has taken graduate work in nuclear engineering.

E. N. LIDE
Associate Scientist

With 13 years of experience, Mr. Lide designs instrumentation for nuclear measurements. He previously served as a Senior Research Engineer, in which capacity he designed electrical instrumentation for aircraft structural testing. He was Electronics Research Branch Head at the USN Underwater Sound Laboratory, where he designed instrumentation for underwater sound measurements and data handling equipment. He has also served as Electronics Engineer, Research Engineer, Instructor of Electrical Engineering, and Electrical and Electronics Officer in the U. S. Air Force.

His academic achievements include a BS in electrical engineering, plus further study at the Harvard-MIT Radar School and graduate work in electrical engineering. He holds patents on a radio sound meter and a portable capacity meter. He has published papers in the Journal of the Acoustical Society of America.

L. H. McCALL, JR.
Senior Nuclear Engineer

With 9 years experience, Mr. McCall is leader of the mechanical equipment design group and is responsible for design and fabrication of reactor components and accessory systems. His responsibilities include also modification of equipment for nuclear use, design of handling equipment, and preliminary design studies for nuclear facilities.

Before joining Lockheed, Mr. McCall participated in the design of the Convair Nuclear Facility and design of ground handling equipment for the ANP Program.

He has a BS degree in mechanical engineering.

L. A. TURNER
Associate Scientist

With 7 years of experience, Mr. Turner is responsible for the design of electronic instrumentation associated with radiation detection systems and for the direction of engineers and technicians constructing these devices. He has also served as a Senior Nuclear Analyst, engaged in the design and construction of electronic instrumentation.

While a Chief Development Engineer, he conducted research and development work on new materials and on construction methods for capacitors of very small size and for capacitors for use under extreme environmental conditions. This work also included construction of conductors and resistors for use in filter assemblies. While a Senior Engineer, he supervised an electronics laboratory. He has also been a Research Assistant engaged in the design, construction, and modification of radar and other electronic devices.

He has a BS and an MS, both in electrical engineering.

The following seven resumes pertain to Testing Capability.

GEORGE V. ASEFF, SR.
Senior Nuclear Engineer

With 18 years of chemical and engineering experience, Mr. Aseff is a member of the Staff of the Nuclear Laboratory Division. He conducts studies in the fields of radiation effects, thermodynamics, and heat transfer. He prepares and directs the preparation of technical reports and specifications applying to current developments.

Mr. Aseff has previously served as lead engineer in the Chemical/ Metallurgical Research Laboratory. He was responsible for providing technical direction and coordination of the group in the research, development, and evaluation of new engineering materials and processes. As an Aircraft Research Engineer, Senior, he has prepared more than 200 Lockheed reports in the field of materials in the past 8 years and has made several patent disclosures to the Company.

In this capacity, he has also acted as consultant to the B-29, B-47, C-130, and JetStar production airplane projects at the Lockheed Georgia Division in matters concerned with materials and materials testing.

Mr. Aseff is a registered professional engineer and a member of the staff of "Chemical Abstracts Journal" for the sections of Metallurgy, Nuclear Phenomena, and others.

He is an active member in a number of professional societies, including the American Society for Testing Materials, American Chemical Society, American Society for the Advancement of Science, and the American Institute of Chemical Engineers.

Prior to joining Lockheed, Mr. Aseff has been employed as a designer and fabricator of special equipment for research, including cryogenics, instructor in general and physical chemistry, engineering department coordinator, sales manager for a color processing plant, and an Army Signal Corps team leader in electronics and electrical equipment.

He holds a BS in chemical engineering from the Case Institute of Technology, an MS in chemistry from Georgia Institute of Technology, and has currently completed a portion of his doctorate work in chemical engineering, specializing in heat transfer and thermodynamics. He has also completed industrial courses in radiography, radioisotopes, airplane systems, and management techniques.

WILLIAM L. BRIDGES
Associate Scientist

With 26 years experience, Mr. Bridges has for the past 2 years been on the Staff of the Nuclear Laboratory Division. He conducts and directs research studies and interprets the results of scientific research, including radiation effects for application to problems of the Nuclear Laboratories. He also reviews for technical content reports and other publications generated in the division.

Mr. Bridges' experience has included several positions as Chemist, Research Chemist, and Materials Engineer. Summarizing his experience for the past 12 years, he was for 4 years a Research Chemist on the nuclear aircraft materials program. This was followed by 6 years as a Research and Development Aircraft Materials Engineer on Aircraft Nuclear Propulsion program and other military aircraft and missiles. In this capacity, he planned, directed, and conducted research programs for determining chemical, physical, and mechanical properties of various aircraft materials, including conventional and exotic nuclear shield materials, high temperature refractories for use in nuclear reactors, liquid metals, honeycomb sandwich structures, structural adhesives, structural plastics, electrical and electronic potting compounds, and plastic foams. In addition, he advised aircraft and missile design engineers on the selection of materials for specific design applications.

Mr. Bridges has a BS in chemistry and physics and has taken additional training in nuclear metallurgy and in nuclear science and engineering.

A. O. BURFORD
Nuclear Group Engineer

With 8 years of experience, Dr. Burford is responsible for radiochemistry, radioactivation analysis, chemical and physical testing, and nuclear requirements pre-analysis for support of Georgia Nuclear Laboratories systems test programs.

He has previously served as a Senior Nuclear Engineer, engaged in radiation effects studies; and as a Senior Operations Research Analyst, engaged in design liaison for the Georgia Nuclear Laboratories. His academic accomplishments include BS, MA, and PhD degrees -- all in nuclear physics.

He is a member of the American Physical Society and the Health Physics Society. He has published papers in the Physical Review and the Surgical Forum and has presented papers at symposia of the American Physical Society.

A. MacCULLEN
Senior Nuclear Engineer

With 16 years of experience, Mr. MacCullen plans subsystem evaluation programs and develops methods and procedures for radiation effects testing of mechanical-hydraulic subsystems. He prepares specifications for specialized test equipment and is Project Engineer for hydraulic subsystem irradiation tests.

While at Lockheed, he has held the positions as Design Group Supervisor, Senior Design Engineer, and Senior Research Engineer; his efforts have been concentrated in hydraulic subsystems design and analyses.

Before joining Lockheed, he held the positions as Design Engineer and Instructor in Mechanical Engineering.

He has a BS and an MS, both in mechanical engineering.

T. R. PHILLIPS
Senior Nuclear Engineer

Mr. Phillips is an Analytical Chemist with 10 years of research and development experience in the atomic energy field.

Mr. Phillips' research and development experience includes 6 years of experience in statistics.

He has held previous positions as Research Chemist, Analytical Chemist, and Research Chemist -- Analytical and Inorganic.

His academic achievements include a BS in chemistry, as well as a number of graduate courses in statistics, advance inorganic chemistry, radiochemistry, advance analytical chemistry, and nuclear physics.

He is a member of the American Chemical Society, the Analytical Chemistry Section of the American Chemical Society, and Gamma Sigma Epsilon, Chemical Society. He is the author of several Atomic Energy Commission reports.

C. E. VIVIAN

With 12 years experience, Mr. Vivian is responsible for design, development, and operation of the hot cell complex, hot materials transport system, warm machine shop, and all remote handling systems and equipment. He is responsible for studies relative to remote handling and for storage and disposal of radioactive or contaminated materials.

Mr. Vivian participated in the initial program to establish design criteria for remote handling facilities at Georgia Nuclear Laboratories. He has also directed remote maintenance studies on aircraft subsystems, which entailed the development of special tools used for disassembly with manipulators.

Before joining Lockheed, Mr. Vivian was a hot cell operator at Los Alamos, where he designed, built, and operated hot cell equipment for remote chemical processes.

Mr. Vivian studied mechanical engineering at the University of New Mexico.

L. A. WILLIAMS
Senior Nuclear Engineer

With 5 years experience, Mr. Williams designs and develops procedures, techniques, and equipment for the operation of the remote operations complex and the hot materials transport systems. He also performs analyses of test systems in the development of techniques and procedures for the remote disassembly and reassembly of test items.

He has been employed as Nuclear Engineer, engaged in the development of special remote handling tools and techniques; Aircraft Research Engineer, engaged in research and development projects in the fields of bleed air contamination detection methods and remote ground handling studies, as well as environmental tests of aircraft systems; and Associate Aircraft Engineer, engaged in developmental testing of hydraulic and control systems.

He was Weapon Systems Project Engineer on the H-34 helicopter and Assistant Weapon Systems Project Engineer on the H-21 helicopter.

He possesses a Bachelor of Aeronautical Engineering degree.

Resumes follow on Messrs. Johnson and Shatzen, who will be participating in Sample Preparation.

E. H. JOHNSON
Shop Foreman, Nuclear Research Shop

With 17 years of experience, Mr. Johnson is responsible for scheduling shop work within the Georgia Nuclear Laboratories and for providing shop support to nuclear research and experimental activities, including the fabrication, construction, and modification of experimental and test equipment and components.

His previous positions with Lockheed include duties as Supervisor, Foreman, and Assistant Superintendent in the Fabrication Division (Machine Shop and Sheet Metal Shop). In these positions, he was responsible for the efficient utilization of machinery, equipment, and manpower; he was also responsible for meeting shop schedules and maintaining quality.

Prior to joining Lockheed, he held positions as Machine Shop Foreman, Machine Tool Estimator, and Assistant Shop Superintendent.

M. L. SHATZEN
Associate Scientist

With 17 years of experience, Mr. Shatzen develops procedures for and performs chemical analyses on materials subjected to nuclear radiation, and he analyzes subsystems for radiation resistance.

He has served Lockheed as a Receiving Inspector, Research Engineer, Senior Research Engineer, and Senior Nuclear Engineer. While a Senior Research Engineer, Mr. Shatzen was responsible for planning and conducting research, development, and qualification tests for plastics, sealants, elastomers, paints, lubricants, hydraulic fluids, and similar products.

During employment elsewhere, he held the positions of Junior Chemist, Chemist, Analytical Chemist, and Chief Chemist and Production Manager.

His academic achievements include a BS in chemistry, as well as a number of graduate courses in methods or analysis, computers, radiography and radioisotopes, and nuclear physics. He is a member of the American Chemical Society, the Georgia Academy of Science, and the American Society for Testing Materials.

Consultants are briefly identified in the following paragraphs.

HENRY J. GOMBERG

Dr. Gomberg is a Research Physicist specializing in nuclear engineering concerned with radiation detection, radiation effects, reactor control and stability, and associated fields.

FRANK C. HOYT
Scientific Advisor to Lockheed Missile and Space Division

Dr. Hoyt directs studies of propulsion systems dependent on nuclear energy sources. He also reviews developments for the conversion of nuclear energy to electric power and propulsion, to enable him to make recommendations to research organizations.

HAROLD F. PLANK
A Staff Scientist at Lockheed Missile and Space Division

Dr. Plank directs and conducts studies on missile and space flight systems that employ nuclear energy as a source for propulsion.

5.3 LOCKHEED FACILITIES

In addition to facilities at the Georgia Nuclear Laboratories for research and development, testing, computing, engineering, and fabrication, Lockheed also has available facilities at Air Force Plant 6 and at the Missiles and Space Division. Included at AFP 6 are an instrumentation and circuits laboratory, as well as structural, mechanical, and metallurgical laboratories. Ample fabrication facilities are also available at the plant. Physics laboratories and a toxic material machining facility are available at the Lockheed Missiles and Space Division. (The facilities of Arthur D. Little, Inc., are noted in Section 5.4.2.)

5.3.1 Georgia Nuclear Laboratories

Laboratory facilities at the GNL include the Radiation Effects Laboratory and the Nuclear Instrumentation Laboratory. Also, a Critical Experiment Facility is available for determining core loadings and performing criticality experiments. The Radiation Effects Laboratory is composed of the following principal work units: the hot-cell mock-up, the systems build-up area, the hot cells, the warm laboratories, a standards and calibration laboratory, a general chemistry laboratory, a radiochemistry laboratory, a counting room, a physical testing and meteorology laboratory, environmental test facilities, and a photographic dark room.

There are two warm laboratories, the electrical-electronic laboratory and the hydraulic-pneumatic laboratory. These laboratories, supported by a well equipped warm machine shop and warm metallurgical facility, are used for pre- and post-irradiation testing. The electrical-electronic laboratory is primarily a facility for determining effects of irradiation on components by means of tests performed either remotely or conventionally. The laboratory also serves as a means for calibrating instrumentation and test articles and for performing qualification tests of electrical and electronic materials and parts. And the laboratory is used to develop any unique electronic instrumentation required for testing. It is equipped with all the meters, generators, power supply facilities, amplifiers, and miscellaneous facilities necessary to perform its intended functions.

The standards and calibration laboratory is housed in an electrically shielded room. It is capable of a high degree of accuracy in measuring various properties such as voltage, current, frequency, time, internal resistance, pressure, temperature, flow, weights, dimensions, vibration, and strains.

The general chemistry laboratory includes capabilities for performing classical and unique analyses and syntheses in support of the various programs. In addition to the usual chemicals and equipment, the laboratory is equipped with balances (semimicro-analytical, micro-analytical, special purpose types), centrifuges, constant temperature baths, an electro-analyzer, a fractometer (vapor phase, Kromatog), a lubricity tester, pH meters, a photoelectric calorimeter, a polarograph, a filtrator, a vapor pressure tester, vacuum equipment, and X-ray diffraction equipment.

The physical test and metallurgy laboratory has the equipment to perform standard mechanical and physical properties tests. It contains such equipment as an Arcweld Model D creep-rupture tester of six-ton capacity, Brinell and Rockwell hardness testers, microscopes, an abrader for use in abrasion-resistance measurements on elastomers and related materials, a metallograph, a Kentron micro-hardness tester, heat-treating furnaces, a 20,000-pound tensile testing universal machine, vibration equipment, and equipment used to prepare specimens for metallographic analysis. Should Lockheed perform this cryogenic program for NASA, this laboratory will be equipped with the necessary equipment to perform the proposed physical properties tests at cryogenic temperatures. This equipment will include a Collins Helium Liquefier and the supporting refrigeration equipment. Equipment for generating liquid nitrogen is presently available.

The facilities of the Nuclear Instrumentation Laboratory are used to design and construct instruments used in measuring radiation fluxes, to instrument test articles for nuclear flux instruments, to make nuclear measurements, and to calibrate measuring equipment. The laboratory contains ample electronics equipment, as well as special items, including dosimeters, spectrometers, thermal-neutron counters, calorimeters, instrumentation for special radiation hazards measurements, and necessary miscellaneous equipment.

The Critical Experiment Facility houses the Critical Experiment Reactor, which is a low-power (thermal power - 80 watts) open-pool type reactor, using highly enriched uranium for fuel. This reactor will be used to perform critical experiments relative to the equipment to be installed in the Plumbrook Reactor.

5.3.2 Air Force Plant 6

The instrumentation and circuits laboratory, equipped with the most modern equipment, yields an extremely flexible and versatile capability. This includes the design of special instrumentation required for specific programs.

Extensive test equipment is available at the structures laboratory for determining mechanical properties of structural materials and for establishing specification or conformance to specifications. This laboratory provides a means for making materials property investigations, vibration and fatigue tests, and static tests. Equipment is available for testing small structural components as well as full scale structural assemblies.

Facilities are available at the metallurgical laboratory for metallurgical micro- and macro-graphic investigations.

Supporting equipment at AFP 6 includes capabilities for sectioning, mounting, polishing (mechanical or electrolytic), and etching metallic specimens; examining metallurgical specimens (both visual and photographic) at magnifications of 1 to 2000 diameters under bright field, dark field, and polarized illumination; making hardness determinations (Rockwell and Brinell) and micro-hardness surveys (Knoop and DPH); determining surface roughness (rms) and surface contour; defining plating or coating thickness; and accomplishing metallurgical, photographic, and darkroom work in both black and white and color.

Additionally, the metallurgical laboratory includes heat treatment facilities capable of reaching temperatures as high as 2400°F, with specialized heating applications, such as localized hardening and softening, brazing, and melting, and complete facilities for X-ray diffraction and fluorescent analysis. The laboratory facility is supported by the services of a complete chemistry laboratory.

Supporting all these facilities is the Engineering Scientific and Technical Information Department. There, an integrated and continuous scientific and technical information program is planned, developed, and maintained. Consultant services are provided on current and anticipated information problems and requirements. Direct affiliations are maintained with AEC, ASTIA, NASA, the Library of Congress, Army, Navy, Air Force, and other governmental and industrial information centers.

5.3.3 Machine Shop and Fabrication Facilities

Machine shop and fabrication facilities for this program are presently available at three locations -- the Georgia Nuclear Laboratories, the Lockheed Missiles and Space Division, and AFP 6. In addition, Lockheed is constructing a new shop in Atlanta, Georgia. The capabilities of all these facilities are described in this section.

5.3.3.1 GNL Shop Facilities

A mechanical maintenance and research machine shop in the Radiation Effects Laboratory area is used to fabricate test components and equipment, to modify and construct tools for remote operations, and to perform any machine work that may be required.

5.3.3.2 Atlanta Shop Facilities

Lockheed is currently equipping a new nuclear machine shop and fabrication facility in Atlanta, which is scheduled for early completion. This facility will include a development shop, a subcritical shop, and an electrical-electronic shop for handling and fabricating nuclear materials and supporting test processes. The shop area includes 4,800 square feet of space, and an adjoining building with 21,000 square feet of potential manufacturing and assembly area is available for expansion of the shop as needed.

5.3.3.3 Missiles and Space Division Shop Facilities

A complete shop for machining toxic materials, such as beryllium, is maintained in a specially air-conditioned room at the Lockheed MSD. All machines are enclosed in air boxes held in a condition of slight vacuum. Special centrifuge and filtering equipment protects the workers and outside areas from contamination by dust and heavier particles of the toxic materials being machined.

5.3.3.4 Air Force Plant 6 Shop Facilities

Lockheed has available at its Marietta plant ample facilities for performing all fabrication type operations, including many precision machines suitable for preparing test specimens.

5.3.4 Computing Facilities

The Mathematical Analysis Department furnishes high-speed digital and analog computational services. To provide such services, some of the best electrical digital and analog computer equipment commercially available is used. The digital equipment consists of an IBM-704 and a Bendix Digital Differential Analyzer. The analog facilities include a Beckman EASE electronic analog computer and a Computer Engineering Associates Direct Analogy Electric Analog Computer. A well trained and experienced staff of applied mathematicians, physicists, engineers, and other specialists is available for complete service. Auxiliary punch card equipment is available to aid in preparing programs and data for the IBM-704 system. This equipment consists of key punches, verifiers, a card-to-paper tape punch, a paper tape-to-card converter, a reproducer, a collator, an electronic card sorter, and an IBM-407 electronic accounting machine.

5.4 ARTHUR D. LITTLE, INC.

The special cryogenic capabilities of Arthur D. Little, Inc., are described in this section. This company is one of the oldest, largest, and most diversified research organizations in the United States. Since its founding, in 1886, and subsequent incorporation in 1909, the Company has expanded so that today its staff numbers over 1,000 people, more than half of whom are professionally trained scientists and engineers versed in nearly every field of science and technology.

The Company is divided into several major operating divisions, each associated with a general field of technical, scientific, or economic activity. These segments are individually subdivided into a number of relatively specialized technical groups, operating within the overall sphere of interest of the parent division. Thus, groups dealing in applied stress analysis, heat transfer, or hydrodynamics are administered by the Engineering Division; those specializing in applied chemistry and plastics are administered by the Research and Development Division; while basic scientific research is handled in the Advanced Research Division.

The policy of the Company is to provide maximum fluidity of the professional staff across divisional and group boundaries. This flexibility of operation enables an unusually wide range of talent and experience to be focused on any given problem. Task forces of Arthur D. Little, Inc., staff members can be assembled for each project or stage of a project; the team thus formed combines the skills appropriate to the job in question. This versatility of organization, coupled with extensive and flexible facilities, accounts in a large part for the successful handling of a variety of assignments.

5.4.1 Experience

Extensive experience in solving research and development problems for industry and government has been gained in dealing with problems that require more than specialized technical information or standard research techniques. This has often included helping to define problems, placing them in the right perspective, and attacking them from the viewpoint of several scientific disciplines.

The range of scientific talent and engineering skill at hand is not limited to the professional staff alone. Expert consulting liaison is maintained with staff members of nearby Massachusetts Institute of Technology; Harvard University, and similar institutions.

Arthur D. Little, Inc., has been engaged for many years in work for various agencies of the United States Government and has undertaken numerous subcontracts for industrial prime contractors. This has provided a thorough knowledge of the procedures and practices common to government contract research and engineering.

5.4.2 Facilities

The Cambridge laboratories and offices of Arthur D. Little comprise a total area of approximately 300,000 square feet. The laboratories are designed for optimum efficiency in conducting research and development work and they permit flexible operation.

Special purpose laboratories are available for conducting temperature and humidity experiments and work in low temperatures, the biological sciences, flavor and odor problems, explosives and propellants, and radioactive materials.

Special research tools include a solar imaging furnace for high-temperature research to 3200°C, ultraviolet and infrared spectrophotometers, X-ray diffraction equipment, an electron microscope, a mass spectrometer, vacuum coaters, high-pressure equipment, and low-temperature research equipment. A digital computer and associated data processing equipment are also available.

Process engineering facilities at Arthur D. Little include equipment for studying unit operations in distillation, filtration, evaporation, drying, liquid-liquid extraction, and heat transfer.

A separate pilot plant building at the Acorn Park Laboratories provides over 2,000 square feet of floor space, as well as a laboratory for small-scale bench work and process control purposes. The facilities also include a complete installation for a fluidized bed operation.

A shop area of over 27,000 square feet is devoted to prototype development and fabrication. This facility includes an adequate machine shop, a high- and low-bay erection and assembly areas, and equipment for operation, test, and inspection of completely assembled units and integrated systems. Shop personnel have had many years experience on prior assignments and have developed an unusually high degree of skills and craftsmanship in precision machining and assembly, high vacuum techniques, and the development of test programs to ensure reliable operating units.

Where unusual machine tool facilities are required, the services of numerous machine tool specialists located in and around the New England area are available. Final assembly and test is always undertaken at the facilities where the system can best be tested as a complete unit. Both engineering and shop personnel are available for installation, maintenance, and servicing at any time.

Because of the wide variety of development programs undertaken in the engineering shop, the physical facilities must be of a general nature. Emphasis has been on acquiring a staff with training and experience over a broad field. The present staff includes specialists in all types of welding, instrumentation, vacuum technology, control systems, precision assembly, experimental fabrication assembly, low-temperature technology, use of special materials and techniques, and magnetic circuitry.

5.4.3 Cryogenic Capabilities

Development of specialized cryogenic processes and equipment has been one of the main interests at Arthur D. Little, Inc., during the past decade. Experience gained in designing, fabricating, and operating a wide range of prototypes under field conditions has provided extensive information in cryogenic process design, machine design, fluid dynamics, high vacuums, piping, structural analysis, thermal stresses, and other technical areas allied to the field of cryogenics. Several of the projects typical of those the Company has conducted in the past few years are discussed in the following paragraphs.

Extensive work on the propellant loading systems for the Atlas, Titan, and Thor missiles has resulted in a fully integrated cryogenic process design team. With strong experience in the problems associated with large-scale handling of cryogenic fluids, the team is capable of unusually advanced engineering in thermodynamics, fluid dynamics, and other specialized fields associated with the design of cryogenic systems.

Arthur D. Little, Inc., has designed special equipment for the handling of liquid oxygen and has constructed a scaled test facility at Cambridge. Here, during the past year, has been carried out an extensive test program, in which investigations have been conducted on the following:

- Thermal stresses that are set up in the pipelines during the flow of cryogenic fluids
- Effects of weather conditions on the rate of evaporation of liquid oxygen and nitrogen from insulated and uninsulated tanks of various sizes and shapes
- Quantity of liquid oxygen boiled off in cooling down transfer lines and components during transfer

- Sensitivity of materials to detonation under impact in the presence of liquid oxygen

- Various methods and devices for gaging and measuring the density of liquid oxygen in simulated missile tanks

- Two-phase fluid flow dynamics in flow through various pipeline configurations and assorted hardware

- Transient pressures associated with line cooldown

- Frost formation uninsulated surfaces cooled by liquid oxygen or nitrogen

- Pressurized gas transfer of liquid oxygen and nitrogen from storage tanks including studies of gas diffuser designs, condensation phenomena, and energy output to the transferred fluid

- Pumping, with single or parallel pumps, such fluids as liquid oxygen and nitrogen

- Problems involved in providing tight gaskets and seals exposed to cryogenic fluids

The design of propellant loading systems for these missiles within the relatively short time schedules has required the formation of a closely knit team of scientists and engineers with a wide variety of skills; it has also required solving problems in the field of thermodynamics, fluid flow, stress analysis, chemistry, physics, and electronics.

In addition to being responsible for research and design work on the propellant loading systems for Atlas, Titan, and Thor, Arthur D. Little, Inc., is participating in the Atlas Evaluation Test program at Edwards Rocket Base and will be associated with similar operations for the Titan missile.

Typical of activities in the cryogenic field is the work on refrigerated transport dewars for liquefied hydrogen. The design and development of the components of this system required intimate knowledge of machine design, thermodynamics, heat transfer, fluid flow, lubrication, and a host of other specialties. The components included the following:

- A special refrigerator employing helium gas as the refrigerant

- A liquid hydrogen transfer line with the necessary elbows and quick-disconnect couplings

The valving and associated transfer tubing developed under this contract have proved to be operationally useful and effective, and 18 of these 2000-liter refrigerated dewars were constructed.

This program represented a significant advance in the field of cryogenics. The equipment was designed to store, transport, and handle fairly large quantities of liquid hydrogen with very little loss. The successful operation of these units when they were first built permitted broader use of hydrogen for two important reasons:

- Liquid hydrogen could be stored while conversion from the ortho to the para form takes place without loss despite the heat evolved in this process.

- The units permitted more effective use of hydrogen liquefiers in that the product could be utilized when and where desired rather than adjacent to the liquefier at the time of manufacture.

Some of the refrigerators have been adapted for use as research tools. One, for example, was redesigned and rebuilt to provide refrigeration to condense the entire nitrogen gas stream in a high-Mach-number, rarefied-gas-flow wind tunnel. Another unit is used to provide 20°K refrigeration for radiation damage studies in one hole of a nuclear reactor. It has run more than 4,000 hours, operating 24 hours per day for one- and two-week periods with only routine maintenance.

Another project was a study of the separation of deuterium by means of low-temperature techniques. The program included theoretical and pilot-plant studies of heat-exchanger configurations for the freeze-out of nitrogen in a hydrogen stream and a calorimetric study of various types of insulation. The program included construction and operation of a pilot plant.

For the Air Materiel Command, an air-transportable liquid-oxygen plant of 10-ton-per-day nominal capacity, known as the Type A-4, was successfully developed, designed, fabricated, and installed. The unit, which uses atmospheric air as the source of oxygen, was designed for a low-pressure process cycle involving a reversing heat exchanger that performs the dual functions of efficient exchange of heat and the removal of impurities such as water vapor and carbon dioxide from the input air. Refrigeration is supplied by direct expansion of a portion of the input air in a turbo-expander, and separation of liquid oxygen is accomplished in a rectifying column.

In the A-4 generator program, efficiency, minimum size and weight, self-sufficiency except for fuel and lubricating oil, and purity of product were the primary objectives.

Arthur D. Little, Inc., has designed and developed a 10,000-psi liquid-nitrogen pump and vaporizer. The successful operation of this system depended to a great extent on the development of special packing and vaporizer, all of which required extensive thermodynamic and machine-design analysis. Because of the low temperature encountered, the components were fabricated of stainless steel. The chrome-plated piston of the pump operates through a packing-gland cell at a temperature of -320°F. The system is hydraulically operated. The project included the testing of an experimental unit as well as the construction of a larger (40,000 scfh) system, now installed and successfully operating at Edwards Air Force Base.

Other contracts have included the design of a 500-lb-per-hr-skid-mounted liquid-oxygen generator, the design and fabrication of a two-ton-per-day trailer-mounted gaseous-oxygen plant, the design and fabrication of a helium refrigerator for use in recondensing the boil-off losses from a large oxygen-storage tank, the prosecution of an extensive calorimetric program for evaluating reflective surfaces used in low-temperature apparatus to 20°K, and the design of a trailer-mounted, helium-refrigerated, hydrogen liquefier having a nominal capacity of 150 liters per hour.

A study concerning different methods of transporting liquid fluorine has been completed and a mechanically refrigerated liquid-fluorine semitrailer has been built. The study conducted under this contract was submitted to the client in the form of a comprehensive report, dealing with the physical and chemical properties of fluorine, its physiological effects, and methods of disposal. The report also treats subjects that include materials of construction for tanks and insulation; valves, gages, liquid-level indicators, and associated hardware; methods of storage and transportation, including a comparison of three feasible systems; and transfer methods and equipment.

An 18-liter-per-hour hydrogen liquefier was designed and built for the NACA flight propulsion laboratory in Cleveland. This is the first U. S. hydrogen liquefier to operate with expansion-engine refrigeration; the maximum process pressure is less than 300 psia.

Beginning in 1954, nine semitrailers for the transport of liquid nitrogen and oxygen were produced for an industrial gas producer. These units have capacities up to 3,500 gallons. In years of rugged use over the highways of several states, the sealed vacuum insulation used in these units has an outstanding service record. Losses due to boil-off are less than 3/4 of 1% per day.

Another important civilian program concerns the generation, storage, and handling of large quantities of liquefied hydrocarbons. One part of this program included evaluating a large number of different refrigeration cycles.

In addition to the equipment designed and fabricated for governmental agencies, Arthur D. Little, Inc., is actively engaged in producing cryogenic equipment for industrial research and manufacturing. Proprietary equipment includes several basic research tools that have been developed for use in cryogenics. Among these is the ADL-Collins Helium Cryostat, a helium liquefier, and a refrigerator that can attain temperatures down to 2° Kelvin. Over 150 of these units have been installed.

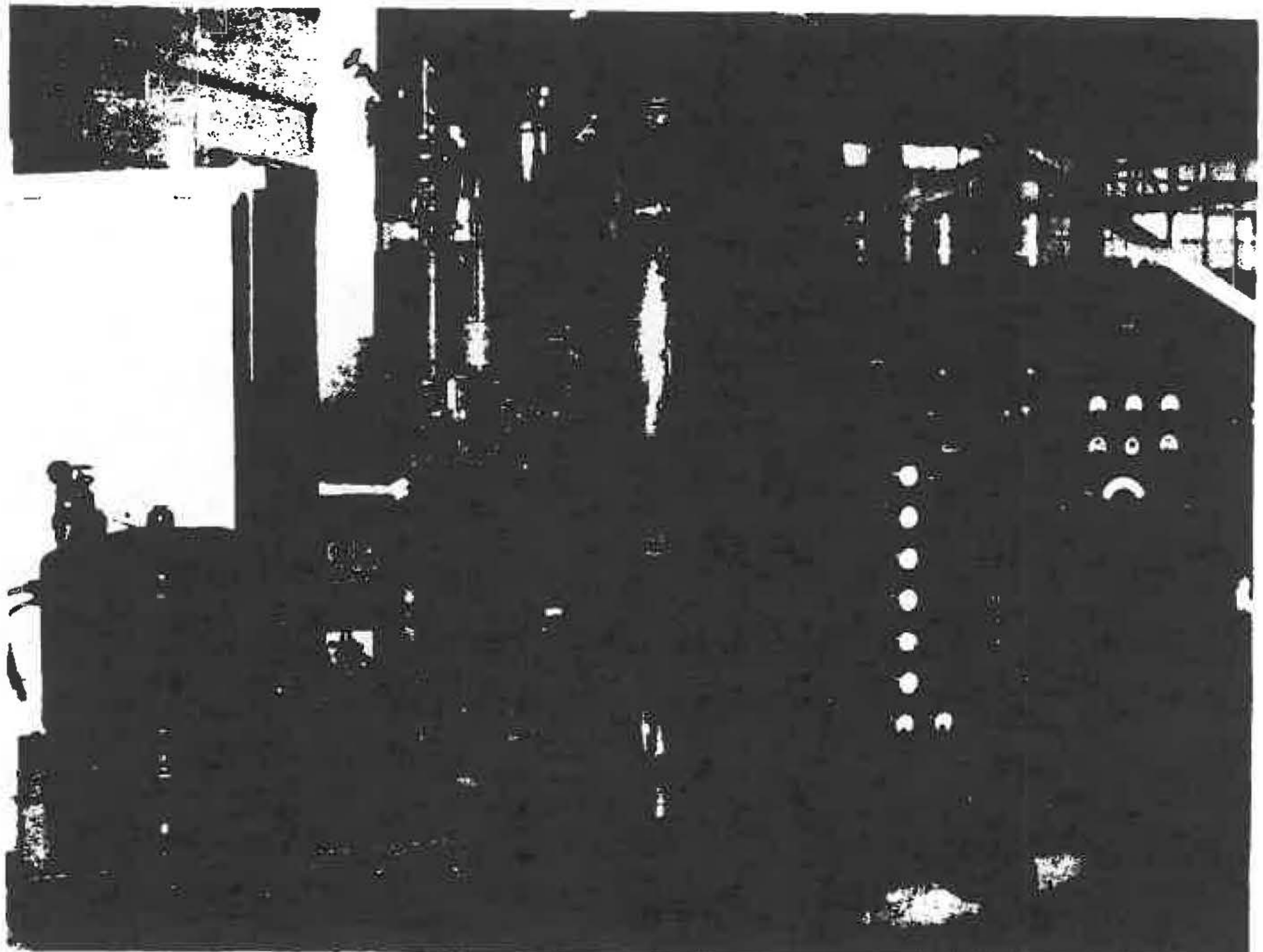

36°R REFRIGERATOR FOR OAK RIDGE NATIONAL LABORATORY

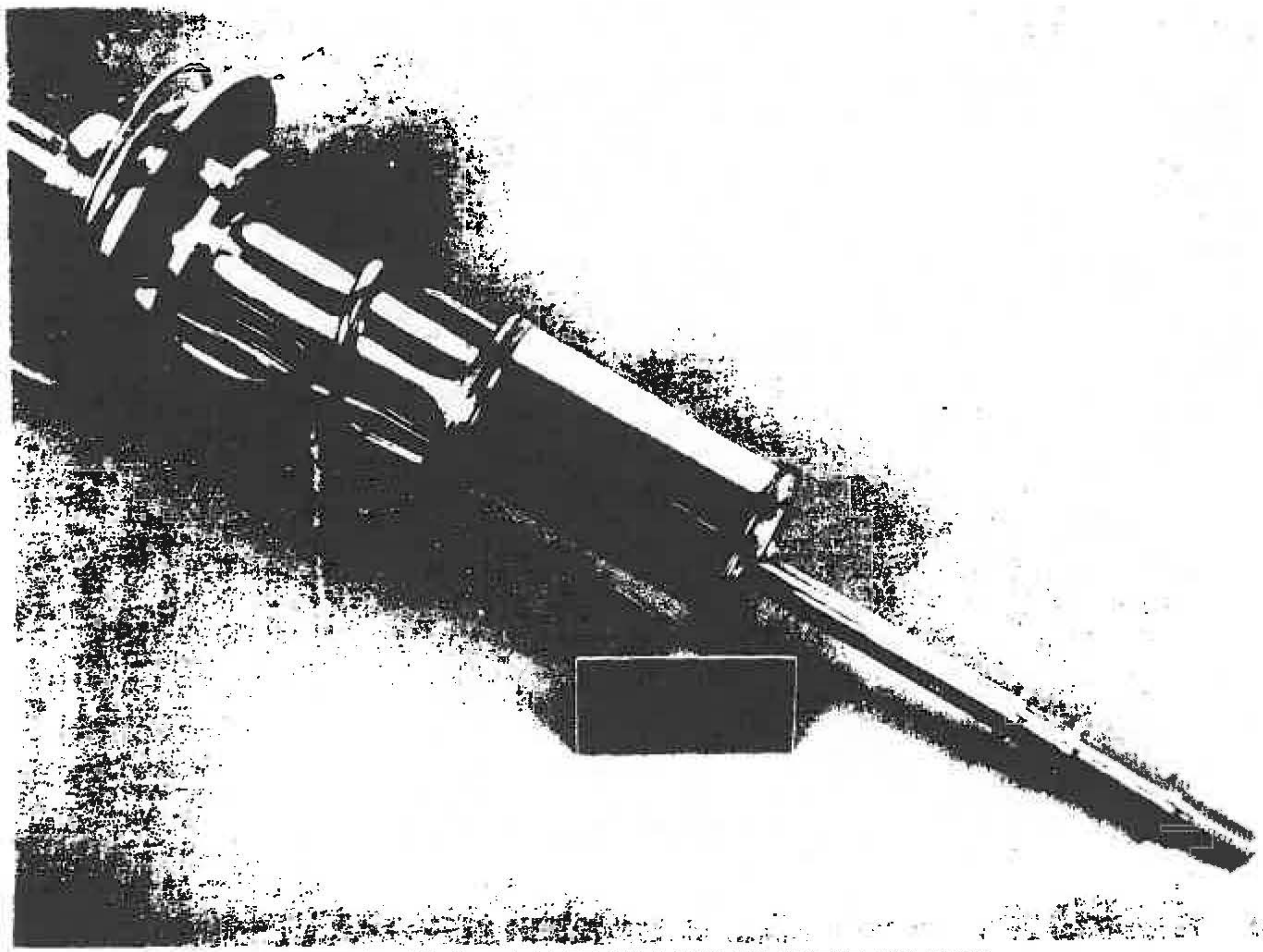

INTERIOR OF 20,000-LB TENSILE TEST CRYOSTAT FOR 7.5°R

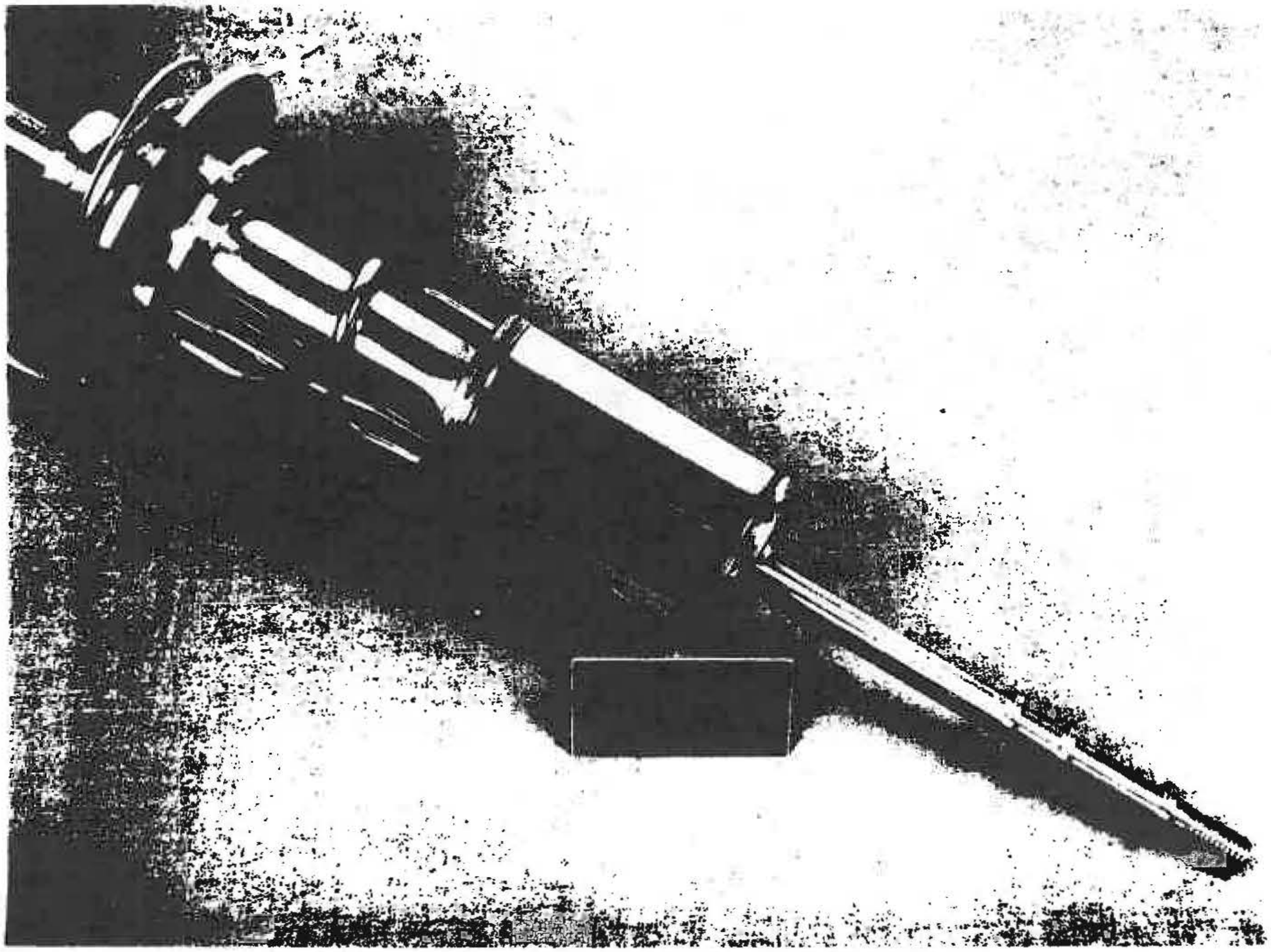

INTERIOR OF 20,000-LB TENSILE TEST CRYOSTAT FOR 7.5°R

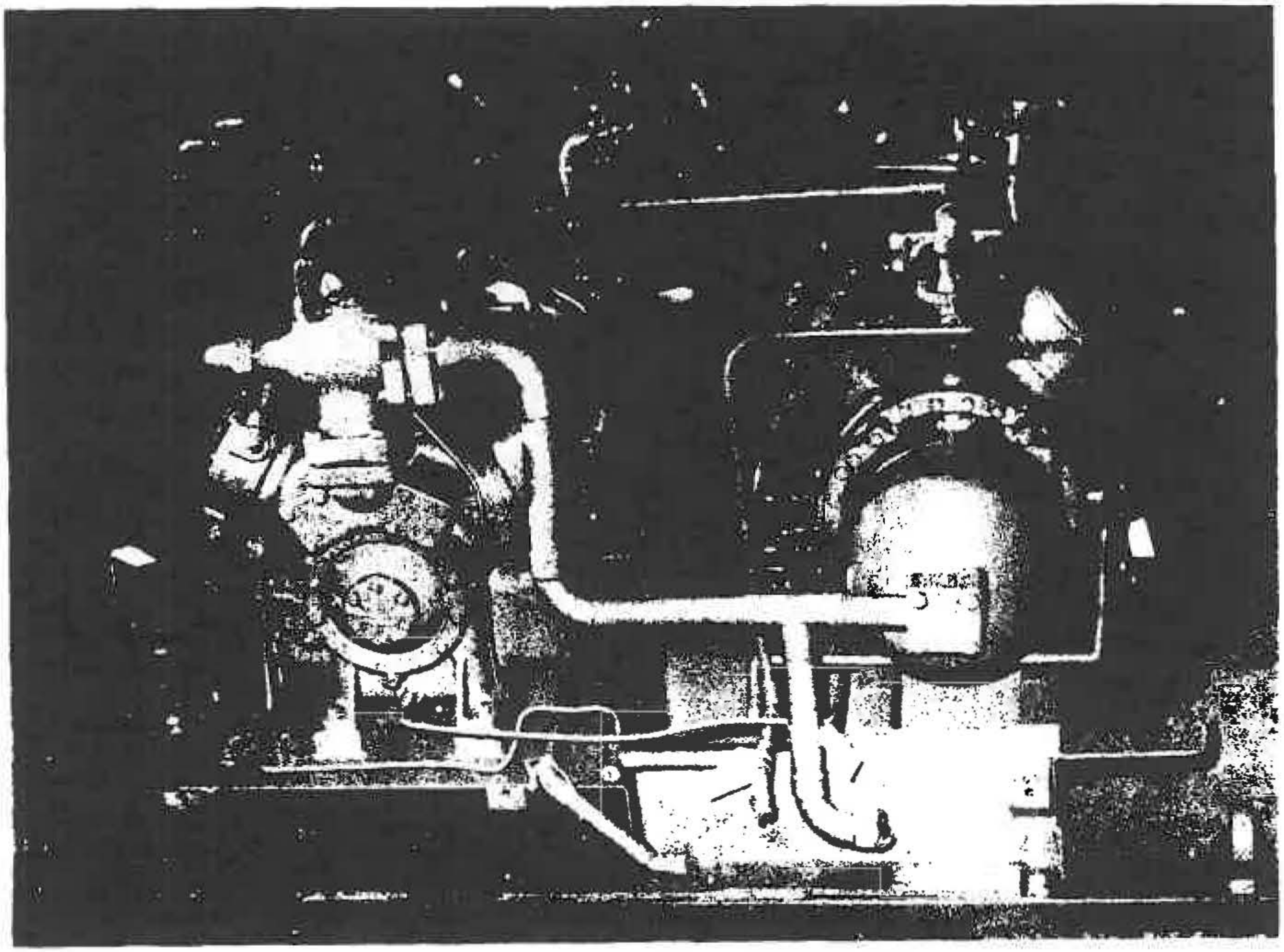

COMPRESSOR SKID FOR ORNL REFRIGERATOR

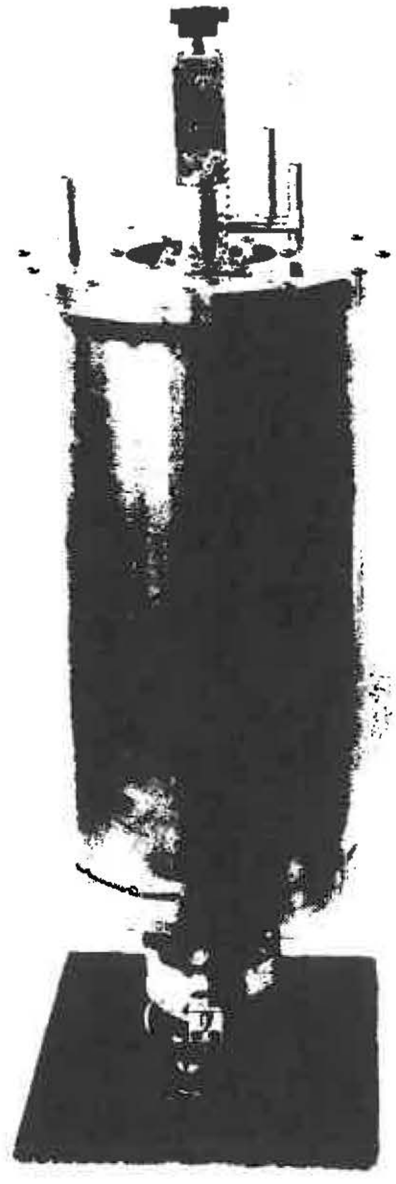

LIQUID-HELIUM COLD CELL FOR USE WITH AN X-RAY DIFFRACTOMETER

6. SCHEDULE

A schedule of design, construction, installation, and testing for the proposed program is shown in Figure 37. The assumption is made that the beam hole shields can be installed in May and the first test at Plumbrook can begin in September. This is, of course, contingent upon the schedule of the Plumbrook reactor. If criticality and first experiment dates of this reactor are altered, this portion of the schedule must be altered accordingly.

CONFIDENTIAL

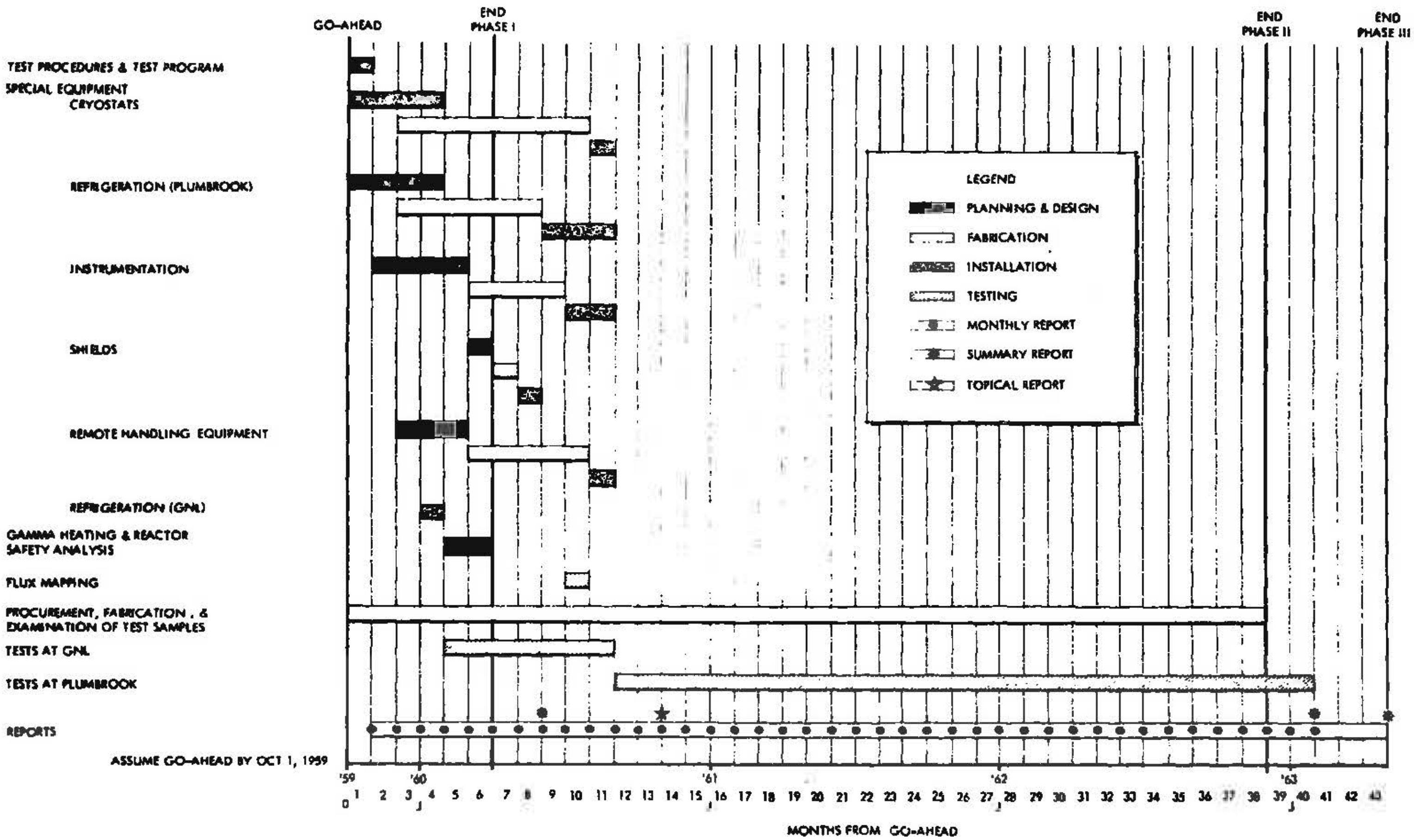

FIGURE 37 SCHEDULE FOR PROGRAM ON NUCLEAR RADIATION EFFECTS IN MATERIALS AT CRYOGENIC TEMPERATURES

CONFIDENTIAL

APPENDIX - A

TABLE

The test program, is tabulated in Tables I through III, Tables IV through IX and Tables XI and XII list for each particular test the several conditions of interest. Table X summarizes the materials and tests for a particular application, thus corresponds to Table I of RFQ HS-225.

CONFIDENTIAL

TABLE I - TEST PROGRAM, PART I - CORRELATION

Test Conditions	Type of Specimen	Tensile	Fatigue	Creep	Tensile Impact	Tensile Notch	Buckling	Tensile Shear	Number of Materials	Number Tests Per Material	Total Tests
Round Specimens											
Room Temp.	Reg.	5		5	5				3	15	45
Room Temp.	Min.	5		5	5				3	15	45
139° R	Reg.	5		5	5				3	15	45
139° R	Min.	5		5	5				3	15	45
Flat Specimens											
Room Temp.	Reg.	5	5	5		5	5	5	3	30	90
Room Temp.	Min.	5	5	5		5	5	5	3	30	90
139° R	Reg.	5	5	5		5	5	5	3	30	90
139° R	Min.	5	5	5		5	5	5	3	30	90

CONFIDENTIAL

TABLE II TEST PROGRAM, PART I, SCREENING

Test Conditions	Tensile	Fatigue	Creep	Tensile Notch	Tensile Impact	Buckling	Shear	Wear	Number of Materials	Number Tests per Material	Total Tests
Pressure Shell											
Room Temperature	5	5		5		5			3	20	60
36° R	5	5		5		5			3	20	60
$10^{17} n/cm^2$ at 36° R	5			5					3	10	30
Tank											
Room Temperature	5			5		5			6	15	90
36° R	5			5		5			6	15	90
$10^{17} n/cm^2$ at 36° R	5			5					6	10	60
Pump											
Room Temperature	5	5	5		5				14	20	280
36° R	5	5	5		5				14	20	280
$10^{17} n/cm^2$ at 36° R	5				5				14	10	140
Bearings											
Room Temperature								5	63	5	315
36° R								5	63	5	315
$10^{17} n/cm^2$ at 36° R								5	63	5	315
Seals											
Room Temperature								5	14	5	70
36° R								5	14	5	70
$10^{17} n/cm^2$ at 36° R								5	14	5	70
Room Temperature		5					5		7	10	70
36° R		5					5		7	10	70
$10^{17} n/cm^2$ at 36° R		5					5		7	10	70

CONFIDENTIAL

TABLE III TEST PROGRAM PART II

Test Conditions	Stress Condition	Tensile	Tensile Notch	Buckling	Fatigue	No. of Matls.	No. of Tests Per Matl.	Total Tests
Pressure Shell								
Room Temp.		27	27	27	27	2	108	216
T_1 ($36^\circ R$)		27	27	27	27	2	108	216
$5x10^{17} n/cm^2$ at T_1		27	27	27	27	2	108	216
$5x10^{17} n/cm^2$ at T_1	Stressed	6	6	6	6	2	24	48
T_2		6	6	6	6	2	24	48
$5x10^{17} n/cm^2$ at T_2		6	6	6	6	2	24	48
$5x10^{17} n/cm^2$ at T_2	Stressed	6	6	6	6	2	24	48
T_3		6	6	6	6	2	24	48
$5x10^{17} n/cm^2$ at T_3		6	6	6	6	2	24	48
$5x10^{17} n/cm^2$ at T_3	Stressed	6	6	6	6	2	24	48
TANK								
Room Temp.		27	27	27	27	2	108	216
T_1 ($36^\circ R$)		27	27	27	27	2	108	216

CONFIDENTIAL

TABLE III TEST PROGRAM PART II (Continued)

Test Conditions	Stress Condition	Tensile	Tensile Notch	Buckling	Fatigue	No. of Matls.	No. of Tests Per Matl.	Total Tests
TANK (Cont'd.)								
10^{17} n/cm^2 at T_1		27	27	27	27	2	108	216
10^{17} n/cm^2 at T_1	Stressed	6	6	6	6	2	24	48
5×10^{15} n/cm^2 at T_1		6	6	6	6	2	24	48
5×10^{15} n/cm^2 at T_1	Stressed	6	6	6	6	2	24	48
2×10^{16} n/cm^2 at T_1		6	6	6	6	2	24	48
2×10^{16} n/cm^2 at T_1	Stressed	6	6	6	6	2	24	48
T_2		6	6	6	6	2	24	48
10^{17} n/cm^2 at T_2		6	6	6	6	2	24	48
10^{17} n/cm^2 at T_2	Stressed	6	6	6	6	2	24	48
5×10^{15} n/cm^2 at T_2		6	6	6	6	2	24	48
5×10^{15} n/cm^2 at T_2	Stressed	6	6	6	6	2	24	48
2×10^{16} n/cm^2 at T_2		6	6	6	6	2	24	48

CONFIDENTIAL

TABLE III TEST PROGRAM PART II (Continued)

Test Conditions	Stress Condition	Tensile	Tensile Notch	Buckling	Fatigue	No. of Matls.	No. of Tests Per Matl.	Total Tests
TANK (Cont'd.)								
$2x10^{16} n/cm^2$ at T_2	Stressed	6	6	6	6	2	24	48
T_3		6	6	6	6	2	24	48
$10^{17} n/cm^2$ at T_3		6	6	6	6	2	24	48
$10^{17} n/cm^2$ at T_3	Stressed	6	6	6	6	2	24	48
$5x10^{15} n/cm^2$ at T_3		6	6	6	6	2	24	48
$5x10^{15} n/cm^2$ at T_3	Stressed	6	6	6	6	2	24	48
$2x10^{16} n/cm^2$ at T_3		6	6	6	6	2	24	48
$2x10^{16} n/cm^2$ at T_3	Stressed	6	6	6	6	2	24	48

Test Conditions	Stress Condition	Tensile	Fatigue	Creep	Tensile Impact	No. of Matls.	No. of Tests Per Matl.	Total Tests
PUMP								
Room Temp.		27	27	27	27	1	108	108
T_1 (36^oR)		27	27	27	27	1	108	108

CONFIDENTIAL

TABLE III TEST PROGRAM PART II (Continued)

Test Conditions	Stress Condition	Tensile	Fatigue	Creep	Tensile Impact	No. of Matl.s	No. of Tests Per Matl.	Total Tests
PUMP (Cont'd)								
10^{17} n/cm^2 at T_1		27	27	27	27	1	108	108
10^{17} n/cm^2 at T_1	Stressed	6	6	6	6	1	24	24
5×10^{15} n/cm^2 at T_1		6	6	6	6	1	24	24
5×10^{15} n/cm^2 at T_1	Stressed	6	6	6	6	1	24	24
2×10^{16} n/cm^2 at T_1		6	6	6	6	1	24	24
2×10^{16} n/cm^2 at T_1	Stressed	6	6	6	6	1	24	24
T_2		6	6	6	6	1	24	24
10^{17} n/cm^2 at T_2		6	6	6	6	1	24	24
10^{17} n/cm^2 at T_2	Stressed	6	6	6	6	1	24	24
5×10^{15} n/cm^2 at T_2		6	6	6	6	1	24	24
5×10^{15} n/cm^2 at T_2	Stressed	6	6	6	6	1	24	24
2×10^{16} n/cm^2 at T_2		6	6	6	6	1	24	24

TABLE III TEST PROGRAM PART II (Continued)

Test Conditions	Stress Condition	Tensile	Fatigue	Creep	Tensile Impact	No. of Matls.	No. of Tests Per Matl.	Total Tests
PUMP (Cont'd.)								
$2x10^{16} n/cm^2$ at T_2	Stressed	6	6	6	6	1	24	24
T_3		6	6	6	6	1	24	24
$10^{17} n/cm^2$ at T_3		6	6	6	6	1	24	24
$10^{17} n/cm^2$ at T_3	Stressed	6	6	6	6	1	24	24
$5x10^{15} n/cm^2$ at T_3		6	6	6	6	1	24	24
$5x10^{15} n/cm^2$ at T_3	Stressed	6	6	6	6	1	24	24
$2x10^{16} n/cm^2$ at T_3		6	6	6	6	1	24	24
$2x10^{16} n/cm^2$ at T_3	Stressed	6	6	6	6	1	24	24

Test Conditions	Stress Condition	Tensile	Buckling	Fatigue	Creep	Impact	No. of Matls.	No. of Tests Per Matl.	Total Tests
REFLECTOR									
Room Temp.		5	5	5	5	5	1	25	25
T_1 (36^oR)		5	5	5	5	5	1	25	25

CONFIDENTIAL

TABLE III TEST PROGRAM PART II (Continued)

Test Conditions	Stress Condition	Tensile	Buckling	Fatigue	Creep	Impact	No. of Matls.	No. of Tests Per Matl.	Total Tests
REFLECTOR (Cont'd.)									
10^{18} n/cm^2 at T_1		5	5	5	5	5	1	25	25
10^{18} n/cm^2 at T_1	Stressed	5	5	5	5	5	1	25	25
T_2		5	5	5	5	5	1	25	25
10^{18} n/cm^2 at T_2		5	5	5	5	5	1	25	25
10^{18} n/cm^2 at T_2	Stressed	5	5	5	5	5	1	25	25
T_3		5	5	5	5	5	1	25	25
10^{18} n/cm^2 at T_3		5	5	5	5	5	1	25	25
10^{18} n/cm^2 at T_3	Stressed	5	5	5	5	5	1	25	25

Test Conditions	Bellows Ductility	Bellows Endurance	Bellows Torsion	No. of Matls.	No. of Tests Per Matl.	Total Tests
SEALS						
Room Temp.	5	5	5	1	15	15
T_1 (36°R)	5	5	5	1	15	15

CONFIDENTIAL

TABLE III TEST PROGRAM PART II (Continued)

Test Conditions	Bellows Ductility	Bellows Endurance	Bellows Torsion	No. of Matls.	No. of Tests Per Matl.	Total Tests
SEALS (Cont.d)						
10^{17}n/cm^{2}at T_1	5	5	5	1	15	15
5×10^{15}n/cm^{2}at T_1	5	5	5	1	15	15
2×10^{16}n/cm^{2}at T_1	5	5	5	1	15	15
T_2	5	5	5	1	15	15
10^{17}n/cm^{2}at T_2	5	5	5	1	15	15
5×10^{15}n/cm^{2}at T_2	5	5	5	1	15	15
2×10^{16}n/cm^{2}at T_2	5	5	5	1	15	15
T_3	5	5	5	1	15	15
10^{17}n/cm^{2}at T_3	5	5	5	1	15	15
5×10^{15}n/cm^{2}at T_3	5	5	5	1	15	15
2×10^{16}n/cm^{2}at T_3	5	5	5	1	15	15

TABLE III TEST PROGRAM PART II (Continued)

Test Conditions	Wear	No. of Matls.	No. of Tests Per Matl.	Total Tests
SEALS (Cont'd.)				
Room Temp.	27	3	27	81
T_1 (36^oR)	27	3	27	81
$10^{17} n/cm^2$ at T_1	27	3	27	81
$5x10^{15} n/cm^2$ at T_1	6	3	6	18
$2x10^{16} n/cm^2$ at T_1	6	3	6	18
T_2	6	3	6	18
$10^{17} n/cm^2$ at T_2	6	3	6	18
$5x10^{15} n/cm^2$ at T_2	6	3	6	18
$2x10^{16} n/cm^2$ at T_2	6	3	6	18
T_3	6	3	6	18
$10^{17} n/cm^2$ at T_3	6	3	6	18

CONFIDENTIAL

TABLE III TEST PROGRAM PART II (Continued)

Test Conditions	Wear	No. of Matls.	No. of Tests Per Matl.	Total Tests
SEALS (Cont.d)				
5×10^{15} n/cm^2 at T_3	6	3	6	18
2×10^{16} n/cm^2 at T_3	6	3	6	18
BEARINGS				
T_1 (36°R)	27	3	27	81
10^{17} n/cm^2 at T_1	27	3	27	81
5×10^{15} n/cm^2 at T_1	6	3	6	18
2×10^{16} n/cm^2 at T_1	6	3	6	18
T_2	6	3	6	18
10^{17} n/cm^2 at T_2	6	3	6	18
5×10^{15} n/cm^2 at T_2	6	3	6	18
2×10^{16} n/cm^2 at T_2	6	3	6	18

TABLE III TEST PROGRAM PART (Continued)

Test Conditions	Wear	No. of Matls.	No. of Tests Per Matl.	Total Tests
BEARINGS (Cont'd.)				
T_3	6	3	6	18
10^{17} n/cm^2 at T_3	6	3	6	18
5×10^{15} n/cm^2 at T_3	6	3	6	18
2×10^{16} n/cm^2 at T_3	6	3	6	18

CONFIDENTIAL

TABLE IV - TENSILE TESTS

	Alloys	Alloy Forms	Batches	Thickness of Alloy	Grain Directions	Stress Condition	Test Temps.	Dose Levels	Total Specimens
PART I									
Correlations Standard & Miniature	3	2	1	1	1	1	2	0	120
PART I									
Screening	21	2	1	1	1	1	2	1	345
PART II									
Basic Program	4	2	3	1	2	2	4	5	881

ALLOYS:

Aluminum 2014, 2024, 5052, 6061, 7075
Alco 355
AM 35
Beryllium
Inconel X
Monel
Stainless Steel 301, 304, 304 L, 347, 17-4PH, 17-7PH
*Stainess Steel 416, 431
Titanium 6% Al, 4% V; Titanium 4% Al, 5% V
Tool Steel

* It is believed that these alloys will be eliminated from the basic program due to brittle properties at 36°R.

CONFIDENTIAL

CONFIDENTIAL

TABLE V - TENSILE NOTCH TESTS

	Alloys	Alloy Forms	Batches	Thickness of Alloy	Grain Directions	Stress Condition	Test Temps.	Dose Levels	Total Specimens
PART I Correlations Standard & Miniature	3	1	1	1	1	1	2	0	120
PART I Screening	21	2	1	1	1	1	2	1	345
PART II Basic Program	3	2	2	1	2	2	4	5	881

ALLOYS:

Aluminum 2014, 2024, 5052, 6061, 7075
Alco 355
AM 35
Beryllium
Inconel X
Monel
Stainless Steel 301, 304, 304 L, 347, 17-4PH, 17-7PH
*Stainless Steel 416, 431
Titanium 6% Al, 4% V; Titanium 4% Al, 5% V
Tool Steel

*It is believed that these alloys will be eliminated from the basic program due to brittle properties at 36°R.

CONFIDENTIAL

TABLE VI - BUCKLING TESTS

	Alloys	Alloy Forms	Batches	Thicknesses of Alloy	Grain Directions	Stress Conditions	Test Temps	Dose Levels	Total Specimens
PART I Screening	9	1	1	1	1	1	2	0	150

ALLOYS:
- Aluminum 2014, 5052
- Stainless Steel 301, 304L
- Inconel X
- Tool Steel
- Beryllium
- Titanium 4% Al, 5% V; 6% Al, 4% V

CONFIDENTIAL

TABLE VII - CREEP TESTS

	Alloys	Alloy Forms	Batches	Thickness of Alloy	Grain Directions	Stress Condition	Test Temps.	Dose Levels	Total Specimens
PART I									
Screening	14	2	1	1	1	1	2	0	260
PART II									
Basic Program	2	2	2	1	2	2	4	4	245

ALLOYS:

Aluminum 2014, 6061, 7075
Alco 355
Beryllium
Stainless Steel AM 35, 17-4PH, 17-7PH, 304, 347
*Stainless Steel 416, 431
Titanium 6% Al, 4% V; 4% Al, 5% V

*It is believed that these alloys will be eliminated from the basic program due to brittle properties at 36°R.

CONFIDENTIAL

TABLE VIII - FATIGUE TESTS

	Alloys	Alloy Forms	Batches	Thicknesses of Alloy	Grain Directions	Stress Conditions	Test Temps	Dose Levels	Total Specimens
PART I									
Correlations Standard & Miniature	3	1	1	1	1	1	2	0	60
PART I									
Screening	21	2	1	[illegible]	1	1	2	1	275
PART II									
Basic Program	3	2	2	[illegible]	2	2	4	5	881

ALLOYS:
- Aluminum 2014, 2024, 5052, 6061, 7075
- Alco 355
- Am 35
- Beryllium
- Inconel X
- Monel
- Stainless Steel 301, 304, 304L, 347, 17-4PH
- *Stainless Steel 416, 431
- Titanium 6% Al, 4% V; Titanium 4% Al, [illegible] V
- Tool Steel

* It is believed that these alloys will be eliminated from the basic program due to brittle properties at 36°R.

TABLE IX - WEAR TESTS

	Test Materials	Forms	Batches	Stress Conditions	Test Temps	Dose Levels	Total Specimens
PART I							
Screening	12	2	1	1	2	1	1155
PART II							
Basic Program	7	2	1	1	4	3	765

TEST MATERIALS:

Stainless Steel 440 C, 304, 17-7 PH
Stellite
Tool Steel
Monel
Ceramic
Phenolic
Amorphous Carbon impregnated with Barium Fluoride
Amorphous Carbon impregnated with Cadmium Iodide
Graphitic Carbon impregnated with Barium Fluoride
Graphitic Carbon impregnated with Cadmium Iodide

CONFIDENTIAL

CONFIDENTIAL

TABLE X - COMPONENTS, MATERIALS, AND TESTS

COMPONENT	MATERIAL			TESTS
Tank	Aluminum, 2014	Titanium, 4% Al, 5% V		Tensile
	Aluminum, 5052	Stainless Steel, 301		Tensile Notch
	Titanium, 6% Al, 4% V	Stainless Steel, 304 L		Buckling
				Fatigue
Pressure Shell	Inconel X	Tool Steel (fcc)		
Pump	Aluminum, 2024	Stainless Steel, 304		Tensile
	Aluminum, 5052	Stainless Steel, 347		Fatigue
	Aluminum, 6061	Stainless Steel, 416		Creep
	Aluminum, 7075	Stainless Steel, 431		Tensile Impact
	Alco, 355	Am, 35		
	Titanium, 4% Al, 5% V	17-4 PH		
	Titanium, 6% Al, 4% V	17-7 PH		
Bearings	Balls	Lubricants	Races	
	Stainless Steel 440C	Gaseous Helium	Stainless Steel, 440C	Wear
	Stellite	Moly-disulfide	Stellite	Hardness
	Ceramic	Solid Film	Tool Steel (fcc)	
			Monel	
			Phenolic	
			Phenolic	
			Ceramic	

CONFIDENTIAL

TABLE X - COMPONENTS, MATERIALS, AND TESTS (Continued)

COMPONENT	MATERIAL	TESTS
Seals	Stainless Steel, 304	Wear
	Stainless Steel, 17-7 PH	
	Stainless Steel, 440C	
	Chrome Plate	
	Amorphous Carbon impregnated with Barium Fluoride	
	Amorphous Carbon impregnated with Cadmium Iodide	
	Graphitic Carbon impregnated with Barium Fluoride	
	Graphitic Carbon impregnated with Cadmium Iodide	
	Ceramic	
Bellows	Aluminum, 2014	Fatigue
	Aluminum, 5052	Tensile Shear
	Titanium, 6% Al, 4% V	Bellows Ductility
	Titanium,4% Al, 5% V	Bellows Endurance
	Stainless Steel, 301	Bellows Torsion
	Stainless Steel, 304L	
	Monel	
Reflector	Beryllium	Tensile
		Buckling
		Fatigue
		Creep
		Impact

CONFIDENTIAL

CONFIDENTIAL

TABLE XI - BELLOWS TESTS

	Alloys	Alloy Forms	Batches	Stress Conditions	Test Temps.	Dose Levels	Total Specimens Bellow Ductility	Bellow Endurance	Bellow Torsion
PART II Basic Program	1	1	1	1	4	3	65	65	65

ALLOY:
To be selected in Part I of the test program.

CONFIDENTIAL

TABLE XII - TENSILE SHEAR TESTS

	Alloys	Alloy Forms	Batches	Thickness of Alloy	Grain Directions	Stress Conditions	Test Temps.	Dose Levels	Total Specimens
PART I Screening	7	1	1	1	1	1	2	1	165

ALLOYS:
Aluminum 2014, 5052
Stainless Steel 301, 304L
Titanium 4% Al, 5% V; 6% Al, 4% V
Monel

CONFIDENTIAL

APPENDIX B

STATISTICAL APPROACH

Observations in all experimental work are subject to error. Under conditions that produce large errors, it is difficult to decide whether a particular result is genuine or due to experimental error. If the error is great, there are two generally accepted methods of reducing it. The experimental techniques can be refined ,or the experiment can be repeated a number of times and the results averaged.

The number of samples will vary, depending on expense, convenience, required accuracy, and other factors. To take more observations than required for establishing conclusions with a given level of significance is extravagant -- particularly in experiments involving irradiation, which tend to be both tedious and expensive.

To make a proper statistical evaluation of any experiment, not only should a variety of samples and a sufficient number of repeats be included, but considerations should be given to inherent variables in the experimental program.

The consideration of each inherent variation involves different phases of a study of systematic errors and, in itself, requires considerable time. However, by use of refined techniques, proper equipment, and calibrated instruments, the following possible variables are assumed to be constant:

Cryogenic temperature $\pm$ 2 °R
Specimen size differences
Reactor flux

To determine the effects of cryogenic temperatures, radiation, andother possible variations -- at the least expense -- a statistical approach has been used in the actual planning, or design, of the program, as well as in the interpretation of the resulting data. There are a number of statistical methods for designing experiments; the proposed designs are based on the principles of the randomised block, Youden square, and factorial experimentation. The first two methods may be considered as representative of the classical, one-variable-at-a-time approach. In the factorial method, however, all the items that are required to be varied are varied simultaneously. This, in effect, gives the maximum amount of information about the experimental system for a given amount of work. The advantages of this design are as follows:

- It provides much greater efficiency; estimates of a given standard of accuracy for the effects can be obtained from a much smaller total number of observations.

- Information is given on the extent to which the factors interact, i.e., the way in which the effects of one factor are influenced by the other factors. The experiments will, therefore, give a wider inductive basis for any conclusions that may be reached.

The proposed program will consist of two parts -- screening testing for material elimination and actual testing of selected materials. The resulting data will be statistically evaluated, and every effort will be made to obtain the most information at the least expense. Some of the data will be reduced by analysis, as collected, to be certain that sufficient details are being gathered and that the important variables are being observed before the equipment or prepared conditions are disbanded. For example, determination of interactions may lead to a different concept of the experiment and may indicate the need for additional data. In-progress data analysis, even though it is only approximate, can often save time, money, and manpower on a planned program by indicating that the original plan needs modifying to produce the results expected from the experiment.

The in-progress analysis, dealing with statistical significance tests, could be accomplished by rank methods, in which the serial numbers 1, 2, 3 ... N are substituted for actual data in an order (rank) corresponding to the magnitude of the experimental figures. While these methods are not as efficient statistically as the classical t, F, and Chi square tests, they possess three distinct advantages as follows:

- They do not require the assumption of normal distribution for the data.
- They are rapid and simple.
- They are particularly adapted to situations where data exist only in rank.

PART I

Chemical analyses of each material tested will be required; each sample will be analyzed in triplicate. Individual results for each determination will be required along with reported means or averages.

Five samples of each material will be tested. This number is adequate for the production of statistically significant results, and it does not require an experimental program of prohibitive proportions. The choice of five samples is based upon an examination of two statistical measures, the limit of error of a mean and the standard error of a mean.

The limit of error (LE) of a mean ($\overline{X}$) at a given confidence level depends upon the number of observations (N) from which the mean was computed.

$$LE = tS/N^{\frac{1}{2}}$$

Where: t = Student's factor, based on the degrees of freedom (N-1) and the probability level.

S = standard deviation $= \left(\dfrac{\Sigma X^2 - \left(\frac{\Sigma X}{N}\right)^2}{N-1}\right)^{\frac{1}{2}}$

and,

$$\overline{X} = \frac{X_1 + X_2 - - - X_N}{N} = \frac{\Sigma X}{N}$$

Then $\overline{X}$ = LE at a selected probability or confidence level. If LE is based on the 95 per cent probability level, it is interpreted to mean that 95 per cent of the time the true value of X lies between $\overline{X}$ + LE and $\overline{X}$ - LE.

As S decreases, the precision of $\overline{X}$ increases. Values for $t/N^{\frac{1}{2}}$ are shown here, t and N being constant for any given set of data.

$t/N^{\frac{1}{2}}$ Values

$S \pm \sigma$

N	PROBABILITY LEVEL		
	90%	95%	99%
2	± 4.464	9.011	± 45.147
3	1.685	2.487	5.737
4	1.177	1.591	2.920
5	0.953	1.239	2.055
6	0.822	1.049	1.646
7	0.753	0.923	1.399
10	0.580	0.716	1.031
15	0.455	0.554	0.769

It is apparent that each new observation above five produces a relatively small decrease in the limit of error of the mean.

The standard error of a mean is inversely proportional to the square root of the number of observations; that is,

$$SE_{\overline{X}} = S/N^{\frac{1}{2}}.$$

Values for 1/N are shown on the following page.

STANDARD ERROR OF A MEAN

N	$1/N^{\frac{1}{2}}$ Values
2	0.707
3	0.577
4	0.500
5	0.447
6	0.408
7	0.378
10	0.316
15	0.258

The averaging of four observations decreases the standard error of the mean to one-half that of a single observation; the standard error or the mean of fifteen observations is approximately one-quarter that of a single test. Here again, when more than five samples are used, the small gain in precision is at the expense of other factors.

The process of repeating an experiment a number of times and averaging the results to reduce the error is inefficient. This may be shown in a different way. Since the magnitude of $tS/N^{\frac{1}{2}}$ is a function of the number of observations, the number of observations required to increase the precision of the mean to a prescribed level can be estimated from the formula:

$$N = \left(2S_R/LE_R\right)^2$$

Where $S_R = \dfrac{100S}{\bar{X}}$

and $LE_R = tS_R/N^{\frac{1}{2}}$ (in this case, the level of precision desired).

The number of observations required to increase the precision of the mean from 10 to 0.1 per cent is shown on the following page for various values of the relative standard deviation (S_R).

Increase in Precision of the Mean as a Function of the Number of Observations with t at 95% Probability Level

NUMBER OF OBSERVATIONS

LE_R \ S_R	0.5	1.0	2.0	3.0	5.0
10					1
5				1	4
4			1	2	6
2		1	4	9	25
1	1	4	16	36	100
0.5	4	16	64	144	400
0.2	25	100	400	900	2,500
0.1	100	400	1,600	3,600	10,000

In order to understand the use of the above table and formula, consider the following set of data:

10.1	$N = 4$
9.8	$\bar{X} = 10.0$
10.2	
9.9	$S = 0.18$ or 0.2
	$S_R = (0.2)\ (100/10 = 2\%$
	$X \pm LE\ 95\% = 10.0 \pm 0.3$
	$X \mp LE_R = 10.0 \pm 2\%$

If the prescribed level of precision in this case is 1 per cent, the number of observations required to increase the precision of the mean to 1 per cent is:

$$N = (2S_R/LE_R)^2$$

$$S_R = 2\%$$
$$LE_R = 1\%$$

Therefore, 16 observations are necessary to increase the precision of the mean from 2 to 1 per cent. And 36 observations are needed to increase the precision of a mean from 3 to 1 per cent.

It should be pointed out that should the standard deviation or variance of a test mean be too large, additional determinations will be made; however, no more than necessary will be made consistent with the test.

PART II

The testing program for Part II is shown in Table III. The program was designed to establish instrument repeatability, day-to-day reproducibility, heat-treat repeatability during sample preparation, effects of chemical composition, operator-to-operator reproducibility, and the total over-all deviation as well as the effects of cryogenic and radiation environments. For sheet material, statistical analysis will reveal, without requiring more testing, heterogeneity, if present, and whether or not it has any effects on results.

The program is divided into two sections, A and B. The testing schemes for Section A and Section B are shown at the end of this Appendix. Data resulting from Section A testing, in addition to determining the effects of the sample parameters (composition and heat treatment) and test parameters (temperature and radiation), as well as serving as a quality control program, will be used as reference data for other test parameters.

The proposed approach for Part II could be considered as a minimum program. Some testing methods, e. g., fatigue, may give too large a standard error of the mean; and additional testing may be necessary. In Section B, the number of samples to be tested could decrease or increase, depending upon the analysis of the data resulting from Section A.

The following references are suggested for further information on statistical methods:

Brownlee, K. A., "Industrial Experimentation," Chemical Publishing Co., Inc., Brooklyn, 1949

Cochran, W. G. and Cox, G. M., "Experimental Designs," John Wiley and Sons, Inc., New York, 1950

Goulden, C. H., "Methods of Statistical Analysis," John Wiley and Sons, Inc., New York, 1952

Hoel, P. G., "Introduction to Mathematical Statistics," John Wiley and Sons, Inc., New York, 1947

Youden, W., "Statistical Methods for Chemists," John Wiley and Sons, Inc., New York, 1951

CONFIDENTIAL

SCHEME - SECTION A OF PHASE II TEST PROGRAM

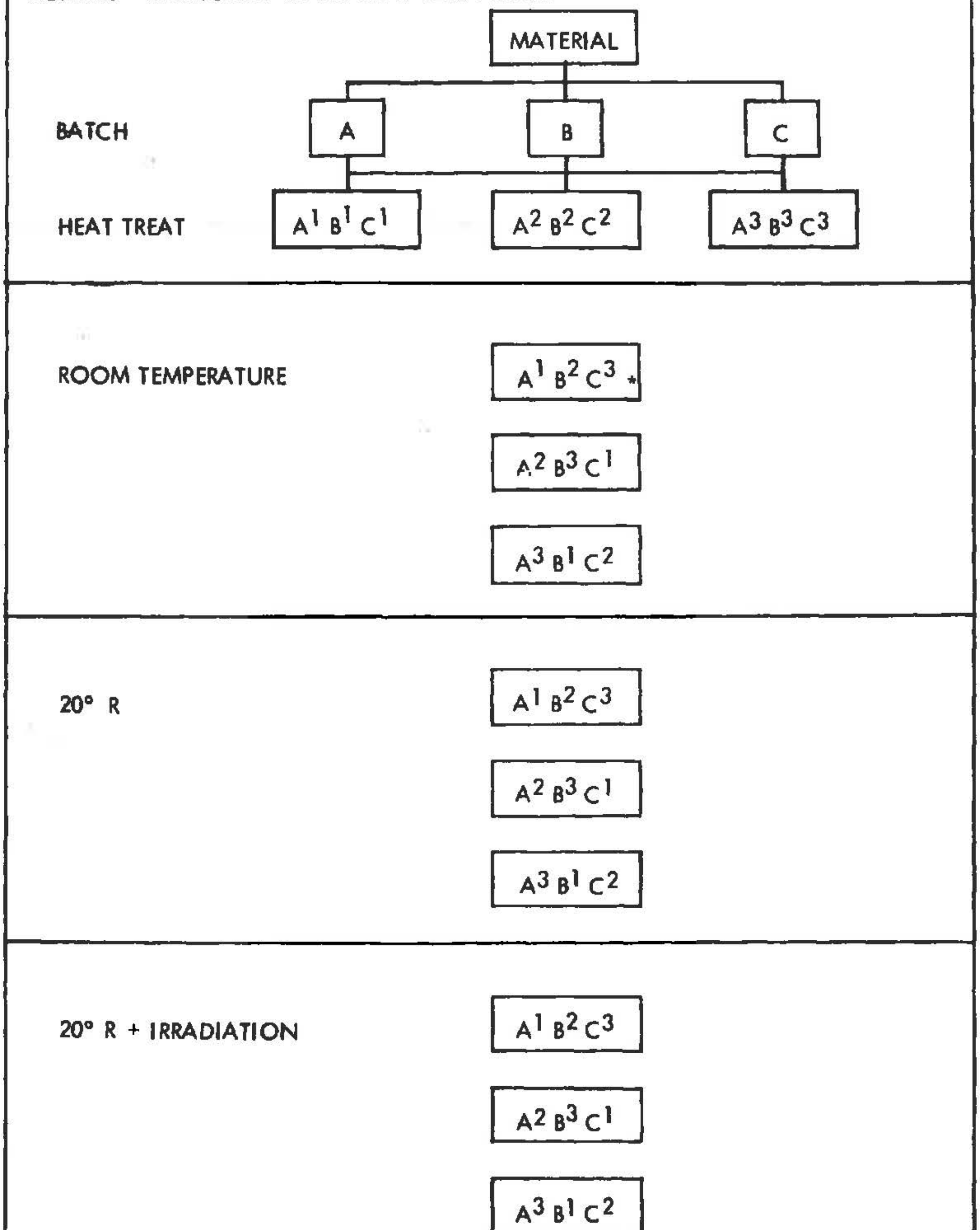

* PER SAMPLE PARAMETER THREE DETERMINATIONS

TWENTY-SEVEN SPECIMENS ARE REQUIRED FOR ONE DETERMINATION.

CONFIDENTIAL

CONFIDENTIAL

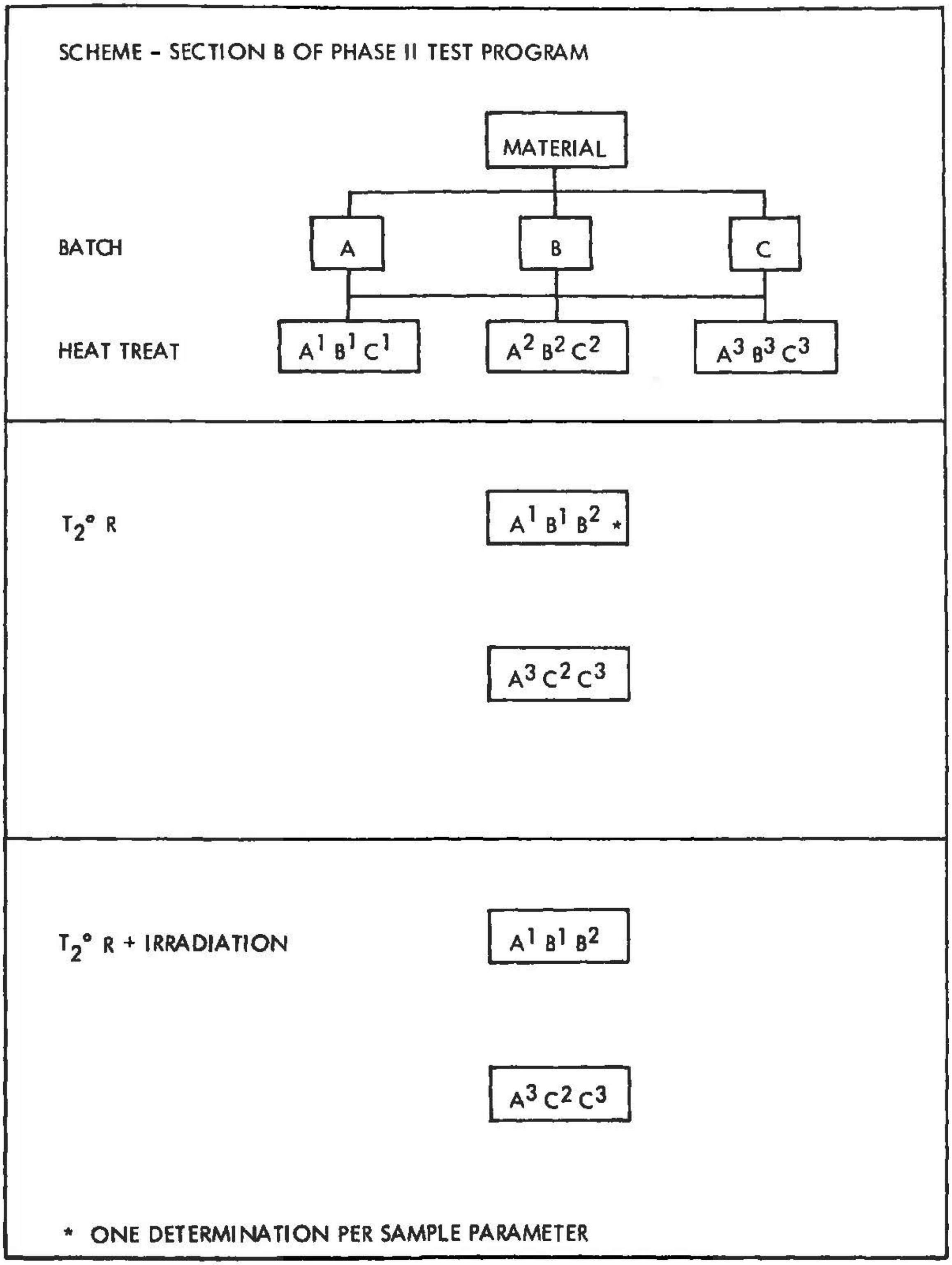

SIX SPECIMENS REQUIRED FOR ONE DETERMINATION.

CONFIDENTIAL

APPENDIX C

REMOTE DISASSEMBLY
OF AIRCRAFT SUBSYSTEMS

Abstract:

Preliminary investigation of the various aircraft subsystems has shown that there is a need for manipulator-operated disassembly tools. Some of these tools have been developed, along with electrical and hydraulic fittings that are easily adapted for remote connecting and disconnecting with the Model 8 manipulators. In some cases, a system can be specially constructed for ease of disassembly by using modular assembly. Examples of this modular construction are the RDZ-1 radio receiver and the radiation-resistant television camera.

INTRODUCTION

A preliminary study of aircraft subsystems proposed for irradiation has shown that there are a number of problem areas relative to the remote disassembly of these subsystems. Some of these problems can be solved easily by use of standard items such as quick disconnect AN plugs and hydraulic connectors. But for the most part, the solution to these problems requires that the equipment, components, and subsystems be modified to permit disassembly with standard manipulators. To accomplish remote disassembly of irradiated subsystems, strict requirements for electrical and hydraulic connectors, tie downs, control locations, and hooks or bales for remote crane handling as well as for construction methods must be incorporated into the preliminary design of the subsystem and its components. However, care must be exercised so that modification of the subsystem for remote disassembly does not impair the function of the subsystem.

Whenever possible, modular construction of components into subsystems is used. This type of construction is necessary to permit any one section of an irradiated subsystem or component to be removed for further disassembly and testing. This type of construction also permits a damaged section to be replaced with another system, in order to dynamically test the rest of the subsystem.

While the Georgia Nuclear Laboratory was still under construction, disassembly studies and remote handling tool development were being conducted at Air Force Plant 6 in Marietta, Georgia. Figure A-1 shows a mock-up that was constructed to accomplish this program. All of the GNL hot cell features are incorporated in the mock-up to duplicate the viewing and remote handling characteristics that will exist when an irradiated subsystem is being disassembled. This view of the cell shows the Model 8 manipulators, the General Mills E-2 manipulator, the sodium vapor lamps, and the simulated flatcar of the hot materials handling system.

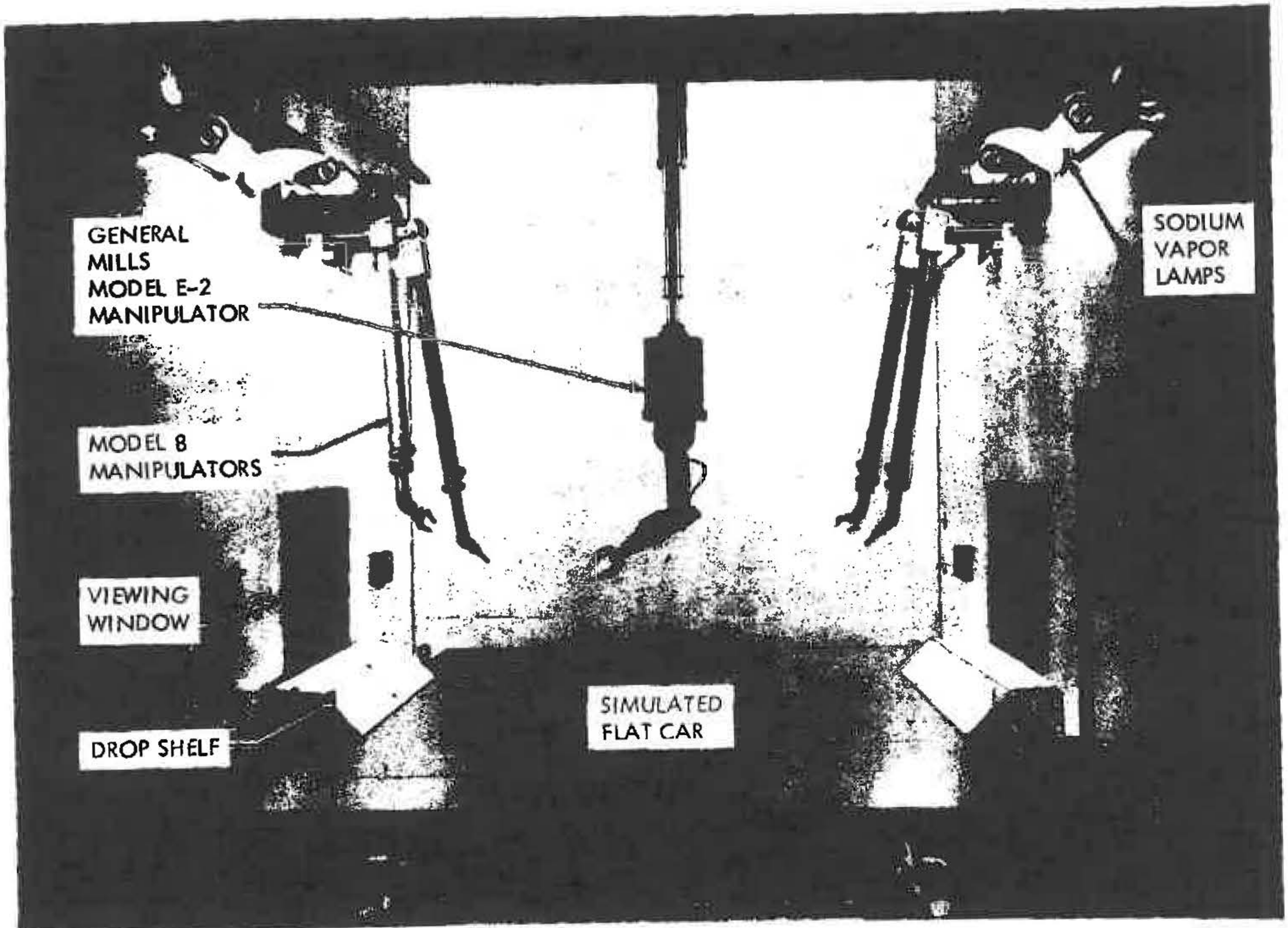

FIGURE A-1 CROSS SECTION OF THE HOT CELL MOCK-UP AT AFP 67

REMOTE HANDLING TOOLS

As manipulators are the tools with which the task of disassembly is performed, their capacity, reach, and dexterity is of prime importance when the modification criteria are established. If the normal capacity of the manipulator must be exceeded, or if the modification becomes too complicated and costly, the manipulator capabilities are increased by the development of special remote handling tools.

Remote handling tools can be fabricated from special designs, or commercial tools can be purchased and modified to be operated by the manipulators. An example of a modified commercial tool is shown in Figure A-2. This tool, a seven-pound Black and Decker No. 100 heavy-duty impact wrench with 1/2 in. bolt diameter capacity, is capable of delivering 1800 impacts per minute. Using the jig shown in Figure A-2, the modified impact wrench is remotely attached or detached from the Model 8 manipulator.

To attach the impact wrench to the manipulator arm, the handle and the on-off switch is removed. The holding frame is built to fit the contour of the "wrist" of the manipulator. An indexing gear, with a control cable running from the indexing pin to the sliding control assembly, is attached to the holding frame. The sliding control assembly permits the tongs to keep the indexing pin disengaged from the gear until the desired position is attained. As the indexing control pin is located on the same assembly, directly below the on-off switch, the manipulator tongs can easily index or turn the switch on or off by moving to the proper position and applying a squeeze motion.

When the tool is indexed to the proper position, the grip is relaxed and the index pin slides into position. As this holds the tool in position, the tongs are relaxed and moved to the on-off switch located directly above the cable control pin to operate the tool. Pneumatic impact wrenches seem to be a better tool for the job, as they weigh less than comparable electrical wrenches. Since

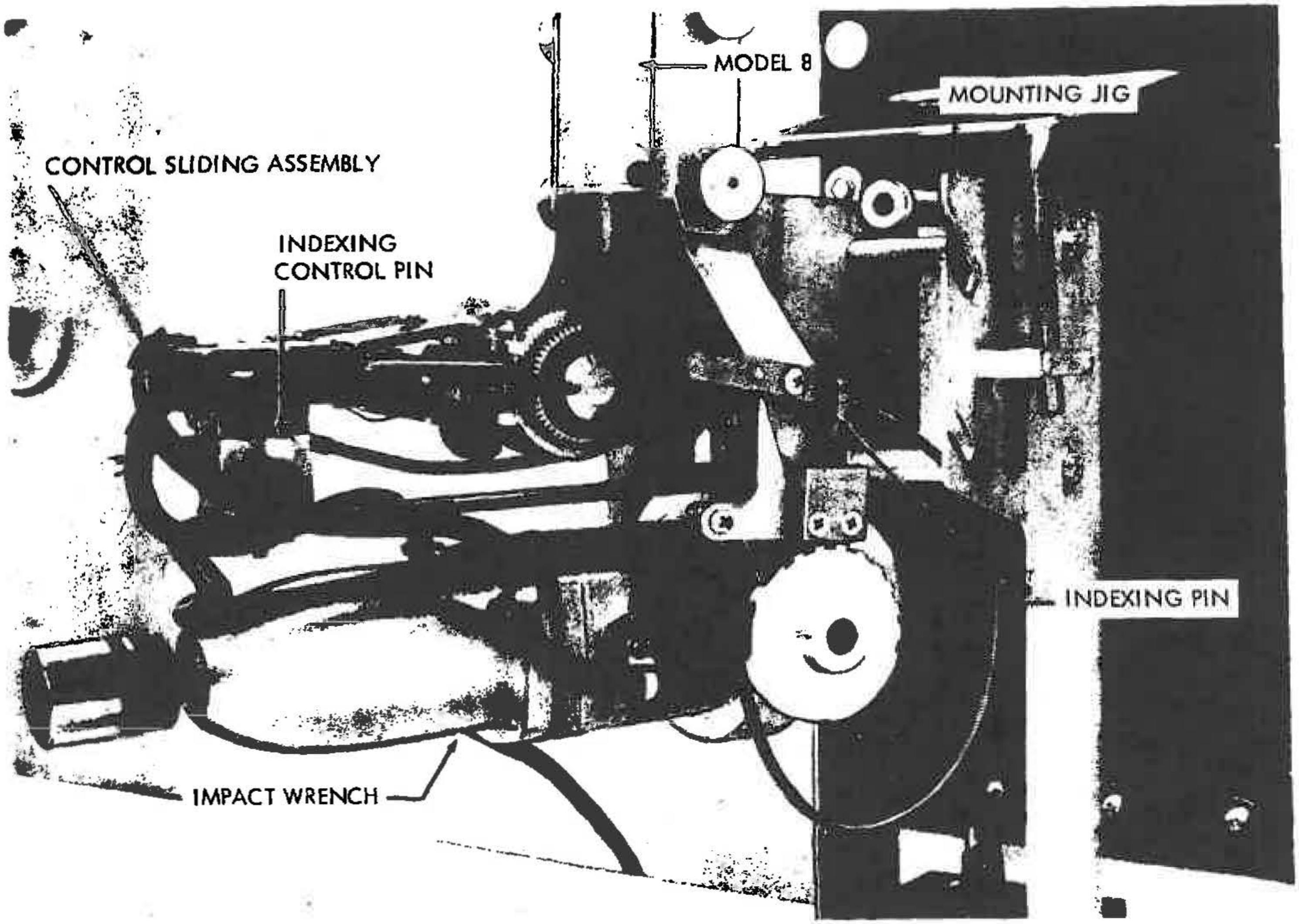

FIGURE A-2 IMPACT WRENCH BEING MOUNTED ON MODEL-8 MANIPULATOR the exhaust tends to scatter contamination, however, pneumatic tools have limited acceptance unless the exhaust is directed away from the contaminated item.

A preliminary investigation of wire cutters for remote disassembly indicates that it is extremely difficult to apply enough pressure to the tool to cut wire of significant size. As the gripping power of the Model 8 manipulators is limited, it was necessary to develop a tool that would deliver a greater cutting force. This was accomplished by increasing the effective lever arm, in the manner shown in Figure A-3. The cutter is designed and fabricated to remotely detach and attach to the Model 8 manipulator in the same way as the standard remotely-removable tongs. This is accomplished with the flange and flange clamp shown in Figure A-4. The cutting action is obtained by squeezing the grips together. This action causes the cutting bar to be forced against the slotted end portion of the tool. This method can be used to cut wire up to #14 AWG. The slender cutting portion of the tool permits its insertion into crowded areas where it hooks onto the wire that is to be cut. In this manner, various electronic items are removed from a chassis for individual radiation damage testing. As this cutter has limited capacity, a pneumatic cutter was designed with considerably higher capacity than the mechanical wire cutter.

Almost any hand tool can be adapted to the manipulators for remote handling and disassembly, and at present several tools have been designed. These include an electric screw driver, a tube-puller, a soldering iron, and a hydraulic universal attachment than can be adapted for shearing, gripping, or rotation. All of these tools have been designed for remote detachment from and attachment to the Model 8 manipulator.

VIEWING

It is important in any hot cell work for the operator's view of the work area to be as nearly complete as possible. Close viewing is

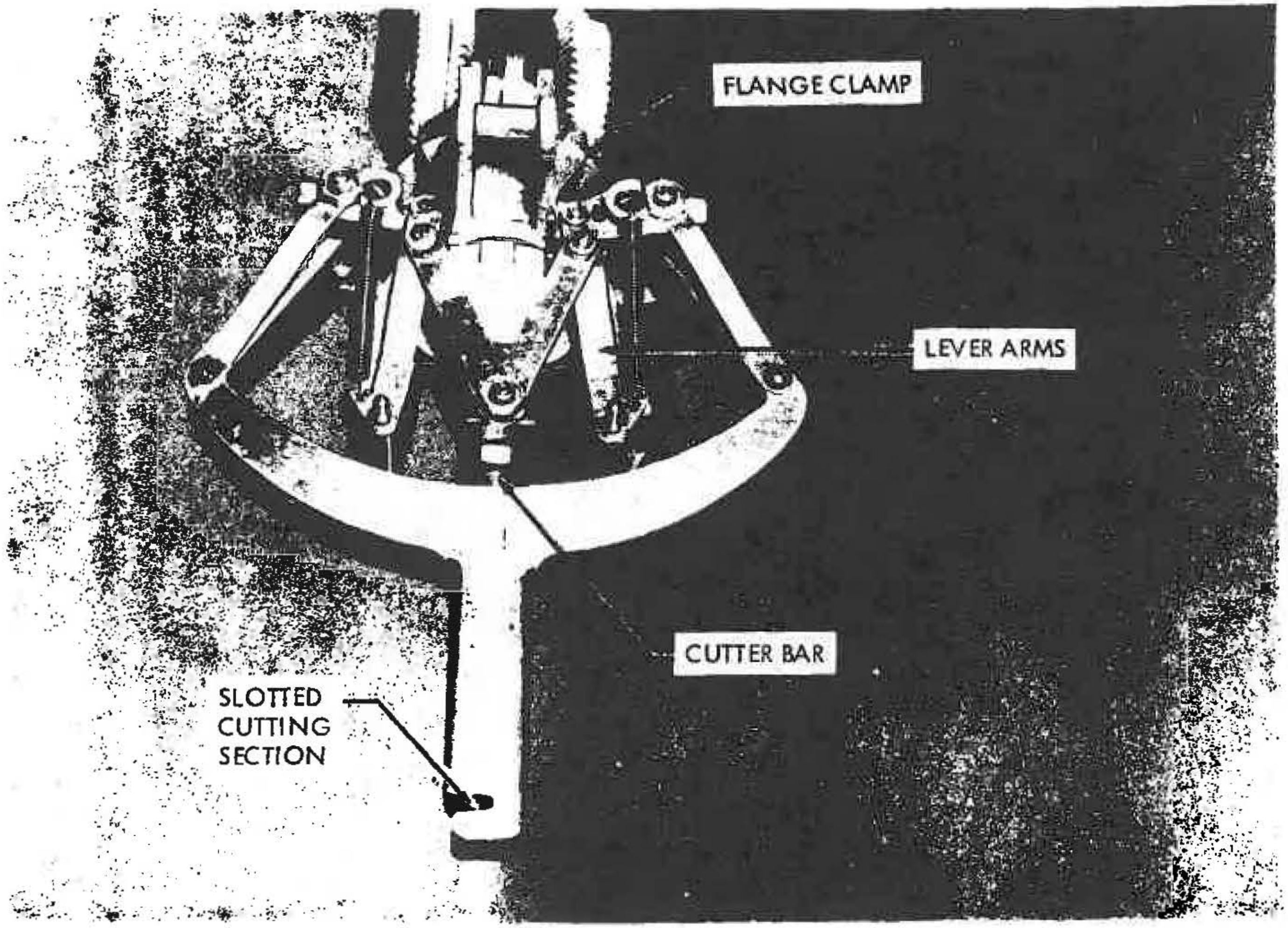

FIGURE A-3 REMOTELY DETACHABLE AND ATTACHABLE WIRE CUTTER TOOL

FIGURE A-4 ATTACHMENT OF CUTTING TOOL ON MANIPULATOR extremely important in the disassembly of complex and delicate subsystems. The standard hot cell window, while giving increased vision due to the index of refraction of the lead glass, does not offer an appreciable degree of magnification. There are a number of visual aids available for hot cell use. A television system with remote pan and tilt and a remotely operated Zoomar lens has been used by some industries for a number of years. One obvious drawback to this system is that the lens browns due to irradiation. A good lens, with non-browning glass, has not yet been manufactured. A periscope with non-browning lenses is commercially available, and it is of great assistance in hot cell work for reading micrometers, gages, and dials. But since the operator must remove his hands from the manipulator to view his objective, this viewing system is not very effective in remote disassembly work.

Since the operator must view his work closely and still operate the manipulator, it was decided that a pair of binoculars installed on an adjustable holding bracket mounted outside the cell would not only meet the visual requirements but would also eliminate the problem of lens browning. A pair of 6 x 30 binoculars was mounted directly above the window on a ball jointed holding rod, as shown in Figure A-5. This type of mount permits the operator to adjust the binoculars and subsequently view his work without removing his hands from the manipulator. The only change required is to adjust the focal range of the binoculars to coincide with the space limitation of the hot cells. The 6 x 30 binoculars are indeed an improvement to the hot cell viewing system; but the field of view is not wide enough, and there is a definite need for more magnification. Preliminary investigations on the modification of a pair of 8 x 50 binoculars has shown that to obtain the focal range desired the convergence angle will also have to be changed.

CONNECTORS

The Model 8 manipulator can disconnect and connect practically any of the standard AN connectors. Some of the quick-disconnect

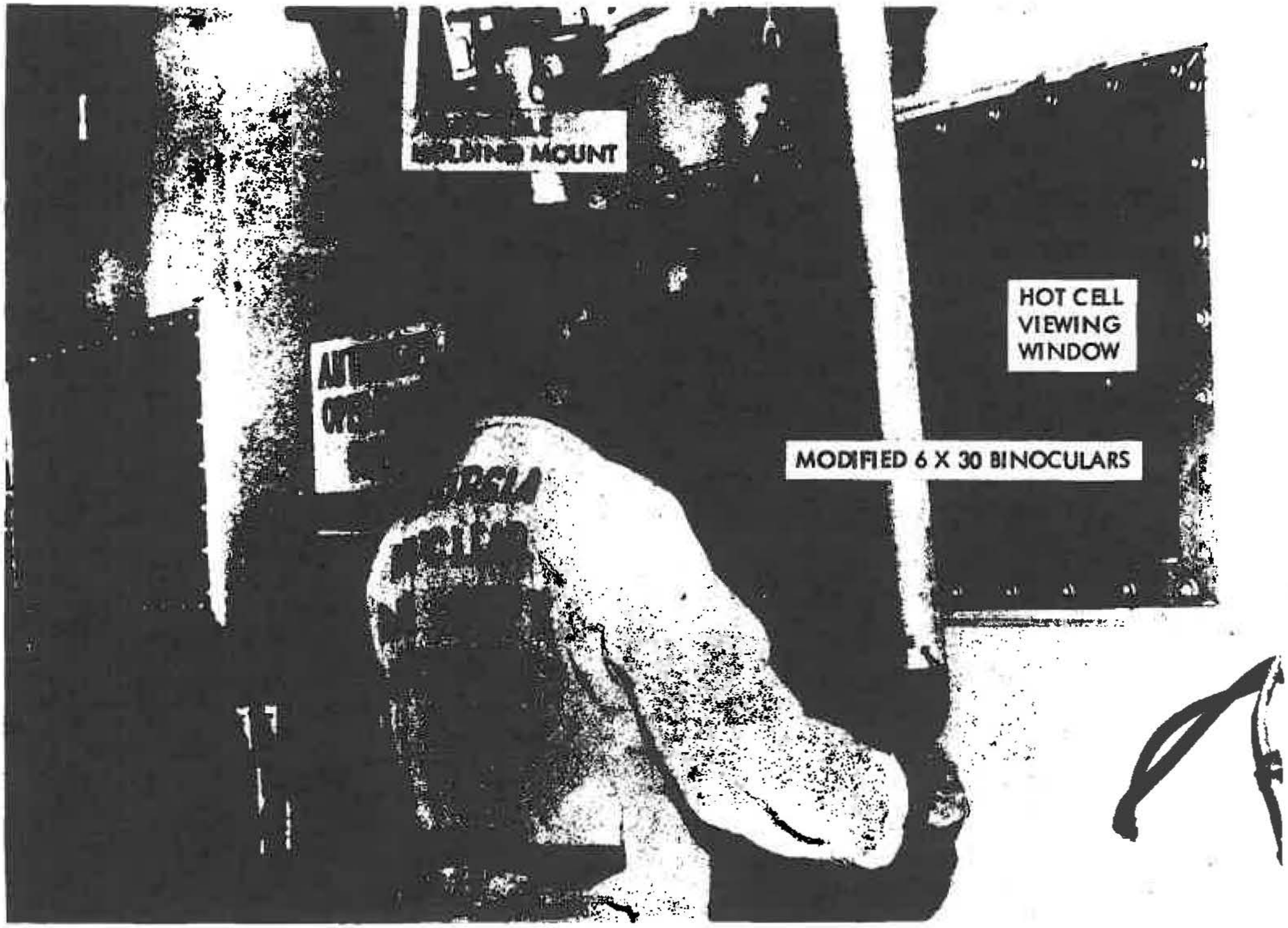

FIGURE A-5 VISUAL AIDS

connectors are obviously better adapted for remote operation than the multi-thread or twist lock connectors. The remote disconnection of any type of connector requires that it be easily accessible to the manipulators. By locating as many connectors as is feasible on a junction board that is easily accessible, remote disconnections and connections of electrical leads is considerably simplified.

Pneumatic and hydraulic fittings introduce a different type of problem. To have a leak-proof seal, a fitting ordinarily requires the application of high torque. In making a hydraulic coupling the lines are usually filled with air and have to be bled. When a hydraulic fitting is disconnected, oil leakes from the line; and in the case of an irradiated systems this leak would spread contamination. A coupling to be remotely connected and disconnected must be self-sealing; it must be capable of being connected and disconnected by the Model 8 manipulators; it must require one or less revolutions to complete the coupling; and it must have sufficient pressure rating to perform the tests. The Aeroquip self-sealing hydraulic and pneumatic coupling shown in Figure A-6 meets all of these requirements. Fluid lines can be disconnected without loss of fluid or introduction of air into the system. Removal of components from a subsystem using these couplings is measured in minutes rather than hours; and as the coupling is easily connected and disconnected by the Model 8 manipulator, special tools are not required. The present pressure rating is 3000 psi at temperatures from -65°F to 160°F.

MODULAR SYSTEM CONSTRUCTION

As has been mentioned before, module construction greatly enhances the capability of manipulators to disassemble irradiated subsystems and components. The RDZ receiver shown in Figures A-7 and A-8 is modified to utilize module construction; it is an example of what can be done to a complicated system to facilitate remote disassembly and testing.

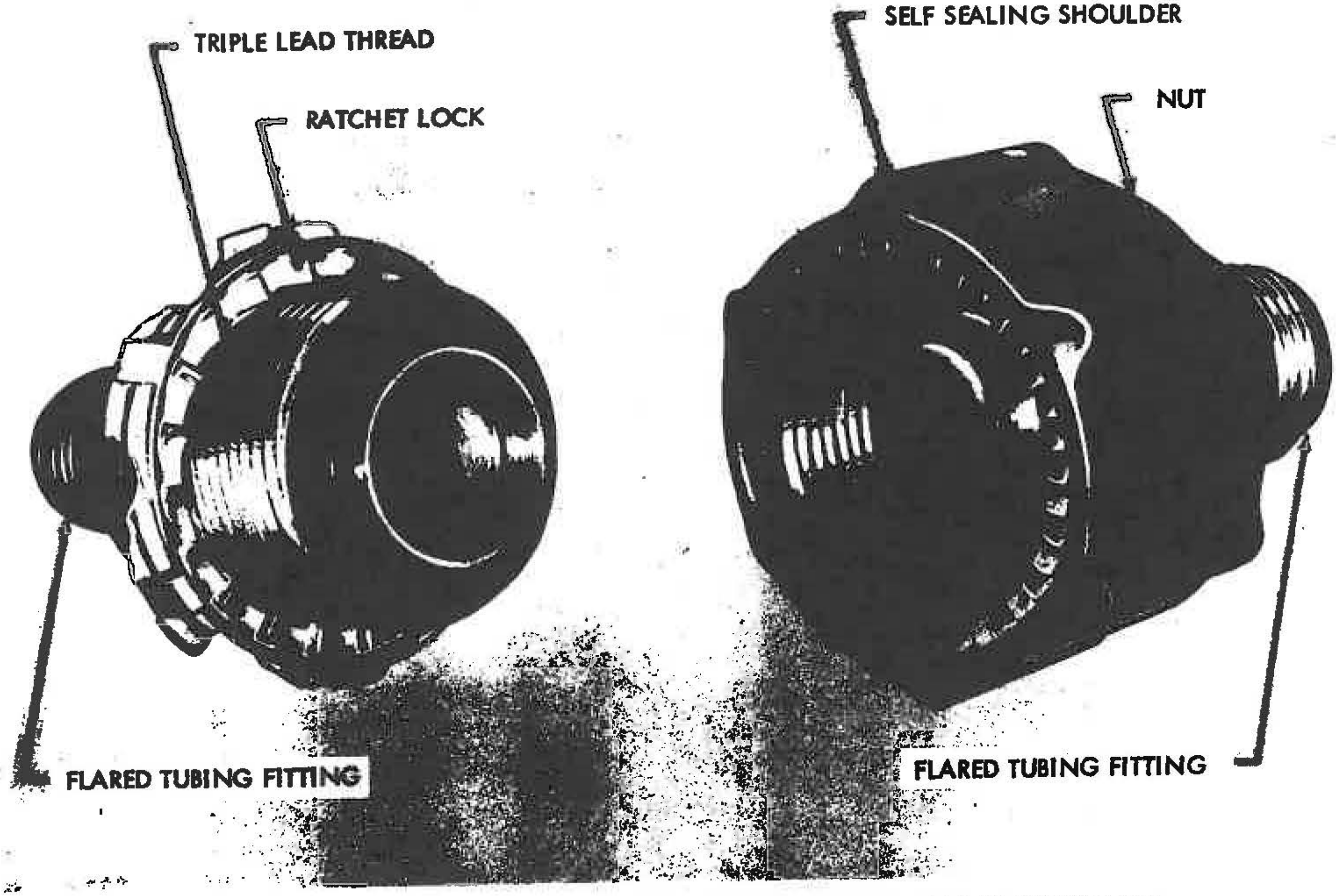

FIGURE A-6 SELF-SEALING HYDRAULIC AND LOW PRESSURE PNEUMATIC COUPLINGS

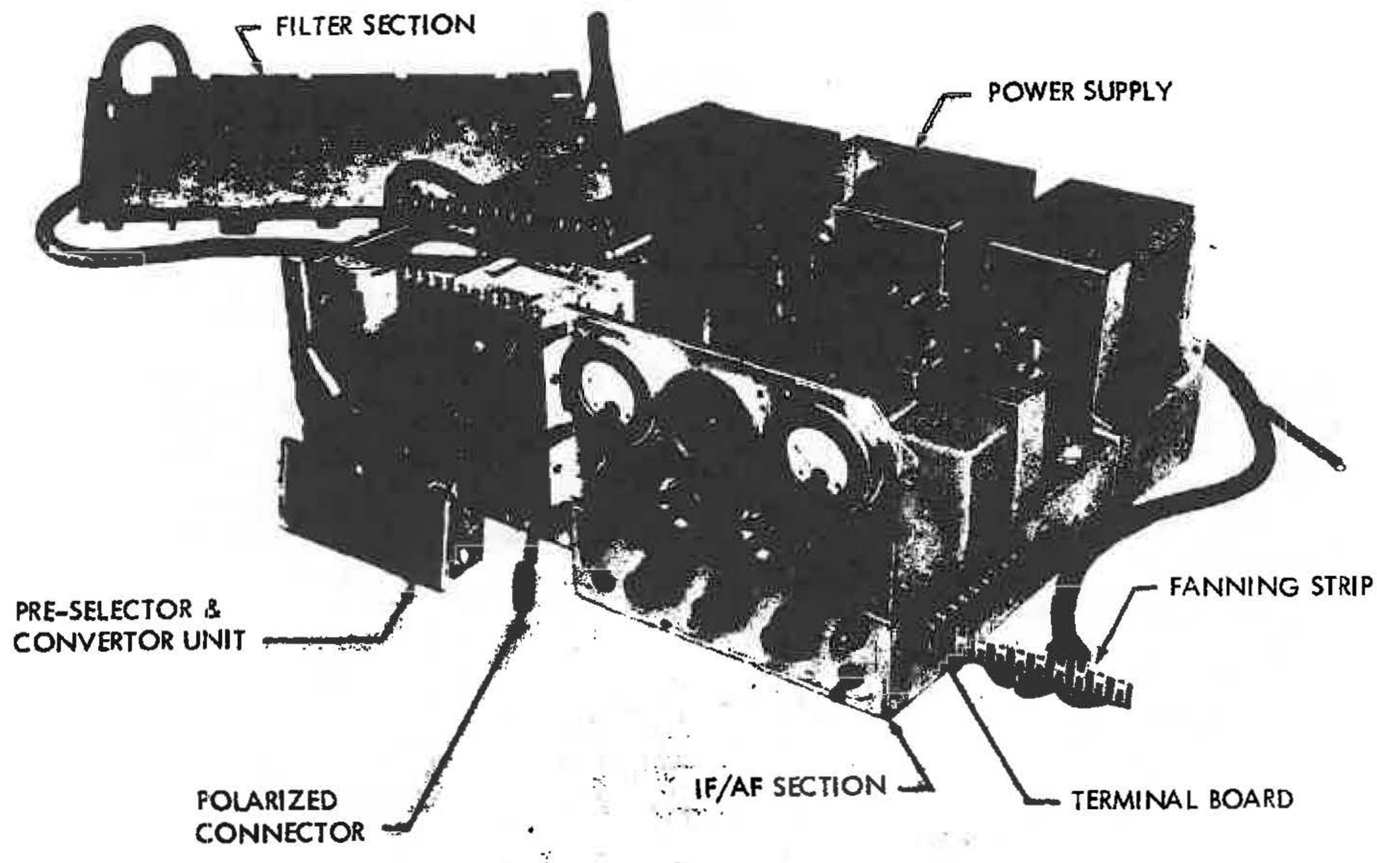

FIGURE A-7 RDZ RADIO RECEIVER

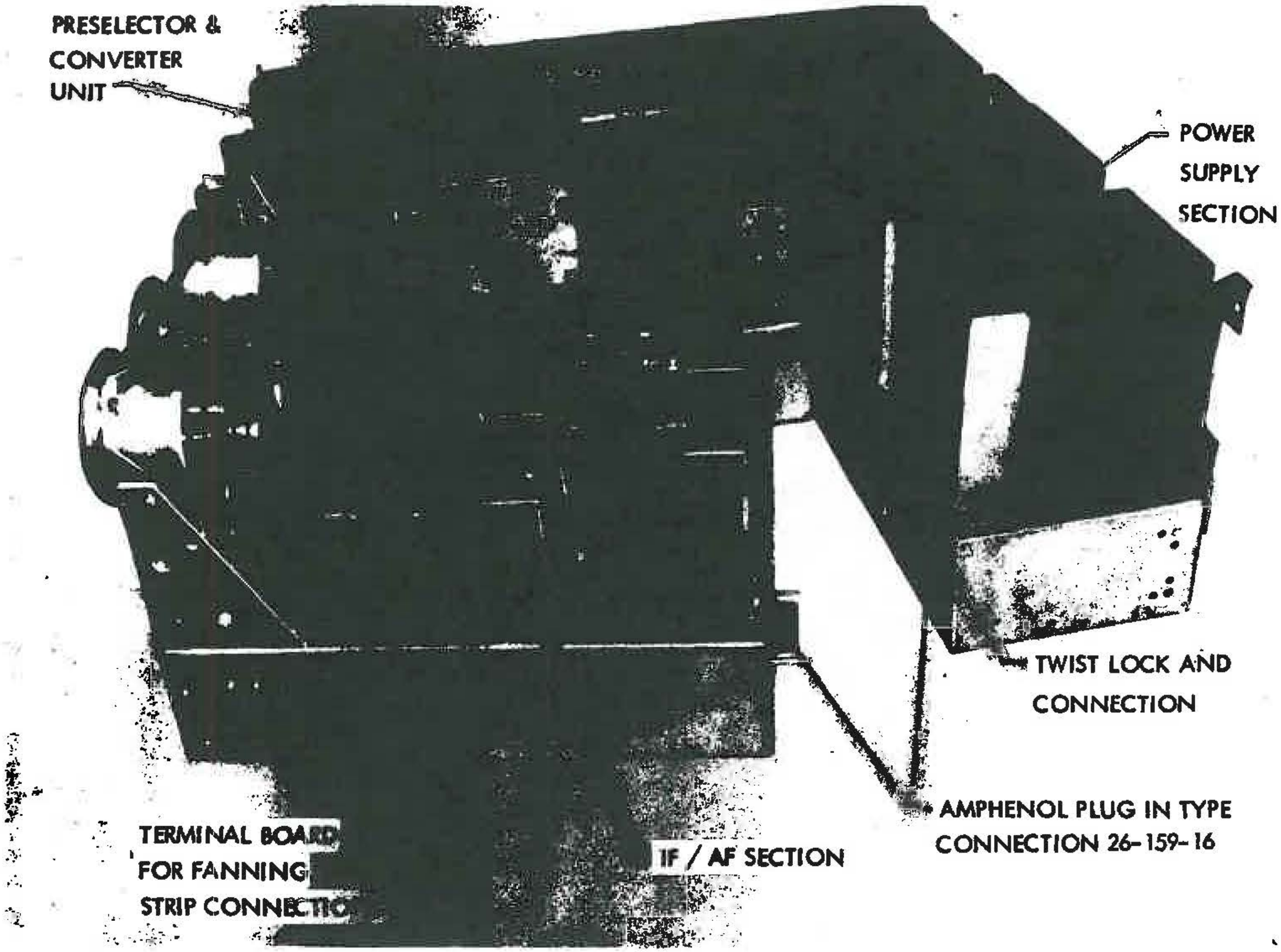

FIGURE A-8 PARTIALLY DISASSEMBLED RDZ RADIO RECEIVER

The modification consists of assembling the receiver in four basic sections:

- Power supply
- Filter section
- IF/AF section
- Pre-selector and converter unit

The power supply, the IF/AF section, and the pre-selector and converter unit are tied together with four Phillips-head fasteners, which are easily removed with an electrically-operated screw-driver. The filter unit is mounted on the chassis as an integral part of the subsystem, but it is isolated mechanically. For sure tool alignment, all screws and bolts are replaced with Phillips-head screws. This type of screw provides for easier alignment with a remotely operated electric screw driver than does the standard slotted screw. The amphenol pin-polarized connector was chosen, because it requires a low insertion and withdrawal force and because the pins permit plug-in without danger of mismating. This type of connector is easily and quickly removed even when the connector is out of sight within the equipment as shown in Figures A-7 and A-8. Also shown in Figure A-7 are the fanning strips that replace the standard terminal strips. These fanning strips permit the manipulators to make a multiple connection; and although individually fastened to the terminal strip, they are fixed in a position so that they can all be either connected or disconnected at the same time.

The soldered connections, between the power supply and the IF/AF section, the power supply, and the pre-selector and converter unit, are replaced with an amphenol plug-in type connector number 26-159-16, as shown in Figure 8. This connector mates the various units electrically and permits easy disassembly, since the plug is located to mate when placed in position and slid forward. Guide pins on the plug and its mate assist in aligning the units.

Receiving tubes equipped with guide pins can be easily removed and replaced by using a standard tube puller adapted for remote handling.

Subminiature tubes having no guide pin will be a little troublesome since the pins are easily bent and since, if positive alignment is not possible, they might be forced into a mismating. This problem can be partially solved by placing a guide mark on the tube and a corresponding mark on the socket. This permits the operator to be certain of the alignment before he applies insertion pressure. Another solution to this particular problem is to solder a standard guide pin socket to the base of the miniature tube socket for a permanent double socket arrangement.

A radiation-resistant television camera, designed and fabricated by Lockheed Aircraft Corporation, California Division, is quite similar in design for disassembly to the RDZ receiver described. For testing purposes, this prototype model is larger and more intricate mechanically than will be required in later operational units. This approach and the module type of construction is made to facilitate complete disassembly of the test model with the manipulators described.

Here again the module type of construction provides for relatively easy disassembly of the entire camera. Slides or slots, shown in Figure A-9, are provided so that the lens and the vidicon coils are accessible and easily removable. Electronic circuits are on bread boards of the plug-in type that require very little soldering for assembling or disassembling. Although the bread boards are accessible and soldering can be done with a minimum of trouble, an improvement could likely be made by replacing the bread boards with fanning strips. The use of a piano hinge to attach the cover to the rear of the camera base affords accessibility to the interior to permit changes by remote handling equipment, as shown in Figure A-10.

Figure A-9 shows the outer structure of the camera case, including the hinged lever assembly, cooling ducts, and lens slide. The ejection system for removing the plug from the vidicon tube is shown in Figure A-11. The lever is pulled by the manipulator, and this effects a straight pull to remove the plug from the vidicon tube. Once this plug is removed, the vidicon tube can be removed from the coils; then the coils themselves can be removed.

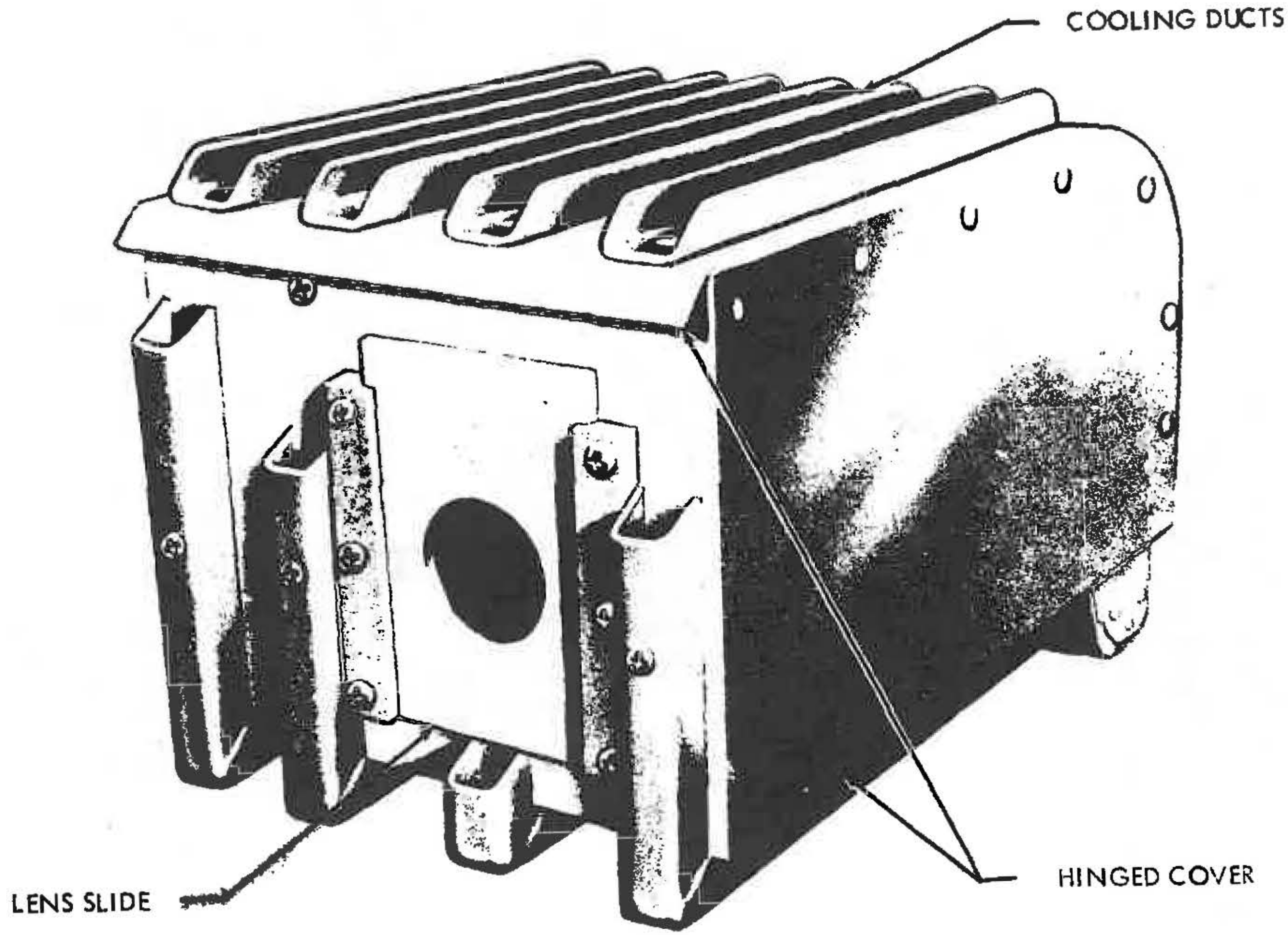

FIGURE A-9 CAMERA CASE

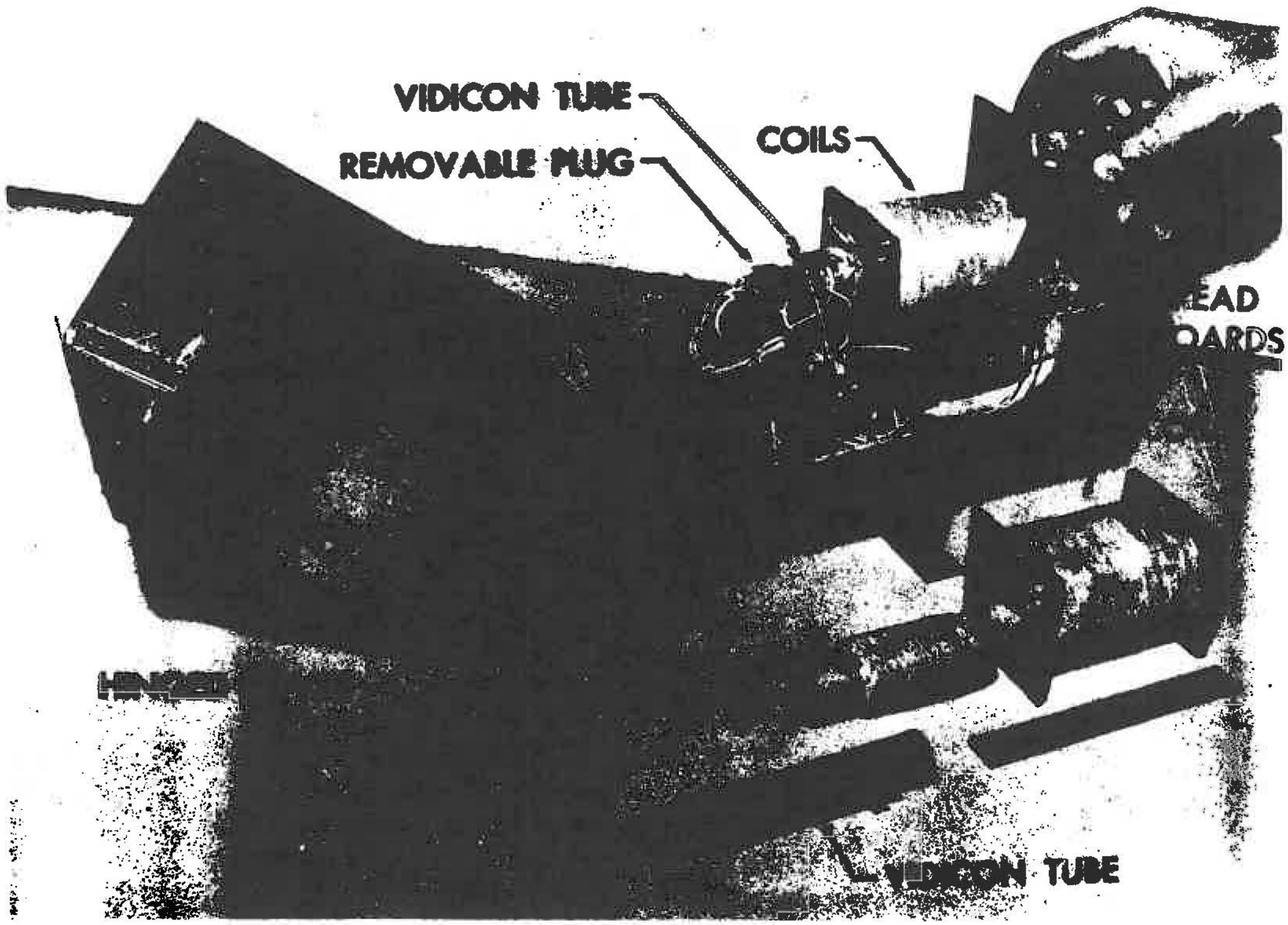

FIGURE A-10 CAMERA INTERIOR (INCLUDING A DISASSEMBLED VIDICON SYSTEM)

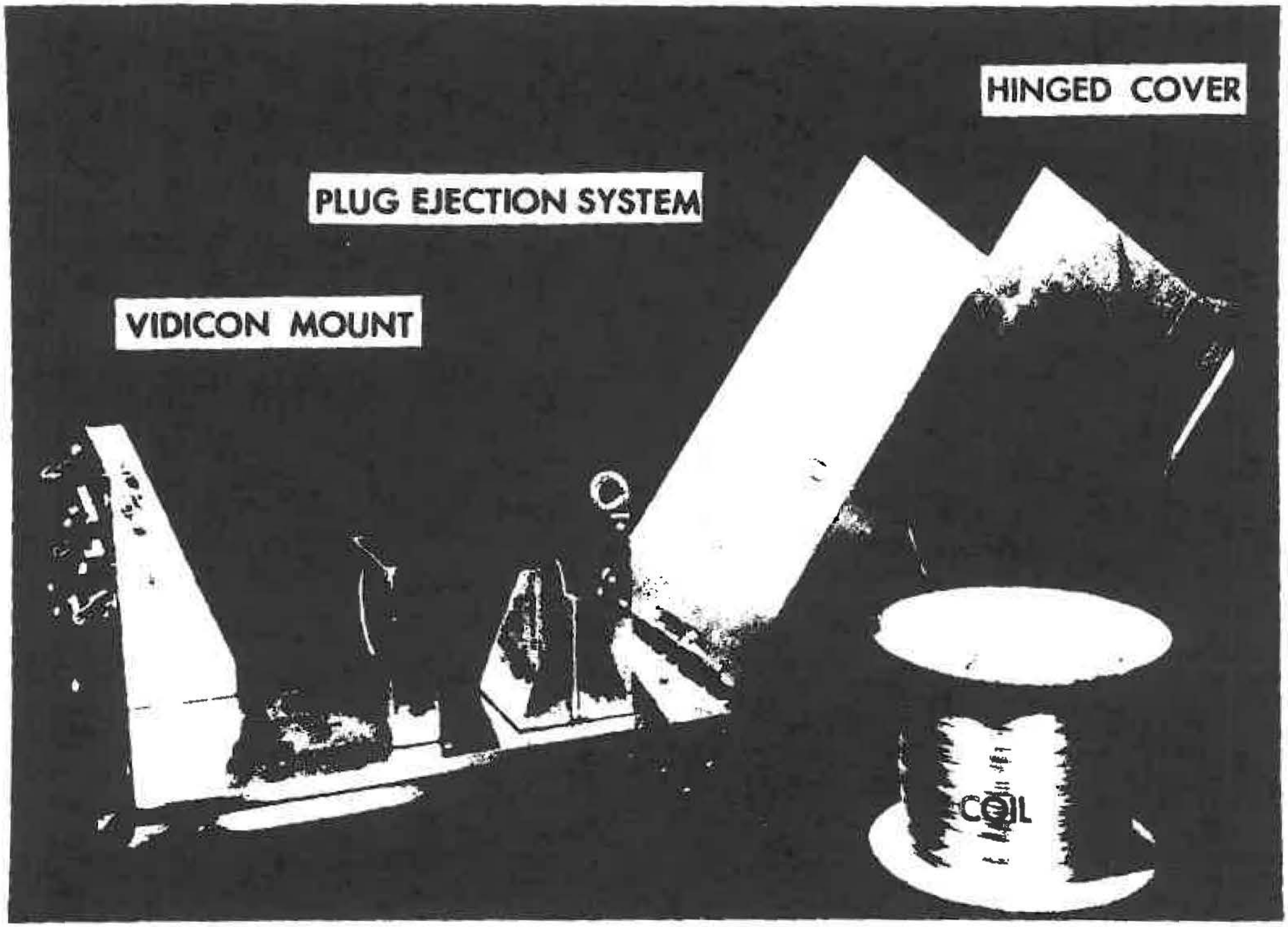

FIGURE A-11 CAMERA INTERIOR (VIDICON MOUNTING AND EJECTION SYSTEM)

APPENDIX D

THE REMOTE DISASSEMBLY AND REASSEMBLY OF THE RADIO SET AN/ARC-34

INTRODUCTION

The following material is a guide for the remote disassembly and reassembly of Radio Set AN/ARC-34, an airborne transceiver, using hot cell equipment. This equipment includes the Central Research Laboratories Model 8 manipulators, the General Mills E-2 manipulator, the Kollmorgen Model 301 periscope, and the Wollensak 6 x 30 binoculars. Included in this pre-irradiation study are the analyses, techniques, modifications, special tool development, and procedures that were established. These operations were conducted in the hot cell mock-up facility at the Georgia Nuclear Laboratories, Air Force Plant 67, Dawsonville, Georgia, shown in Figure B-1. This hot cell mock-up operation will ensure the success of remote operations on an irradiated AN/ARC-34. In the event of a total or partial failure of some of the radio subassemblies, vacuum tubes, diodes, or other electronic items, these items will be replaced remotely.

OBJECT

All the remote handling requirements will be met. The operational studies in the hot cell mock-up will answer most questions that might arise. A satisfactory view of those vital components and electronic items of the AN/ARC-34 will be obtained. Vital components and electronic items will be reached and handled with hot cell tools already developed. Modifications to the Radio Set and special tools will be required. The exact procedures will be used in the disassembly, replacement of all vital components and items, and the reassembly of the AN/ARC-34. The following components will be removed and replaced:

- Receiver, Subassembly
- Modulator, Radio
- Selector Control Subassembly
- Control Monitor
- Receiver, Radio
- Amplifier, Oscillator

FIGURE B-1 HOT CELL MOCK-UP

PROCEDURE

1. Pre-analysis and Planning

A pre-buildup study of the AN/ARC-34, considering its size (7-1/2 in. x 10 in. x 21 in.), weight (45 lb), and adaptability for remote handling with the Model 8 manipulators, was made. The AN/ARC-34, being an airborne receiver-transmitter, is small and compact and has many components and parts. Each component contains electronic circuits, condensers, diodes, and vacuum tubes of various sizes. The removal of these components and parts requires very careful handling. The extraction of vacuum tubes and other small items is difficult because of the very compact nature of the radio system. Viewing and locating these parts require extensive use of hot cell optical instruments -- binoculars, periscope, and convex mirror.

2. Complexity and Accessibility

Because of the vast complexity and inaccessible location of some of the components and items, two large exploded isometric drawings, Figures B-2 and B-3, were made showing the components on both sides of the Radio Set. All electrical connectors and disassembly screws are shown in these drawings.

Complexity of the radio system had the greatest single effect on the time requirements for mock-up activities. Most of the vacuum tubes and diodes were inaccessible and required the removal of the component for the replacement of those items.

3. Special Tools and Equipment

A rectangular mount rack constructed of aluminum angles was designed to hold the AN/ARC-34 on the test car. The mount rack

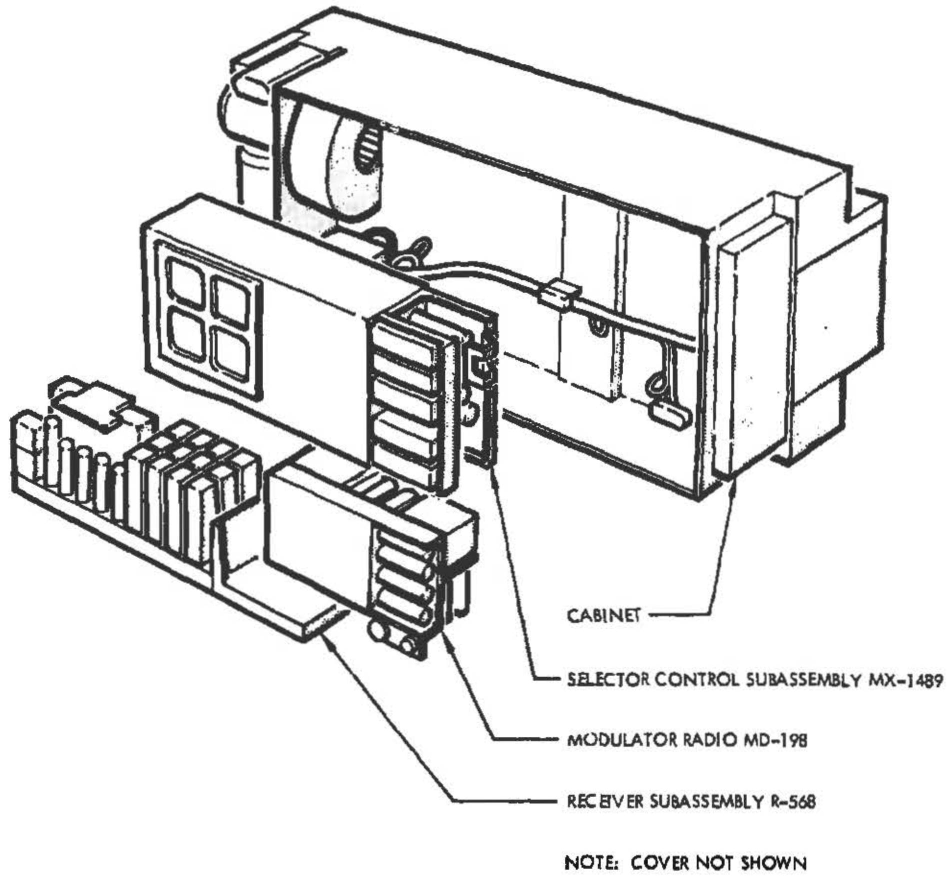

FIGURE B-2 AN/ARC-34, VIEW I

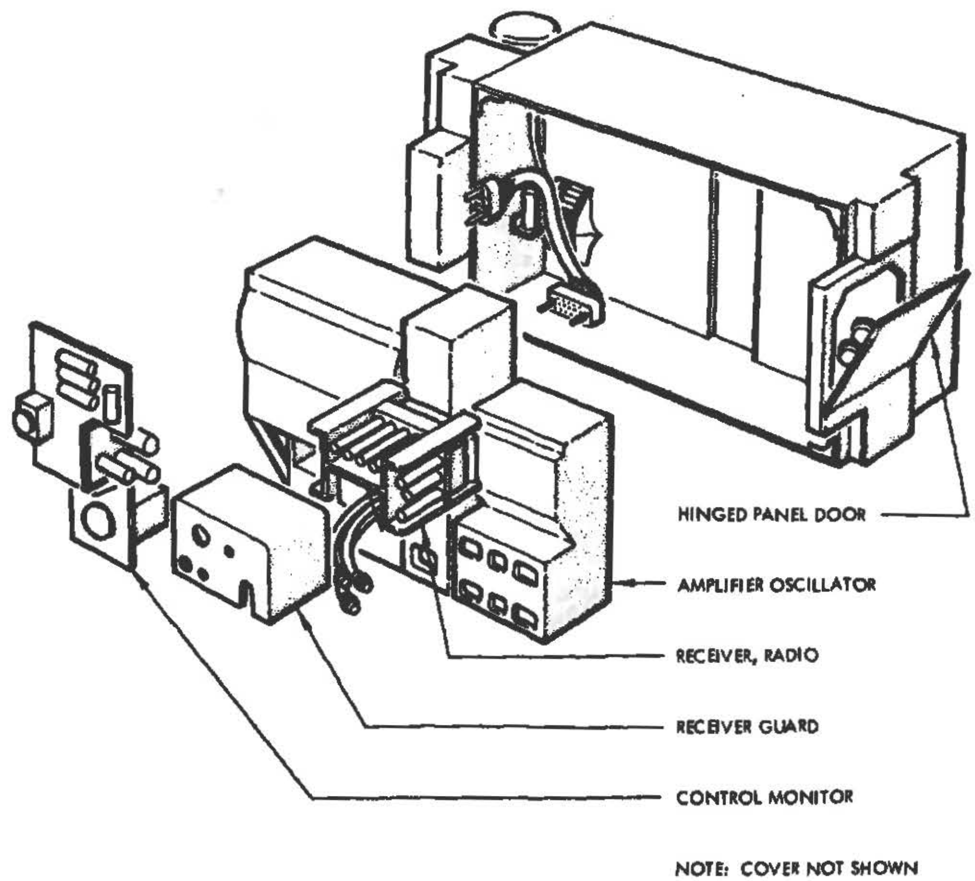

FIGURE B-3 AN/ARC-34, VIEW II

used in the hot cell mock-up duplicates the actual mount rack to be used in the radiation testing of the AN/ARC-34. It is shown in Figure B-4. This rack is equipped with a circular knurled knob on one end, allowing the manipulator operator to rotate the radio set on a horizontal axis located about 19 inches above the top of the test car. This rack was developed to facilitate remote handling, removal of components, and easier viewing. Normal hot cell equipment was utilized during this mock-up operation. This equipment includes closed circuit TV camera and monitoring system, cell wall periscope, high powered binoculars, portable spotlight, and a convex viewing mirror. Special hot cell tools already in use include the wire cutter and the "Lazy Susan" tool rack.

Most of the existing hot cell tools were analyzed with respect to the tool requirements for the disassembly and reassembly of the AN/ARC-34. Many of these tools were found to be too large and too tiring for the manipulator operators to utilize in remote operation on the Radio Set.

Two ratchet-type screw drivers were modified both in length and blade size as shown in Figure B-5. A special screw driver, Figure B-4, was developed with an off-set handle. This was necessary so that the manipulator operators could see very small screws in the radio set without the manipulator claw and screw driver handle being in the line of sight.

Other tools developed were a variety of steel handles to remove the components from the radio cabinet. Most of the components plug into electrical connectors directly beneath the subassembly; considerable force is required to separate these connectors. The Model 8 manipulators are too large in most cases to grasp the components without damaging the delicate electrical parts. The handles are easily attached to the components and provide a safe method of handling. This greatly reduces the possibility of dropping the subassembly during disassembly. Obviously, dropping a subassembly would cause considerable damage.

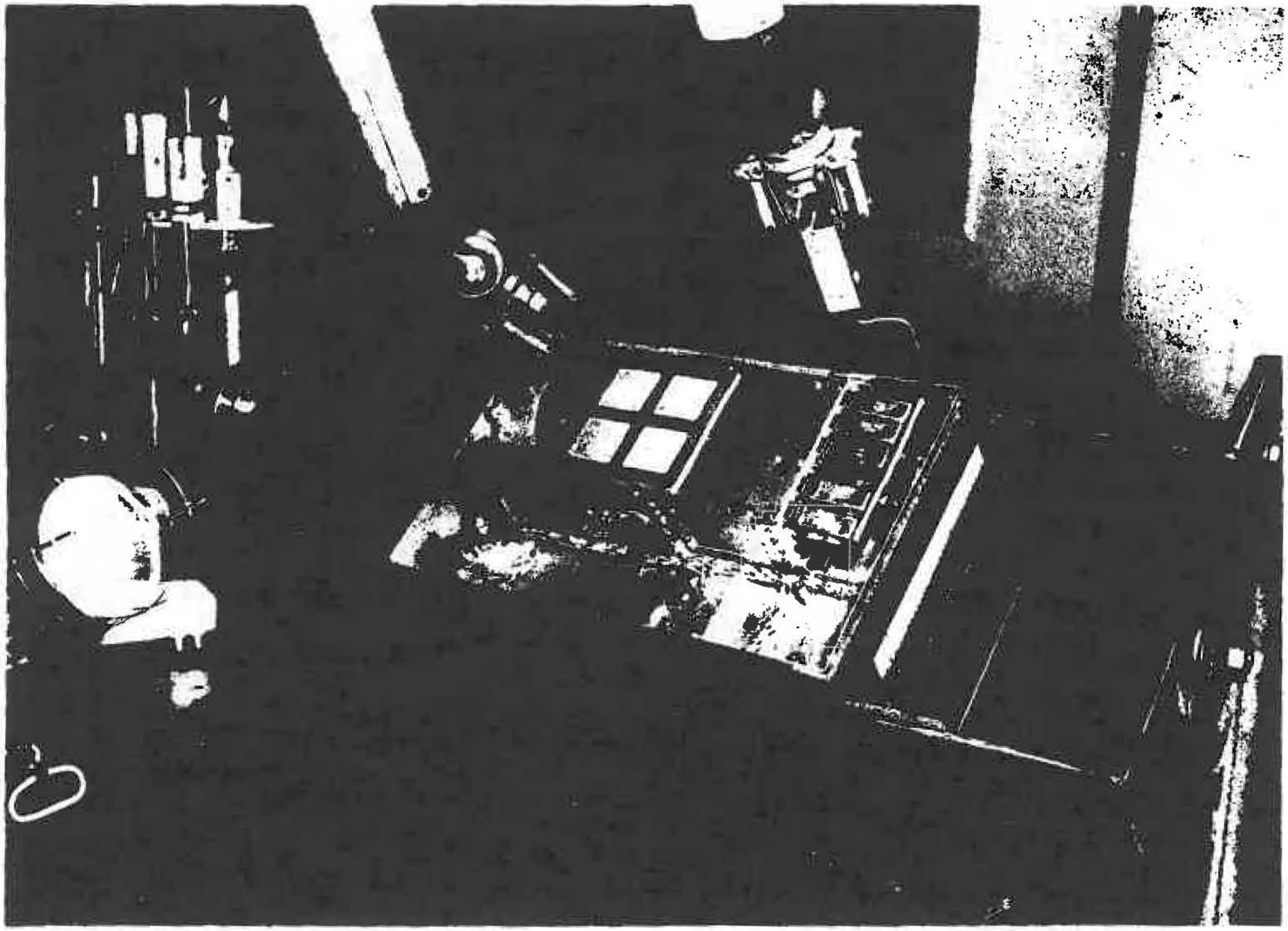

FIGURE B–4 OFFSET SCREWDRIVER

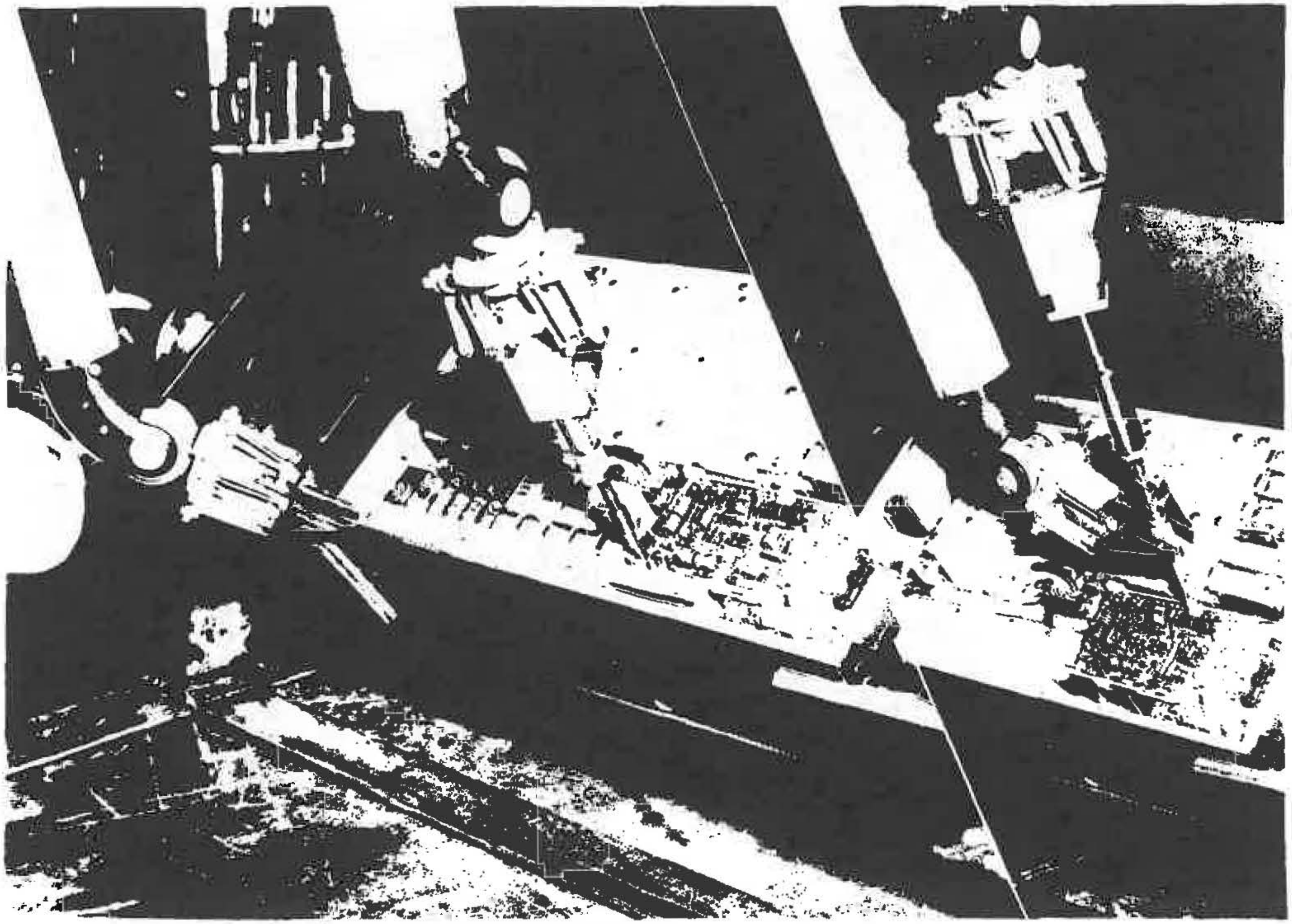

FIGURE B-5 RATCHET SCREWDRIVERS

Existing vacuum tube pullers were modified with rubber tips to extract and replace vacuum tubes. A different size was required for each different size tube in the radio set. The type constructed of thin steel tubing with a tapered slot on both sides and extending almost the length of the tube proved to be the most effective for Model 8 manipulator usage.

4. Subsystem Modification Requirements

Modifications for some specific components and items in the AN/ARC-34 are:

- Modulator Radio: Replace the three existing red disassembly screws on this element with three screws of the same diameter, but having raised heads 3/4 of an inch in depth. Paint these screw heads white for easier identification.

- Paint white spots for identification on the edges and screw holes of the components where the tool handle ends will engage.

- Increase the lengths of the electrical cables having twist type connectors for easier remote disconnection.

- Identify vacuum tubes with their alignment into their respective female sockets.

- Paint the top of electrical connectors marked P696 and P697 white for easier identification.

The following components of the AN/ARC-34 were removed remotely in the order shown during the hot cell mock-up operation:

(a) Receiver Subassembly (R-568/ARC-34)
(b) Modulator, Radio (MD-198/ARC-34)

(c) Selector Control Subassembly (MX-1489/ARC-34)
(d) Control Monitor (C-1256/ARC-34)
(e) Receiver, Radio (R-567/ARC-34)
(f) Amplifier-Oscillator (AM-868/ARC-34)

5. Job Instructions

The AN/ARC-34 was mounted in the mount rack described previously in Paragraph 3. The mounted radio was then placed upon a test car and the car was positioned inside the hot cell mock-up at the Radiation Effects Laboratory building. The actual procedure for the component disassembly of the AN/ARC-34 was performed in the hot cell mock-up and will be utilized as a guide in future hot cell operation.

The first disassembly operation is to remove the top cover from the radio set *. Loosen the three screws on the right end of the cover one turn to the left. These screws are spring attached and will spring out when they have been loosened enough. Remove the cover by raising the right end up and pushing to the left.

The first component to be removed is the Receiver Subassembly located at the lower left of the radio set. Loosen the three white disassembly screws several turns to the left. The screws will dangle loose when they have been loosened enough. Next, pick

* All the special tools developed were painted white and then identified with black bands. For example, one black band for the receiver subassembly, two black bands for the modulator radio, etc. The manipulator operator is furnished a tool identification chart. The white and black colors proved to be more easily seen than other colors when viewed through the cell windows.

up the special tool handle with one black band *. See Figure B-6. Insert one end of the tool under the handle on the left front of the component. Insert the right end of the tool under the flange of the protruding end of the component on the upper right front. (All the tool handles are made springy for easier manipulation into their correct positions. Also, being springy, these tools will grasp the components with a firmer and tighter grip.) Pull straight out on the handle and the component will disconnect from the radio chassis.

The next component to be removed is the Modulator Radio located in the lower right front of the radio set. This is accomplished by loosening the three white screws in the same manner as before. These screws again will dangle free. The tool handle with two black bands is positioned diagonally across the front of the component as shown in Figure B-7. One tool end is inserted in a hole at the lower left of the component; the other tool end is inserted in a hole at the upper left of the component. Both holes are spotted with white paint for easier identification. The component is lifted straight out of the electrical connector located beneath the component.

* The AN/ARC-34 used in the mock-up test did not contain the instrumentation cables leading into both the top and the bottom cover of the radio set. On the actual instrumentated AN/ARC-34 to be irradiated, these instrumentation cables will have to be disconnected before the covers can be removed. These cables will be fastened to the covers by aluminum connector blocks. Loosening two screws on each connector block allows the cables to be disconnected from the female sockets within the radio set.

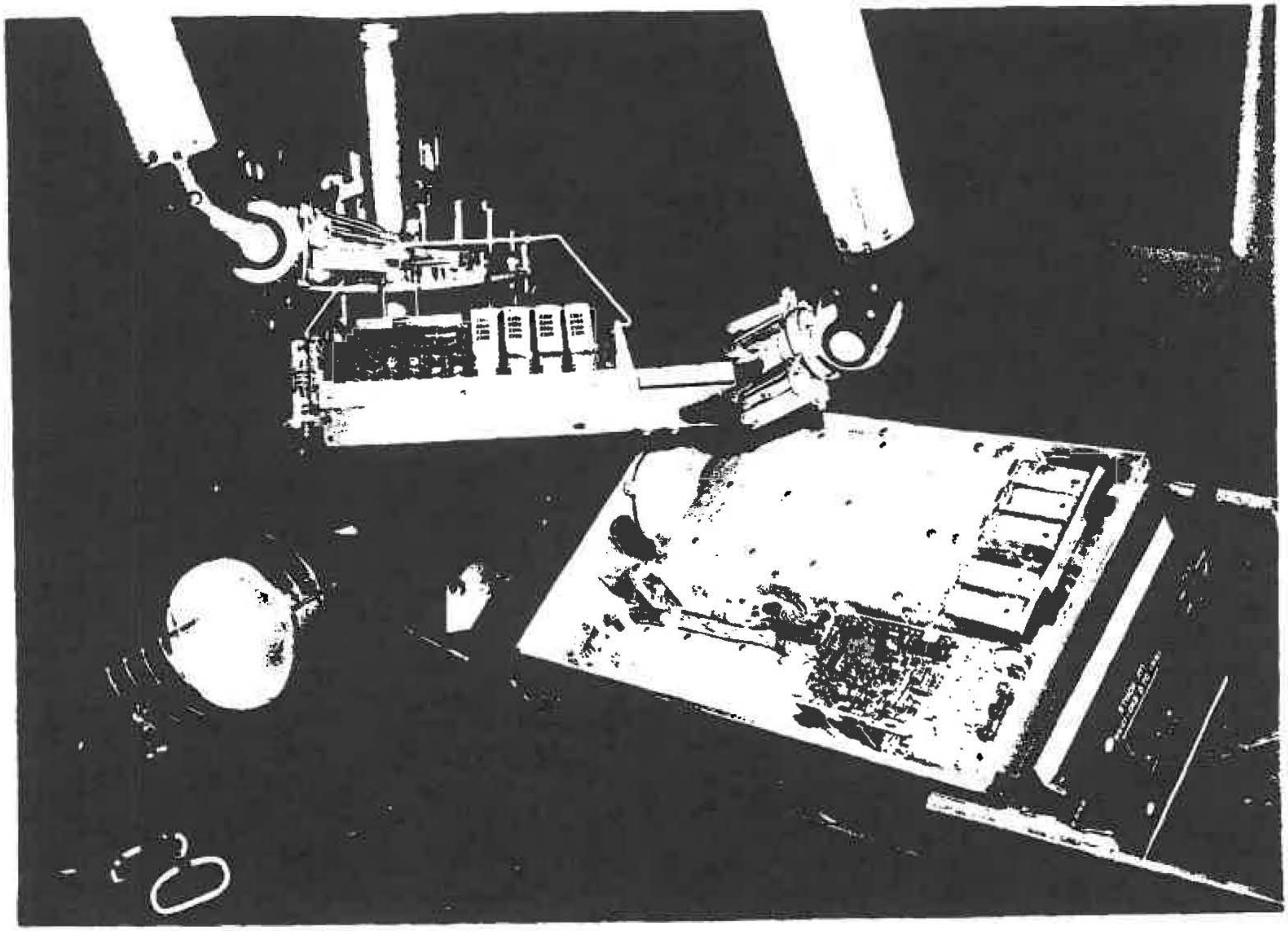

FIGURE B-6 RECEIVER SUBASSEMBLY

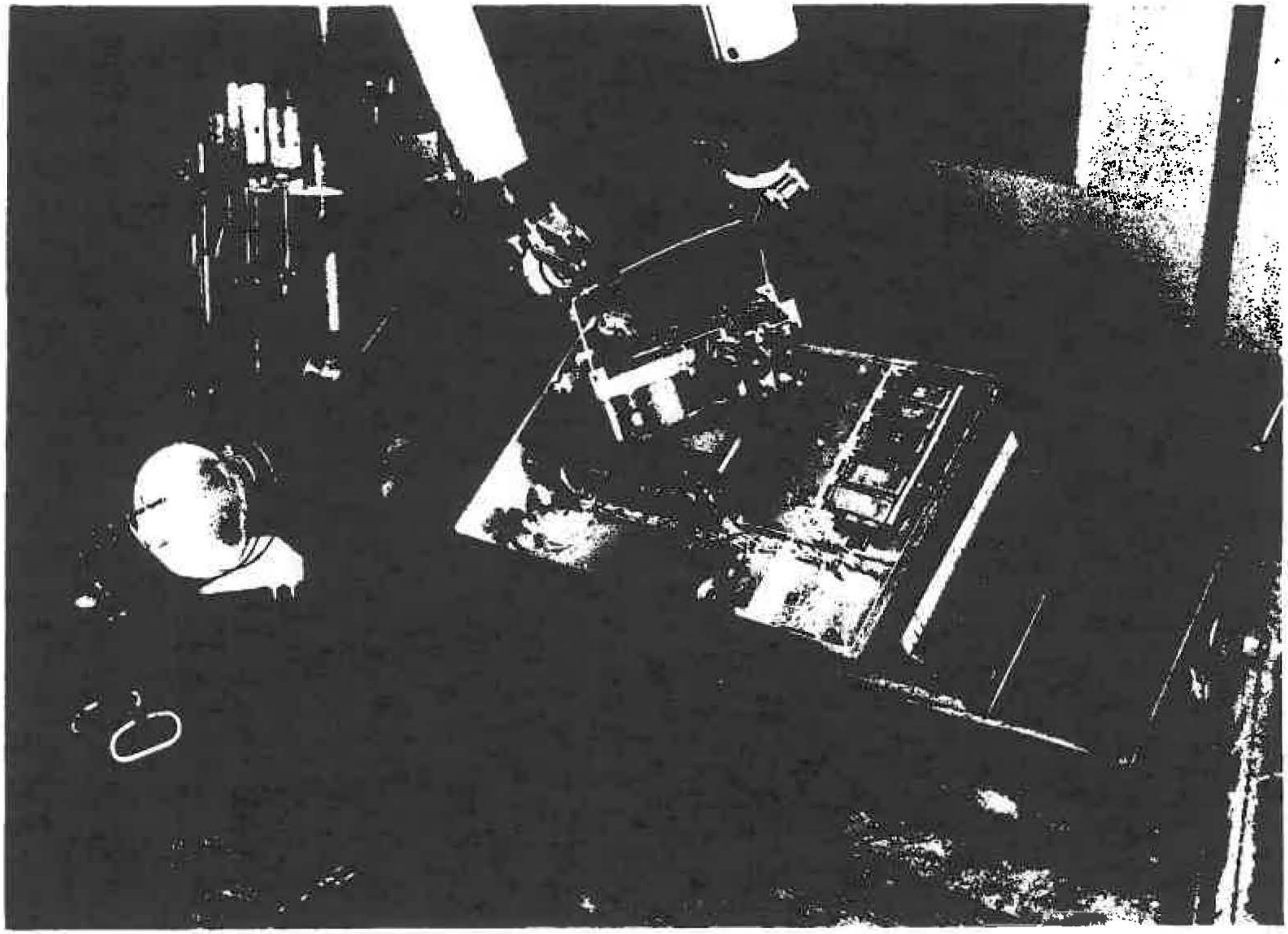

FIGURE B-7 MODULATOR RADIO SUBASSEMBLY

There is now only one component remaining in the radio set on this side. This is the large Selector Control Subassembly. It has four screws, painted white, in each corner of the component. Loosen each screw about four turns to the left. This component has two tool handles, each having three black bands for identification. See Figure B-8. Engage the ends of both tools under the heads of the four screws. Tighten these screws on the ends of the tools. Lift the component about three inches out of the two electrical connectors beneath. A twist-type connector cable leading from the component to the radio chassis must be disconnected before the component can be removed. Disconnect the cable and lift the component out of the radio set. This completes the component disassembly on the top half of the AN/ARC-34.

Turn the radio set over by loosening the large knurled knob on the mount rack. The lower portion of the set is now positioned toward the manipulator operator. Tighten the knob, and the radio set is now in position for the remote disassembly of the bottom half of the set.

Remove the cover by loosening the four white screws, two on each end. Turn each screw once to the left. Lift the cover off by prying up under the right end with a screw driver.

The Control Monitor component is removed first. Locate the three white disassembly screws and loosen them. No tool handle is necessary to remove this component. Remove the Control Monitor by lifting straight out.

Pull the twist-type cable connector with the orange band located just in front of the Receiver Guard at the upper right of the set out of the two clips and disconnect the cable.

Disconnect the twist-type cable connector with the green band next. The twist type cable connector with the red band located on the right side of the Receiver Guard is disconnected also.

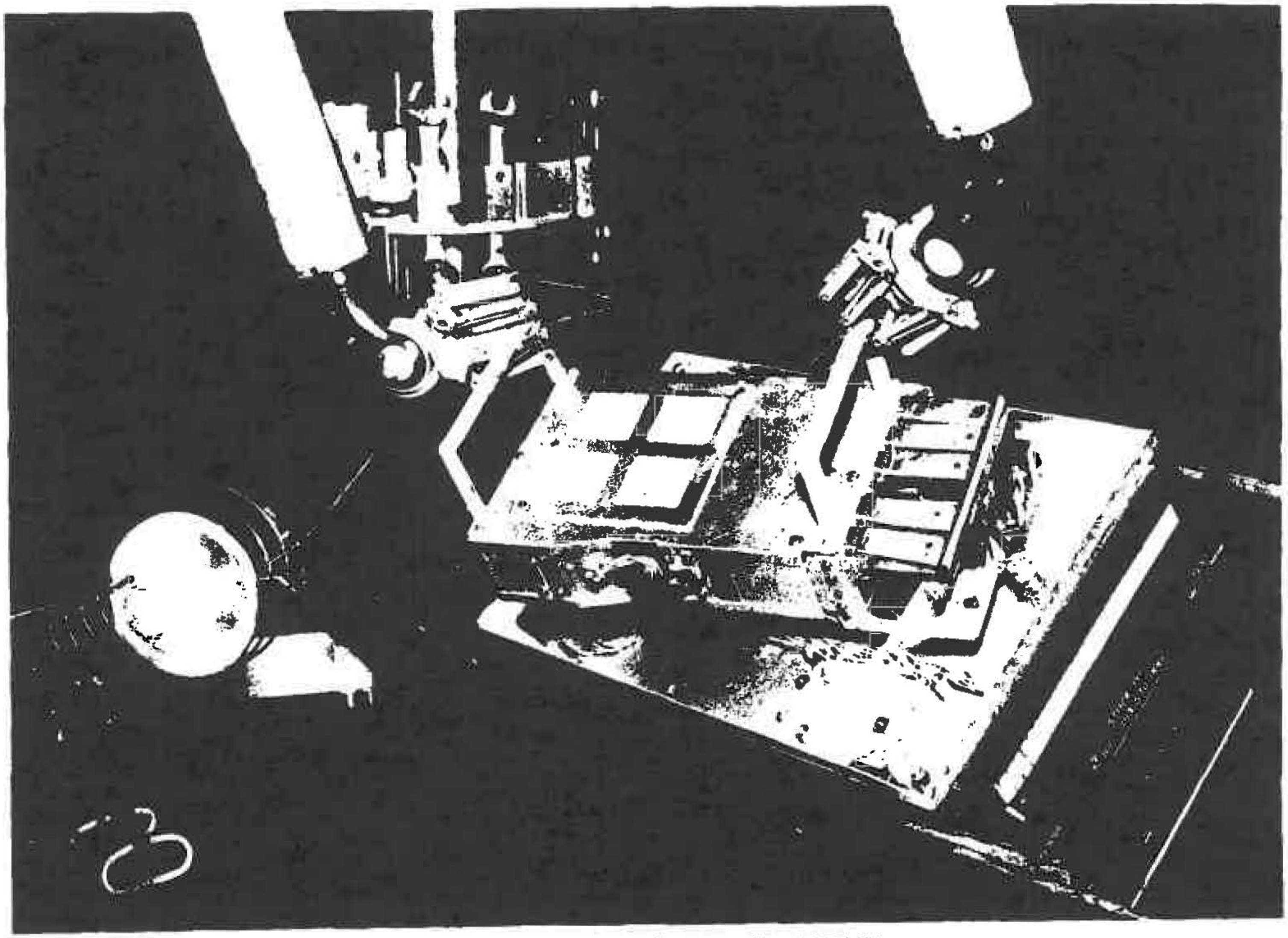

FIGURE B-8 SELECTOR CONTROL SUBASSEMBLY

Now loosen the two white screws on the Receiver Guard. Pick up the tool handle with four black bands shown in Figure B-9. The right end of the tool is inserted under the big slot on the Receiver Guard and the other end is inserted under the small hole on the left end of the compartment. These places are identified by white paint spots. Pull the Receiver Guard out a short distance. At this point, the three loose cable ends must be pushed through the big slot in the Receiver Guard. Now lift the Receiver Guard straight out.

Attach the tool with five black bands to the Receiver Radio component by screwing the two screws on the handle into the two raised and tapped posts on the component shown in Figure B-10. The component is then lifted straight out.

The final component to be removed is the large, heavy Amplifier-Oscillator. The white connector marked P696 located at the lower left of the component must be unplugged. Also unplug the white connector marked P697 located at the upper right of the component. Unscrew the two socket-head cap screws located on the lower exterior of the radio cabinet and remove them from the radio cabinet. Pick up the two tools with six black bands shown in Figure B-11. Insert the end of the tools where the white identification spots are located. The component, being heavy, requires careful handling. Lift the component straight out of the cabinet. This completes the component disassembly of the AN/ARC-34 Radio Set.

The AN/ARC-34 components are reassembled in the reverse order. Reassembly requires greater care in handling the components, because almost all of the components have to be inserted into electrical connectors. This is done almost "blindly" and the "feel" of a good connection has to be done remotely with the Model 8 manipulators.

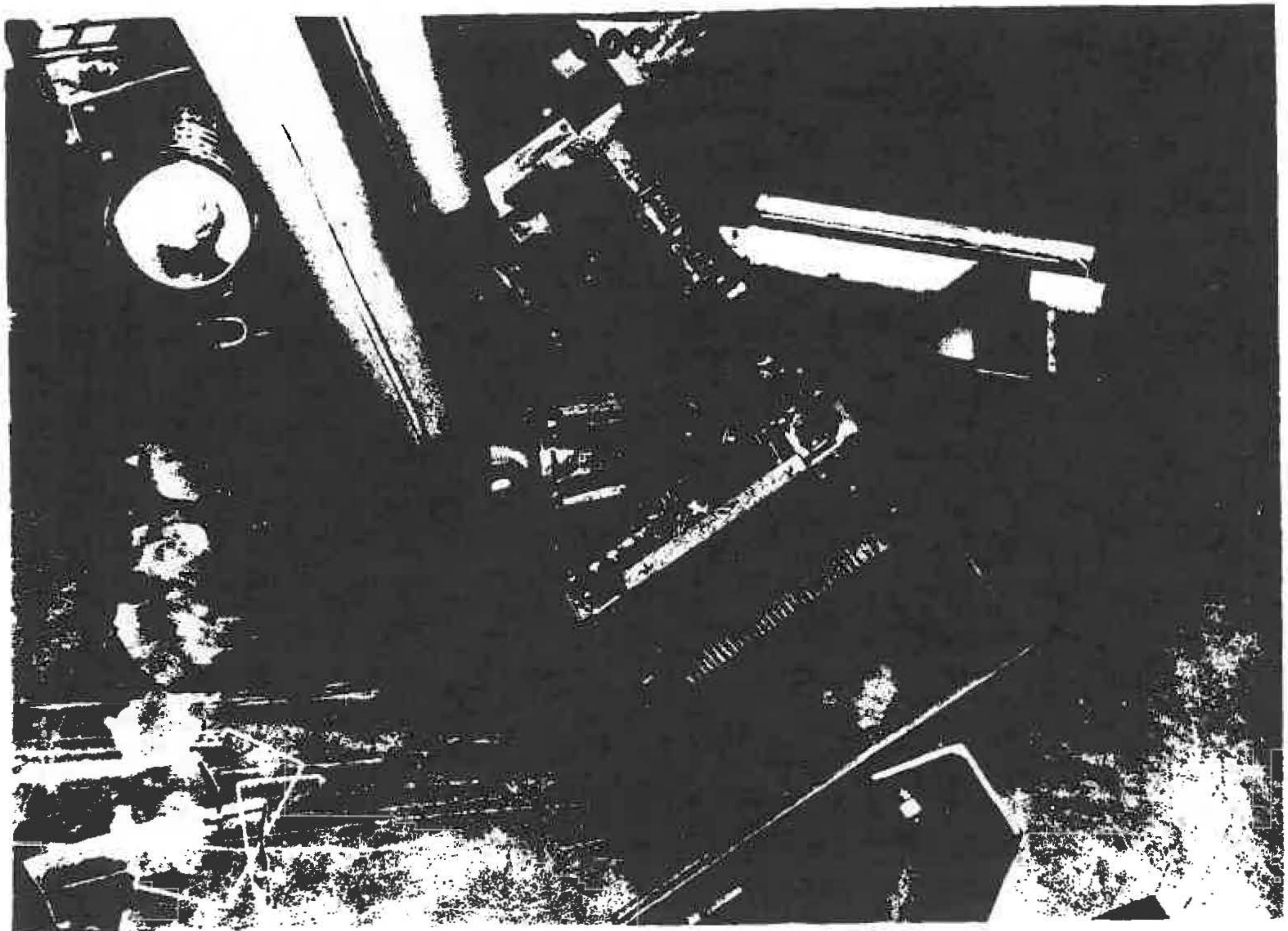

FIGURE B-9 GUARD RECEIVER SUBASSEMBLY

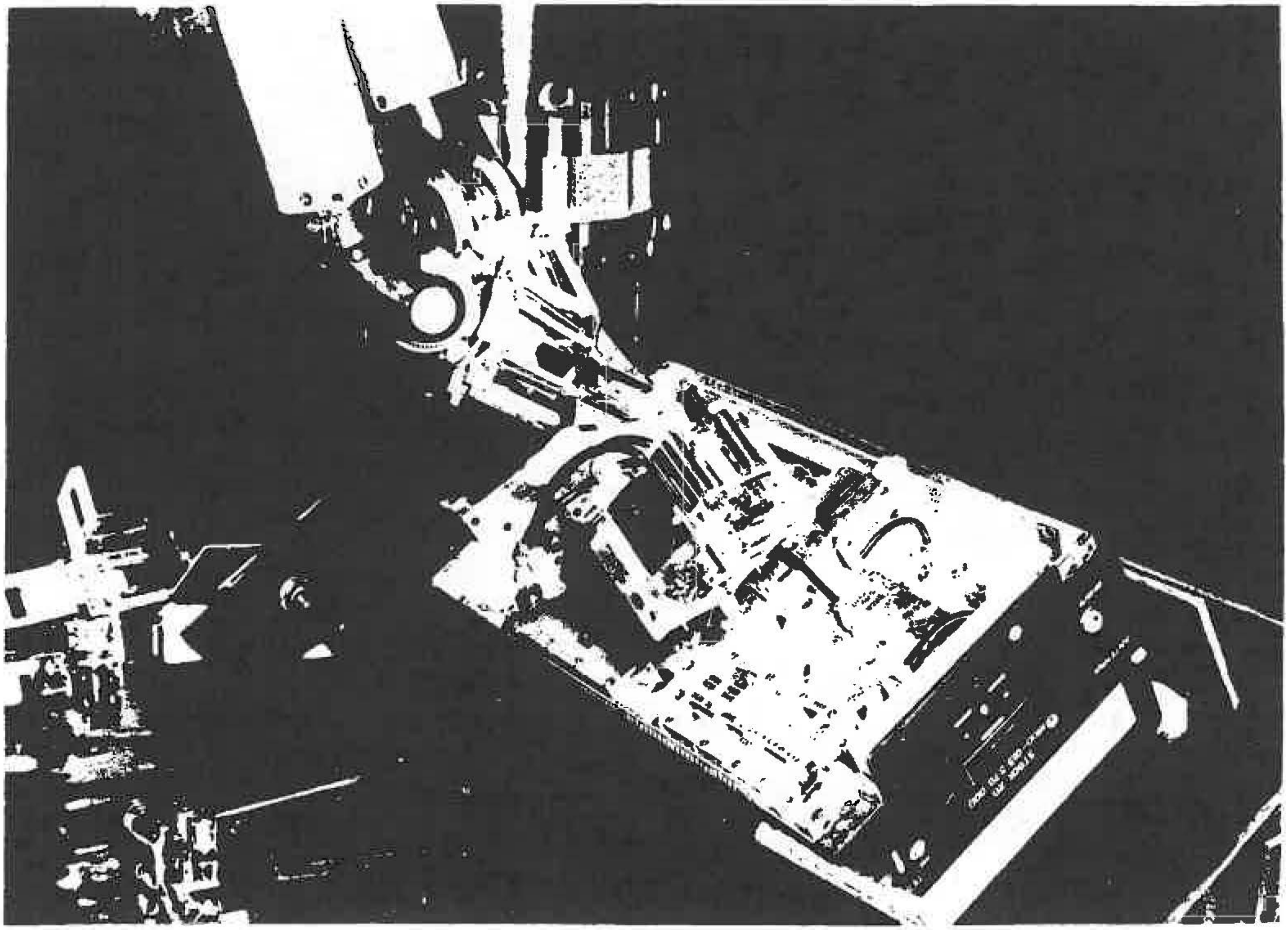

FIGURE B-10 RADIO RECEIVER SUBASSEMBLY

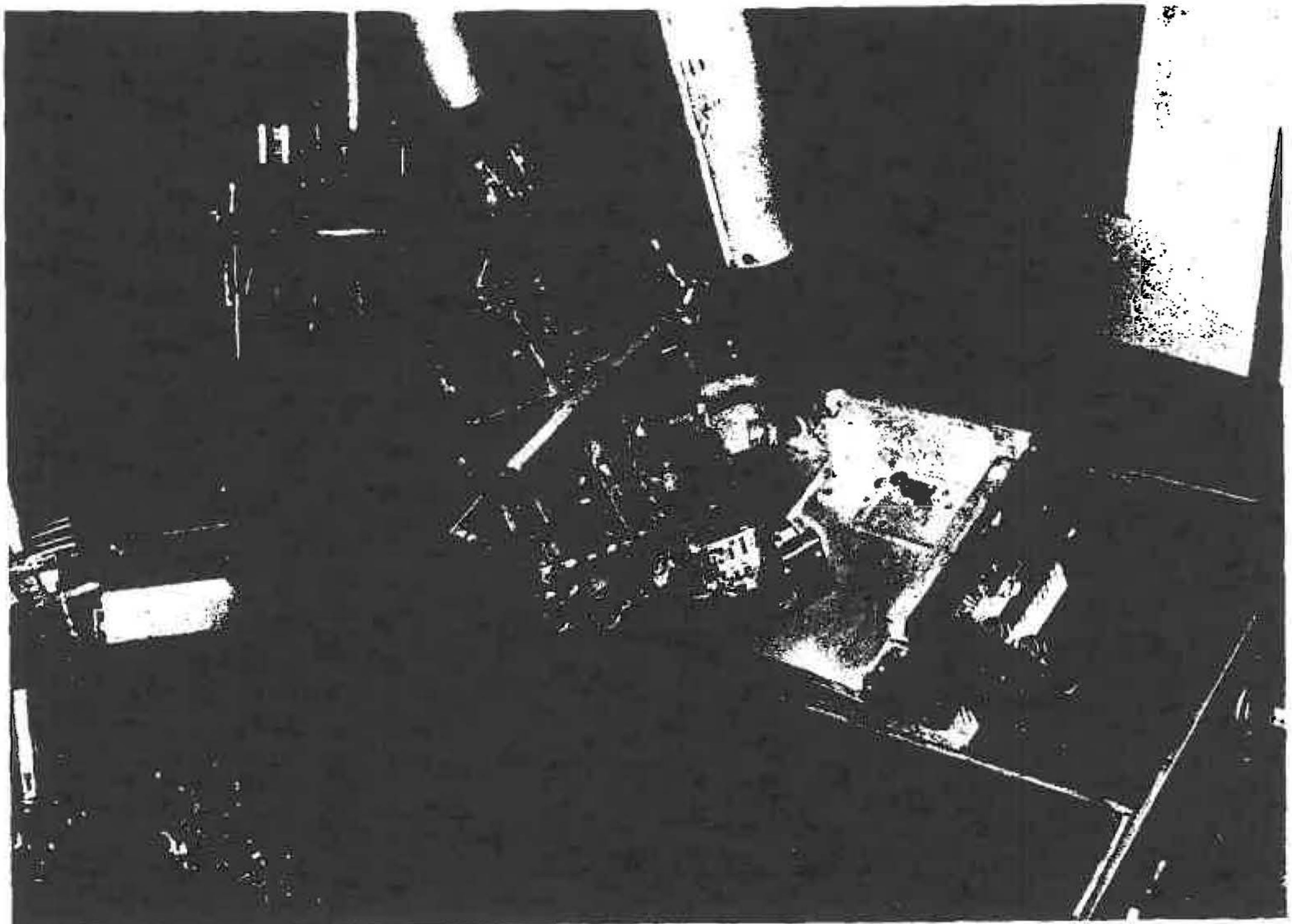

FIGURE B-11 AMPLIFIER, OSCILLATOR SUBASSEMBLY

Reassemble the components in the order shown below:

a. Amplifier-Oscillator
b. Receiver Radio
c. Receiver Guard - This requires the use of a string to tie the three loose ends of the electrical cables together. The cables have to be pulled through the large slot on the guard before the guard can be placed over the receiver.
d. Control Monitor
e. Selector Control Subassembly
f. Modulator, Radio
g. Receiver Subassembly
h. Replace the cover on this side of the set.

This completes the reassembly of the AN/ARC-34.

CONCLUSIONS

The AN/ARC-34 can be disassembled and reassembled remotely using Model 8 manipulators.

APPENDIX-E

REFERENCES

1. Boas, W. and Schmid, E., Zeits. f. Physik, 61:767 (1930).

2. deHaas, W. J. and Hadfield, R., Phil. Trans. Roy. Soc., (A) 232, 297 (1933).

3. Eldin, A. S. and Collins, S. C., J. Applied Physics, 22:1296 (1957).

4. McCammon, R. D. and Rosenberg, H. M., Proc. Roy. Soc. (A) 234: 221 (1957).

5. Bechtold, J. H. and Wessel, E. T., Proc. of the Office of Naval Research Symposium on Molybdenum, Detroit, 1956.

6. Basinski, Z. S. and Sleeswyk, A., Acta Met., 5:176 (1957).

7. Smith, R. L. and Rutherford, J. L., Trans. Amer. Inst. Min. Met. Eng., 209:857 (1957).

8. Cottrell, A. H., Trans. Met. Soc. A.I.M.E., 212:192 (1958).

9. Rosenberg, H. M., Met. Rev., 3:357 (1958).

10. Blewitt, T. H., Coltman, R. R., and Redmond, J. K., J. Applied Physics, 28:651 (1957).

11. Zambrow, J. L. and Fontana, M. G., Trans. Amer. Soc. Metals, 41:480 (1949).

12. Spretnak, J. W., Fontana, M. G. and Brooks, H. E., Ibid, 43:547 (1951).

13. Bishop, S. M., Spretnak, J. W., and Fontana, M. G., Ibid., 45:993 (1953).

14. McCammon, R. D. and Rosenberg, H. M., Proc. Roy. Soc. (A) 242:203 (1957).

15. Cottrell, A. H. and Hull, D., Proc. Roy. Soc. (A) 242:211 (1957).

16. Broom, T. and Ham, R. K., Proc. Roy. Soc. (A) 242:166 (1957).

17. Broom, T., Molineaux, J. H., and Whittaker, V. N., J. Inst. Met., 84:357 (1955-56).

18. Wyatt, O. H., Proc. Phys. Soc., (B) 66:459 (1953).

19. Meissner, W., Polanyi, M., and Schmid, E. Z., Physik 66:477 (1930).

20. Glen, J. W., Phil. Mag., (vii) 1:400 (1956).

21. Mott, N. F. and Nabarro, F. R. N., Report of a Conference on Strength of Solids, London (Physical Society) (1948).

22. Dienes, G. J., Effects of Radiation on Materials, Chapt. 1, Reinhold Publishing Corp., New York, (1958).

23. Billington, D. S., Effects of Radiation on Materials, Chapt. 3, Reinhold Publishing Corp., New York (1958).

24. Thompson, D. O. and Holmes, D. K., J. Applied Physics, 27:713 (1956).

25. Steele, R. V. and Wallace, W. P., Met. Prog. 68:114 (1955).

26. Faris, F. E., Proc. Geneva Conf., Paper 747 (1955).

27. Billington, D. S. and Siegel, S., Met. Prog. 58:847 (1950).

28. Kernohan, R. H., Billington, D. S., and Lewis, A. B., J. Applied Physics 27:40 (1956).

29. Kunz, F. W. and Holden, A. N., Acta Met. 2:816 (1954).

30. Mankin, M. J. and Minter, F. J., J. Inst. Metals, 24:399 (1957).

31. Leeser, D. O., Materials and Methods 40:115 (1954).

32. Sutton, C. R. and Leeser, D. O. Nucleonics, 12:8 (1954).

33. Wilson, J. C. and Billington, D. S., Nuclear Eng. and Sci. Congress (1955).

34. Jones, E. R. W., Munro, W., and Hancock, J. Nuclear Energ. 1:181 (1955).

35. Jeppson, M. R., Mather, R. L., Andrew, A., and Yockey, H. P., J. Applied Physics 26:365 (1955).

36. Cottrell, A. H., Met. Reviews 1:479 (1956).

37. Sosin, A., Brinkman, J. A., and Meecham, C. J., Physics Today, 12:30 (June, 1959).

38. Blewitt, T. H., et al, J. Applied Physics 28:639 (1957).

39. Ibid., P. 742.

40. McReynolds, A. W., et al, Phys. Rev. 98 (1955).

41. Broom, T., Advances in Physics 3:26 (1956).

42. Nachbar, W., Discontinuity Stresses in Pressurized Thin Shells of Revolution, LMSD-48483, 17 (March 1959)

ASSIFIED

43. Journal of Research, National Bureau of Standards, Vol. 58, No. 5 (May, 1957).

44. American Society for Testing Materials, Standards 1958, Pt. 4 Method E4-57T.

45. Ibid., Standards 1958, Pt. 5 Method E83-57T.

46. NACA TN-3553, Compressive Crippling of Structural Sections.

47. NACA WR-L-429.

48. NACA TN-3431, Analysis of the Structural and Ultimate Comprehensive Strength of Short Sheet-stringer Panels with Special Reference . . . Sheet and Stringer.

49. NACA TN-1389.

50. TML-24, Applications of a New Structural Index to Compare Titanium Alloys with Other Materials in Airframe Structures.

51. NACA TN-4211, Friction Studies of Various Materials in Liquid Nitrogen.

52. WADC TR-57-455, High Temperature of Solid Dry Film Lubricants.

53. WADC TR-58-499.

54. Coltman, R. R., Blewitt, T. H., and Noggle, T. S., Techniques and Equipment Utilized in Low-Temperature Irradiation.

55. WADC Report 56-408, Interrelation of Fatigue Cracking, Damping, and Notch Sensitivity, (March 1957).

56. WADC Report 56-44, Analytical Methods for Determining Specific Damping Energy Considering Stress Distribution, (June 1957).

57. McAdams, W. H., Heat Transmission, McGraw-Hill, Third Edition, (1952).

58. Conant, C. W. and Kartier, W. E., NASA-Plumbrook Reactor Facility, (1959).

59. Marenchain, F. and Love, T., "Gamma Spectrum From Bulk-Shielding Reactor," Nucleonics, Vol. 12 (1954).

60. Binford, Bettis, and Howe, "Gamma Ray Heating in BSR," Nucleonics, Vol. 15, No. 3, 93, (1956).

61. AECD 3978, Effective Neutron Cross Section for Shielding.

62. NASA-MEMO 12-8-58E, NASA Reactor Facility Hazards Summary, Volumes 1 and 2.

63. ANL-5800, Argonne National Laboratory Handbook No. 5800, p. 280.

64. NARF 55-32T, "Measurement of Dose Rates from Activated Aircraft Materials," Part I, (1955).

65. NARF 57-35T, "Dose Rates from Activated Aircraft Materials," Part V, (1957).

66. Nucleonics, Vol. 17, No. 1, p. 54, (1959).